AN ABSTRACT OF THE DISSERTATION OF

Lu Wang for the degree of Doctor of Philosophy in Microbiology presented on September 8, 2020.

Title: Effects of Anthropogenic Stressors on Seagrass and Coral Microbiomes

Abstract approved:

_____

Ryan S. Mueller

Seagrasses and coral reefs play important roles in nutrient cycling, coastal protection, and maintaining marine biodiversity. However, these coastal marine organisms are declining globally due to anthropogenic stressors, such as rising ocean temperatures, ocean acidification, and eutrophication. These organisms live in close association with their microbiomes, which can be beneficial or detrimental to the host organism, depending upon environmental conditions. This body of work utilized 16S rRNA amplicon and metagenome sequencing to characterize changes in the taxonomic composition and functional potential of seagrass and coral microbiomes under varying environmental stressors. This work was done to gain fuller understanding of seagrass and coral holobiont responses to the changing oceans. Chapter 2 describes the increased prevalence of Dark Spot Syndrome (DSS) in the coral *Siderastrea siderea* associated with thermal stress, and changes in the microbiome associated with diseased corals, exhibiting characteristics of dysbiosis (increased compositional variation amongst diseased samples). Importantly, we found no microbial taxa associated with DSS, and concluded DSS is a general stress

response and not microbe mediated. Chapter 3 presents the effects of eutrophication on *Zostera marina*, or eelgrass. Using a mesocosm experiment, we characterized the microbiome and plant host morphology and physiology responses to nutrient enrichment. Fertilization led to increased plant size and enriched nitrogen and sulfur cycling bacteria in root-associated samples. This study contributes both eelgrass physiology and microbiome responses to eutrophication to the breadth of seagrass literature. Chapter 4 examines changes to the leaf microbiome of the seagrass *Posidonia oceanica* under acidified conditions. Samples were collected from naturally occurring CO_2 vents in Ischia, Italy, which simulate future ocean acidification scenarios. In acidified samples, we identified decreases in relative abundance of microbial carbon fixation genes, and enrichment for heterotrophic bacteria and genes involved in biofilm production. Seagrass transplantation is a major component of restoration efforts after population declines, and Chapter 5 examines the eelgrass rhizobiome response to transplantation. We transplanted eelgrass individuals with and without intact rhizosphere sediment and characterized plant morphology and belowground microbiome succession over 4 weeks. Eelgrass transplanted without intact rhizospheres exhibited declines in root biomass and dysbiosis at the start of the experiment, but after one week, eelgrass plants and their belowground microbiomes demonstrated resilience to transplantation in our mesocosm environment.

As a whole, these studies described demonstrable changes to host-associated microbiomes under future ocean conditions. In particular, this work presents a significant contribution to the nascent field of seagrass microbiome research. These

studies have identified key members of healthy and disturbed seagrass microbiomes; this knowledge can be used to generate hypotheses and future experiments targeting specific host-microbe interactions. This work shows the importance of interdisciplinary collaboration and integration of microbiome data with plant and environmental metrics to gain a full appreciation of the system. Lastly, though these valuable coastal organisms are currently on the decline, the integration of microbiome data may lead to successful management and restoration efforts.

Effects of Anthropogenic Stressors on Seagrass and Coral Microbiomes

by
Lu Wang

A DISSERTATION

submitted to

Oregon State University

in partial fulfillment of
the requirements for the
degree of

Doctor of Philosophy

Presented September 8, 2020
Commencement June 2021

Doctor of Philosophy dissertation of Lu Wang presented on September 8, 2020

APPROVED:

Major Professor, representing Microbiology

Head of the Department of Microbiology

Dean of the Graduate School

I understand that my dissertation will become part of the permanent collection of Oregon State University libraries. My signature below authorizes release of my dissertation to any reader upon request.

Lu Wang, Author

ACKNOWLEDGEMENTS

I express my deepest and most sincere gratitude to everyone who has supported and believed in me during this journey.

Thank you to my committee members for their expertise, patience, and wisdom. I would particularly like to thank and acknowledge my advisor, Dr. Ryan S. Mueller, an all-star scientist and mentor, for guiding me on my scientific journey. I feel extremely lucky to have landed in the Mueller Lab.

Thank you to friends near and far, and to the friends I made along the way, especially fellow microbiology graduate students with whom I could celebrate and commiserate. Special thanks to past and present members of the Mueller Lab, particularly Hanna Delgado, MK English, and Dr. Brandon Kieft.

Thank you to Cinamon Moffett at HMSC, who was vital in the success of chapters 3 and 5. Thank you to Dr. James Kaldy, who passed on seagrass research wisdom. Thank you to everyone who helped me in the field – 100-pound buckets of mud are not easy to carry, and I literally could not have done it alone.

I appreciate all the funding sources who took a chance on me – the Department of Microbiology at OSU (Nicholas L. Tartar Graduate Student Fellowship, Middlekauf Graduate Research Assistant Award, Joan Countryman Suit Scholarship, Teaching Assistantships), OSU Graduate School (Dissertation Completion Award), Hatfield Marine Science Center (Mamie Markham Research Award), South Slough National Estuarine Research Reserve (Margaret Davidson Fellowship FY2019 Spring Quarter), and the Oregon Shell Club.

Lastly, thank you to my loved ones – my mom and dad for their support and encouragement. Thank you to Stephen Black for everything, even coming out to the field with me and inadvertently becoming an expert in seagrass epiphyte removal. And of course, thanks to my cat Magus for keeping me grounded.

CONTRIBUTION OF AUTHORS

Lu Wang: First author in the dissertation and chapters therein, study design and conception, performed experiments, data analysis, manuscript preparation and edits

Andrew A. Shantz: Fieldwork, data analysis, manuscript preparation and edits

Jérôme P. Payet: Field work, sample preparation, manuscript preparation and edits

Thomas J. Sharpton: Data analysis

Amelia Foster: Sample preparation

Deron E. Burkepile: Study design and conception, fieldwork, data analysis, manuscript edits

Rebecca Vega Thurber: Study design and conception, data analysis, manuscript preparation and edits

Gema Hernán: Sample collection

Jorge Terrados: Sample collection

Fiona Tomas: Study design and conception, manuscript preparation and edits

MK English: Performed experiments, data analysis, manuscript preparation and edits

Ryan S. Mueller: Study design and conception, performed experiments, data analysis, manuscript preparation and edits

TABLE OF CONTENTS

Page

TABLE OF CONTENTS (Continued)

Page

TABLE OF CONTENTS (Continued)

Page

TABLE OF CONTENTS (Continued)

Page

TABLE OF CONTENTS (Continued)

Page

LIST OF FIGURES

Figure Page

LIST OF FIGURES (Continued)

LIST OF TABLES

LIST OF APPENDICES

LIST OF APPENDIX FIGURES

LIST OF APPENDIX TABLES

DEDICATION

This dissertation is dedicated to my mom, dad, and my family in China. I would not be where I am today without their sacrifice and support.

1 Introduction

Seagrasses and corals are coastal ecosystem engineers that create and shape the surrounding environment into complex habitats, and act as foundations for coastal biodiversity. Their ecosystem services include water filtration, nutrient cycling, wave protection, support of fisheries stocks, and recreational and cultural value (Doney *et al.* 2012; Nowicki *et al.* 2017; Lei and Nepf 2019). Coral reefs provide food and resource security and provide habitats for fish and invertebrates (Elliff and Kikuchi 2017; Hughes *et al.* 2017; Woodhead *et al.* 2019). Loss of corals has been associated with loss of reef fishes and collapse of coastal food webs (Pratchett, Hoey and Wilson 2014). Seagrass meadows reduce pathogen load in coastal waters, stabilize marine sediments, and provide habitat and food web support for coastal fauna (Lamb *et al.* 2017; Whitfield 2017; Sherman and DeBruyckere 2018; Holmer 2019). Seagrass wrack can also be used for insulation and other building material (Sherman and DeBruyckere 2018). Importantly, seagrass meadows have potential for blue carbon - sequestration of allochthonous and autochthonous carbon (Oreska *et al.* 2018), which has consequences for mitigation of global change due to human activities. Seagrass loss leads to coastal erosion (Walter *et al.* 2020), loss of carbon stocks (Arias-Ortiz *et al.* 2018), and disruptions in abundance and behavior of coastal megafauna (Nowicki *et al.* 2019).

Taken together as a holobiont, the microbiome and host organisms contribute to ecosystem functioning and structure (Wilkins *et al.* 2019). Corals possess a unique microbiome (Rohwer *et al.* 2001), which protects host health by preventing the establishment of opportunistic and pathogenic microbes and increasing resilience

against disturbance (Rosenberg *et al.* 2007; Glasl, Herndl and Frade 2016; McDevitt-Irwin *et al.* 2017; Welsh *et al.* 2017). Most notably, coral animals live in mutualism with the dinoflagellate Symbiodiniaceae, which provide their hosts with photosynthetic carbon in exchange for nutrients (Rosenberg *et al.* 2007). Members of the coral microbiome participate in carbon, sulfur, and nitrogen cycling, and can provide nitrogen for both Symbiodniaceae and the coral host (Bourne, Morrow and Webster 2016; McDevitt-Irwin *et al.* 2017). Corals experiencing dysbiosis are more likely to suffer from bleaching and necrosis (Glasl, Herndl and Frade 2016).

Seagrasses possess endophytic and epiphytic microbiota associated with various compartments (roots, rhizosphere, leaves), which have been shown to be distinct from that of the bulk sediment and water column (Jensen, Kühl and Priemé 2007; Garcias-Bonet *et al.* 2012; Cúcio *et al.* 2016; Fahimipour *et al.* 2016; Ettinger *et al.* 2017; Crump *et al.* 2018; Ugarelli, Laas and Stingl 2018; Hurtado-McCormick *et al.* 2019; Zheng *et al.* 2019). Microbes on the seagrass leaf, or phyllosphere (Lindow and Brandl 2003), are associated with their hosts via symbioses that involve potential consumption of host metabolic waste products, such as methanol (Crump *et al.* 2018), conversion of amino acid to inorganic nitrogen for seagrasses uptake (Tarquinio *et al.* 2018), enhancement of seagrass growth via the production of phytohormones (Celdrán *et al.* 2012), and inhibition of pathogens through competitive exclusion or direct antagonism (Wilkins *et al.* 2019). Additionally, microbes associated with seagrass roots and rhizospheres can increase nutrient availability through nitrogen fixation (Welsh 2000; Garcias-Bonet *et al.* 2016; Crump *et al.* 2018). These microbes also metabolize detritus and seagrass-derived carbon

(Kaldy *et al.* 2006), and cycle sulfur mainly through sulfate reduction and sulfide oxidation (Isaksen and Finster 1996; Jensen, Kühl and Priemé 2007; Cúcio *et al.* 2016, 2018).

Global change and anthropogenic stresses will leave lasting impacts on oceans and marine life in the next century (Doney *et al.* 2012, 2020). These environmental changes include eutrophication, coastal anoxia, ocean acidification, and changes in sea water temperature and upwelling (Doney *et al.* 2012), which will negatively affect marine organisms and perturb global biogeochemical cycles (Gruber 2011). Corals and seagrasses experience these stressors in part due to human development and runoff, harmful fishing practices, and intensified storm surge (Norström *et al.* 2016; Sherman and DeBruyckere 2018). The individual and synergistic effects of these stressors on marine habitats are leading to global declines of coral reefs and seagrass meadows (Waycott *et al.* 2009; Hughes *et al.* 2017).

Environmental stressors can trigger responses in marine host associated microbiomes, which can disrupt symbiotic relationships and impact host responses to environmental stressors (Apprill 2017). For example, the composition and function of the sponge microbiome can be largely disrupted under temperature and pH stress (Hentschel *et al.* 2012; Botté *et al.* 2019). Environmental stress such as heat waves, ocean acidification (OA), sedimentation, pH stress, and eutrophication can all have negative effects on the coral holobiont (Vega Thurber *et al.* 2009; Bourne, Morrow and Webster 2016; McDevitt-Irwin *et al.* 2017). Corals exposed to these stressors experience shifts in the microbiome from beneficial microbes to opportunistic and pathogenic microbes usually found in diseased corals, and shifts in functional

potential towards genes associated with virulence and stress (Vega Thurber *et al.* 2009; Neave *et al.* 2016; Webster *et al.* 2016a; Biagi *et al.* 2020). Additionally, bleaching can shift the coral microbiome from a healthy community to one dominated by *Vibrio sp*., which is commonly associated with coral disease (Bourne *et al.* 2008; Munn 2015; van Oppen and Blackall 2019).

Less work has been done on the composition and function of seagrass microbiomes with respect to global change. Studies have directly measured microbe-driven biogeochemical activities in relation to environmental stress, such as changes in eutrophication and increased temperature (Kilminster and Garland 2009; George *et al.* 2020). Other studies have found that light limitation and pH stress enriches the seagrass microbiome for pathogenic microbes (Hassenrück *et al.* 2015; Martin *et al.* 2018a). Given the potential roles of the microbiome to seagrass ecosystem functioning and the lack of knowledge of seagrass microbiomes compared to other marine systems, it is important to further explore potential responses of the seagrass microbiome to environmental stressors.

In this dissertation, I characterize changes in the coral and seagrass microbiome in response to several key stressors, and link microbiome shifts to host health and biogeochemical cycling. In chapter 2, I characterize how the microbiomes of two coral species respond to eutrophication and thermal stress, and subsequent coral bleaching and disease. In chapters 3 and 4, I characterize how seagrass microbiomes respond to nutrient pollution and ocean acidification (OA), respectively. In light of global seagrass loss and restoration efforts, chapter 5 examines changes in the seagrass microbiome after transplanting with and without rhizosphere sediment.

This work contributes to the field of marine microbiomes by examining the effects of synergistic stressors on the coral microbiome, and by contributing towards achieving an understanding of the seagrass microbiome.

Increasing development and human settlement in coastal regions can lead to sedimentation, runoff, and pollution of shorelines (Smith *et al.* 2000). High nutrient inputs cause coastal eutrophication, which can lead to coral microbial dysbiosis, disease, and bleaching (Morrow *et al.* 2012; Vega Thurber *et al.* 2014; Ziegler *et al.* 2016). Interestingly, anthropogenic nitrogen and phosphorus inputs can cause disparate responses in corals (Ezzat *et al.* 2016; Shantz, Lemoine and Burkepile 2016). In addition to these nutrient stresses, thermal stress can also negatively affect corals, leading to coral bleaching, increases in microbial virulence (Gruber 2011; Doney *et al.* 2012), and coral dysbiosis (Bourne *et al.* 2008; Tout *et al.* 2015). The research presented in Chapter 2 used an *in situ* nutrient exposure experiment in the Florida Keys to characterize the individual effects of nitrogen and phosphorus on the health and associated microbiomes of Scleractinian corals *Agaricia sp.* and *Siderastrea siderea*. Concurrent to running this experiment, the Florida Keys experienced the warmest temperatures on record, followed by mass coral bleaching (Manzello 2015). Thus, this experiment presented the opportunity to break down individual and potentially additive or synergistic effects of nutrient pollution and heat stress on corals and their microbiomes.

Results of this experiment showed that individual nutrient inputs interacted differently with heat stress to cause bleaching in *Agaricia sp.* and Dark Spot Syndrome (DSS) in *Siderastrea siderea*. DSS causes brown lesions on corals, which

may not be lethal, but may increase susceptibility to bleaching. Nitrogen addition exacerbated bleaching severity and prevalence in *Agaricia* corals, and led to a slower recovery. Heat stress increased the prevalence of DSS in *S. siderea*, and phosphorus-treated individuals experienced the most severe disease symptoms. Metagenomes generated from *S. siderea* mucus samples showed that heat and nutrient stress correlate with changes in the composition and function of microbiomes. Alpha diversity of microbiomes increased across all nutrient treatments of *S. siderea* samples collected from September, one month after the peak of the heat wave. Alpha diversity was not affected by disease state, but was more variable in diseased microbiomes compared to healthy microbiomes. Most notably, genes for replication and repair were enriched in all months of the experiment (August, September, and October), compared to the start of the experiment in July. DSS-afflicted corals had distinct microbiomes from healthy corals, though there was no taxon correlated with DSS. In conclusion, the thermal anomaly and nutrient inputs interacted to cause bleaching and disease in *Agaricia sp*. and *S. siderea*, as well as disruptions of the *S. siderea* microbiome.

Eutrophication can also be harmful to seagrass populations (Short and Burdick 1996; Short and Wyllie-Echeverria 1996; Burkholder, Tomasko and Touchette 2007; Govers *et al.* 2014b). Increased nutrient inputs can lead to opportunistic algal blooms and light reduction, which can reduce seagrass growth and meadow size, and lead to plant death (Short, Burdick and Kaldy 1995; Ruiz and Romero 2001; Hauxwell, Cebrián and Valiela 2003; Schmidt *et al.* 2012). Some seagrass species do not possess nitrogen feedback mechanisms and can suffer from nitrogen toxicity under excess

nutrient concentrations (Burkholder, Mason and Glasgow 1992; van Katwijk *et al.* 1997). Additionally, eutrophication also can increase hydrogen sulfide concentrations in seagrass meadows (Govers *et al.* 2014a), a phytotoxin that negatively impacts seagrass survival (Holmer and Bondgaard 2001; Pedersen, Binzer and Borum 2004). Eutrophication can also stimulate seagrass microbial respiration, resulting in decreased residence times for carbon stored in seagrass meadows (Jiang *et al.* 2018). Depending on the environmental conditions, microbial activity within these communities may have large impacts on carbon storage, nutrient availability, and host health. Chapter 3 of this dissertation examines the effects of nutrient pollution on the seagrass *Zostera marina*, or eelgrass, and its associated microbiome. We predicted that nutrient enrichment would lead to eelgrass declines either via nitrogen toxicity or algal and epiphyte blooms, or both. Additionally, we hypothesized that the eelgrass microbiota shift via nutrient enrichment towards opportunistic and pathogenic microbes, and heterotrophic sulfur cycling bacteria.

The experiment for chapter 3 took place at in the Experimental Seawater Facility at Hatfield Marine Science Center (HMSC) in Newport, Oregon. Eelgrass shoots were collected from Yaquina Bay, Oregon, and transferred to mesocosm tanks. Fertilized mesocosms were enriched with Osmocote slow release fertilizer (a combination of nitrogen, phosphorus, and potassium). Nutrient concentration, eelgrass morphology, and microbiome composition were characterized over the course of four weeks. To examine microbial community changes, 16S amplicon sequencing data was generated from eelgrass compartments of leaves, roots, and rhizosphere, as well as from the water column and bulk sediment. Fertilized plants

retained higher number of leaves compared to ambient plants, and suffered no negative effects compared to ambient plants. Contrary to previous seagrass eutrophication studies, fertilization did not result in algal proliferation, suggesting that eutrophication leads to different ecosystem responses depending on site conditions, such as mixing and residence time of water. Eelgrass microbiomes were distinct across compartments and between eelgrass samples and environmental samples. The main fertilization effect on the eelgrass microbiome was seen in root-associated samples, which were enriched for nitrogen- and sulfur-associated bacteria. These results show that in future eutrophic conditions, sulfur cycling may be enhanced, and carbon stocks may be depleted at a faster rate due to nutrient stimulation of heterotrophic sulfur and nitrogen cycling bacteria.

In addition to eutrophication, another threat facing global oceans is ocean acidification (OA). Rising atmospheric CO_2 is absorbed by oceans, changing marine carbonate chemistry, reducing the availability of calcium carbonate and negatively affecting calcifying organisms such as fish, corals, calcifying algae, and molluscs (Kroeker *et al.* 2010; Gazeau *et al.* 2013; Doney *et al.* 2020). Increased bicarbonate concentrations in the ocean will also create unpredictable consequences for marine microbes, biogeochemical cycling, primary productivity and nitrogen fixation (Gruber 2011; O'Brien *et al.* 2016). Interestingly, seagrasses are hypothesized to thrive under OA conditions due to their ability to utilize CO_2 and bicarbonate for carbon fixation (Larkum *et al.* 2017; Doney *et al.* 2020), though some responses may vary (Apostolaki *et al.* 2014; Zayas-Santiago *et al.* 2020). Seagrasses grown under OA conditions have higher growth rates, C/N ratio, and density (Jiang, Huang and

Zhang 2010; Garrard *et al.* 2014; Hernán *et al.* 2016), though these rates can plateau after an acclimation period (Hall-Spencer *et al.* 2008; Hernán *et al.* 2016). Expanding seagrass meadows and productivity could produce more niche habitats for local fauna (Garrard *et al.* 2014), buffer negative side effects of ocean acidification such as low pH through primary productivity (Su *et al.* 2020a), and enhance blue carbon deposition within seagrass meadows (Garrard and Beaumont 2014). Due to the positive response of seagrass productivity to OA conditions, we hypothesized that this increased productivity would support the seagrass microbiome via exudation of excess photosynthates. We also predicted that increased availability of CO_2 and seagrass-derived carbon would lead to nitrogen and phosphorus limitations in acidified conditions. Chapter 4 of this dissertation examines the differences in the microbial community and functional potential of the seagrass species *Posidonia oceanica* under OA and ambient conditions.

For this study, *P. oceanica* leaf samples were collected from ambient and acidified waters near naturally occurring volcanic CO_2 vents in Ischia, Italy. Water at the ambient site (S1) had a pH of 8.08, while sites (S2, S3) in acidified areas had pH measurements of 7.75 and 6.59. Previous reports of this area found the highest level of seagrass productivity (measured as shoot density) at acidified sites along with significant loss of coralline algae (Hall-Spencer *et al.* 2008; Martin *et al.* 2008). This natural acidified gradient allowed us to study changes of the *P. oceanica* microbiome as a result of long-term acclimation to naturally high pCO_2 and low pH conditions. Initial analysis of the 16S amplicon sequencing data of the *P. oceanica* leaf microbiome saw no difference between the intermediate and low pH sites (S2 and

S3), but communities in both of these sites were different than those found on seagrass leaves from the ambient pH site (S1). Ambient leaf microbiomes were enriched with *Granulosicoccus sp.*, *Jannaschia sp.*, unclassified Gammaproteobacteria species, and the cyanobacteria *Chroococcciopsis* PCC-6712. Acidified leaf microbiomes were enriched in *Vibrio sp.*, Gammaproteobacteria species, *Endozoicomonas sp.* within the Oceanospirillales order, and unclassified Hyphomicrobiaceae. To characterize the differences in microbial functional potential between sites, metagenome samples were generated from 3 replicates taken from sites S1 and S3. Most notably, genes for starch and sucrose metabolism were enriched in acidified metagenomes, while genes for ABC transporters and carbon fixation were enriched in ambient samples. These results provide evidence for differential microbial life strategies amongst the leaf microbiome within the two conditions, in which the ambient microbiome may be relatively nutrient limited and enriched for microbial autotrophs. Conversely, acidified microbiomes appear to be enriched microbial heterotrophs, that may use over-produced seagrass-derived metabolites, such as sucrose. These results indicate that the microbiome under acidified conditions may be more reliant on seagrass-derived carbon, shedding light on the shifting relationship between microbes and seagrasses under future OA conditions.

Chapter 5 of this dissertation explores the effects of transplantation on the seagrass microbiome. Seagrass meadows can be restored to their previous structure and community functions (Thom *et al.* 2008; Aoki and McGlathery 2018) through a variety of methods including transplanting of bare roots or sod transplants, which include the intact root sediment (Boyer and Wyllie-Echeverria 2010). Historically,

sod transplants have had higher rates of success compared to bare root transplants (Boyer and Wyllie-Echeverria 2010). We hypothesized that this discrepancy may be in part due to the role of the rhizosphere, or the microbial community associated with plant roots, which may promote plant health by alleviating abiotic stressors, promoting root development, altering root formation via phytohormones, and increasing soil fertility via nitrogen fixation (Yang, Kloepper and Ryu 2009a; Turner, James and Poole 2013). The undisturbed and intact sediment surrounding the eelgrass root in sod transplants allows microbes in the rhizosphere to function uninterruptedly, while the bare root transplants, which lack a rhizosphere, may experience a lag in rhizosphere function while it redevelops. Plant roots may recruit microbes in part via labile organic compounds in the form of root exuded photosynthates, including amino acids, sugars, vitamins, and oxygen (Donnelly and Herbert 1998), facilitating an organic-rich environment containing an active microbial community. Here, we hypothesized that eelgrass transplanted with an intact rhizosphere will grow more robustly compared to eelgrass transplanted with a disrupted rhizosphere. Additionally, we aimed to shed light on microbial succession and recruitment of the eelgrass root and rhizosphere microbiome.

To conduct this experiment, eelgrass plants were collected from Yaquina Bay, with and without an intact rhizosphere, and individually planted within PVC containers in an outdoor mesocosm at HMSC. Plants were measured for morphological characteristics and development of the rhizosphere and root microbial communities over the course of the 4-week experiment. Transplants without an intact rhizosphere (wash treatments) initially possessed distinct belowground microbiomes

from those with an intact rhizosphere (sod treatments). Microbiome of washed plants recovered to match that of the sod transplants within 14 days, which also coincided with changes in the rhizosphere sediment mass, and root biomass. Notably, carbon- and sulfur-cycling bacteria, such as Sulfurovaceae and Ruminococcaceae, showed similar successional patterns in both rhizosphere and root samples, where relative abundances were low in wash treatments at the beginning of the experiment, but gradually increased in relative abundance towards the end of the experiment. The results of this experiment showed that seagrasses and their microbiomes are resilient to transplantation stress under these conditions. However, rhizosphere and root disturbance in the first few weeks post transplantation may affect initial eelgrass establishment in the field, potentially having implications on long-term success.

Changing ocean conditions will impact marine animals, plants, microbes, and the ecosystem services provided by these ecologically and economically important organisms. The collective chapters of this dissertation shed light onto how the microbiome of two vital ecosystem engineers, corals and seagrasses, will respond to environmental stressors such as eutrophication, warming, and ocean acidification. Chapter 2 examined the microbiome responses of two coral species to heat stress and eutrophication, and showed that these two stressors have interactive effects on both bleaching and disease. Chapter 3 presents the first study to examine the microbiome responses to eutrophication in the seagrass *Zostera marina*. These results show that though effects of eutrophication may not be seen in plant morphological traits, belowground microbial metabolism may be stimulated by nutrient inputs, providing implications for sulfide and carbon concentrations in seagrass meadows under future

ocean conditions. Chapter 4 examines the effects of OA conditions on the leaf microbiome of *Posidonia oceanica,* showing that increased pCO_2 has significant effects on the metabolic potential of the *P. oceanica* microbiome, implying that OA can affect the strength of the mutualism between host and microbiota. Chapter 5 characterizes the succession of the *Zostera marina* root and rhizosphere microbiome after transplantation disturbance. Results show that the seagrass microbiomes are resilient to transplantation, and revealed important taxa associated with the core *Z. marina* belowground microbiome. These studies contribute to the growing field of seagrass microbiome research by providing the first study characterizing the eelgrass microbiome composition responses to nutrient pollution, expanding upon the effects of OA conditions on the seagrass leaf microbiome, and providing the first study characterizing seagrass rhizosphere microbiome successional dynamics. These studies also attempted to link stressors and microbiome changes to plant health, as well as linking combined stressors to coral health. These observational studies yield hypotheses for future studies, including identification of promising mutualistic taxa within seagrass microbiomes. Future work can characterize the range of these taxa amongst seagrass species and marine macrophytes, as well as determining the mechanism of mutualism through cultivation and inoculation studies. Additionally, many of the conclusions for this dissertation reference seagrass exudation, which should be measured in future studies. Lastly, future studies should look at synergistic effects of multiple stressors on seagrasses and their microbiomes, as these conditions may most realistically align with future conditions.

2 Corals and their microbiomes are differentially affected by exposure to elevated nutrients and a natural thermal anomaly

Lu Wang

Andrew A. Shantz

Jérôme P. Payet

Thomas J. Sharpton

Amelia Foster

Deron E. Burkepile

Rebecca Vega Thurber

Published: March 2018 (doi: 10.3389/fmars.2018.00101)

Frontiers in Marine Science

Avenue du Tribunal Fédéral 34, CH – 1005 Lausanne Switzerland

Vol. 5

2.1 Abstract

Nutrient pollution can increase the prevalence and severity of coral disease and bleaching in ambient temperature conditions or during experimental thermal challenge. However, there have been few opportunities to study the effects of nutrient pollution during natural thermal anomalies. Here we present results from an experiment conducted during the 2014 bleaching event in the Florida Keys, USA, that exposed *Agaricia* sp. (Undaria) and *Siderastrea siderea* corals to 3 types of elevated nutrients: nitrogen alone, phosphorous alone, and the combination of nitrogen and phosphorus. Overall, bleaching prevalence and severity was high regardless of treatment, but nitrogen enrichment alone both prolonged bleaching and increased coral mortality in *Agaricia* corals. At the same time, the elevated temperatures increased the prevalence of Dark Spot Syndrome (DSS), a disease typically associated with cold temperatures in *Siderastrea siderea* corals. However, nutrient exposure alone did not increase the prevalence or severity of disease, suggesting that thermal stress overwhelms the effects of nutrient pollution on this disease during such an extreme thermal event. Analysis of 78 *Siderastrea siderea* microbial metagenomes also showed that the thermal event was correlated with significant shifts in the composition and function of the associated microbiomes, and corals with DSS had microbiomes distinct from apparently healthy corals. In particular, we identified shifts in viral, archaeal, and fungal families. These shifts were likely driven by the extreme temperatures or other environmental co-variates occurring during the 2014 bleaching event. However, no microbial taxa were correlated with signs of DSS. Furthermore, although nutrient exposure did not affect microbial alpha diversity, it did significantly

affect microbiome beta-diversity, an effect that was independent of time. These results suggest that strong thermal anomalies and local nutrient pollution both interact and act independently to alter coral health in a variety of ways, that ultimately contribute to disease, bleaching, and mortality of reefs in the Florida Keys.

2.2 Introduction

Ocean warming and coastal pollution are two of the most widespread threats to coral reefs. Increases in sea surface temperatures of just a few degrees can exceed the thermal tolerance of many tropical corals, causing coral bleaching and warm-water associated epizootics that together threaten up to one-third of all coral species (Carpenter *et al.* 2008). Although it has been widely publicized that the frequency of coral bleaching will increase over the coming century (Magris, Heron and Pressey 2015; Hooidonk *et al.* 2016), increasing frequency and severity of coral diseases may pose a greater threat to reefs than bleaching events (Maynard *et al.* 2015). At the same time, nutrient enrichment in nearshore waters is one of the major anthropogenic forces altering coastal ecosystems (Halpern *et al.* 2008) and can drive the increased prevalence of coral diseases and bleaching on reefs worldwide (Vega Thurber *et al.* 2014; Maynard *et al.* 2015). For example, field surveys suggest that the prevalence of coral disease is often correlated with nutrient concentrations (Haapkylä *et al.* 2011; Kaczmarsky and Richardson 2011).

While the effects of coastal nutrient pollution on bleaching tolerance and disease have garnered a great deal of interest (Bruno *et al.* 2003; Wooldridge and Done 2009; Wagner, Kramer and van Woesik 2010; Vega Thurber *et al.* 2014; Wooldridge 2020), little is known about the interactions between nutrients,

temperature stress, and coral diseases. Troublingly, large increases in coastal nitrogen loading are projected to occur alongside ocean warming as a result of climate change (Sinha, Michalak and Balaji 2017), adding urgency to our need to understand the interactive effects of nutrients and temperature stress on coral health.

Nitrogen (primarily as nitrate) and phosphorus are two major nutrient pollutants in terrestrial run-off (Howarth 2008), and the effects of each of these nutrients on coral physiology are distinct. Enrichment with nitrogen causes *Symbiodinium* to rapidly proliferate (Hoegh-Guldberg and Smith 1989; Muscatine *et al.* 1989; Marubini and Davies 1996; Cunning and Baker 2013), disrupting the translocation of nutrients between *Symbiodinium* and their coral hosts, and thus compromising the animal's energy budget (Shantz, Lemoine and Burkepile 2016). Furthermore, nitrogen enrichment can result in limitation of other important nutrients. For example, nitrogen-induced phosphorus limitation is linked to reduced thermal tolerance in corals (Wiedenmann *et al.* 2013). Because the ability of corals to survive bleaching events is influenced by, among other things, a coral's energy reserves (Schoepf *et al.* 2015), nitrogen enrichment also reduces coral resilience in the face of bleaching events by jeopardizing coral energy budgets.

In contrast, surplus phosphorus increases stress tolerance in corals (Béraud *et al.* 2013; Wiedenmann *et al.* 2013). Under typical conditions, the impacts of phosphorus enrichment on coral physiology are small (Shantz and Burkepile 2014; Ferrier-Pagès *et al.* 2016). However, under thermal stress, phosphorus uptake rates increase because phosphorus is required to maintain symbiont density, photosynthesis, and carbon translocation (Ezzat *et al.* 2016). Thus, while coastal

pollution can impact coral physiology, the interactive effects of pollution and warming are likely mediated by the ratio of nitrogen:phosphorus delivered to the environment.

Less is known about the relative impacts of nitrogen and phosphorus on coral diseases, such as Dark Spot Syndrome (DSS) in scleractinian corals. DSS is one of the most common diseases of corals in the Florida Keys, representing 71% of all diseased corals and typically afflicting 26% of *Montastrea annularis* colonies and 8% of *Siderastrea siderea* colonies on most reefs (Porter *et al.* 2011). DSS is identified by darkened pigmentation of the coral tissue resulting in purple, black, or brown lesions that can either be circular or elongate (Weil 2004; Gochfeld, Olson and Slattery 2006). A necrotizing disease, DSS can cause affected tissues to die at a rate of 4.0 cm/month in *S. siderea* corals (Cervino *et al.* 2001). Though it is often not obviously deleterious to whole coral colonies, it is a known marker for more aggressive diseases such as Black Band Disease and Yellow Band Disease (Richardson 1998; Cervino *et al.* 2001). Additionally, DSS affected corals are more likely to bleach than their healthy counterparts (Brandt and McManus 2009).

Nutrient loading increases the severity of coral diseases (Bruno *et al.* 2003; Voss and Richardson 2006) and in some instances, may cause disease outbreaks. For example, Vega Thurber et al. (Vega Thurber *et al.* 2014) showed that combined nitrogen and phosphorus enrichment increased both the severity and frequency of DSS in *S. siderea*, an abundant coral on reefs in Florida. Substantial evidence exists showing that nutrient enrichment drives changes in the microbial communities associated with corals (Thompson *et al.* 2015; Zaneveld *et al.* 2016; Shaver *et al.*

2017), and these changes are often associated with increases in pathogenic bacteria and the appearance of disease signs (for review see, McDevitt-Irwin *et al.* 2017). However, the relative role of nitrogen vs. phosphorus in shaping disease susceptibility and the coral microbiome is currently underexplored. To date, we are not aware of any studies that have investigated how phosphorus modifies the susceptibility of corals to diseases.

In the summer of 2014, an anomalous thermal event occurred in the Florida Keys, providing the opportunity to study how nutrient pollution interacted with thermal stress to impact coral bleaching and disease. We evaluated how increases in two nutrients (nitrate and phosphate) separately and in combination can exacerbate the effects of thermal stress on coral disease and bleaching. To address this question, we exposed individuals of two species of corals, *Siderastrea siderea,* and *Agaricia sp*. (Undaria) in the field to nitrogen alone, phosphorus alone, and the combination of each, in addition to control corals with no nutrients, for 6 months while following the visual health of corals throughout the experiment. Furthermore, we evaluated the microbial ecology of the control and exposed corals before, during, and after nutrient enrichment and thermal stress.

2.3 Methods

2.3.1 Nutrient Enrichment Experimental Design

To evaluate the effects of nutrient enrichment on natural coral colonies, we conducted an *in situ* nutrient enrichment experiment at Pickles Reef (N24.99430, W80.40650) in the Florida Keys from July 14, 2014 to January 12, 2015 (Figure 2.1). Along two 30 m transects, approximately 20 m apart, at a depth of ca. 5–6 m, we

haphazardly selected 20 *Agaricia* sp. (Undaria) and 20 *Siderastrea siderea* colonies at least 10 cm^2 in area and visually deemed to be in good health. Individual coral colonies were randomly assigned to a nutrient treatment with either (1) nitrogen and phosphorus, (2) nitrogen, (3) phosphorus, or (4) left untreated to serve as controls, with five replicates per treatment.

To achieve our enrichments, we deployed nutrient diffusers constructed from PVC pipes with holes drilled throughout that were filled with either slow-release nitrate (150 g, 12% NO_3), phosphate (45 g, 40% PO_4), or both, and wrapped in mesh as described in Zaneveld et al. (Zaneveld *et al.* 2016, Figure S2.1). We stationed each nutrient diffuser 10 cm from the target coral, and replaced the fertilizer monthly. We have successfully used this method in the past to enrich sections of the reef (Vega Thurber *et al.* 2014; Zaneveld *et al.* 2016). Water column NO_3 and PO_4 concentrations collected near the diffusers 24 h after deployment were ca. 4.5- and 2.4-fold higher in N and P respectively than concentrations at control sites (3.18μM NO_3 and 0.34 μM PO_4 vs. 0.71 μM NO_3 and 0.14 μM PO_4). Per previous experiments, the nutrients from these apparatuses were shown to diffuse within approximately 1m from the experimental area.

2.3.2 Disease and Bleaching Surveys

From July 2014 to January 2015, corals were surveyed monthly by SCUBA to track changes in their health throughout the course of the experiment (Supplementary Table 2.1). For each coral, divers recorded whether bleaching or disease symptoms were visually present and photographed the coral from a fixed position with an object of known length. Using ImageJ (v1.50), we analyzed photos from each monthly

survey to estimate the total surface area of each coral, as well as the area of each colony afflicted by disease or bleaching (Abramoff, Magalhaes and Ram 2004). A portion of a coral was considered bleached when it no longer retained any pigmentation and the white coral skeleton was visible through the tissue. Bleached or diseased areas were divided by total surface area to calculate the percentage of the total colony surface afflicted as measures for disease and bleaching severity. In addition, tissue mortality was estimated from each coral by comparing the area of live tissue on each coral with the coral's initial live tissue area from our pre-treatment surveys. At the end of our final round of surveys in January, we also estimated bleaching recovery as the proportion of bleached tissue that had regained pigmentation. Although we recorded both bleaching and disease measurements for both coral species, here we only report measurements of DSS in *S. siderea* and bleaching in *Agaricia* sp.; only a single colony of *Agaricia* sp. ever showed disease, and only a single *S. siderea* colony showed signs of bleaching (data not shown).

2.3.3 Coral Mucus and Seawater Sampling

Coral mucus from each colony, as well as seawater samples, were collected by divers at four time points to generate microbial metagenomes. A pretreatment sample was collected in July of 2014, followed by monthly samples in August, September, and October. To investigate the role of microbes and viruses in the etiology of DSS, metagenomes were only made for the *Siderastrea siderea* corals. *Agaricia* sp. (Undaria) mucus samples were not explored using metagenomes due to the high mortality rate of our *Agarcia* specimen that ultimately resulted in low replication over time and treatment.

Surface coral mucus was collected by gently agitating the colony surface with a sterile syringe, as detailed in Zaneveld et al. (Zaneveld *et al.* 2016). Specifically, on all corals, we agitated the top of the animal, collecting mucus across the entire surface. We chose to sample mucus due to the benign effect of sampling upon the coral, and due to its role in providing a barrier for the coral from pathogens (Zaneveld *et al.* 2016). Mucus samples were brought back to the boat, where they were transferred into sterile 15 mL falcon tubes, immediately frozen on dry-ice for transport, and then stored at −80°C prior to nucleic acid extraction. Seawater samples were collected in duplicate 50 mL falcon tubes from 1 m above each transect and stored frozen as described above.

We also used mucus samples from a previous enrichment experiment (Zaneveld *et al.* 2016) to generate comparative *S. sideraea* metagenomes from corals growing under normal temperature conditions. In August of 2012, 25 apparently healthy and 25 DSS afflicted corals were selected from within control and nutrient enriched plots. In this enrichment experiment, only combined nitrogen and phosphorus was used to mimic nutrient pollution (for details see Vega Thurber *et al.* 2014). Mucus samples were collected in the same manner as described above and processed in the exact same manner for metagenome generation and analysis as described below.

2.3.4 Microbial Metagenome Library Generation and Sequencing

Thawed mucus and seawater samples were pre-filtered through 5.0μm pore-size EMD Millipore Millex (Millipore) syringe filters to remove larger particles. Viral and microbial size- particles from resulting filtrates were further concentrated using

the 30 kDa cutoff Amicon Ultra-15 centrifugal filter units (Millipore). DNA from microbial concentrates was then extracted using the MasterPure Complete DNA purification kit (Epicenter, Illumina). Purified DNA extracts served as input for the NexteraXT DNA library preparation (Illumina) to generate multiplexed metagenome libraries for high-throughput sequencing, following the manufacturer's recommendations. Multiplexed sample libraries were cleaned using AMPure XP magnetic beads (Agencourt) and checked for quality and size distribution on a Bioanalyzer 2100 (Agilent), prior to being pooled in equimolar concentrations for sequencing. Whole genome shotgun sequencing was conducted on the HiSeq2000 platform (Illumina) at the CGRB facility at the Oregon State University, yielding 2 × 100 bp long paired-end reads. This approach resulted in 86 metagenomes including 6 seawater samples, and 80 coral metagenomes that spanned 4 time points, 4 treatments, and 5 replicate colonies per treatment (Table S2.2). Two metagenomes were removed from the analysis due to their low number of reads and one seawater sample from August and one seawater sample from September were lost during shipment. The resulting 84 metagenomes had an average of 4,753,686 reads, with about 77% of reads remaining after quality-control. These metagenomes are freely and publicly available online at the Sequence Read Archive (SRA; #SRP133535 for the 2014 metagenomes and #SRP133699 for the 2012 metagenomes) and our own websites:

http://files. cgrb.oregonstate.edu/Thurber_Lab/NOAA_SSids/, and

http:// files.cgrb.oregonstate.edu/Thurber_Lab/DSS/.

2.3.5 Bioinformatic Analyses of Metagenomic Data

We used the program Shotcleaner (https://github.com/sharpton/shotcleaner) to filter out host and symbiont sequences and low- quality reads with quality scores below 25. This program also trimmed Illumina adapters and combined duplicate sequences. Shotcleaner is a workflow program that integrates an ensemble of programs such as Trimmomatic v0.35 (Bolger, Lohse and Usadel 2014), Bowtie2v 2.3.2 (Langmead and Salzberg 2012), and FastQC (Andrews 2010). For this analysis, the coral, *Acropora digitifera* (RefSeq NW_015441057.1) was used as the reference host, because the *Siderastrea siderea* genome was not currently available. Sequences from the coral endosymbiont *Symbiodinium* were filtered out using the *Symbiodinium minutum* genome (GenBank DF242864.1). Host and symbiont genomic reads were filtered out using Bowtie2, which aligned the metagenome reads to the host and symbiont genomes. Bowtie2 was run using default "end-to-end" parameters set to "-sensitive." In short, both the read and its reverse complement were aligned end-to-end to the host and symbiont genomes. Mismatch penalties ranged from a minimum of 2 and a maximum of 6, depending on the quality value of the read character. A lower quality score would lead to a lower penalty to the overall alignment score in the case of a mismatch. Gap penalties were 5 to open a gap, and 3 for a gap extension, for both the read and reference sequences.

We used the program Kraken (v.0.10.5) to conduct taxonomic assignment of the filtered metagenomics reads (Wood and Salzberg 2014). Paired-end reads were analyzed using the "- -paired" option, which concatenates the pair and increases classification sensitivity (Wood and Salzberg 2014). Then a custom MiniKraken database was built, comprising all Archaea, Bacteria, Fungi, Protozoans and Viruses

RefSeq released genomes, using the k-mer length of 25. The resulting database contained all k-mers and the lowest common ancestor of genomes that possess any particular k-mer. Annotations were made by alignment of metagenomic reads to k-mers in the database. The Kraken output was then transformed into a taxonomy table using kraken-translate, with the option "--mpa- format."

We also used the program ShotMAP for functional annotations (Nayfach *et al.* 2015). ShotMAP utilizes Prodigal (https://doi.org/10.1186/1471- 2105- 11- 119) to predict genes in unassembled shotgun reads *ab initio* and compares the predicted protein coding sequences against a protein family database using alignment algorithms. For this analysis, KEGG (release 73.1) was used as the reference database (Kanehisa *et al.* 2016). ShotMAP was run using the option "–ags-method none," as the genome size estimation tool was not compatible with this dataset. ShotMAP outputs for all 85 metagenomes were combined using compare_shotmap_samples.pl. ShotMAP outputs were sorted by KEGG identification numbers and grouped via KEGG BRITE functional hierarchies to level B (excluding the categories drug development, human diseases, and organismal systems). Given that KEGG ID numbers are often associated with multiple pathways, we weighted KEGG IDs based on the number of pathways in which they were assigned. For each sample, we calculated the average count of all instances in which a pathway is associated with a KEGG ID (average count of unique KEGG IDs). We also took the sum of these averages for each KEGG ID. Then, we took the ratio of the average count of unique KEGG IDs and the sum of the average count of unique KEGG IDs. This ratio determines which pathways are more abundant in the metagenomes, relative to all

other pathways that also were assigned to that KEGG ID. This approach therefore results in a ratio that determines how well-represented a pathway is relative to other pathways associated with that KEGG ID in the sampling environment. The unique average count/sum of unique average count ratios for each KEGG pathway were used for all subsequent analysis and statistics.

2.3.6 Statistical Analyses for Environmental and Metagenomic Data

Comparisons of mean monthly temperature data from the NOAA Molasses Buoy (a station approximately 5 km from the experimental site) in the Upper Florida Keys were performed using a Kruskal-Wallis and Dunn's *post-hoc* test in SigmaPlot Version 11 (Table S2.3). Differences in bleaching and disease prevalence were analyzed using generalized linear mixed models with a binomial distribution and logit link function in the lme4 package (Bates *et al.* 2015) in R (R Core Team 2018). To assess significance, fitted models were tested against a null model that included only time and the random colony effect via likelihood ratio tests.

We analyzed the effects of enrichment on bleaching and disease severity using mixed-effects models. For these models, we used the logit-transformed severity scores as the response variable and included nitrogen, phosphorus, and date as interacting fixed factors and a random effect for coral colony. When significant effects were present, we conducted Tukey's *post- hoc* analyses using the glht() function in the multicomp package (Hothorn, Bretz and Westfall 2008). Treatment and time were considered fixed effects, and a random effect was included for coral colonies. For analyses of bleaching and disease prevalence and severity, we excluded July data points, as July was the start of the experiment and corals were deliberately

selected to have no signs of disease or bleaching. Additionally, we used data from our final surveys to test for differences in the recovery of bleached tissue and tissue mortality using two-factor ANOVA that included nitrogen and phosphorus enrichments as interacting factors. Both the recovery and mortality data were logit transformed to meet assumptions of parametric statistics.

Prior to statistical analysis, we first normalized metagenomic taxonomic raw results to relative abundance. Differences in taxonomic relative abundance between nutrient treatments and over time were tested using generalized linear mixed models using the lme4 package in R, with treatment and time as fixed effects, and individual corals as random effects (Bates *et al.* 2015). *Post-hoc* tests were conducted using the multicomp package in R (Hothorn, Bretz and Westfall 2008). Statistical analysis comparing relative abundance of functional pathways found in the metagenomes over time and among treatments were also done as described above. All metagenomic data graphs were visualized using ggplot2 (Wickham 2016).

We used the indicator species analysis function in Mothur v1.39.3 (Schloss *et al.* 2009) to generate microbial Operational Taxonomic Units (OTUs) indicative of the microbiome of apparently healthy or diseased *S. siderea*. We used the indicator() command with a shared OTU table and a design file containing the relevant metadata. An indicator value, ranging from 1 to 100, decides the indicator status of an OTU in a group of pre- determined sites or samples. The indicator value of an OTU is a calculation of its abundance and fidelity in a group of sites (how often the OTU is present in all sites of a group) (Dufrêne and Legendre 1997). Ten thousand random permutation of sites among groups tests the statistical significance of an OTU's

indicator species status. We used a cutoff indicator value of 30 to obtain the strongest indicators of any group. This threshold ensures that an OTU is present in over half of the samples in a group, and that its relative abundance in that group is at least 50% (Dufrêne and Legendre 1997).

To check for effects of time and treatment on microbial diversity indices, alpha and beta-diversity were measured for both time and treatment separately and together using the Phyloseq package in R, with the estimate_richness() function for Chao1 calculations, and the distance() function on normalized data for Bray-Curtis indices (McMurdie and Holmes 2013). Chao1 values were compared over time and between treatments using Kruskal-Wallis and Dunn's *post-hoc* test (Table S2.4). Bray-Curtis data were further analyzed using the Adonis function in the Vegan package in R, and *post-hoc* testing was performed using the RVAideMemoire package using pairwise.perm.manova(), which conducts pairwise tests on matrix data using Adonis (Hervé 2018; Oksanen *et al.* 2018).

2.4 Results

2.4.1 Time and Treatment Variably Affect *Agaricia* sp. Bleaching

In 2013–2014, the Florida Keys experienced the warmest winter and summer on record up to that date (Manzello 2015). These anomalously high temperatures were likely the main driver of the 2014 bleaching event as portions of the Florida Keys, including our study site, reached between 6 and 12 Degree Heating Weeks (NOAA and Coral Reef Watch and US Department of Commerce 2014; Barnes *et al.* 2015). Our experiment began on July 14th, 2014, just preceding the NOAA bleaching alert warning for the study area (Figure 2.1). The average hourly temperature on July

14th was 29.8°C. By August, the Upper Keys surpassed the thermal stress thresholds (max monthly mean sea surface temperature + 1°C) and significant bleaching occurred (Manzello 2015). During this time, the maximum mean monthly temperature at our site was 30.8 ± 1.1°C in August, with the warmest time point within our experimental time period falling on August 15th at 31.9°C (Figure 2.1). The mean daily temperature in August was significantly higher than all other months during metagenome sampling (Kruskal Wallis, $p < 0.05$).

The thermal stress event in 2014 induced severe bleaching in our *Agaricia* sp. corals (Figure 2.2). While no corals showed signs of bleaching in July, all corals began to bleach in August. By early September, 100% of the *Agaricia* sp. corals were bleached to some degree, regardless of nutrient treatment (Figure 2.2A). However, 4 months later, in January 2015, the control *Agaricia* sp. corals had mostly recovered with only 1 out of 5 control corals remaining bleached. In contrast, bleaching prevalence in surviving enriched corals remained between 50 and 66% depending on the treatment, however, this effect was not statistically significant [$\chi^2_{(3)} = 1.475$, $p = 0.692$]. Similarly, we were unable to detect an impact of nutrients on bleaching severity in *Agaricia* sp., as upwards of 90% of the surface area of all colonies were bleached by September (Figure 2.2B). Interestingly, nitrogen tended to impede recovery of bleached coral tissue (Figure 2.2C), although differences were not statistically different from other nutrient treatments [$F_{(1, 15)} = 4.053$, $p = 0.06$]. Furthermore, reduced recovery in nitrogen only enriched corals coincided with increased mortality. By January, mean tissue loss for the control *Agaricia* was 67 ± 12% vs. 92.5 ± 3.2% of tissue lost in nitrogen alone exposed *Agaricia* (Figure 2.2D).

2.4.2 Thermal Stress Associated with Dark Spot Syndrome in *Siderastrea siderea*

Across all treatments, the average prevalence of DSS in the experimental corals increased from 0% in July, to >40% in August, and peaked at >60% by September (Figure 2.3A). All of the nitrogen alone and combined nitrogen and phosphorus treated corals exhibited signs of disease by September. By October, half of the diseased corals in the control treatments had recovered (e.g., 80% in September to 40% in October) while more than 60% of the nutrient-enriched corals showed signs of DSS from October until January, suggesting that, like bleaching, nutrient exposure prolongs disease signs (Figure 2.3A). Overall, while a trend existed, we again did not detect a significant effect of enrichment on DSS prevalence [$\chi^2_{(3)} = 6.25$, $p = 0.09$].

Throughout the experiment, disease severity was lowest in August (3.9%, $p < 0.001$) and highest in November (14.9%) and December (14.8%) (Figure 2.3B). Disease severity in November and December were statistically higher than in August ($p < 0.001$), September ($p = 0.02$, $p = 0.005$), and October ($p < 0.001$). Amongst treatments, disease severity again tended to be higher in the nutrient exposed corals, with the controls exhibiting the lowest mean disease severity (5.4%) compared to nitrogen alone (7.3%), phosphorus alone (12.1%), and nitrogen and phosphorus combined (17.2%) diseased tissue levels. However, despite a visual trend there were no statistical differences in disease severity among nutrient types.

To track how time, treatment, or the interaction shifted overall diversity metrics of the microbiome, we generated shotgun metagenomes for all of the *S. siderea* and compared the community structure and function among the different coral microbiomes. There was a significant change in microbial alpha diversity

metrics over time (Figure 2.4A). *Post-hoc* tests showed that alpha diversity differed between August and September ($p < 0.01$), September and October ($p < 0.01$), and July and October ($p = 0.01$). September samples, which had the highest amount of DSS recorded, had the highest overall alpha diversity, with an average Chao1 OTU index of ~5,277 ± 71.29 OTUs, compared to July (4,888 ± 203.44), August (4,420 ± 203.66), and October (4,130 ± 204.58) (Figure 2.4A). Nutrient exposure had no significant effect on alpha-diversity *(*$p > 0.01$, Figure 2.4A).

Although nutrients did not alter coral microbiome alpha diversity, nutrient enrichment did increase microbial beta- diversity, or sample to sample variation (Figure 2.4B; $p = 0.01$). As visualized on an ordination plot, control samples clustered together, while the phosphorus enriched samples were aligned along Axis 1, and the nitrogen enriched samples were aligned along Axis 2 (Figure 2.4B). *Post-hoc* tests showed significant differences between the combined nitrogen and phosphorus samples compared to control and nitrogen enriched samples ($p = 0.04$ & $p = 0.03$, respectively). Surprisingly there were no differences in beta-diversity over time (Adonis, $p = 0.11$), nor was there a significant interaction of time and nutrient treatments on beta-diversity (Adonis, $p = 0.96$).

2.4.3 *Siderastrea siderea* Microbiome Community Structure Shifts

In addition to alpha and beta-diversity analysis, we conducted metagenomics analysis to determine if different taxa, groups of taxa, or functions were differentially affected by time, treatment, or the interaction. Hierarchical taxonomic and functional analysis showed clear effects of time but few effects of nutrient addition on different individual or groups of microbial organisms (Table 2.1). Overall the mean number of

microbial and viral annotations within the coral metagenomes were: 3.66% Archaea, 21.19% Bacteria, 1.14% Virus, and 61.24% Eukarya (excluding the host and symbiont). Archaea were composed of 82.90% Euryarchaeota, 10.35% Crenarcheota, and 6.06% Thaumarcheota. The Bacteria were composed primarily of Proteobacteria (36.10%), Firmicutes (28.52%), Bacteroidetes (16.15%), Actinobacteria (4.19%), and Cyanobacteria (2.84%). The top five viral families consisted of *Myoviridae* (25.98%), *Siphoviridae* (9.26%), *Mimiviridae* (7.89%), *Baculoviridae* (7.61%), and *Poxviridae* (5.81%). Approximately half of all the Eukaryotic reads (32.11%) were assigned as Fungi, consisting of the following top five phyla: Ascomycota (75.22%), Basidiomycota (17.75%), Microsporidia (1.56%), Chytridiomycota (0.64%), and Entomophthoromycota (0.04%). An average of 12.75% of the metagenome reads were unclassified. While time significantly affected the composition of the microbiome, (see below) there were no significant differences at any taxonomic level in relative abundance of different taxonomic groups among nutrient treatments ($p > 0.01$; Figure S2.2).

2.4.4 Coral-Associated Viral Consortia Shift During Thermal Stress

Among the highest hierarchical categories, three taxonomic groups significantly changed with time: viruses, Archaea, and Fungi (Table 2.2). For example, viral annotations showed shifts in the early part of the coral collections, with September corals consisting of a significantly higher relative abundance of viral annotations compared to July ($p = 0.01$) and August ($p = 0.006$) (Figure 2.5). The relative abundance of viral reads went from 1.07% in July, to 1.24% in September, declining again to 1.12% in October. A large part of this increase in viral annotations

came from the order Caudovirales (dsDNA bacteriophages) which were significantly higher in September compared to July ($p = 0.005$) and August ($p = 0.03$) (Table 2.2). These September samples contained a higher abundance of annotations assigned to the family *Myoviridae* than July ($p = 0.002$) and August samples ($p = 0.007$) where they increased from ~25% in July and August to 29.34% in September (Table 2.2). Around 70% of the *Myoviridae* annotations were unclassified, while 23.11% were classified as T4-like viruses. In October, *Myoviridae* annotations decreased back to 25.58%, similar to those in July (23.61%) and August (23.73%) samples (Table 2.2). Of the eukaryotic viral families, only the *Poxviridae* were found to change over time. Annotations to these nucleocytoplasmic large DNA viruses were highest in July, but then decreased in relative abundance in September ($p = 0.03$) and October ($p = 0.013$).

2.4.5 Coral-Associated Archaea Shift in Abundance During Warming

Along with the viruses, there were shifts in the Archaea associated with the *Siderastraea* corals. At the class level, the Thermoplasmata had lower abundance in July (2.78%) than in August (2.91%; $p = 0.02$). In the case of Thermococci, the October metagenome contained higher relative abundance of 6.68% compared to 6.16% in July ($p < 0.001$) and 6.20% in September ($p = 0.02$). This class consisted solely of the order Thermococcales, and within that, the family Thermococcaceae. Additionally, the relative abundance of Desulfurococcaceae in July (1.38%) was lower than that in August (1.45%) ($p = 0.045$).

2.4.6 Coral-Associated Fungi Shift Across the Thermal Stress Event

Within the Eukaryotes there was a statistically significant change in fungal orders over time, with several orders of low relative abundance fungi becoming slightly more abundant in the October metagenomes. Agaricales, a Basidiomycota, had a relative abundance of 3.24% in August and increased to 3.33% in September ($p < 0.001$) and October ($p = 0.008$). Another Basidiomycota, the Tremellales, also had higher relative abundance in October, 1.62%, compared to August (1.57%; $p = 0.001$). The Sordariomycetes order, Magnaporthales, had a higher relative abundance of 1.30% in October compared to 1.25% in August ($p = 0.03$), and 1.25% in September ($p = 0.01$).

2.4.7 Indicator Species of Healthy Coral Microbiomes

We conducted indicator species analysis on healthy and diseased *S. siderea* microbial metagenome samples to find the taxa most indicative of either healthy or diseased states. The indicator species of apparently healthy *S. siderea* included solely fungi and viruses. Fungal indicators include *Olpidium brassicae*, an unclassified Entomophthoromycete, *Polychytrium aggregatum* in the order Polychytriales, and *Pluteus saupei*, in the order Agaricales. Fourteen virus families also showed up as indicator taxa in healthy *S. siderea* microbiomes. These include Astroviridae, Baculoviridae, two OTUs within Betaflexiviridae, Bromovoridae, Circoviridae, Closteroviridae, two OTUs within Geminiviridae, Nyamiviridae, two OTUs in Polyomaviridae, Potyviridae, Secoviridae, two OTUs within Siphoviridae, Tombusviridae, and two OTUs within Totiviridae. Interestingly, we found no taxa indicative of diseased *S. siderea* microbiomes.

2.4.8 Coral Microbiome Function is Altered During Thermal Stress

One advantage of metagenomes is the ability to quantify shifts in both the taxonomic structure of a microbiome as well as the functional potential of that community. Overall the functional potential of the coral microbiome showed the following distribution of classified functions: 9.77% Cellular Processes, 14.75% Environmental Information Processing, 24.23% Genetic Information Processing, and 51.25% Metabolism. We found that the functional potential of the coral microbiomes shifted across time but not with treatment (Table 2.3). Within the broadest hierarchical level, KEGG category 1, there was a higher abundance of genes for "genetic information processing" in October (24.75%) compared to July (23.91%; $p = 0.008$). This category houses the subcategories of "transcription," "translation," "folding," "sorting and degrading," and "replication and repair." Genes for "translation" were more abundant in October (9.51%) compared to July (9.29%) ($p = 0.02$), and genes for "replication and repair" were found to be lowest, at 6.76%, in July, compared to 6.92% in August ($p = 0.04$), 6.98% in September ($p < 0.001$), and 6.95% in October ($p < 0.001$).

In contrast, genes for "amino acid metabolism" were lower in October (9.05%) than July (9.66%) ($p = 0.03$) and September (9.89%) ($p = 0.04$) while genes for "metabolism of cofactors and vitamins" were also lower in October (6.62%) compared to July (6.84%) ($p = 0.02$). Lastly, genes for "xenobiotics biodegradation and metabolism" were more abundant in July (1.25%) and September (1.21%) compared to August (1.18%) ($p = 0.02$) and October (1.13%) ($p < 0.001$, $p = 0.01$).

Within the highest resolution KEGG categories, the subcategory "genetic information processing" showed that only a few genes increased in abundance over

time while many were reduced. For example, genes for “homologous recombination” were higher in October (1.52%) than in July (1.45%; $p < 0.001$) while “nucleotide excision repair” genes were more abundant in September (1.49%) than in October (1.36%; $p = 0.007$). But genes assigned to functional subcategories within “environmental information processing, cellular processes, and metabolism” tended to be more abundant in July compared to later months with “ABC transporter” genes higher in July (4.89%) than September (4.77%; $p = 0.001$) and October (4.81%; $p = 0.04$), and genes for the “two-component system” also being elevated in July (3.03%) compared to September (2.86%; $p = 0.001$). “Photosynthesis” genes were more abundant in July (0.26%) than in August (0.23%; $p = 0.008$), and genes for “alanine, aspartate, and glutamate metabolism” were higher in July (1.43%; $p = 0.007$) and September (1.46%; $p = 0.007$) compared to October (1.30%).

2.4.9 Thermal Stress Shifts the Microbiomes of DSS Afflicted Corals

Although there is no ascribed etiological agent responsible for DSS, by subdividing the data into corals with and without DSS, we found metagenomic evidence that corals experiencing DSS are unique microbiologically. Like nutrient exposure, DSS samples exhibited increased beta-diversity (Adonis, $p = 0.011$) compared to apparently healthy ones (Figure 2.6A). However, there was no significant difference in alpha diversity (Chao1 index) between DSS and non-DSS coral microbiomes (Welch’s *T*-test, $p = 0.24$). To test if the thermal stress event altered the microbiomes, we compared only the August 2014 DSS ($n = 10$) and apparently healthy samples ($n = 8$) to another metagenomic dataset ($n = 42$) from coral mucus collected in August 2012. The 2012 samples (23 DSS and 19 apparently

healthy) came from *S. siderea* corals that were either exposed to nutrient enrichment or control conditions. Compared to 2014, the 2012 samples were only experiencing moderate thermal stress (~6 DHW) (Zaneveld et al., 2016). The 2012 DSS and apparently healthy corals had indistinguishable microbiomes regardless of treatment and disease, and they clustered separately from the 2014 microbiome samples (Figure 2.6B, Adonis, $p \leq 0.001$).

2.5 Discussion

In 2014, corals in the Florida Keys experienced severe thermal stress of 6–12 degree heating weeks depending on location. We found that this thermal anomaly was associated with increased bleaching and disease alongside changes in the alpha diversity of the microbiome and distinct shifts in different groups of taxa associated with the corals, particularly fungi and viruses. Shifts in the function of the microbiomes were also correlated with time. Nutrient exposure, on the other hand, only caused clear shifts in beta-diversity of the microbiomes, a finding that was independent from time, and thus likely not a result of the thermal anomaly.

2.5.1 Nutrient Exposure May Prolong Temperature-Mediated Bleaching in *Agaricia* Corals

Nutrient exposed corals were more likely to remain bleached 5 months after thermal stress compared to control corals. Though all *Agaricia* spp. corals bleached after the thermal stress event in August, recovery trended in favor of the corals in ambient conditions (80% recovered), compared to the corals in nutrient- stressed conditions (less than 50% recovered) (Figure 2.2A). All corals experienced high bleaching severity after thermal stress in August, however, only control corals and corals exposed to phosphorus completely recovered by January; corals exposed to

nitrogen alone, or nitrogen and phosphorus did not fully recover by the end of the experiment (Figure 2.2B). Though not of statistical significance, likely due to our low replication within each category, these trends suggest that nitrogen and phosphorus behave in different ways to influence susceptibility and resilience to bleaching.

2.5.2 Coral Disease Linked to Thermal Stress

Disease prevalence in all *S. sideraea* corals (Figures 2.3A,B) went from 0% in July 2014 to ~80% within 2 months. DSS declined by October to 40% in the controls but remained steady at this level until January when we ended the experiment. This was a somewhat unexpected finding, because DSS generally peaks in the winter months, not the summer (Borger 2005; Gochfeld, Olson and Slattery 2006), although one other study found that DSS prevalence can increase with higher water temperatures (Gil-Agudelo and Garzón-Ferreira 2001). Interestingly, the prevalence of disease also remained above 50% from September to the conclusion of the experiment for all nutrient treatments, suggesting only in the presence of elevated nutrients during thermal events reduces coral resilience by prolonging disease and/or preventing recovery.

2.5.3 *Siderastrea siderea* Disease and Microbial Diversity

Diversity within the *S. siderea* microbiome changed significantly over time with alpha diversity peaking in September across all treatments. Interestingly, the September alpha diversity metrics also had low variability compared to samples from other months. In contrast to microbial alpha diversity, the beta diversity of the metagenomes varied with both nutrient treatment and disease status. In particular, we

found that beta-diversity in the combined nitrogen and phosphorus enriched corals differed from both the control and the nitrogen-treated corals.

Similarly, DSS-afflicted coral microbiomes were significantly different from healthy colonies, linking DSS with the coral microbiome, although it is unclear if this is a cause or an effect. Yet this difference in beta diversity in the microbiomes of stressed and diseased corals aligns with the Anna Karenina principle, which states that the microbiomes of stressed animals are usually in an unstable dysbiosis, due the host being unable to regulate its microbial community (Zaneveld, McMinds and Thurber 2017).

We used metagenomics instead of 16S analysis because we and others had previously found no correlation in microbial taxa shifts associated with DSS using 16S analysis (Borger 2005; Kellogg *et al.* 2014; Meyer *et al.* 2016). Using this approach, we again found no single taxon or groups of taxa that were associated with the disease. Yet in a study focusing on *Stephanocoenia intersepta*, the microbes of healthy and diseased patches of coral were characterized and found to differ among health states (Sweet *et al.* 2013). In DSS lesions, but absent in healthy tissue, four types of potentially pathogenic bacteria were identified (*Corynebacterium*, *Acinetobacter*, *Parvularculaceae,* and *Oscillatoria*) along with the pathogenic fungi, *Rhytisma acerinum*, implicating that DSS in *S. intersepta* is caused not by a single pathogen but rather by a collection of taxonomically diverse microbes (Sweet *et al.* 2013). More recently, the transmission of DSS between *S. siderea* individuals was also experimentally tested, but there was no evidence of direct or indirect (water-

borne) transmission of DSS symptoms, suggesting that DSS is not an infectious disease but rather a physiological one (Randall *et al.* 2016).

We analyzed two metagenomic datasets of apparently healthy and DSS afflicted *S. siderea* from two different years (2012 and 2014) that were significantly different in terms of the ambient conditions present. Our indicator species analysis showed a plethora of viral and fungal taxa associated with a healthy coral microbiome, but no indicator species was found for DSS-afflicted coral samples. This provides further evidence that there is likely no pathogen responsible for DSS, although these negative results could be due to the low power of our experiment design. However, given that we find increased beta-diversity in the DSS microbiomes, it is not surprising that we found no taxa or group of taxa that are exclusively associated or significantly elevated in DSS corals. These collective data contribute to the growing body of thought that the signs of this disease are likely manifestations of an alteration of host physiology as a response to severe temperatures and nutrient pollution, manifesting in increased instability of the microbiome.

2.5.4 Thermal Anomaly Associated with Taxonomic Functional Microbiome Shifts

Although there was no significant shift in microbial taxa from nutrient exposure, we did find shifts in certain virus, Archaea, and Fungi over time. Because changes in time and temperature in this experiment were inherently connected, we hypothesize that these taxonomic shifts were directly related to changes in seawater temperatures or some covariate(s). We found a higher proportion of the virus order Caudovirales in September metagenomes compared to other months. Phages targeting

bacteria and archaea are the most abundant viral types found in scleractinian corals (Vega Thurber *et al.* 2017). These phages are thought to be crucial in shaping the coral microbiome and controlling microbial populations. Phages serve as a lytic barrier against potential pathogens (Sweet and Bythell 2017) and have been described as non-host-derived immunity (Barr *et al.* 2013). The viral order Caudivirales has consistently been found in coral viromes (Wood-Charlson *et al.* 2015; Vega Thurber *et al.* 2017; Weynberg *et al.* 2017), with its top three families being *Siphoviridae*, *Podoviridae*, and *Myoviridae*. Most of the Caudovirales reads from this experiment were assigned to the *Myoviridae* family, which consisted mainly of T4-like viruses. The abundance of these lytic phages suggests a high turnover of the microbial community, and may also have obscured any shifts in the bacterial community, including any potential pathogens.

The family *Poxviridae* had a higher relative abundance in July, the start of the experiment, compared to September and October, but there was no dominating viral genus within this family. Members of *Poxviridae* infect insects and terrestrial vertebrates such as humans and birds, but have also been found in dolphins, whales, and sea lions (Bracht *et al.* 2006). Marine *Poxviridae* often make up the top five viral families found in coral viromes (Vega Thurber *et al.* 2017; Weynberg *et al.* 2017). These eukaryotic viruses either infect the coral host or eukaryotic members of the microbiome, yet this taxon tends to be more abundant in healthy coral viromes compared to diseased or bleached viromes (Vega Thurber *et al.* 2017), which may explain the decline of the relative abundance of *Poxviridae* in *S. siderea* metagenomes as thermal stress increased and coral health declined. Interestingly,

neither *Myoviridae* nor *Poxviridae* were identified as indicator species for a healthy *S. siderea* microbiome. However, the plethora of viral OTUs found to be indicative of the microbiome of a healthy coral host show the importance of viruses in shaping the coral-associated microbial community.

The Archaeal members of the *S. siderea* holobiont consisted mainly of Crenarchaeota and Euryarchaeota. While they are not known to form species-specific symbioses with their coral host, they are hypothesized to participate in nutrient cycling (Wegley *et al.* 2004). For example, it is hypothesized that the Crenarchaeota cycle nitrogen via ammonia oxidation (Siboni *et al.* 2008). In this study, we did not find any correlation between Archaeal communities and nutrient exposure. Instead, we found three Archaeal members of the microbiome to shift across time. Both the Euryarchaeota, Thermoplasmata, and the Crenarchaeota, Desulfurococcaceae, had higher relative abundance in August, when seawater temperature reached its peak.

Fungi, particularly endolithic fungi, have long been acknowledged as endemic members of the scleractinian coral holobiont (Bentis, Kaufman and Golubic 2000; Ainsworth, Fordyce and Camp 2017). Though most marine fungi are thought to be opportunistic, with the exception of *Aspergillus sydowii*, the confirmed pathogen of Caribbean sea fans (Smith *et al.* 1996), the role of endolithic fungi in coral tissue has yet to be confirmed. These fungi are hypothesized to participate in nutrient cycling by participating in symbiotic relationships with nitrogen-fixing bacteria. One early metagenome study of the *Porites astreoides* holobiont found fungal reads to make up the majority of classified eukaryotic sequence sequences (Wegley *et al.* 2007). Most of these fungal reads consisted of Ascomycota, which are in many healthy coral

holobionts (Wegley *et al.* 2007). Similarly, Ascomycota made up 75% of the fungal reads in this study. Ascomycetes also dominated the fungal community in another coral metagenome study of the *Porites compressa* holobiont (Vega Thurber *et al.* 2009), but in that study, nutrient enrichment did not affect the composition of the fungal community. Again, we saw the same result in this study, in which certain fungal orders shifted with time and temperature, but not with nutrient addition. Other hypothesized roles of these fungi include competition with algal members of the holobiont, contribution to coral resistance to disease and bleaching, and parasitism upon the coral host (Yarden 2014; Ainsworth, Fordyce and Camp 2017). In this study, we found an Entomophthoromycete, a Chytridiomycete, and an Agaricomycete as fungal indicator species of healthy *S. siderea*, showing that at least some fungal species exist in either a commensal or mutualistic relationship with the coral host.

Functional analysis of the *S. siderea* microbial metagenome showed several contrasts between the start of the nutrient enrichment experiment in July, and the end of metagenome sampling in October. Prior to the bleaching event there was a higher relative abundance of genes for metabolism of cofactors and vitamins, and metabolism of amino acids—in particular alanine, aspartate, and glutamate. Additionally, prior to the thermal stress there was a higher relative abundance of photosynthesis genes (compared to August), two-component system genes (compared to September), ABC transporter genes (compared to September and October), and genes for xenobiotics biodegradation and metabolism (compared to August and October).

In contrast, microbial metagenomes of the latter months showed distinct functional potential. This manifested in the higher abundance of genes in October metagenomes for translation, replication and repair, homologous recombination, and a higher abundance of genes for nucleotide excision repair in September. The elevation of these genes categories could be interpreted as a shift in the community to more stress resistant taxa as a result of the thermal anomaly.

2.6 Conclusions

We conducted an *in situ* nutrient enrichment experiment in the Upper Florida Keys on *Agaricia* sp. and *Siderastrea siderea* corals in 2014, which coincided with a bleaching event due to a thermal anomaly. These unique environmental conditions allowed us to study the effects of high temperature and nutrient pollution on these corals. Elevated temperatures resulted in higher bleaching prevalence and severity of *Agaricia* sp. regardless of nutrient treatment and resulted in higher disease prevalence and severity in *Siderastrea siderea*. In the *Siderastrea siderea* metagenomes, there were several shifts in viral, archaeal, and fungal families across sampling time points, most notably a severe increase in the *Myoviridae* viruses associated with the aftermath of the thermal anomaly. Interestingly, we found no microbial taxa correlated with DSS.

2.7 Experimental Design Considerations and Future Work

Due to the low number of replicates in each coral category, there was a likelihood of Type II errors (false negatives). For example, many statistical tests failed to meet the standard *p*- value requirements after multiple corrections tests, especially since many animals died during the experiment. Trends in our data are thus

likely suggestive of important patterns that should be tested and confirmed in the future. Repeat experiments with a higher number of replicates are suggested to provide better statistical power. Additionally, we acknowledge that many of our statistically significant results show shifts in the relative abundance of taxonomic or functional assignments of less than 3%. Whether these shifts are biologically significant and meaningful is debatable. However, for some groups, even small changes that occur in the background of host and symbiont genetic information is likely to be biologically important. In particular, viral genomes are typically many orders of magnitude shorter in length than bacterial or eukaryotic genomes, thus they make up a very small percentage of any host associated metagenome. Additionally, in other systems, it is well established that presence and absence of rare taxa have been found to be significant due to potentially high metabolic activity of low abundance bacteria and fungi members of microbial consortia (Kurm *et al.* 2017). Therefore, any statistically significant shift in the taxonomic composition of viruses could have meaningful consequences in the microbial community. Yet for shifts we discovered within fungi and Archaea, interpretations of such small shifts in the relative abundance of genes associated with these taxa should be tempered.

Lastly, to confirm the hypothesis that DSS is a physiological stress response, and not caused by a disease agent, we suggest future work to include transcriptome analysis of DSS-infected *S. siderea,* and the transcriptome analysis of the *Symbiodinium* associated with DSS-infected *S. siderea*. Studying differential gene expression in DSS-afflicted and healthy corals and *Symbiodinium* can provide answers for disease symptom initiation, progression, and restriction.

2.8 Author Contributions

RV and DB designed the experiment. AS, DB, and JP conducted the fieldwork. JP and AF generated the metagenomes. LW, AS, TS, DB, and RV performed the analysis. LW, AS, JP, RV, and DB wrote the manuscript.

2.9 Acknowledgments

We thank numerous volunteers for assistance with the experiment, and the Florida Keys National Marine Sanctuary for permits (FKNMS-2009-047 and FKNMS-2011-090). This research was funded by the NOAA Coral Reef Conservation Program Grant #NA14NOS4820090 to RV and DB with additional support from an NSF Biological Oceanography Grant (#OCE-1130786) to DB and RV.

Month	Treatment	Archaea (%)	Bacteria (%)	Fungi (%)	Protozoan (%)	Virus (%)	Unclassified (%)
July	Control	3.61 ± 0.05	21.09 ± 0.24	32.16 ± 0.15	29.39 ± 0.17	1.1 ± 0.02	12.66 ± 0.25
July	Nitrogen	3.71 ± 0.09	21.89 ± 0.92	30.62 ± 0.46	29.97 ± 0.66	1.05 ± 0.01	12.76 ± 0.49
July	Nitrogen + Phosphorus	3.87 ± 0.04	22.48 ± 0.42	32.23 ± 0.42	28.32 ± 0.31	1.11 ± 0.02	11.99 ± 0.21
July	Phosphorus	3.57 ± 0.07	20.72 ± 0.52	31.99 ± 0.23	29.49 ± 0.42	1.07 ± 0.02	13.16 ± 0.35
July	Seawater	3.88 ± 0.1	33.76 ± 1.27	22.6 ± 0.56	24.19 ± 0.32	1.59 ± 0.03	13.99 ± 0.46
August	Control	3.62 ± 0.04	20.94 ± 0.23	31.94 ± 0.19	29.56 ± 0.21	1.11 ± 0.02	12.82 ± 0.31
August	Nitrogen	3.6 ± 0.08	20.82 ± 0.23	31.85 ± 0.48	29.44 ± 0.19	1.12 ± 0.02	13.17 ± 0.6
August	Nitrogen + Phosphorus	3.49 ± 0.04	21.08 ± 0.89	32.69 ± 0.62	28.5 ± 1.25	1.03 ± 0.04	13.21 ± 0.31
August	Phosphorus	3.58 ± 0.07	20.46 ± 0.29	32.08 ± 0.34	29.78 ± 0.22	1.06 ± 0.01	13.04 ± 0.46
August	Seawater	3.72 ± NA	31.67 ± NA	21.09 ± NA	25.61 ± NA	1.68 ± NA	16.23 ± NA
September	Control	3.8 ± 0.05	22.74 ± 1.64	30.8 ± 1.67	28.32 ± 0.93	1.56 ± 0.39	12.78 ± 0.54
September	Nitrogen	3.76 ± 0.06	21.14 ± 0.15	32.42 ± 0.15	29.23 ± 0.07	1.17 ± 0.02	12.28 ± 0.28
September	Nitrogen + Phosphorus	3.8 ± 0.05	22.9 ± 1.69	30.71 ± 1.87	28.16 ± 0.81	1.47 ± 0.29	12.97 ± 0.68
September	Phosphorus	3.67 ± 0.04	20.98 ± 0.19	32.84 ± 0.36	28.83 ± 0.38	1.14 ± 0.02	12.55 ± 0.16
September	Seawater	3.58 ± NA	20.32 ± NA	32.07 ± NA	29.75 ± NA	1.12 ± NA	13.16 ± NA
October	Control	3.64 ± 0.02	20.67 ± 0.13	32.41 ± 0.23	29.63 ± 0.2	1.14 ± 0.02	12.51 ± 0.2
October	Nitrogen	3.66 ± 0.08	20.65 ± 0.26	32.55 ± 0.31	29.37 ± 0.13	1.15 ± 0.02	12.63 ± 0.43
October	Nitrogen + Phosphorus	3.59 ± 0.11	21.01 ± 0.36	34.1 ± 1.07	28.15 ± 1.05	1.04 ± 0.06	12.1 ± 0.35
October	Phosphorus	3.64 ± 0.08	20.78 ± 0.31	32.97 ± 0.47	29.15 ± 0.37	1.1 ± 0.02	12.35 ± 0.45
October	Seawater	3.73 ± 0.01	27.24 ± 0.72	22.84 ± 0.36	26.45 ± 0.2	3.67 ± 0.24	16.07 ± 0.07

Data are separated by time (month of sampling) and treatment (control, nitrogen alone, phosphorus alone, and nitrogen and phosphorus combined).

Table 2.1 | Mean relative taxonomic composition and standard error of the mean of different microbial groups identified from *Siderastrea siderea* coral metagenomes

Taxonomic Shifts	July (%)	August (%)	September (%)	October (%)	Pairwise comparisons
ARCHAEA					
Thermoplasmata	2.78 ± 0.025	2.91 ± 0.053	2.85 ± 0.027	2.84 ± 0.069	*July < August
Thermococci	6.17 ± 0.094	6.45 ± 0.091	6.20 ± 0.093	6.68 ± 0.119	**July < October; *September < October
Desulfurococcaceae	1.38 ± 0.018	1.45 ± 0.022	1.39 ± 0.018	1.41 ± 0.022	*July < August
FUNGI					
Agaricales	3.27 ± 0.028	3.24 ± 0.027	3.33 ± 0.023	3.33 ± 0.025	**August < September; **August < October
Magnaporthales	1.25 ± 0.0084	1.25 ± 0.011	1.25 ± 0.0085	1.30 ± 0.013	*August < October; *September < October
Tremellales	1.59 ± 0.014	1.57 ± 0.017	1.60 ± 0.012	1.62 ± 0.019	**August < October
VIRUS					
Caudovirales	39.17 ± 0.27	40.05 ± 0.68	45.35 ± 2.43	40.35 ± 0.54	**July < September; *August < September
Myoviridae	23.67 ± 0.20	24.15 ± 0.35	28.99 ± 2.06	24.60 ± 0.46	**July < September; **August < September
Poxviridae	6.39 ± 0.15	5.82 ± 0.19	5.39 ± 0.22	5.71 ± 0.15	*September < July; *October < July

*$p < 0.05$; **$p < 0.01$.

Table 2.2 | Statistically significant shifts in taxonomic groups across time in *Siderastrea siderea* metagenomes as measured by generalized linear mixed models with Tukey's *post-hoc* test.

Functional Shifts	July (%)	August (%)	September (%)	October (%)	Pairwise comparisons
KEGG 1					
Genetic information processing	23.91 ± 0.22	24.34 ± 0.18	24.01 ± 0.28	24.75 ± 0.09	**July < October
KEGG 2					
Amino acid metabolism	9.66 ± 0.14	9.50 ± 0.16	9.89 ± 0.33	9.05 ± 0.10	*October < July; *October < September
Metabolism of cofactors and vitamins	6.84 ± 0.042	6.71 ± 0.051	6.87 ± 0.073	6.62 ± 0.055	*October < July
Replication and repair	6.76 ± 0.052	6.92 ± 0.050	6.98 ± 0.021	6.95 ± 0.036	*July < August; **July < September; **July < October
Translation	9.29 ± 0.089	9.42 ± 0.050	9.28 ± 0.050	9.51 ± 0.043	*July < October
Xenobiotics degradation and metabolism	1.25 ± 0.026	1.18 ± 0.019	1.21 ± 0.011	1.13 ± 0.027	*August < July; **October < July; *October < September
KEGG 3					
ABC transporters	4.89 ± 0.019	4.81 ± 0.024	4.77 ± 0.022	4.81 ± 0.030	**September < July; *October < July
Alanine, aspartate, and glutamate metabolism	1.43 ± 0.027	1.40 ± 0.036	1.46 ± 0.042	1.30 ± 0.026	**October < July; **October < September
Homologous recombination	1.45 ± 0.014	1.49 ± 0.009	1.49 ± 0.008	1.52 ± 0.019	**July < October
Nucleotide excision repair	1.43 ± 0.020	1.43 ± 0.017	1.49 ± 0.035	1.36 ± 0.019	** October < September
Two-component system	3.03 ± 0.058	2.90 ± 0.036	2.86 ± 0.023	2.92 ± 0.039	**September < July
Photosynthesis	0.26 ± 0.023	0.23 ± 0.017	0.26 ± 0.034	0.23 ± 0.015	**August < July

*$p < 0.05$; **$p < 0.01$.

Table 2.3 | Statistically significant shifts in functional assignments across time in *Siderastrea siderea* metagenomes as measured by generalized linear mixed models with Tukey's *post-hoc* test.

2.11 Figures

Figure 2.1 (following page) | Experimental design and temperature profile from field site. **(A)** Data from NOAA Molasses buoy show that mean monthly sea surface temperatures in 2014 were significantly elevated both in the winter and summer months (red lines) compared to the monthly means from 1987–2008 (blue lines). Error bars indicate the standard error of means of all temperature data available for that month. **(B)** During this summer, we monitored control and nutrient exposed *Agaricia* corals for bleaching prevalence, severity, and recovery as well as tissue loss from July (pretreatment) to January 2015. Photos I and II represent *Agaricia* corals from July and September, respectively. *Siderastrea* control and nutrient exposed corals were also monitored for disease prevalence and severity across the course of the experiment. Photos III and IV represent *Siderastrea* corals from July and September, respectively. *Siderastrea* mucus samples for metagenomes (indicated by the stars) were only collected at the pretreatment time point (July 14, 2014) and three post treatment months: August 13th, Sept 14, and October 14th.

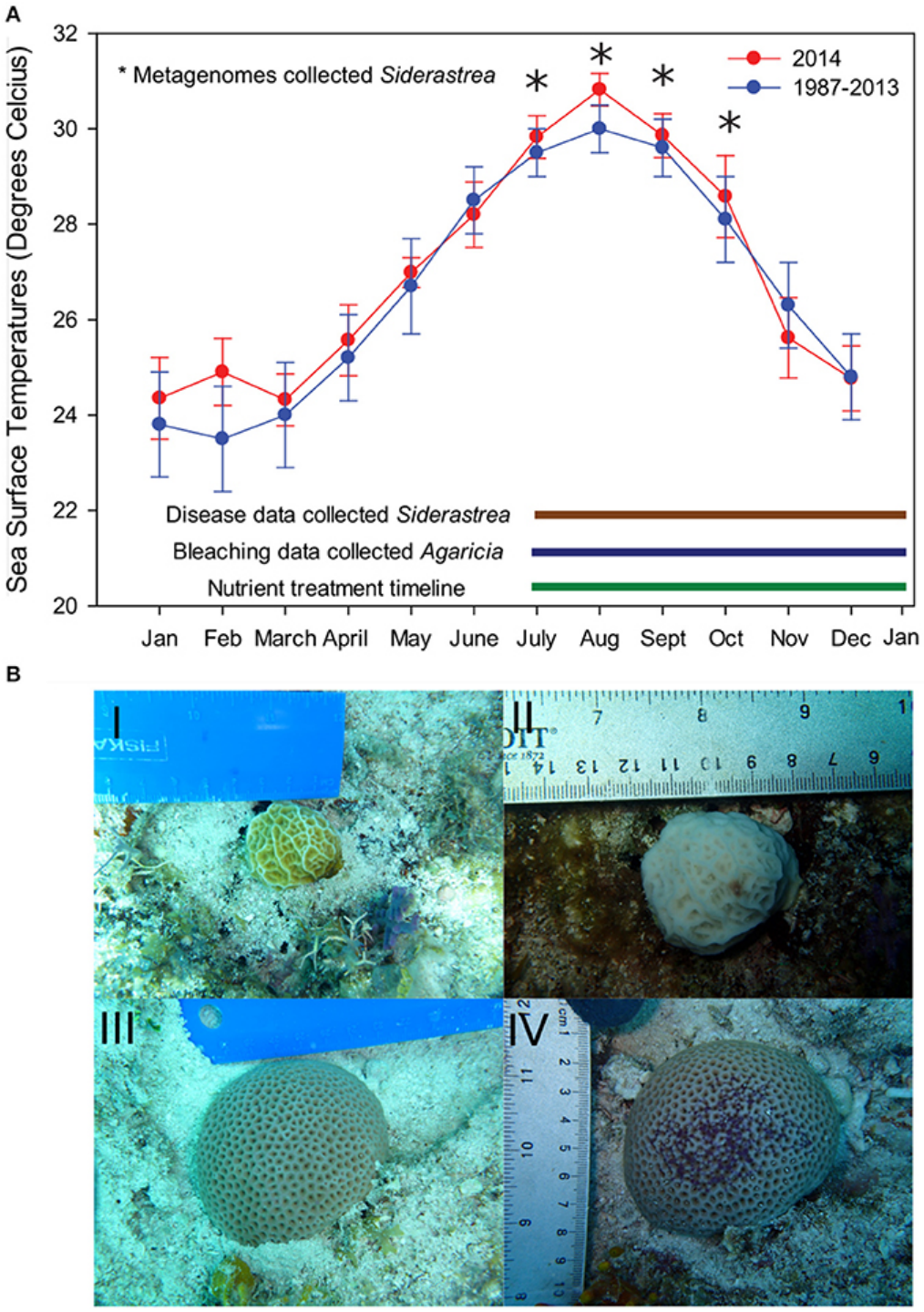
A
Sea Surface Temperatures (Degrees Celcius)
32
30
28
26
24
22
20
* Metagenomes collected Siderastrea
2014
1987-2013
Disease data collected Siderastrea
Bleaching data collected Agaricia
Nutrient treatment timeline
Jan
Feb
March
April
May
June
July
Aug
Sept
Oct
Nov
Dec
Jan
B
I
II
III
IV

Figure 2.1

Figure 2.2 (following page) | (A) Proportion of *Agaricia* spp. in each treatment experiencing bleaching during our monthly surveys. **(B)** The average severity of bleaching, calculated as the percentage of colony surface area with no pigmentation, during each survey point. **(C)** The average percentage of previously bleached tissue in each colony that had regained pigment and recovered from bleaching by January, 2015. *P*-values are from a two-factor ANOVA. **(D)** The average percentage of each coral's surface area that died between pretreatment surveys in July, 2014, and final surveys in January, 2015.

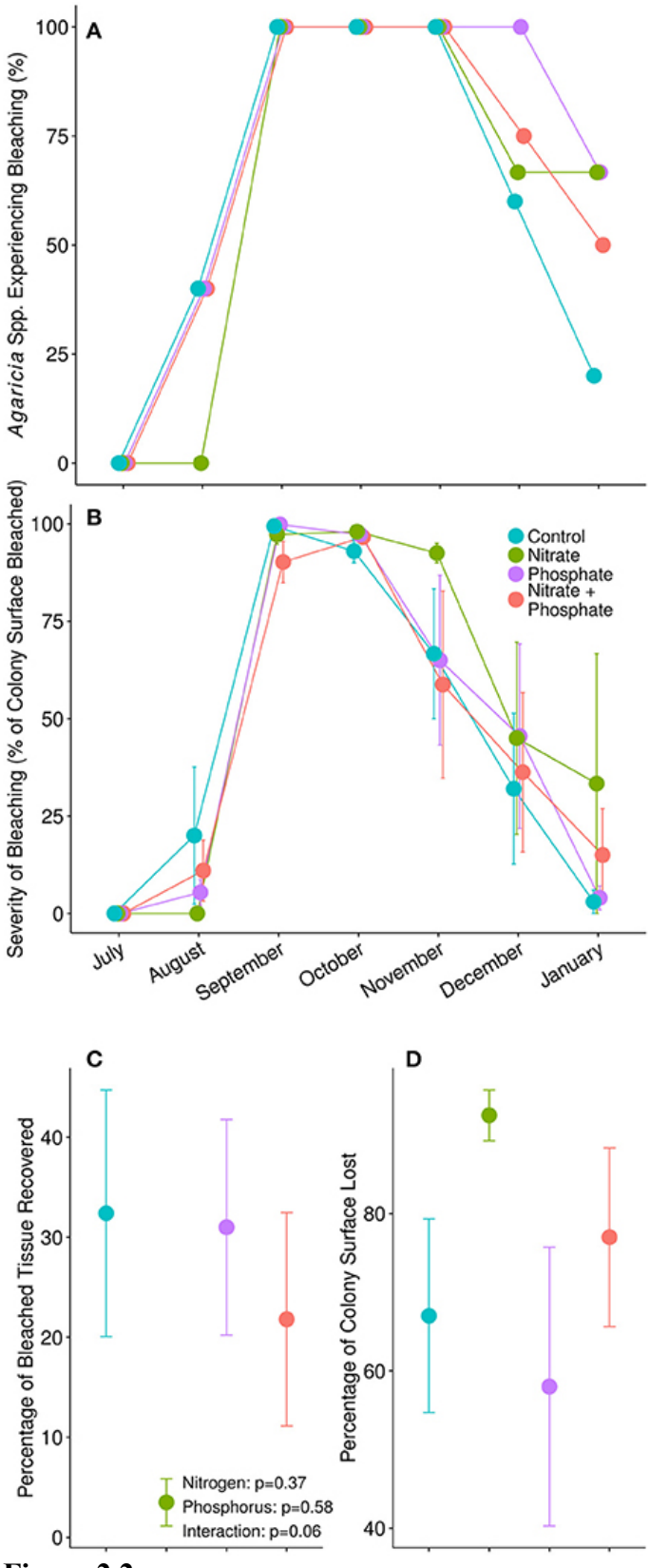
A
Agaricia Spp. Experiencing Bleaching (%)
100
75
50
25
0
B
Severity of Bleaching (% of Colony Surface Bleached)
Control
Nitrate
Phosphate
Nitrate + Phosphate
July
August
September
October
November
December
January
C
Percentage of Bleached Tissue Recovered
Nitrogen: p=0.37
Phosphorus: p=0.58
Interaction: p=0.06
D
Percentage of Colony Surface Lost

Figure 2.2

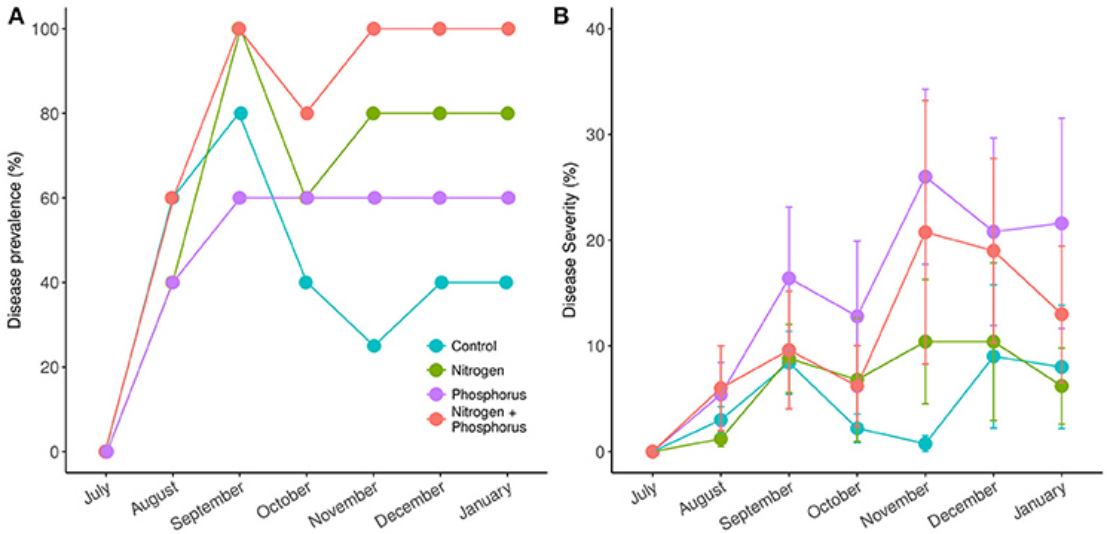

Figure 2.3 | Prevalence **(A)** and severity **(B)** of Dark Spot Syndrome in *Siderastrea siderea* corals during the course of study. Measurements taken in July were taken prior to nutrient treatment, while August, September, and October measurements were taken post treatment. Disease prevalence was calculated as the proportion of diseased individuals at each time point. Disease severity was calculated as the proportion of diseased tissue in each individual.

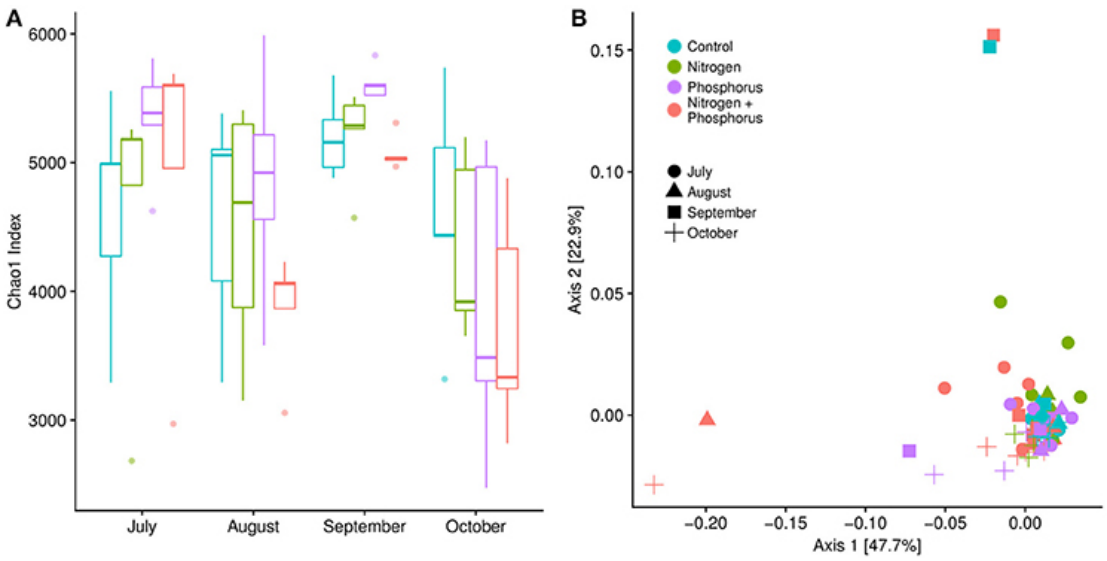

Figure 2.4 | (A) Alpha diversity of the microbial communities associated with *Siderastrea siderea* over time, calculated using the Chao1 index. Microbial alpha diversity in September was statistically different from alpha diversity metrics in August and October (Kruskal-Wallis test: $p < 0.01$; FDR-corrected Games-Howell *post-hoc* test: $p < 0.01$). **(B)** Beta diversity was calculated using a Bray-Curtis dissimilarity matrix and plotted on an MDS (multidimensional scaling) graph. Beta-diversity metrics were not different over time, but were instead significantly different between treatments (Adonis, $p = 0.01$). Pair-wise comparisons showed that the beta-diversity metrics were different between control sites and combined nutrient sites, and nitrogen and combined nutrient sites (Adonis, $p = 0.042$ and 0.03).

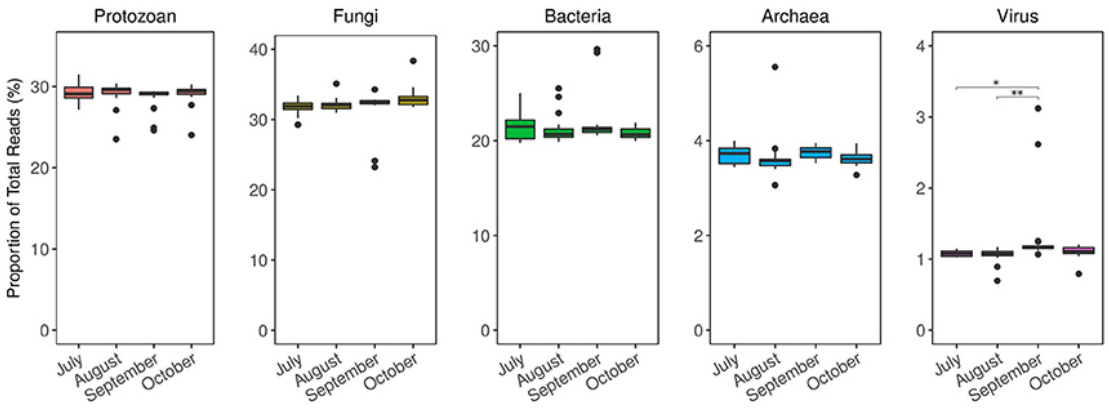

Figure 2.5 | Taxonomic distribution of *Siderastrea siderea* coral microbiomes from metagenome analysis over time. Results are normalized as the relative abundance of each taxa at every time point. The microbiome composition among domains remained relatively stable throughout time, except for viral annotations. The relative abundance of viral annotations was higher in September, compared to July ($p = 0.01$) and August ($p < 0.01$). *$p \leq 0.05$; **$p \leq 0.01$.

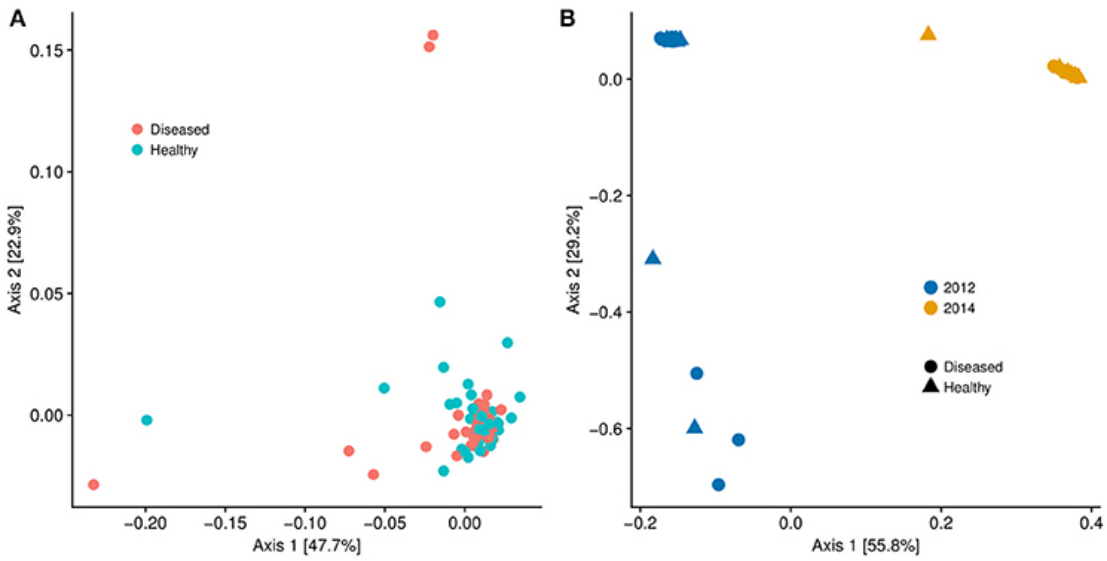

Figure 2.6 | (A) Multidimensional scaling graph of beta diversity of microbial communities of *Siderastrea siderea* samples broken into diseased and healthy groups. The microbiome of the diseased corals was statistically different from the microbiome of the healthy corals (Adonis, $p = 0.01$). **(B)** Multidimensional scaling graph of beta diversity of microbial communities of *Siderastrea siderea* corals. The 2012 data points were taken from *Siderastrea siderea* microbial metagenome data from a nutrient-enrichment experiment conducted in August of 2012. The 2014 data points were metagenomes from the current dataset sampled in August of 2014, which was subject to nutrient enrichment and high water temperatures. There was no statistical difference between the diseased and healthy microbiomes in 2012 and 2014, but there was a difference between the 2012 and 2014 samples (Adonis, $p < 0.01$).

3 Nutrient enrichment increases size of *Zostera marina* shoots and enriches for sulfur and nitrogen cycling bacteria in root-associated microbiomes

Lu Wang

Fiona Tomas

Ryan S. Mueller

Published: August 2020 (doi.org/10.1093/femsec/fiaa129)

FEMS Microbiology Ecology

Delftechpark 37a, 2628 XJ Delft, The Netherlands

Vol. 96

3.1 Abstract

Seagrasses are vital coastal ecosystem engineers, which are mutualistically associated with microbial communities that contribute to the ecosystem services provided by meadows. The seagrass microbiome and sediment microbiota play vital roles in belowground biogeochemical and carbon cycling. These activities are influenced by nutrient, carbon, and oxygen availability, all of which are modulated by environmental factors and plant physiology. Seagrass meadows are increasingly threatened by nutrient pollution, and it is unknown how the seagrass microbiome will respond to this stressor. We investigated the effects of fertilization on the physiology, morphology, and microbiome of eelgrass (*Zostera marina*) cultivated over four weeks in mesocosms. We analyzed the community structure associated with eelgrass leaf, root, and rhizosphere microbiomes, and of communities from water column and bulk sediment using 16S rRNA amplicon sequencing. Fertilization led to a higher number of leaves compared to that of eelgrass kept under ambient conditions. Additionally, fertilization led to enrichment of sulfur and nitrogen bacteria in belowground communities. These results suggest nutrient enrichment can stimulate belowground biogeochemical cycling, potentially exacerbating sulfide toxicity in sediments and decreasing future carbon sequestration stocks.

3.2 Introduction

Seagrasses are aquatic angiosperms commonly found along coastlines and estuaries worldwide (Short *et al.* 2007). Seagrass meadows maintain a variety of important ecosystem services such as providing habitat and food for coastal fauna (Whitfield 2017; Nowicki *et al.* 2019), mitigating wave action (Lei and Nepf 2019),

improving water quality (Nowicki *et al.* 2017), and sequestering both autochthonous and allochthonous sources of carbon (Oreska *et al.* 2018; Prentice *et al.* 2019), thereby mitigating the effects of climate change (Fourqurean *et al.* 2012). Recent studies have revealed the potential importance of mutualisms between seagrasses and their microbiome – the community of microorganisms directly associated with the seagrass leaf, root, and rhizosphere (Fahimipour *et al.* 2016; Ettinger *et al.* 2017; Crump *et al.* 2018) – in altering the functioning of these ecosystems and the services they provide (Barbier *et al.* 2011; Ugarelli *et al.* 2017). For example, the seagrass microbiome can positively affect plant productivity by promoting seagrass growth through the synthesis and release of phytohormones (Celdrán *et al.* 2012) and protecting seagrasses from hydrogen sulfide toxicity through its oxidation (Isaksen and Finster 1996; Holmer, Frederiksen and Møllegaard 2005).

Sediments of seagrass meadows are hotspots of nitrogen (N) and sulfur (S) cycling (Welsh 2000: 200; Garcias-Bonet *et al.* 2016; Marietou 2016; Aoki and McGlathery 2018; Holmer 2019). In seagrass sediments, these biogeochemical cycles are driven by specific microbial taxa whose activities are stimulated in part by access to freshly exuded organic rhizodeposits (López *et al.* 1995; Martin *et al.* 2018b) and by plant-generated oxygen gradients around roots (Duarte, Holmer and Marbà 2005). Therefore, the belowground sediment microbial community is an important primary consumer of fixed carbon from seagrasses (Holmer *et al.* 2004; Kaldy *et al.* 2006). In turn, the seagrass microbiome can mitigate some forms of nutrient limitation, such as N limitation, by converting organic nitrogen and atmospheric nitrogen to ammonium, which can then be assimilated by plants (Welsh 2000: 200; Nielsen *et al.* 2001;

Garcias-Bonet *et al.* 2016; Tarquinio *et al.* 2018). Diazotrophic bacteria are particularly active in the root-associated sediment (i.e., the rhizosphere), where N-fixation activity is ~40-fold greater than in the bulk sediment (Nielsen *et al.* 2001). The importance of the contributions of nitrogen-fixing bacteria of the seagrass microbiome is clearly exemplified in the case of the seagrass *Posidonia oceanica*, where it is estimated to account up to 100% of the total nitrogen demand of the plant host (Agawin *et al.* 2016). Thus, the microbiome can act as a key component that helps to offset nutrient deficits when N is limiting to seagrasses.

An overabundance of nutrients can also negatively affect seagrass productivity, with eutrophication being identified as an important cause of observed global seagrass population declines (Waycott *et al.* 2009). Sources of nutrient pollution include nitrogen and phosphorus in runoff from agricultural (Grech, Coles and Marsh 2011) or residential applications (Lapointe, Barile and Matzie 2004; Orth *et al.* 2006; Román, Fernández and Méndez 2019). Eutrophication can lead to seagrass loss through several direct or indirect mechanisms (Burkholder, Tomasko and Touchette 2007). Eutrophication typically enhances macroalgae and phytoplankton blooms in seagrass meadows leading to decreased light availability in the water column, which can be exacerbated by increased sediment resuspension resulting from loss of seagrasses, deepening seagrass declines (McGlathery 2001; Hauxwell, Cebrián and Valiela 2003; Ralph *et al.* 2007; Waycott *et al.* 2009; Schmidt *et al.* 2012). In addition, eutrophication can directly impact seagrasses via ammonium toxicity, creating a carbon imbalance in the plant that can lead to death via loss of structural integrity (Burkholder, Mason and Glasgow 1992; van Katwijk *et al.* 1997;

Touchette, Burkholder and Glasgow 2003; Burkholder, Tomasko and Touchette 2007: 200).

Microbes may also play an indirect role in the effects of eutrophication on seagrasses. Nutrient pollution can impact nitrogen and sulfur cycling, which, in turn, can have downstream feedback effects on the plant host (Duarte, Holmer and Marbà 2005). For example, sediment sulfate reduction and nitrogen cycling rates (nitrogen fixation, denitrification) increase with nitrogen and phosphorus enrichment (Holmer *et al.* 2001, 2004; Pérez *et al.* 2007). N and S cycling, and organic matter mineralization may be enhanced both by increased nutrient availability (López *et al.* 1998) and increase in seagrass root exudation in response to eutrophication (Liu *et al.* 2017a), leading to oxygen depletion. Anoxic conditions promote sulfate reduction, leading to build-up of hydrogen sulfide, which requires oxygen for its oxidation to non-toxic forms of sulfur. Seagrasses are vulnerable to sulfide toxicity in anoxic and sulfidic sediments and are prone to increased mortality rates in these conditions (Holmer and Bondgaard 2001; Pedersen, Binzer and Borum 2004; Holmer, Frederiksen and Møllegaard 2005). Thus, the seagrass microbiome and microbes within the bulk sediment could exacerbate the effects of eutrophication, impacting the well-being of seagrass meadows.

While there have been previous studies observing the effects of nutrient pollution on seagrass meadows, many of these have focused on sediment chemistry (Holmer *et al.* 2004; Pérez *et al.* 2007; Liu *et al.* 2017a). It is currently unclear how the seagrass microbiome is influenced by changing nutrient conditions, and how these changes affect the plant host (York *et al.* 2017). Indeed, studies that examined the

effects of nutrient loading in seagrass meadows have only examined bulk sediment microbial communities, with results indicating that nutrients can play a major role in enhancing abundance of pathogens (Liu *et al.* 2018) and microbial taxa associated with organic matter degradation (Guevara *et al.* 2014). However, these studies have not examined the effects of nutrient loading on the seagrass microbiome itself, missing the belowground sediment spatial gradient from the root to bulk sediment, as well as other plant-mediated effects of eutrophication on the seagrass microbiome. To fill this gap in knowledge, we conducted a nutrient manipulation experiment with eelgrass (*Zostera marina*), the most widespread seagrass species globally (Short and Green 2003), following plant responses along with microbiome responses of water column, bulk sediment, and the seagrass leaf, root, and rhizosphere to nitrogen and phosphorus additions over the course of four weeks.

3.3 Materials and Methods

3.3.1 Sediment and Seagrass Collection and Processing

We collected sediment from an intertidal eelgrass bed in Yaquina Bay, OR in May 2017. Sediment was transported to the Hatfield Marine Science Center (HMSC) facilities, sieved through 6 mm stainless steel mesh, and added to eight experimental mesocosm tanks up to a depth of 10 cm. Experimental tanks (~190 liters) were connected to a continuous seawater flow-through system at an indoor Experimental Seawater Facility located at HMSC and were held at ambient temperatures for four weeks prior to seagrass transplantation.

Apical eelgrass shoots were collected in June 2017 and immediately transported to adjacent HMSC facilities. To standardize our experimental eelgrass

samples, we clipped secondary shoots from the apical shoot, gently removed the pre-existing leaf epiphytes, trimmed the leaves to 50 cm, and trimmed the rhizome to the fifth node to ensure that the four most metabolically active nodes were included with each shoot (Kaldy 2012). Twenty-five apical shoots were randomly assigned to each tank and treatment group, transplanted into the prepared sediment within each tank at uniform intervals, and allowed to acclimate to conditions (e.g., light, temperature, and water) for three weeks prior to initiating experimental treatments. Transplanted seagrass rhizosphere and root associated microbiomes recover within 2 weeks to match that of seagrasses transplanted with intact rhizospheres (Wang *et al.,* submitted; see chapter 5). Tank seawater was maintained at a height of 25 cm, and temperature controlled at 10.00 ± 2 °C, similar to the average ambient water temperature of 10.93 ± 0.03 °C. Flow rate variation was minimized between tanks and maintained between 3.50-4.36 L/min. LED lights were used to provide 200 µmol photons sec^{-1} m^{-2} at the tank surface on a 12:12 hour light:dark regimen.

3.3.2 Experimental Setup

Four replicate nutrient-enrichment tanks were treated with 400 g of Osmocote 14:14:14 (8.6% Ammonium, 5.4% Nitrate, 14% Phosphate, 14% Potassium). To evenly distribute the fertilizer, Osmocote was separated into 100 g mesh parcels which were then placed into 2 x 8-inch PVC piping drilled with holes around the perimeter (Hessing-Lewis *et al.* 2015). Pipes with or without fertilizer were mounted on bamboo sticks and placed at the four corners of each fertilized tank. Fertilization treatment lasted four weeks, with a replacement of fertilizer parcels with new fertilizer after the first two weeks. Based on estimated water flow (~5.7 $kl \cdot d^{-1}$) and

fertilizer dissolution rates (8.28 $g \cdot d^{-1}$), we estimated that the fertilizer treatments would continuously add 7 μM of ammonium and 1.27 μM of nitrate to the water column.

3.3.3 Sampling Scheme

We measured plant traits (photosynthesis rate and leaf growth rate) at defined time points throughout the four weeks of the experiment. Photosynthesis rates were calculated as net oxygen accumulation ($mg \cdot l^{-1}$) using a dissolved oxygen probe (Luminescent Dissolved Oxygen Probe, Hach LDO10105) and were measured on days 1, 7, 14, 21, and 28. Measurements were taken by placing a leaf clipping (10 cm) from the second youngest leaf of one shoot per tank into a clear 50 ml conical tube filled with seawater and incubating for 2-3 hours in the respective tank. Net oxygen concentrations were measured at four intervals ranging between 30 minutes to 1 hour. We estimated net oxygen accumulation rate per hour by graphing oxygen measurements over time (in minutes), obtaining the slope, and multiplying the slope by 60.

Weekly leaf growth of two plants was measured via the hole punch method (Zieman 1974) on days 7, 14, and 21 of the experiment. Plants remaining at the end of the experiment (4-7 per tank) were collected and surveyed for plant growth characteristics, including leaf count, leaf length, number of rhizome nodes, and presence of any secondary shoots. Plants were frozen until processed for dry weight, before which leaves were stripped of epiphytes. Plant biomass and epiphytes were oven-dried separately for 48 hours at 60 °C.

Samples for DNA extraction and microbiome sequencing were collected on days 0 (prior to nutrient deployment), 1, 3, 7, 14, 15, 17, 21, and 28 to capture immediate and delayed responses. At each time point, two replicate plants with ~10 cm of sediment core were removed from each tank using a 30 mm diameter corer and destructively sampled. After collection, eelgrass was dissected into above and belowground segments. An 8-cm segment from the second youngest leaf, the youngest root bundle, and the rhizosphere sediment were removed from each plant. We manually removed leaf epiphytes prior to DNA extraction. We defined the rhizosphere as the sediment attached to seagrass roots after pulling the whole plant from the sediment core. Additionally, two 1-liter replicate samples of the water column microbiome (i.e., cells concentrated onto 0.2 μm PES filter membranes) and bulk sediment cores (i.e., sediment with no visible microalgae collected ca. 10 cm away from the closest eelgrass individual) were collected from each tank. All processed samples were placed in individual 2 ml DNA LoBind tubes (VWR International) and held at -20 °C before transporting from HMSC to the main campus of Oregon State University, where they were kept at -80 °C until DNA extraction.

3.3.4 Inorganic Nitrogen Analysis of Water Samples

We collected samples for nitrogen concentration measurements from the water column, and from pore water samples of bulk, residual core, and rhizosphere sediments. The residual core samples consisted of remaining sediment from eelgrass cores after the removal of whole plants and the root-associated rhizosphere sediment. Sediments were centrifuged at 3000 rpm for 5 minutes and the supernatants containing porewater were removed and stored at -80 °C. Porewater nitrate and

ammonium concentrations were measured using methods from Hood-Nowotny *et al.*, (Hood-Nowotny *et al.* 2010) and Qiu *et al.*, (Qiu, Liu and Zhu 1987), respectively.

3.3.5 Microbial Biomass DNA Extraction and PCR

We extracted microbial community DNA from samples using a CTAB phenol-chloroform extraction method detailed in Crump *et al.*, (Crump *et al.* 2003). Sequencing libraries of the v4-v5 hypervariable regions of 16S rRNA genes were created using a one-step PCR with universal 515FB-806RB primers (Thompson *et al.* 2017) at a final concentration of 200 nM and Accustart II PCR ToughMix polymerase (Quanta Bio) under the following amplification cycling conditions: 94 °C for 3 min; 25 cycles of 94 °C for 45 seconds, 50 °C for 60 seconds, 72 °C for 90 seconds; 72 °C for 10 minutes. PNA (peptide nucleic acid) blockers were added to leaf sample amplifications at 0.25 μm final concentrations to decrease amplification of seagrass chloroplast DNA (PNA Bio; Lundberg *et al.* 2013). PCR products were size purified with Agencourt AMPure XP beads following the standard protocol (Beckman Coulter, Inc), quantified by Agilent TapeStation 4200, pooled at normalized concentrations, and sequenced on the Illumina MiSeq (Reagent Kit v3; 2x300bp) at Oregon State University's Center for Genome Research and Biocomputing (CGRB). The raw sequence data can be accessed in the NCBI Sequence Read Archive under BioProject PRJNA563458.

3.3.6 Statistical Analyses of Plant Trait and Nutrient Concentrations

Plant trait data were tested for normality using the Shapiro test in R (R Core Team 2018). Statistical differences of each plant trait between fertilized and ambient conditions at the end of the experiment were examined using Student's T-tests or

Wilcoxon rank sum tests. We used the ‘lme4’ package in R to fit linear mixed-effects models to test for treatment, time, and their interaction as fixed effects and for tank as a random effect on growth rate and photosynthesis data (Bates *et al.* 2015). For nutrient data, we first assessed the appropriate probability distribution for each dataset using the ‘car’ package in R (Fox and Weisberg 2019) and fit generalized linear mixed-effects model using the ‘MASS’ package in R (Venables and Ripley 2002). We also conducted separate tests of mixed-effects models on belowground compartment nutrient comparisons, with treatment, time, and sampling compartment as fixed effects, and tank as random effects. We used the Tukey’s HSD post hoc comparisons implemented in the ‘multcomp' package to calculate Benjamini-Hochberg adjusted p-values for multiple hypothesis testing (Hothorn, Bretz and Westfall 2008). Average values and standard errors are reported as summary statistics, unless otherwise stated.

3.3.7 Amplicon Sequence Processing and Statistical Analyses of Microbial Community Data

16S amplicon sequence reads were processed using mothur v1.39.3 (Schloss *et al.* 2009), which joined paired reads using the make.contigs() command with the option trimoverlap=T and screened reads with excess ambiguous base calls and inappropriate lengths. Unique contigs were aligned to the SILVA 16S rRNA reference alignment version 123 (Quast *et al.* 2013) using the ‘align.seqs()’ command with default settings, removed of chimeras with chimera.uchime(), and classified using the RDP classifier version 14 (Wang *et al.* 2014). Reads were clustered using the default Opti clustering method in mothur at 97% similarity to produce OTUs (Operational Taxonomic Units). Reads assigned to chloroplast and mitochondria were

removed from subsequent analyses. We subsampled to the library with the lowest number of reads (935) to obtain an OTU table for downstream analysis (Lozupone and Knight 2005; Weiss *et al.* 2017). After column filtering of the multiple sequence alignment ('filter.seqs()' of mothur), a midpoint rooted phylogenetic tree was produced from the resulting alignment with FastTreeMP (v. 2.1.7) implementing the General Time Reversible model of nucleotide evolution (Tavaré and Miura 1986; Price, Dehal and Arkin 2010). Beta-diversity patterns were assessed across samples using weighted and unweighted UniFrac metrics (Lozupone and Knight 2005). The 'pcoa()' command of mothur was applied to resulting distance matrices, and the 'adonis' function in the 'vegan' package of R (Oksanen *et al.* 2018) assessed significant differences between treatment groups using PERMANOVA (Permutational multivariate analysis of variance) (Anderson 2017). We utilized the 'pairwise.perm.manova()' function in the 'RVAideMemoire' package for post hoc tests on PERMANOVA results (Hervé 2018).

Based on the experimental treatment design, we grouped samples into the first and second halves of the experiment (each two-week period) to gain insight into processes that corresponded with initial and successive nutrient additions (Jurburg *et al.* 2017; Kurm, Geisen and Hol 2018). PERMANOVAs on the UniFrac distance metrics of the separate seagrass mesocosm compartments (leaf, root associated, rhizosphere associated, bulk sediment, and water column) detected significant differences between immediate (i.e., during the first two-week period) and more sustained (i.e., during the second two-week period) effects of nutrient additions on the microbial communities (Table S3.1).

To visualize community structure of ambient eelgrass microbiomes, we graphed the log-transformed OTU counts of all taxonomic orders present at over 1% relative abundance using the 'heatmap.2' function in the 'gplots' package in R (Warnes *et al.* 2016). The 'indicator()' function in mothur was used to detect species with biases in abundance and/or occurrence due to experimental treatment effects or in specific eelgrass compartments. We chose an indicator value cutoff of 25 so that each significant taxon was present in at least 50% of a given group, and at a relative abundance of at least 50% in the group (Dufrêne and Legendre 1997). All graphs were generated using 'ggplot2' of R (Wickham 2016).

3.4 Results

3.4.1 Water Column and Porewater Nitrogen (N) Concentrations

We investigated differences in water column and porewater nitrate and ammonium concentrations between treatment groups (fertilized and ambient) and between sediment compartments over the course of the experiment. Nitrate and ammonium concentrations in water column and porewater samples responded differently to nutrient fertilization, with the magnitude and direction of the response varying and being specific to the compartment examined and the nutrient itself (Figure S3.1, Table S3.2). For instance, when comparing water column ammonium and nitrate concentrations, a significant effect of the fertilization treatment and the interaction between treatment and time was observed for nitrate, but not ammonium (Table S3.2). Nitrate water column concentrations increased an average of 2.5-fold in the fertilized treatment across all sampling dates, with a general increase in concentrations after 15 days (Figure 3.1E).

Belowground compartments exhibited different trends in N concentrations than water column samples. On average, porewater ammonium concentrations in the rhizosphere, residual core sediment, and bulk sediment were all higher in fertilized samples compared to those from tanks under ambient conditions (Figure S3.1C). Similarly, average nitrate concentrations in the bulk sediment porewater and residual core sediment porewater from fertilized samples were higher than those found in ambient samples (Figure S3.1D). However, this trend did not hold for nitrate concentrations in rhizosphere porewater, which were higher in ambient than fertilized samples, particularly after day 15 of the experiment (Figure 3.1H).

Significant differences in ammonium and nitrate concentrations between compartments were also observed. Water column samples were consistently lower in concentrations of both nutrients compared to belowground compartments across all samples. When comparing belowground compartments alone, opposite trends were observed for ammonium relative to nitrate. Average ammonium concentrations consistently and significantly decreased moving across the spatial gradient of the bulk sediment porewater to the rhizosphere porewater (Table S3.2; bulk sediment: 142.34 ± 11.77 μM, residual core sediment: 89.11 ± 7.32 μM, rhizosphere sediment: 68.69 ± 11.69 μM). On the other hand, belowground nitrate concentrations demonstrated the opposite trend, with the lowest concentrations in bulk sediment samples (Table S3.2; bulk sediment: 18.24 ± 2.92 μM, residual core sediment: 20.21 ± 3.06 μM, rhizosphere sediment: 64.49 ± 9.64 μM) (Figure S3.1D).

3.4.2 Nutrient Fertilization Effects on Plant Traits

Of all plant traits measured, only the number of leaves per shoot were significantly different between fertilization treatment groups (Table 3.1). Fertilized eelgrass on average had a significantly higher number of leaves per plant than ambient treatments (5.22 ± 0.31 vs. 3.90 ± 0.24; Table 3.1). Additionally, albeit not statistically significant, the proportion of fertilized plants with secondary shoots tended to be higher than for ambient plants (28.6% ± 20.1 vs. 6.3% ± 3.1). For plants in both treatments groups, average photosynthesis rates (oxygen accumulation) significantly decreased over the course of the experiment, while other factors generally indicative of overall growth increased over the course of the experiment. Leaf growth rate was an average of 1.24 ± 0.10 cm · d^{-1}, and total leaf length over the course of the experiment increased by 11.37 ± 2.83 cm while the number of rhizome nodes increased by 3.24 ± 0.18. Plants in both treatments at the end of the experiment exhibited similar dry leaf biomass (0.36 ± 0.03 g), epiphyte load (375.25 ± 40.60 mg epiphyte · g dry $leaf^{-1}$), and survivorship (~6 plants remaining).

3.4.3 Microbial Communities of Eelgrass Mesocosms

There were significant differences in microbiome structure between eelgrass-associated compartments (leaf, root, and rhizosphere), and non-host associated samples (water column and bulk sediment) (Table 3.2, Figure 3.2, 3.3). OTUs within the Gammaproteobacteria, Bacteroidetes, and Rhodobacteraceae taxonomic groups were present at high relative abundance (>2%) in all compartments (Figure 3.3). *Nitrosopumilus sp., Candidatus Pelagibacter*, and *Tenacibaculum sp.,* a member of the Flavobacteriaceae, were dominant only in water column samples, at an average relative abundance of 2.11 ± 0.05%, 3.04 ± 0.05%, and 8.43 ± 0.20%, respectively.

OTUs of several genera that were more abundant in leaf samples than any other compartment included *Sulfitobacter sp.* (7.38 ± 0.15%), *Methylophilus sp.* (6.71 ± 0.31%), *Glaciecola sp.* (4.60 ± 0.10%), and *Granulosicoccus sp.* (3.33 ± 0.19%). *Methylophilus sp.* was the only genus dominant in both above- and belowground plant-associated samples, with a relative abundance of 1.37 ± 0.04% in root associated samples. Taxa dominant only in belowground samples included OTUs assigned to *Sulfurovum sp.* (1.97 – 4.72%), and unclassified OTUs within the Desulfobulbaceae (2.07 – 4.32%) and Desulfobacteraceae (1.40 – 5.85%). Interestingly, these taxa were all found in highest relative abundance within the bulk sediment. In contrast, *Arcobacter sp.* was dominant solely in rhizosphere and root associated samples, at 2.36 ± 0.43% and 2.21 ± 0.04%, respectively.

3.4.4 Nutrient Fertilization Effects on Microbial Community

Microbial communities from all compartments except for the bulk sediment exhibited significant changes in structure as a result of sustained fertilization (i.e., during weeks 3 and 4 of the experiment). There was a significant treatment effect on the community structure of the leaf and water microbiota after continued fertilization, particularly in regard to low-abundance taxa (Table 3.2). Additionally, there were sustained fertilization effects in belowground (root and rhizosphere) eelgrass microbial communities regarding both low and high-abundance taxa (Figure 3.4, Table 3.2).

3.4.5 Nutrient Fertilization Effect on OTUs

Rhizosphere microbiomes demonstrated a significant response to fertilization during the second half of the experiment. Taxa that increased in occurrence and

abundance as a result of sustained fertilization within these communities included OTUs classified to *Glaciecola*, *Rubritalea*, *Methylophaga*, the sulfur cycling taxon *Sulfurospirillum*, and unclassified OTUs belonging to the Flavobacteriaceae, Bacteroidetes, and Acidobacteria Gp22. Conversely, indicator taxa of the ambient rhizosphere communities included OTUs assigned to *Haliscomenobacter*, *Lutibacter*, *Sulfitobacter*, and unclassified OTUs belonging to Actinobacteria, Alphaproteobateria, Brocadiaceae, Flavobaceriaceae, Gammaproteobacteria, Rhodobacteraceae, Saprospiraceae, and Verrucomicrobiaceae (Table S3.4).

Indicator taxa of root microbiomes that were found in greater occurrence and abundance on fertilized eelgrass roots during the second nutrient addition included OTUs classified to *Sulfurovum*, *Arcobacter, Sulfurospirillum, Vibrio, Cytophaga, Colwellia*, and unclassified OTUs belonging to *Desulfobacteraceae, Bacteroidetes, Gammaproteobacteria, Flavobacteriaceae, Acidobacteria Gp23, Marinifilum, Bacteriovoraceae,* and *Proteobacteria* (Figure 3.5, Table S3.4). In contrast, the indicator OTUs of the unfertilized roots were assigned to distinct taxonomic groups comprised of *Glaciecola*, *Sulfitobacter*, *Winogradskyella*, *Granulosicoccus*, *Litorimonas*, *Lewinella*, *Lutibacter*, *Ekhidna*, *and Luteolibacter*, with unclassified OTUs belonging to the Alphaproteobacteria, Verrucomicrobiaceae, Gammaproteobacteria, Marinicella, Rhodobacteraceae, Bacteroidetes, Proteobacteria, Saprospiraceae, Hyphomonadaceae, Flavobacteriaceae, and Flammeovirgaceae.

Given the prevalence of S cycling taxa found to be indicators of fertilized root samples, we calculated the cumulative relative abundances of taxa known to oxidize or reduce sulfur compounds (i.e., Campylobacterales, Desulfobacterales,

Desulfovibrionales, and Desulfomonadales) over the course of the experiment to determine the overall trajectory of this group in response to fertilization. In the first two weeks of the experiment, these taxa comprised of 13.02 % (± 1.64) of all OTUs in ambient samples, and 15.41 % (± 2.94) of all OTUs in fertilized samples. In the second two weeks of the experiment, in contrast, these taxa decreased to 7.62 % (± 2.51) of ambient root communities, compared to an increase to 20.27 % (± 3.74) in fertilized root communities.

3.5 Discussion

The results of our mesocosm experiment with *Zostera marina* reveal significant positive effects of nutrient enrichment on plant morphology and important changes in host-associated microbiomes. We detected positive growth effects of fertilization on seagrass traits, with nutrient addition mainly enhancing aboveground leaf abundance and secondary shoot production. In past field and mesocosm fertilization experiments, seagrass responses have been highly variable, ranging from enhanced growth (Udy and Dennison 1997) to population declines (Short, Burdick and Kaldy 1995; Taylor *et al.* 1995; Govers *et al.* 2014a). These variations in responses highlight the importance of factors such as nitrogen or phosphorus-specific limitations (Armitage *et al.* 2005), and species-specific responses (Ferdie and Fourqurean 2004). Given that eelgrass generate one rhizome segment per leaf (Short and Coles 2001), and that we found no differences in final rhizome node count between treatments, we conclude that the final number of leaves retained on plants from each treatment group implies that fertilized and ambient eelgrass generated new leaves at similar rates, but differed in leaf retention. Here, the plants under ambient

conditions may have lost more leaves over the course of the experiment as a mechanism to recycle nitrogen and phosphorus from older leaf tissue once new leaf material is grown (Chapin III, Schulze and Mooney 1990; Stapel and Hemminga 1997).

Our results show that eelgrass possess a distinct microbiome from the surrounding environment (i.e., the water column and bulk sediment) (Jensen, Kühl and Priemé 2007; Cúcio *et al.* 2016; Ettinger *et al.* 2017; Crump *et al.* 2018), and that this microbiome is different between seagrass tissues/compartments (Fahimipour *et al.* 2016; Ettinger *et al.* 2017; Crump *et al.* 2018) Similar to other studies (Hargreaves, Williams and Hofmockel 2015; Fahimipour *et al.* 2016; Mazel *et al.* 2018; Jones *et al.* 2019), our results support a mechanism of environmental and host filtering in structuring host-associated microbiomes and suggest that eelgrass-associated microbes are enriched from surrounding environments by direct plant-microbe symbioses and/or inter-species competition on the plant surface. (i.e., microbes from the water column are enriched on eelgrass leaves, and microbes from the bulk sediment are enriched in the rhizosphere sediment, which are enriched on the roots).

Seagrass leaves are sites of carbon (Dorokhov, Sheshukova and Komarova 2018) and nutrient exchange (Hemminga, Harrison and Lent 1991; Rolny *et al.* 2011; Tarquinio *et al.* 2018) between the host plant and epiphytic microbes and eukaryotic epibionts. This resource exchange likely contributes to the selection of a seagrass-leaf-associated microbiome, making seagrass leaves a unique microbial environment compared to the coastal water column (Lu *et al.* 2015; Crump *et al.* 2017). Given the

observation that OTUs of the genus *Granulosicoccus* were dominant members of the leaf microbiome in this study, and on algae and the seagrass phyllosphere in previous studies (Kurilenko *et al.* 2010; Park *et al.* 2014; Crump *et al.* 2018), their role in facilitating specific metabolite exchanges in the plant environment is worth pursuing in future studies. Another genus dominant in seagrass-associated samples is *Methylophilus sp.*, which utilizes methanol and methylamine as carbon and energy sources (Doronina, Kaparullina and Trotsenko 2014). Both eelgrass and their epiphytic algae can be sources of methanol through cell division (Galbally and Kirstine 2002; Mincer and Aicher 2016), which can support the metabolic demands of these methylotrophic bacteria. The family Methylophilaceae has been identified as an indicator taxon of eelgrass leaves previously, and microbial taxa expressing genes for energy production via methanol oxidation have been found to be common on *Z. marina* and *Z. japonica* (Crump *et al.* 2018)

Microbial communities in the belowground eelgrass sediment compartments are constrained by nutrient, carbon, and oxygen gradients, and are influenced by plant processes, such as exudation of labile carbon (Nielsen *et al.* 2001; Kaldy *et al.* 2006) and radial oxygen loss (Martin *et al.* 2019). The area immediately surrounding the roots can support high amounts of heterotrophic aerobic metabolism, nitrogen fixation, sulfide oxidation, and sulfate reduction (Brodersen *et al.* 2018), whereas oxygen and labile carbon may not be as readily available in the bulk sediment. Gradients of electron acceptors and donors in relation to seagrass roots have direct effects on biogeochemical cycling (Sipler *et al.* 2017), which, in turn, can impact plant health. We observed that groups involved in sulfur metabolism (Kuever 2014a,

2014b), such as *Arcobacter* and *Sulfurovum* genera, Desulfobulbaceae and Desulfobacteraceae, were enriched in belowground samples, and that the abundances of these taxa changed with respect to distance from the host. The relative abundance of *Arcobacter* was similar in root associated and rhizosphere sediment samples, but lower in bulk sediment samples, whereas *Sulvurovum* was enriched in bulk sediment and rhizosphere sediment samples, and present in lower relative abundance in the root associated samples. *Arcobacter* has been previously found to dominate the eelgrass root microbiome, expressing genes for elemental sulfur and hydrogen sulfide oxidation, nitrogen fixation, and denitrification (Fahimipour *et al.* 2017; Brodersen *et al.* 2018; Crump *et al.* 2018) while *Sulfurovum* can oxidize elemental sulfur using nitrate and oxygen as electron acceptors (Mitchell *et al.* 2014). *Arcobacter* may have a closer plant association than *Sulfurovum*, due to its ability to oxidize hydrogen sulfide and fix nitrogen (Wirsen *et al.* 2002), both of which would be beneficial activities for the plant.

Indicator taxa analysis of root-associated samples in the latter two weeks of this experiment highlight how communities, and, in turn, potential metabolic functioning, may be affected by fertilization. Of the indicator taxa associated with fertilized eelgrass roots, species from four of these (e.g., *Arcobacter*, *Sulfurovum*, *Sulfurospirillum*, and unclassified Desulfobacteraceae) are commonly implicated as important drivers of sulfur (S) and nitrogen (N) cycles (Finster, Liesack and Tindall 1997; Mitchell *et al.* 2014; Crump *et al.* 2018). These biogeochemical cycles are tightly linked in the environment partially due to the fact that the same microbial taxa can perform key reactions in both (Welsh *et al.* 1996b). Importantly, the activities of

belowground microbes involved in these cycles are largely dependent on the composition and quantity of root carbon exudation in seagrasses, which is influenced by nutrient availability (Liu *et al.* 2017a, 2017b). We hypothesize that seagrass root exudation was affected by fertilization treatment, both of which subsequently influenced N and S cycling and the relative abundance of microbes performing these reactions.

Based on the synthesis of these findings, we propose a model whereby fertilization in this experiment changed the abundances of specific belowground microbial taxa, leading to direct and indirect alterations in sulfur and nitrogen cycling processes (Figure 3.6). We suggest that root-associated microbes involved in N and S cycling that are found in high relative abundance under ambient conditions were more carbon-limited in this experiment, due to decreased eelgrass carbon exudation compared to that of fertilized conditions. This hypothesis is supported by the anomalous build-up of nitrate in ambient eelgrass rhizosphere porewater samples of weeks 3 and 4 of the experiment. This nitrate build-up could be caused by a relative limitation of labile carbon in sediments, which would lower nitrate-utilizing metabolic pathways, such as nitrate respiration, denitrification, and dissimilatory nitrate reduction to ammonia, (Figure 3.6), although additional experimentation would be needed to verify changes in these activities.

While we did not observe eelgrass mortality due to fertilization, our results have potential implications for the effect of eutrophication on sulfide toxicity towards seagrasses and carbon sequestration in seagrass meadow sediments. Seagrasses have evolved methods of counteracting sulfide toxicity through radial oxygen loss

(Frederiksen and Glud 2006; Brodersen *et al.* 2015a, 2018), associations with sulfide oxidizing bacteria, and via incorporation of sulfur precipitate in belowground tissue (Hasler-Sheetal and Holmer 2015). However, eutrophication may enhance aerobic respiration and sulfate reduction, resulting in increased sulfide levels in sediments that may exceed detoxification mechanisms. Additional abiotic stressors, which may result from eutrophication (e.g., algal blooms; Holmer, Frederiksen and Møllegaard 2005), may further exacerbate these effects. Eutrophication may also stimulate overall belowground microbial activities, leading to increased respiration and a concurrent reduction of belowground carbon stocks in seagrass meadows (López *et al.* 1998; Holmer *et al.* 2004; Jiang *et al.* 2018). Future *in situ* experiments would be useful to confirm our results done in mesocosm. Additionally, the presence and relative abundance data derived from 16S amplicon sequencing results may not directly translate to microbial function, and further studies should be done to directly measure these microbial processes. Given the importance of seagrass meadows as key coastal ecosystems contributing to the sequestration of substantial amounts of carbon that would otherwise enter the atmosphere (Fourqurean *et al.* 2012; Oreska *et al.* 2018), it is important to further understand the effects of anthropogenic factors on both seagrasses and the seagrass microbiome.

3.6 Funding

This work was supported by the Department of Microbiology (OSU) and the Salvador de Madariaga Program (PRX18/00124) to F. Tomas.

3.7 Acknowledgments

Thank you to J. Hayduk and E. Hayduk for aiding with field work, G. Schwinge and S. Black for help with sample collection, J. Kaldy and F. Chan for lending us equipment, and Hatfield Marine Science Center (HMSC), particularly C. Moffett, for assistance with mescosom set-up at HMSC's Experimental Seawater Facility.

3.8 Tables

Response variable	Effects	Df	Test statistic	P-value	SD
Photosynthesis rate (mg O_2/L min^{-1})	Treatment	1	$\chi^2 = 0.04$	0.833	
	Time	4	$\chi^2 = 30.30$	**<0.001**	
	Treatment x Time	4	$\chi^2 = 7.64$	0.106	
	Tank				0.31
Growth rate (cm/day)	Treatment	1	$\chi^2 = 0.01$	0.938	
	Time	3	$\chi^2 = 5.04$	0.169	
	Treatment x Time	3	$\chi^2 = 3.58$	0.310	
	Tank				<0.001
Leaf length (cm)	Treatment	1	$\chi^2 = 1.79$	0.178	
	Tank				<0.001
Rhizome node count	Treatment	1	$\chi^2 = 0.06$	0.941	
	Tank				0.47
Leaf biomass (g dry weight)	Treatment	1	$\chi^2 = 0.23$	0.629	
	Tank				<0.001
Epiphyte load (mg/g leaf dry weight)	Treatment	1	$\chi^2 = 0.21$	0.649	
	Tank				132.40
Number of leaves per shoot	Treatment	1	$\chi^2 = 4.48$	**0.034**	
	Tank				<0.001
% plants with 2° shoots	Treatment	1	F = 3.53	0.060	
Survivorship	Treatment	1	F = 5.00	0.067	

Table 3.1 | Statistics table of plant traits measured throughout the 4-week experiment and at the experiment's conclusion. The significance of the treatment effect and the time effect, if applicable, were tested using generalized linear mixed models or linear mixed models depending on the best probability distribution fit of the plant trait data. Mesocosm tanks were assigned as random effects. Significance of fixed effects for each model was tested with a Wald's Chi-square test, and significant results ($p < 0.05$) are denoted in bold.

		Weighted UniFrac		Unweighted UniFrac	
Sampling compartment	**Df**	**Pseudo-F**	**P-value**	**Pseudo-F**	**P-value**
Compartment effects, all sampling points					
All sampling compartments	4, 240	80.95	**p = 0.001**, Tukey's post hoc: **p < 0.001**, pairwise comparison of all compartments	22.75	**p = 0.001**, Tukey's post hoc: **p = 0.001**, pairwise comparisons of all compartments
Treatment effects (ambient vs. fertilized), weeks 1 and 2					
Leaf	1, 21	0.48	p = 0.956	2.25	p = 0.899
Water column	2, 16	0.98	p = 0.432	1.14	p = 0.700
Root associated	1, 31	0.44	p = 0.941	1.49	p = 0.481
Rhizosphere	1, 27	1.83	p = 0.076	1.41	p = 0.103
Bulk sediment	1, 23	0.82	p = 0.687	1.20	p = 0.358
Treatment effects (ambient vs. fertilized), weeks 3 and 4					
Leaf	1, 20	0.89	p = 0.544	1.24	**p = 0.032**
Water column	2, 20	1.59	p = 0.064	1.25	**p = 0.025**
Root associated	1, 13	4.44	**p = 0.008**	1.27	**p = 0.008**
Rhizosphere	1, 28	2.11	**p = 0.050**	1.22	**p = 0.042**
Bulk sediment	1, 24	0.98	p = 0.394	1.53	p = 0.136

Table 3.2 | Results of PERMANOVA tests conducted on weighted and unweighted UniFrac metrics of microbiomes associated with *Zostera marina* sampling compartments; leaf, water column, roots, rhizosphere sediment, and bulk sediment, to elucidate the effects of fertilization. Tests compared microbial communities associated with the different sampling compartments, as well as differences between ambient and fertilized samples within each sampling compartment. Statistically significant results ($p < 0.05$) are denoted in bold.

3.9 Figures

Figure 3.1 (following page) | Water chemistry measurements. Ammonium and nitrate concentrations in the water column (A, E), bulk sediment porewater (B, F), residual core sediment porewater (C, G), and rhizosphere porewater (D, H) over the 4-week experiment. Significant differences ($p < 0.05$) in nutrient concentrations between fertilized and ambient tanks on a given day are denoted with an asterisk (*).

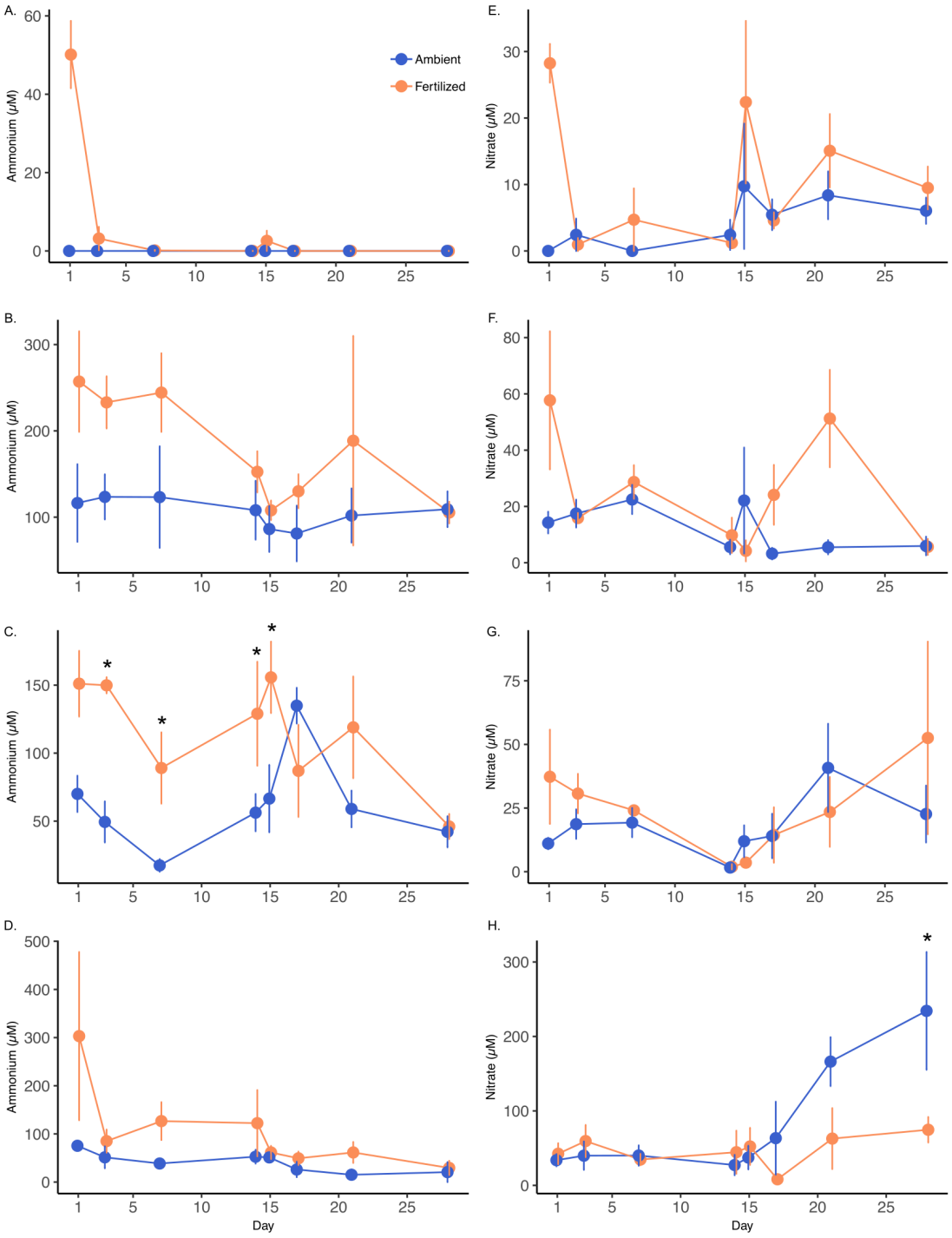

Figure 3.1

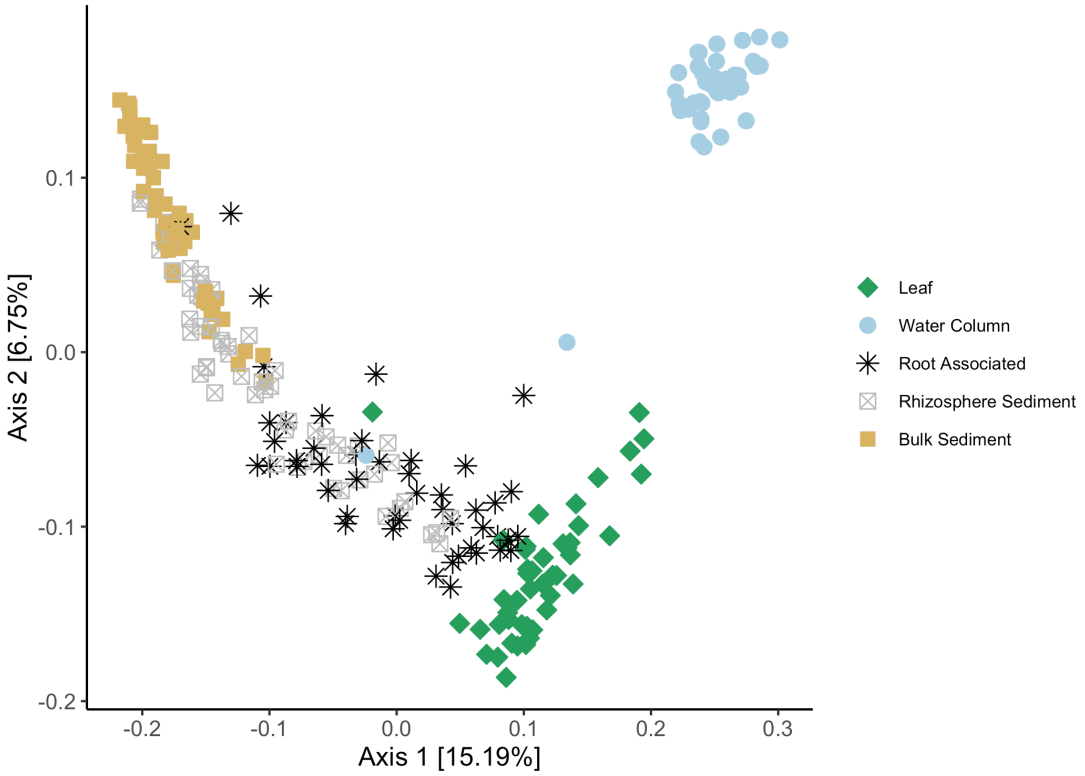

Figure 3.2 | Microbial communities associated with *Zostera marina* leaves, roots, rhizospheres, water column, and bulk sediment. Principle coordinate analysis plot of eelgrass mesocosm microbial community structure with first and second PCoA axes derived from weighted UniFrac metrics calculated from all microbial samples. Microbial communities from different *Z. marina* compartments cluster distinctly from each other (PERMANOVA, $p = 0.001$; $p < 0.001$ for all compartment pairwise post-hoc comparisons).

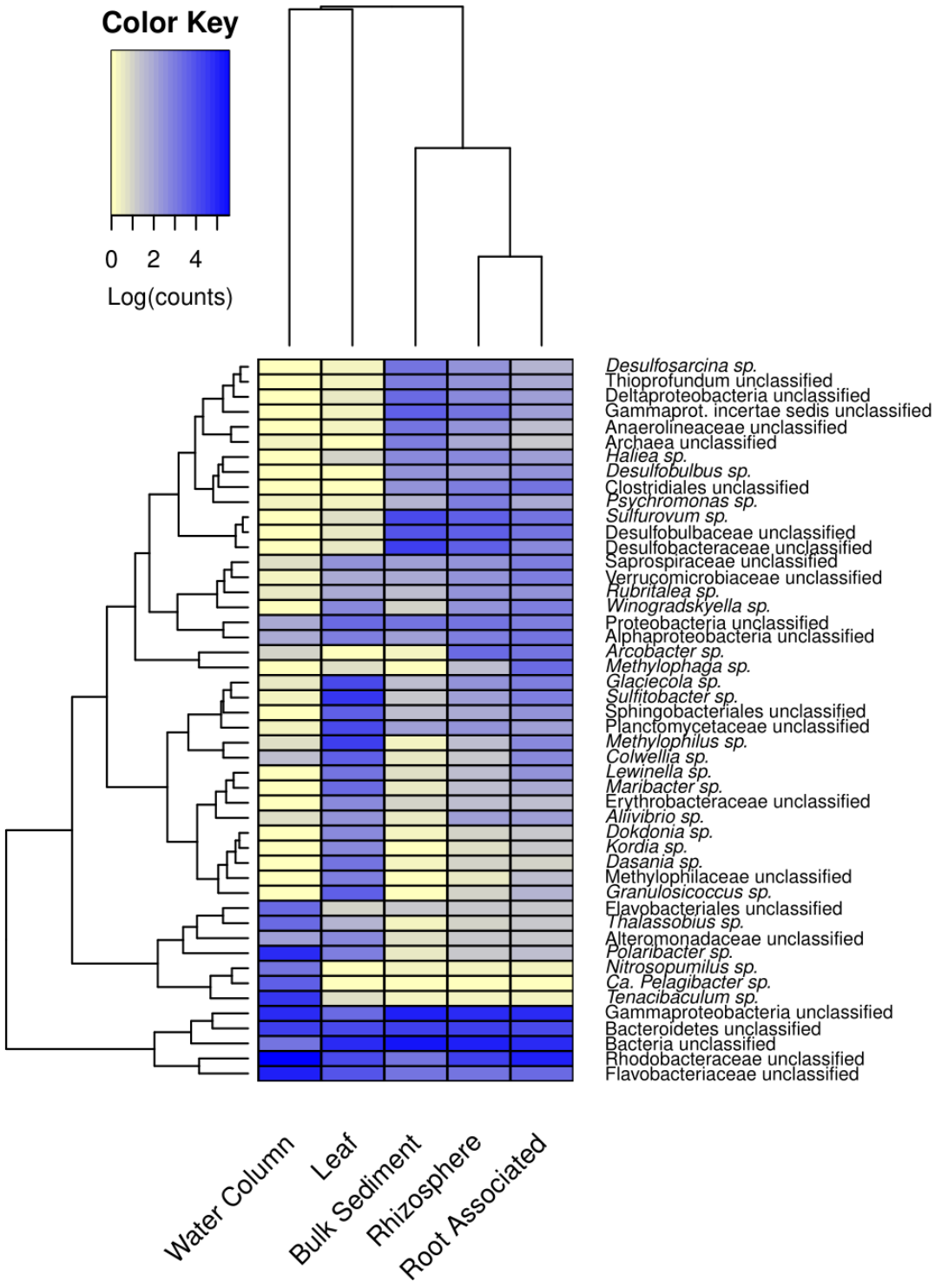

Figure 3.3 | Top genera (>1% relative abundance) of *Z. marina* compartments from all ambient samples. Heatmap depicting log-transformed OTU counts of bacterial genera.

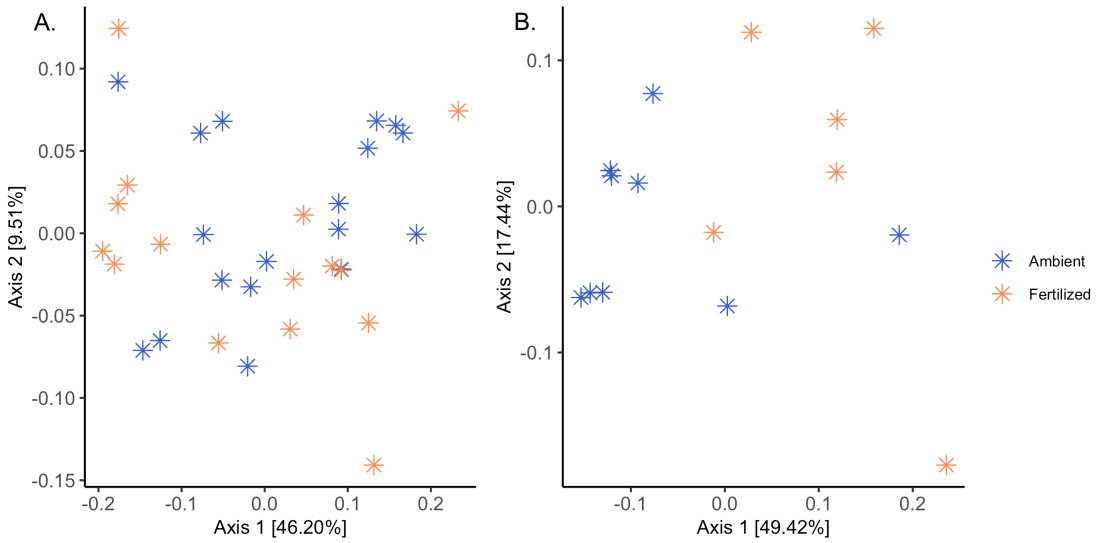

Figure 3.4 | Root microbial community responses to fertilization. PCoA plots of microbial communities associated with *Zostera marina* in weeks 1-2 (A) and weeks 3-4 (B) of roots. Ambient samples are denoted in blue, while fertilized samples are denoted in coral. PCoAs were graphed using weighted UniFrac metrics.

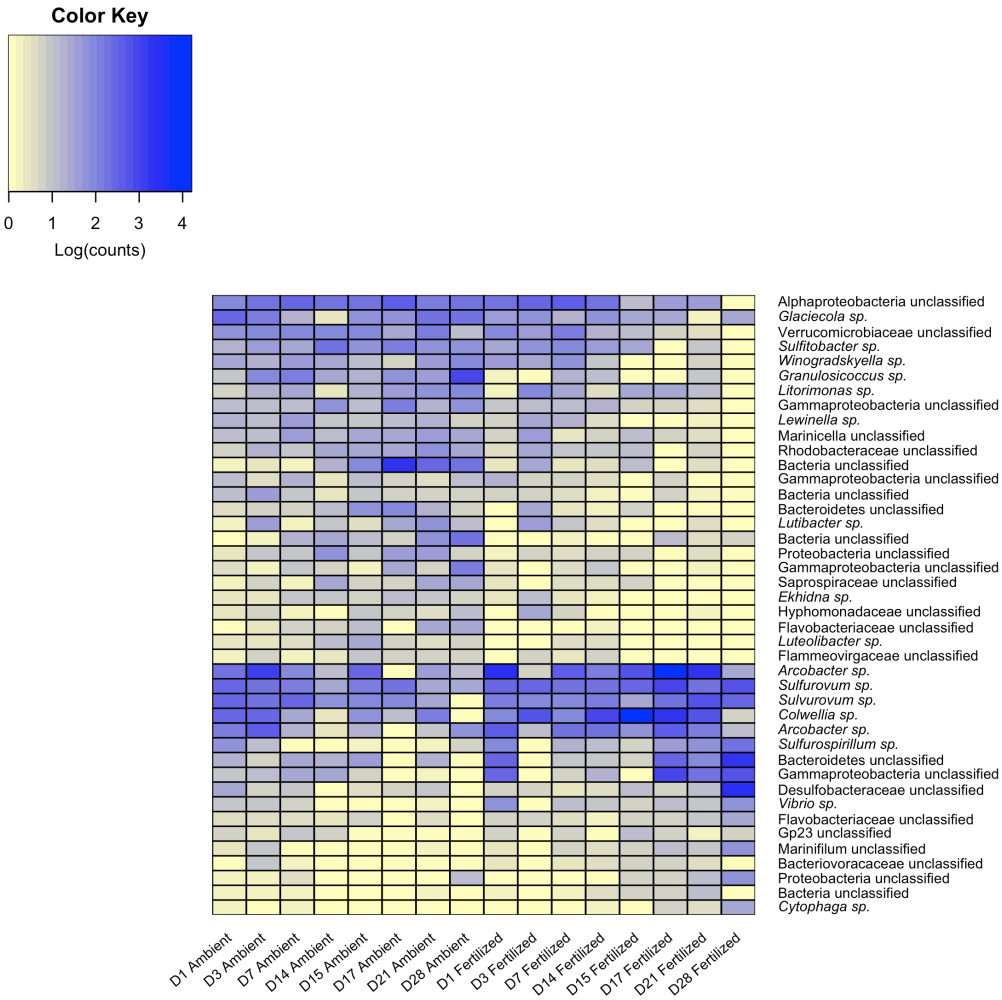

Figure 3.5 | Indicator taxa of ambient and fertilized eelgrass root microbiomes. Heatmap depicting log-transformed counts of indicator taxa associated with root microbial communities of both ambient and fertilized samples from weeks 3 and 4, graphed over the entire 4-week experiment.

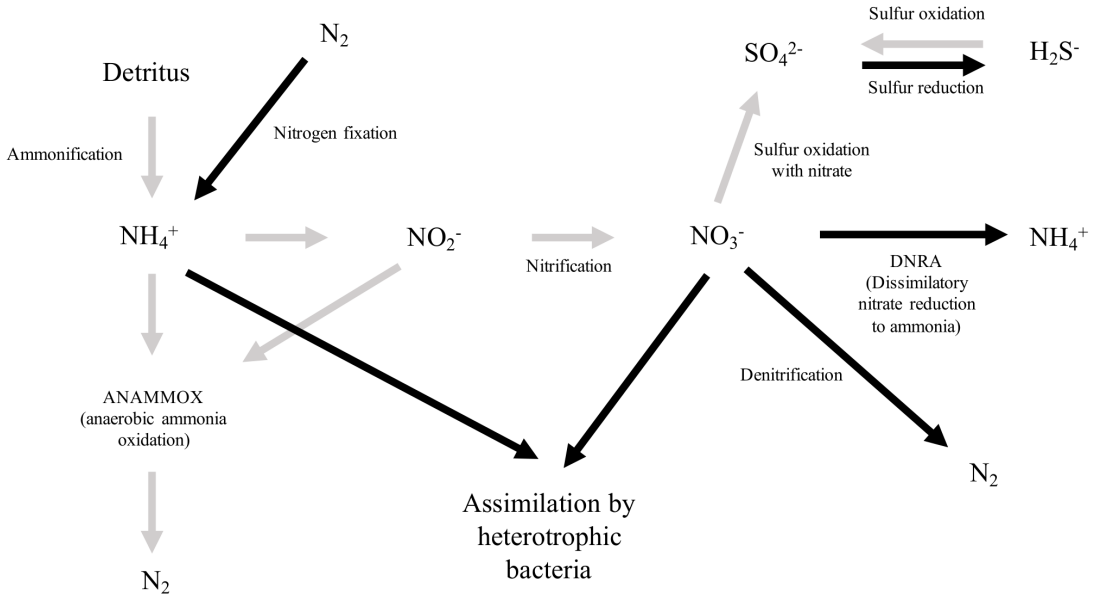

Figure 3.6 | Conceptual model of sulfur and nitrogen cycling responses to fertilization in eelgrass sediments. Pathways with black arrows denote processes that are hypothesized to be supported in fertilized mesocosms by labile carbon availability via eelgrass root exudates. Nitrogen fixation (Welsh 2000; Nielsen *et al.* 2001), carbon assimilation (Holmer *et al.* 2004; Kaldy *et al.* 2006), denitrification (Aoki and McGlathery 2018; Garcias-Bonet *et al.* 2018), DNRA (Aoki and McGlathery 2018), and sulfate reduction (Pollard and Moriarty 1991; Nielsen *et al.* 2001; Pérez *et al.* 2007) are all predicted to be positively affected by labile carbon inputs. Pathways with grey arrows are not hypothesized to be directly affected by labile carbon availability or fertilization.

4 Changes in the *Posidonia oceanica* leaf microbiota composition and functional potential under high pCO_2 and low pH conditions

Lu Wang

Fiona Tomas

Gema Hernán

Jorge Terrados

Ryan S. Mueller

Manuscript in preparation

4.1 Abstract

The ocean acts as a sink for anthropogenic carbon emissions, and as a result, significant drops in ocean pH are projected to occur within the next century, leading to ecological consequences for marine macro and microorganisms. Seagrasses are projected to potentially benefit from ocean acidification, because they utilize both CO_2 and HCO_3^- as sources of carbon. As seagrasses and their microbiota are metabolically linked, this increased carbon availability may yield changes in the seagrass microbiome. For this study, *Posidonia oceanica* leaves were sampled from acidified and ambient sites off of the coast of Ischia, Italy, in which naturally occurring volcanic CO_2 vents acidify surrounding ocean waters. We used both 16S rRNA amplicon sequencing and metagenome analysis to investigate differences between the acidified and ambient *P. oceanica* leaf microbiota. Results showed distinct differences in the leaf microbiota based on site variables, which was not seen in the water column microbiota. Representative metagenomes of acidified and ambient sites provided evidence for enrichment of autotrophic microbes in ambient sites and heterotrophic microbes in acidified sites. Genes enriched in ambient sites include those involved in carbon fixation and ABC transporters, while genes enriched in acidified sites include those in sucrose and starch metabolism and biofilm formation. These results indicate that diverse metabolic pathways may be supported within acidified phyllospheres by environmental niches within microbial biofilms and increased seagrass productivity.

4.2 Introduction

The ocean absorbs 25% of anthropogenic CO_2 emissions, and as a result, marine carbonate chemistry is heavily impacted by increasing global CO_2 production (Bindoff *et al.* 2019). CO_2 reacts with water to form H_2CO_3, which can dissociate into H^+ and HCO_3^- (bicarbonate) (Doney *et al.* 2020). The resulting increase in hydrogen ions lowers the pH of seawater, leading to ocean acidification (OA). If anthropogenic emissions are left unchecked, ocean pH is expected to decrease by ~0.3 by 2100 (Bindoff *et al.* 2019). Additionally, excess hydrogen ions will bind to existing carbonate ions to form more bicarbonate, and in the process deplete the bioavailability of carbonate ions that would otherwise be used by shelled organisms and other calcifiers as calcium carbonate (Doney *et al.* 2020). Thus, this increase in the partial pressure of CO_2 (pCO_2) in the ocean is expected to negatively impact calcifying organisms such as corals and calcareous algae (Kroeker *et al.* 2010; Doney *et al.* 2020). In contrast, seagrasses, which are thought to be restricted in their photosynthetic capacity by limiting inorganic carbon concentrations in most environments, have generally been shown to thrive under OA conditions (Koch *et al.* 2013; Zayas-Santiago *et al.* 2020), due to their use of CO_2 for carbon fixation (Larkum *et al.* 2017). Seagrasses under experimentally high pCO2 and low pH conditions have been reported to exhibit higher productivity and photosynthetic rates compared to control plants (Invers *et al.* 2001; Jiang, Huang and Zhang 2010; Ow, Collier and Uthicke 2015). Seagrass meadows may be able to mitigate OA through removal of bicarbonate, enhanced primary productivity (Unsworth *et al.* 2012a; Koweek *et al.* 2018; Pacella *et al.* 2018; Su *et al.* 2020b) that can lead to sequestration of fixed carbon in sediments (i.e., blue carbon; Fourqurean *et al.* 2012),

and by providing benefits to local invertebrates through increases in habitat niches and food availability (Whitfield 2017).

Recent studies have revealed the unique microbial communities associated with seagrasses, as well as potential mutualisms that may form the basis of symbioses between the seagrass microbiome and the plant host (Cúcio *et al.* 2016; Ettinger *et al.* 2017; Ugarelli, Laas and Stingl 2018; Hurtado-McCormick *et al.* 2019; Wang, Tomas and Mueller 2020). For instance, the seagrass root and rhizosphere microbiomes are thought to contribute to sulfide detoxification in sediments and nitrogen fixation that can deliver organic nitrogen to plants (Garcias-Bonet *et al.* 2016; Crump *et al.* 2018; Cúcio *et al.* 2018). Further, the leaf microbiome is thought to increase nutrient availability through carbon and nitrogen exchange mechanisms (Tarquinio *et al.* 2018) and enhance plant growth through an as yet undetermined mechanism (Celdrán *et al.* 2012). In return, excess photosynthates produced by seagrasses are exuded from both leaves and roots (Kaldy 2012), which are quickly metabolized by members of the seagrass microbiome (Kaldy *et al.* 2006).

Due to the increasing acknowledgement of the role of the microbiome in ecosystem services and host health, research has begun to focus on the effects of changing environmental conditions on the holobiont, which comprises both the host and the microbiome. With regard to OA and pH perturbations, previous experimental and *in situ* studies conducted with corals, sponges, non-calcifying seaweed, and seagrass have shown that marine host-associated microbiomes are affected by changes in pH and OA conditions (Vega Thurber *et al.* 2009; Hassenrück *et al.* 2015; Webster *et al.* 2016b; Aires *et al.* 2018; Botté *et al.* 2019; Biagi *et al.* 2020). These

studies have generally found enrichment for marine pathogenic microbes such as *Vibrio sp*. under OA conditions (Vega Thurber *et al.* 2009; Aires *et al.* 2018) and loss of potential symbionts (Webster *et al.* 2016b). The only study to date characterizing seagrass (*Enhalus acroides*) microbiome response to OA conditions found a decrease in epiphyte cover, particularly crustose coralline algae, and shifts towards pathogenic microbes (Hassenrück *et al.* 2015). However, there is a need for functional profiling in addition to taxonomic information. For example, a previous functional profiling study found a reduction in the uptake potential for carbohydrates and amino acids, and degradation of host-derived metabolites within sponge microbiomes under OA conditions (Botté *et al.* 2019). Evidence from studies on free-living bacteria from the Rhodobacteraceae and Flavobacteriaceae families under OA conditions show a general trend towards enhanced growth efficiency (Teira *et al.* 2012) and organic matter degradation (Piontek *et al.* 2010; Fuentes-Lema *et al.* 2018), while impacting primary productivity and nitrogen fixation (Liu *et al.* 2010; Das and Mangwani 2015; O'Brien *et al.* 2016). These results indicate that OA conditions may favor fast growing, heterotrophic, opportunistic, and potentially pathogenic marine microbes. Taken as a whole, these results have implications for marine biogeochemical cycling as well as host fitness and adaptability. Thus, it is important to characterize the effects of OA on microbiomes and host organisms to better understand ecosystem-wide responses to future ocean conditions.

To characterize the long-term effects of OA conditions on seagrasses and their microbiomes, this study characterized the composition and functional potential of leaf microbiomes, or the phyllobiome, of *Posidonia oceanica* growing in natural pH

gradient consisting of three sites within waters covering volcanic CO_2 seafloor vents in the Mediterrenean Sea (Hall-Spencer *et al.* 2008). Seagrasses and microbes were collected from three field sites located near Ischia, Italy, that range in pH from highly acidified to ambient seawater pH conditions (average pH of sites = 6.59, 7.75, and 8.08). The naturally rich pCO_2 waters provided an opportunity to study the responses of *P. oceanica* and its phyllobiome under near steady-state conditions and after years of continuous exposure, compared to a perturbed state that may arise under experimental settings.

Enhanced seagrass growth and photosynthesis under OA conditions may lead to an influx of fixed carbon to the seagrass microbiome via exudation (Hall-Spencer *et al.* 2008, Kaldy *et al.* 2006, Martin *et al.* 2018). This availability of labile organic matter may stimulate microbial metabolism, potentially priming the microbes to metabolize more carbon and impacting estimates for blue carbon predictions (Paterson and Sim 2013). On a macroscopic level, there are clear ecological effects of OA surrounding Ischia, including increased *P. oceanica* production and shoot density, decreased abundance of coralline algae and other calcifying epiphytes, increased grazing, and negative effects on shelled organisms (Hall-Spencer *et al.* 2008; Donnarumma *et al.* 2014). The ecological effects of OA conditions on the functional potential of microbes associated with these seagrasses remain unexplored.

4.3 Methods

Posidonia oceanica leaf samples were collected from volcanic vents off of Ischia, Italy, in Castello d'Aragonese in July 2014 at approximately 1.5 – 3.5 meters water depth. Vent gasses consisted of 90.1-95.3% CO_2, and no sulfur, as detailed by

Hall-Spencer et al (Hall-Spencer *et al.* 2008). Plant samples were collected from sites near the vents, S2 (pH 7.75) and S3 (pH 6.59), which were 50 meters apart, and from a control site, S1, pH 8.08, 100 meters from the closest vent. Water column samples were taken from all three sites, and seep water samples were taken nearest to the S2 site. All water samples were filtered through a 0.2 µm PES filter membrane on site. Samples were kept on ice, frozen to -80 °C, and shipped on dry ice to Oregon State University in Corvallis, Oregon, where they remained at -80 °C until processing.

DNA was extracted from 8 cm of the second youngest *P. oceanica* leaf after scraping off visible algal epiphytes, and from the 0.2 µm filters via phenol-chloroform extraction (Crump *et al.* 2003). We amplified the v4-v5 hypervariable region of the 16S rRNA gene using a one-step PCR with 200 nM of universal primers 515FB-806RB (Thompson *et al.* 2017) and Accustart II PCR ToughMix polymerase (Quanta Bio). PCR conditions were the following: 94 °C for 3 min; 25 cycles of 94 °C for 45 seconds, 50 °C for 60 seconds, 72 °C for 90 seconds; 72 °C for 10 minutes. PCR products were purified using Agencourt AMPure XP beads following the standard procedure (Beckman Coulter, Inc), quantified using the Agilent Bioanalyzer 2100, pooled to equimolar concentrations, and sequenced on the Illumina MiSeq (Reagent Kit v2; 2 x 250 bp) at Oregon State University's Center for Genome Research and Biocomputing (CGRB).

Taxonomic assignment on the 16S amplicon data was done using DADA2 v.1.12.1 following v1.12 of the pipeline tutorial (Callahan *et al.* 2016), using the Silva SSU database release 132 (Quast *et al.* 2013). Samples averaged 11,973 ± 1,028 reads, with a median of 4,334. The structure of the phyllobiome, the microbial

community inhabiting leaf surfaces, was analyzed using the phyloseq package in R (McMurdie and Holmes 2013; R Core Team 2018). Microbial count data was normalized using the ALDEx2 package in R (Fernandes *et al.* 2014), which calculates centered log-ratios of Monte-Carlo Dirichlet instances for each taxonomic feature. Normalized values of taxonomic features were tested for differential abundance using Welch's T test and subsequent Benjamini-Hochberg P-value corrections. We also report the median effect size of each taxonomic feature, which is calculated within the ALDEx2 package by dividing the median difference in clr (centered log ratio) values by the median of the largest difference in clr values, between ambient and acidified groups. Taxonomic features with corrected P-values less than 0.05 and effect size > |1| were considered differentially abundant between ambient and acidified groups.

Following analysis of 16S amplicon sequencing data, 3 replicates each from sites S1 and S3 were chosen for metagenome analysis to determine changes in functional potential of the *P. oceanica* phyllobiome. Microbiomes of S2 and S3 samples were virtually identical and samples from S3 were chosen to represent acidified samples in subsequent metagenomic analyses. Metagenome libraries were prepared using the Illumina Nextera Flex DNA kit, and sequenced on the Illumina V3 MiSeq (Reagent Kit v3; 2 x 300 bp) at the CGRB. Raw metagenome reads were quality controlled using TrimGalore, a wrapper program consisting of Cutadapt and FastQC (Andrews 2010; Martin 2011; Krueger 2015). TrimGalore v0.6.0 was run using a quality score cutoff of 25, and the –nextera option to remove nextera adapters, with otherwise default parameters. Quality filtered and trimmed reads were assembled into contigs using default parameters with metaSPAdes v3.13.1 (Nurk *et*

al. 2017). The three replicates from each site were co-assembled, resulting in one assembly each for S1 and S3. Assemblies were indexed using Bowtie2 v2.3.4.3 (Langmead and Salzberg 2012).

To filter out plant host reads, we downloaded an available *P. oceanica* transcriptome dataset from NCBI (D'Esposito *et al.* 2016, SRP071971). The transcriptome reads were mapped to the S1 and S3 Bowtie2 indices with standard options. We used samtools idxstats to identify contigs with three or more transcriptome reads mapped, which were determined to be host contamination and removed (Li *et al.* 2009). We chose the cut-off of 3 mapped reads to avoid false positives. Kaiju v1.7.2 was used to assign taxonomy to the quality-controlled sample reads (Menzel, Ng and Krogh 2016), using the NCBI BLAST non-redundant protein database nr, with fungi and microbial eukaryotes (downloaded December 2019). To filter out microbial eukaryote reads, we identified all reads assigned to microbial eukaryotes, and mapped those reads to the assembly indices using Bowtie2, using the same contamination and filtering protocol and threshold as with the host contaminants. We filtered 18,789 and 32,970 putative eukaryotic and plant contigs from samples S1 and S3 respectively, with 1,150,348 and 1,135,102 contigs remaining.

Gene prediction was done using Prodigal v2.6.3, with assemblies S1 and S3, consisting of contaminant-filtered contigs longer than 500 bp (Hyatt *et al.* 2010). Predicted genes were annotated with GhostKOALA (Kanehisa *et al.* 2016) using rpsblast with an E-value threshold of 1E-05. The filtered contigs longer than 500 bp from the S1 and S3 assemblies were indexed using Bowtie2. Quality controlled

metagenome reads were mapped back to these indices using default parameters to produce read coverage data. The number of reads mapping back to each gene was counted using htseq-count v0.9.1 with default parameters (Anders, Pyl and Huber 2015). Read count information from full length genes were used to test for differential gene abundance between acidified and ambient samples using DESeq2 v1.23.0 in R (Love, Huber and Anders 2014). All graphs were plotted in R using ggplot2 (Wickham 2016).

We used the DEICODE plug-in (Martino *et al.* 2019) in Qiime2 (Bolyen *et al.* 2019) to create Aitchison Distance metrics for beta-diversity analysis of both 16S rRNA amplicon sequencing and metagenomic functional results. Both the ASV (Amplicon Sequence Variant) and KO (KEGG Orthology) count tables were used to calculate community structure differences between ambient and acidified treatments. PERMANOVA tests on the resulting Aitchison Distances were also performed using DEICODE via Qiime2.

4.4 Results

4.4.1 Water Column and *P. oceanica* microbiomes at ambient and acidified sites

Microbial communities showed clear differences between sample source and site condition based on Aitchison Distance metrics of Beta-diversity (Figure 4.1). Samples derived from *P. oceanica* leaves, water column, and seep water column clustered separately ($p = 0.001$, pseudo-$F = 27.98$). Within leaf samples, microbial communities derived from acidified (S2, S3) and ambient sites (S1) were significantly different from each other ($p = 0.001$, pseudo-$F = 7.58$). There was no difference in the microbiomes of samples from sites S2 and S3 ($p = 0.430$, pseudo-$F = 0.72$); amplicon

data from these two sites are combined into one acidified treatment for all subsequent analyses. Water column samples from sites S1, S2, and S3 did not differ from each other ($p = 0.286$, pseudo-$F = 0.48$), and were not affected by the pH gradient. Within the leaf samples, the most abundant microbial family was Microtrichaceae (16.74 ± 1.59%), belonging to the Acidimicrobiia class, followed by the Rhodobacteraceae (13.88 ± 0.94%).

Analysis of the leaf microbiome resulted in eight significantly differentially abundant taxa, with four taxa enriched in samples from each pH site (Figure 4.2). Sequences assigned to *Chroococcidiopsis* sp. *PCC-6712* in the Xenococcaceae family, unclassified Gammaproteobacteria D90, *Granulosicoccus* sp. in the Thiohalorhabdalaceae family, and *Jannaschia* sp. within the Rhodobacteraceae family were enriched in ambient samples. Sequences assigned to *Chroococcidiopsis* sp. *PCC-6712* were detected at 0.86 ± 0.27% relative abundance in ambient samples, and not detected in acidified samples. Unclassified Gammaproteobacteria D90 sequences were present at 11.62 ± 1.26% in ambient samples, and 5.50 ± 0.66% in acidified samples, *Granulosicoccus sp.* sequences were present at 5.20 ± 0.80% in ambient samples, and 1.62 ± 0.27% in acidified samples, and *Jannaschia* sp. sequences were present at 1.37 ± 0.25% in ambient samples compared to 0.09 ± 0.07% in acidified samples.

Sequences assigned to *Endozoicomonas* sp. within the Oceanospirillales order, unclassified Hyphomicrobiaceae in the Rhizobiales order, unclassified Gammaproteobacteria UBA4486, and *Vibrio* sp. were all enriched in acidified samples. *Endozoicomonas* sp. sequences were present at 0.03 ± 0.02% in ambient

samples, and 0.66 ± 0.10 % in acidified samples and unclassified Hyphomicrobiaceae sequences were present at 0.02 ± 0.01% in ambient samples and 0.76 ± 0.09 % in acidified samples. Unclassified Gammaproteobacteria UBA4486 sequences were not detected in ambient samples but comprised 0.56 ± 0.07 % of acidified samples. *Vibrio* sp. sequences were 0.03 ± 0.03 % of ambient community samples, but 3.5 ± 0.56 % of acidified samples.

4.4.2 Functional potential of ambient and acidified P. oceanica phyllobiomes

Differential abundance analysis of gene coverage counts from metagenome data showed clear differences in microbial functional potential between the ambient and acidified samples. Out of 8,754 identified KEGG orthologous (KO) gene clusters, 1,113 KOs were classified as differentially abundant between metagenomes from ambient and acidified sites. Functional profiles of ambient and acidified metagenomes were not significantly different based on PERMANOVA tests on Aitchison Distance metrics, however, 69.37% of the variation among the two metagenome groups can be attributed to site differences (Figure S4.1).

4.4.3 Lipid, fatty acid, and alcohol metabolism

Genes associated with two metabolic pathways within lipid metabolism were significantly enriched in acidified samples. Six KOs annotated to be involved in glycerophospholipid metabolism were significantly enriched in acidified samples, while 3 KOs annotated to this pathway were significantly enriched in ambient samples. KOs enriched in acidified metagenomes included acyl transferases (*aas*, K05939; GPAT3_4, K13506) and a cardiolipin synthase (*clsA_B*, K06131).

Differential gene abundance within the fatty acid degradation pathway had an identical pattern. There was a strong bias in the abundance of KOs annotated to be involved in the interconversion of alkanes and fatty acids towards metagenomes from acidified samples (*frmA*, K00121; ALDH, K00128). *frmA* genes, which are responsible for detoxifying formaldehyde to formic acid, were significantly enriched in acidified metagenomes and assigned to taxa within the families Acetobacteraceae, Alcanivoraceae, Bradyrhizobiaceae, Burkholderiaceae, Caulobacteraceae, Erythrobacteraceae, Hyphomicrobiaceae, Ilumatobacteraceae, Leptolyngbyaceae, Phyllobacteriaceae, Rhodobacteraceae, Rhodospirillaceae, Sphingomonadaceae, Thiotrichaceae, and Vibrionaceae.

4.44 Carbon, Nitrogen, and Sulfur Metabolism

The majority of significantly enriched KOs within carbon fixation pathways were biased towards higher relative abundances in metagenomes from ambient samples (Figure 4.3). Of sixteen enriched KOs, thirteen were enriched in ambient metagenomes. Six of the ambient-enriched KOs were annotated to function in Calvin-Benson-Bassham (CBB) cycle, a CO_2 fixation pathway within photosynthesis. These significantly enriched KOs were primarily classified to genera belonging to the Rhodobacteraceae family, including *Jannaschia* sp., and unclassified Hyphomicrobiaceae. There was a trend for enrichment of KOs in the metagenomes of ambient samples annotated to the Wood-Ljungdahl pathway, utilized by anaerobic microbes to fix CO_2. One KO associated with two reactions within the Wood-Ljungdahl pathway was significantly enriched (*folD*, K01491). Two additional KOs

within the Wood-Ljungdahl were enriched in ambient metagenomes (*metF*, K00297; *fdhA*, K05229), but these enrichments were not statistically significant.

Two KOs within the nitrogen metabolism pathway were significantly enriched in ambient metagenomes, while four KOs were significantly enriched in metagenomes of acidified samples (Figure 4.3). Carbonic anhydrase genes (*cah*, K01674), which were enriched in ambient metagenomes and used by bacteria to convert bicarbonate from seawater into CO_2 for C-fixation and N-assimilation reactions, were classified to *Helicobacter* sp., *Ca*. Tendaria, and unclassified Alphaproteobacteria, Chloroflexi, Burkholderiales, and Rhodobacteraceae. Ferredoxin-nitrate reductase genes (*narB*, K00367), which were also enriched in ambient samples and is a key enzyme involved in the first step of nitrate assimilation in bacteria, were classified to *Labrenzia* sp., within Rhodobacteraceae, as well as unclassified Rhodobacteraceae and Bacteroidetes.

Nitrate reductase genes (*narH*, K00371), involved in dissimilatory nitrate reduction, were enriched in acidified metagenomes, and classified to *Labrenzia* sp. along with another unclassified taxon within the Rhodobacteraceae family. Also enriched within acidified samples were KOs associated with detoxifying by-products of nitrate respiration and subsequent scavenging of inorganic N products via arginine biosynthesis (*CPS1*, K01948; *hcp*, K05601).

KOs enriched within the sulfur metabolism pathway were divided evenly between ambient and acidified metagenomes (Figure 4.3). Adenylylsulfate kinase (*cysC*, K00860), sulfate adenylyltransferase subunit 2 (*cysD*, K00957), and cystathione gammasynthase (*metB*, K01739), which are all involved in sulfur

assimilation from sulfate, were enriched in ambient metagenomes. Additionally, a flavocytochrome c sulfide dehydrogenase (*fccB*, K17229) was enriched in ambient samples, and classified to *Roseovarius* sp. within Rhodobacteraceae, and unclassified Gammaproteobacteria. An aliphatic sulfonate transport system permease protein, *ssuC* (K15554), was enriched in acidified samples, with one classification to *Ilumatobacter* sp. A sulfite reductase used in dissimilatory sulfur respiration, *sir* (K00392), was enriched in acidified samples and annotated to unclassified Planctomycetes, Thiotrichales, and Ruaniaceae. Another sulfur respiratory enzyme sulfide:quinone oxidoreductase, *sqr* (K17218), was enriched in acidified samples, and assigned to a diverse array of taxa, including *Granulosicoccus* sp., Rhodobacteraceae species such as *Roseobacter* and *Sulfitobacter*, and unclassified Actinobacteria, Gammaproteobacteria, Planctomycetaeae, Myxococcales, and Proteobacteria.

4.4.5 Organic Carbon Metabolism

Abundances of genes assigned to starch and sucrose metabolism showed a strong enrichment in acidified metagenomes (Figure 4.3). Of nine differentially enriched KOs, eight were enriched in acidified samples. KOs associated with starch degradation (*ISA*; *treX*, K01214; *amyA*; *malS*, K01176) were enriched in metagenomes of acidified samples. The former KO was classified to *Blastopirellula* sp., *Nitrosomonas* sp.*, Marivita* sp.*,* and unclassified Actinobacteria, Acidobacteria, and Rhodospirillales, while genes annotated to K01176 was classified to *Bacillus* sp.*, Nocardiopsis* sp.*, Flagellimonas* sp.*, Leptolyngbya* sp.*,* and unclassified Sphingobacteriales, Chromatiales, and Planctomycetes. KOs associated with starch/glycogen anabolism were also significantly enriched in acidified metagenomes.

These included the ectonucleotide pyrophosphatase/phosphodiesterase (*ENPP1_3*, K01513), glucose-1-phosphate adenylyltransferase (*glgC*, K00975), and starch synthase (*glgA*, K00703). 1,4-alpha-glucan branching enzyme (*glgB*, K00700), responsible for converting amylose to glycogen, was also enriched in acidified metagenomes, but not significantly. K00975 and K00703 are also associated with biofilm formation pathways. The significantly enriched starch/glycogen anabolic genes were assigned to *Frankia* sp., *Nitrosomonas* sp.*, Xenococcus* sp.*, Streptomyces* sp.*, Pseudoalteromonas* sp.*, Blastopirellula* sp.*,* and unclassified Planctomycetes, Rhodospirillales, Rhizobiales, and Rhodobacteraceae. Genes annotated to beta-glucosidase (K01188), which hydrolyze terminal glucose residues from cellulose polymers, were significantly enriched in ambient samples and classified to *Flavivirga* sp. within Flavobacteriaceae.

4.4.6 Environmental Information Processing

Analysis of functional potential within environmental information processing pathways showed differing responses in ABC transporter, two-component systems, and bacterial secretion pathways to acidified conditions. Within annotated ABC transporters, 34 were enriched in phyllosphere metagenomes collected from ambient sites, while 13 were enriched in acidified metagenomes (Figure 4.3). Annotations of ABC transporters enriched in ambient metagenomes indicated the transport of glycerol, tungstate, thiamine, iron, phosphate, multiple sugars, urea, aldouronate, branched-chain amino acids, L-amino acids, polysaccharides, and amino acids (Figure 4.4). Significantly abundant transporters in acidified metagenomes included those putatively involved in the transport of sulfonate, nitrate/nitrite,

lipopolysaccharide export, cell division transport, alpha-glucoside, as well as eukaryotic-like transporter families (Figure 4.4).

With regard to gene clusters annotated to two-component sensing systems (Figure 4.3), genes for the phosphate starvation sensing and transport system (*senX3*, K07768; *phoB*, K07657; *pstS*, K02040) were enriched in ambient samples, and were classified to *Jannaschia* sp., *Granulosicoccus* sp., *Nostocales* sp., *Vibrio* sp., *Nitrosospira* sp., and unclassified Hyphomicrobiaceae. Nitrogen assimilation genes (*glnL*, K07708; *glnG*, K07712; *glnB*, K04751) were enriched in ambient samples, and were classified to *Nitrospira* sp., *Jannaschia* sp., *Granulosicoccus* sp., *Vibrio* sp., and unclassified bacteria within Rhodobacteraceae, Planctomycetes, Gammaproteobacteria, Alphaproteobacteria, and Actinobacteria.

4.4.7 Cellular Processes

KEGG orthologs annotated to be involved in bacterial biofilm formation were enriched in acidified metagenomes (Figure 4.3). In total, 11 KEGG orthologs associated with these biofilm formation pathways were enriched in ambient samples, while 25 were enriched in acidified samples. This difference was driven by a higher diversity of taxa annotated to biofilm formation reads within acidified metagenomes, compared to ambient samples.

Significantly enriched KEGG orthologs for flagellar assembly and motility also showed trends for greater enrichment in acidified samples (Figure 4.3). Genes for the sodium-dependent flagellar motor protein (*motY*, K21218) were enriched in ambient metagenomes, and associated with unclassified Gammaproteobacteria and Oceanospirillales. Genes for flagellar component proteins (*flgE*, *fliF*, *fliG*, *fliK*, and

fliM) were enriched in acidified metagenomes, and associated with unclassified Planctomycetes, Rhodobacteraceae, and Gammaproteobacteria.

4.5 Discussion

This study examined the effects of high CO_2/low pH waters on the phyllobiome composition and functional potential of *Posidonia oceanica* at a naturally occurring CO_2 vent site. The phyllobiome taxonomic composition was significantly different between acidified and ambient sites. This effect indicated a threshold effect of site conditions on the phyllobiome, in which the microbiome taxonomic composition at pH 6.59 and 7.75 were statistically similar, compared to communities at pH 8.08. These changes in the community composition were also reflected in differentially abundant taxa associated with each site. Changes in the phyllobiome functional potential across sample sites reflected key differences in microbial lifestyle adaptations to acidified conditions. Taken together, these microbial results indicate both direct and indirect effects of changing seawater carbonate chemistry on the seagrass phyllobiome.

As host-associated marine microbes, the seagrass phyllobiome will be influenced by environmental factors, host physiology, and other members of the epiphytic community. Seagrass primary productivity is thought to increase under OA conditions, and reflective of this, *P. oceanica* production and shoot density in Ischia is highest at acidified sites (Hall-Spencer *et al.* 2008). The effect of OA on seagrasses is also seen in increases in the C:N ratio of *P. oceanica* seedlings when experimentally conditioned to high pCO_2 flowthroughs (Hernán *et al.* 2016). Seagrass leaves and roots exude excess photosynthates in the form of dissolved organic carbon

(Kaldy *et al.* 2006; Barrón and Duarte 2009), which is used by the epiphytic community (Wetzel and Penhal 1979; Moriarty and Pollard 1982). Seagrass exudation is influenced by environmental perturbations, such as an increase in protein-like dissolved organic matter under light limitation (Martin *et al.* 2018a). As such, these results indicate that enhanced seagrass growth under acidified conditions may influence the phyllosphere community via increased exudation of freshly fixed carbon and other nutrients.

With regard to the effects of OA on epibiont community structuring, numerous studies have reported decreases in coralline algae and increases in filamentous algae in the seagrass macroalgal epiphyte community under high pCO_2 conditions (Hall-Spencer *et al.* 2008; Martin *et al.* 2008; Campbell and Fourqurean 2014; Donnarumma *et al.* 2014; Hassenrück *et al.* 2015). These studies also reported a general decrease in and compositional simplification of epiphyte cover (Donnarumma *et al.* 2014; Hassenrück *et al.* 2015). Changes in algal and microbial eukaryotes can strongly affect the bacterial community associated with seagrass phyllospheres (Hassenrück *et al.* 2015; Bengtsson *et al.* 2017). The significant differences in the phyllobiome of *P. oceanica* sampled from acidified and ambient waters seen in this study are likely driven indirectly by pH effects, through enriched seagrass productivity and subsequent increased availability of organic matter. Results supporting this hypothesis include the pH-driven differences within leaf microbiome communities, which was not seen within the water column samples.

In line with the results of this study, taxa within Oceanospirillales and Vibrionales orders have been previously reported to be enriched on epiphytic

assemblage of macrophytes under OA conditions (Hassenrück *et al.* 2015; Aires *et al.* 2018). *Endozoicomonas* sp. (Oceanospirillales) is a common host-associated organism, found on sea squirts (Schreiber *et al.* 2016), poriferans, molluscs, fish, cnidarians (Neave *et al.* 2016). In particular, their presence is associated with healthy corals, and loss of *Endozoicomonas* sp. is usually indicative of environmental stress (Neave *et al.* 2016). In contrast to our results, members of the *Endozoicomonas* genus within the coral microbiome have been shown to decrease in relative abundance at high pH in both experimental settings (Webster *et al.* 2016a) and near naturally occurring CO_2 vents (Morrow *et al.* 2015). As a symbiont, *Endozoicomonas* sp. are thought to play a role in nutrient exchange and cycling (Morrow *et al.* 2015) by transporting and using proteins and complex organic compounds (Neave *et al.* 2017). As such, the loss of *Endozoicomonas sp.* within stressed coral holobionts may be due to host stress response and a subsequent breakdown of the symbiosis between corals and Symbiodiniaceae, decreasing the availability of fixed carbon. The enrichment of *Endozoicomonas* sp. in acidified leaf metagenomes in this study is possibly driven by an increased availability of fixed carbon driven by increased seagrass productivity under OA conditions. *Vibrio sp.* are enriched in coral microbiomes at low pH (Meron *et al.* 2011), and *V. tubiashii* is more virulent against the blue mussel *Mytilus edulis* under OA conditions (Asplund *et al.* 2014). These previous studies are congruent with our findings and show that seagrass phyllobiomes may harbor an increased abundance of *Vibrio* sp. under OA conditions, and act as a reservoir of pathogens against marine organisms.

Ambient-enriched taxa were typical marine surface-inhabiting microbes. Members of the Rhodobacteraceae family, including *Jannaschia* sp., are commonly found in marine epiphytic communities and may be adapted to a symbiotic lifestyle with marine macrophytes and algae (Dogs *et al.* 2017). Metagenome results suggested that *Jannaschia* sp. in *P. oceanica* phyllospheres play a role in carbon, nitrogen, and phosphorus cycling, as well as in enhancing plant growth through phytohormone production. *Granulosicoccus* sp. (Gammaproteobacteria) has previously been detected and isolated from several marine macrophytes, including seagrass (Kurilenko *et al.* 2010; Crump *et al.* 2018), brown algae (Park *et al.* 2014), seaweed, and kelp (Weigel and Pfister 2019). Metagenome results yielded insights into the functional role of *Granulosicoccus* sp. within the seagrass phyllosphere, including biofilm formation, and phosphate, nitrogen, and sulfur cycling via sulfide oxidation and DMSP metabolism via *dmdA*, which has also been previously detected in the completed *Granulosicoccus antarcticus* genome (Kang, Lim and Cho 2018).

The Cyanobacteria *Chroococcidiopsis* sp. was enriched in ambient conditions. This result may be due to deleterious effects of low pH on cyanobacteria (Hong *et al.* 2017), though overall cyanobacteria production and N_2 fixation responses to OA are highly variable, due a myriad of factors, including sensitivity to CO_2 and variations in nutrient concentrations (Eichner, Rost and Kranz 2014). However, a previous study of seagrass microbial assemblages occurring at CO_2 vents also found a decrease in Cyanobacteria at vent sites (Hassenrück *et al.* 2015). In this study, the enrichment of Cyanobacteria, in combination with enrichment of genes associated with carbon fixation pathways, indicated a trend towards an autotrophic microbial lifestyle under

ambient conditions within *P. oceanica* phyllobiomes. Conversely, the increased relative abundance of heterotrophs such as *Endozoicomonas* sp., *Vibrio* sp., and other Gammaproteobacteria, as well as the enrichment of genes associated with the starch and sucrose metabolism pathway, indicate a trend towards heterotrophic lifestyles in the acidified phyllobiome communities.

Sucrose is the end product of photosynthesis (Stein and Granot 2019), and is stored in seagrass leaves, roots, and rhizomes (Burke, Dennison and Moore 1996; Jiang, Huang and Zhang 2010). Sucrose concentrations have been seen to increase in both adult seagrasses (Jiang, Huang and Zhang 2010) and seedlings (Hernán *et al.* 2016) under increasing pCO_2 concentrations. An increased concentration of sucrose may be supporting heterotrophic microorganisms within the *P. oceanica* phyllobiome under OA conditions, which may, in turn, account for the observed enrichment of starch and sucrose metabolism genes within the acidified metagenomes.

The enrichment of KOs within biofilm formation and flagellar assembly pathways indicate a bias towards enriched biofilm communities under acidified conditions. Previous studies have shown that marine biofilms increase in abundance under high pCO2 and low pH (Lidbury *et al.* 2012; Russell *et al.* 2013). Biofilms offer protection to microbes from environmental stress, such as suboptimal temperature, pH, and salinity, as well as increased access to nutrients and organic compounds due in part to production of extracellular enzymes (Flemming and Wingender 2010; Dang and Lovell 2016; Carvalho *et al.* 2018). The nutrient and oxygen gradients within biofilms allow a greater diversity of metabolic pathways, which are supported by enhanced productivity and availability of fixed carbon within

the seagrass host under OA conditions. The increase in genes for microbial biofilms in the *P. oceanica* phyllobiome under acidified conditions indicate an abundance of biofilms under OA conditions, supporting a broad range of microbial activity and enhancing the biogeochemical cycling capacity of the meadow (Dang and Lovell 2016).

There was a large and diverse array of significantly enriched KEGG orthologs assigned to ABC transporters in ambient samples, relative to the acidified samples, which may be a sign of nutrient limitation. For example, under oligotrophic conditions, SAR11 has been shown to express high proportions of nutrient transporters, specifically for phosphate, amino acids, phosphonate, and sugars, relative to other proteins (Sowell *et al.* 2009). In this experiment, the phyllosphere metagenome under ambient conditions were enriched with ABC transporters for these nutrients, which are often expressed under nutrient limited conditions (Kolowith, Ingall and Benner 2001; Martiny, Coleman and Chisholm 2006). Similarly, the nitrogen regulator *glnL* was enriched in ambient samples, and is present in high amounts during nitrogen limitation (Zimmer *et al.* 2000). This phenomenon was also seen in the sponge microbiome under ambient and OA conditions (Botté *et al.* 2019), though the authors speculated that the sponge microbiome under OA conditions was experiencing a reduction in the amount of carbohydrates and nutrients from the water column and the sponge host. Alternatively, we hypothesize that the enrichment of ABC transporters in the *P. oceanica* phyllobiome under ambient conditions is due to resource limitation, leading to a need for additional nutrient transporters.

The *P. oceanica* phyllobiome structure and functional potential were likely affected by direct effects of pCO_2 concentrations and pH, and indirect effects, including plant host responses to changes in carbonate chemistry. These effects manifested in signals indicating differing microbial lifestyles associated with ambient and acidified phyllobiomes. Ambient phyllobiomes saw signs towards autotrophy and nutrient limitation, while acidified phyllobiomes showed signals for heterotrophy and protective mechanisms against acidification via biofilm formation, which can also contribute to nutrient acquisition and cycling. However, we also acknowledge the limitations of this study, including the fact that functional profiles obtained through metagenome sequencing may not be indicative of actual processes, and conditions at naturally occurring CO_2 vents may not be fully representative of future OA conditions (Vizzini *et al.* 2013). Given these caveats, this study identified trends in microbiome responses to OA, and was able to link members of the *P. oceanica* phyllobiome to potential functions, revealing functional capacities of the microbial community, and responses to future marine conditions. Results of this study suggest that OA may enhance biogeochemical cycling in acidified seagrass meadows as a whole, through increased seagrass productivity and enhanced microbial metabolism within biofilms.

4.6 Acknowledgments

Thank you to Dr. Gema Hernán, Dr. Jorge Terrados, and Captain Vicenzo Morgera for their fieldwork contributions.

4.7 Figures

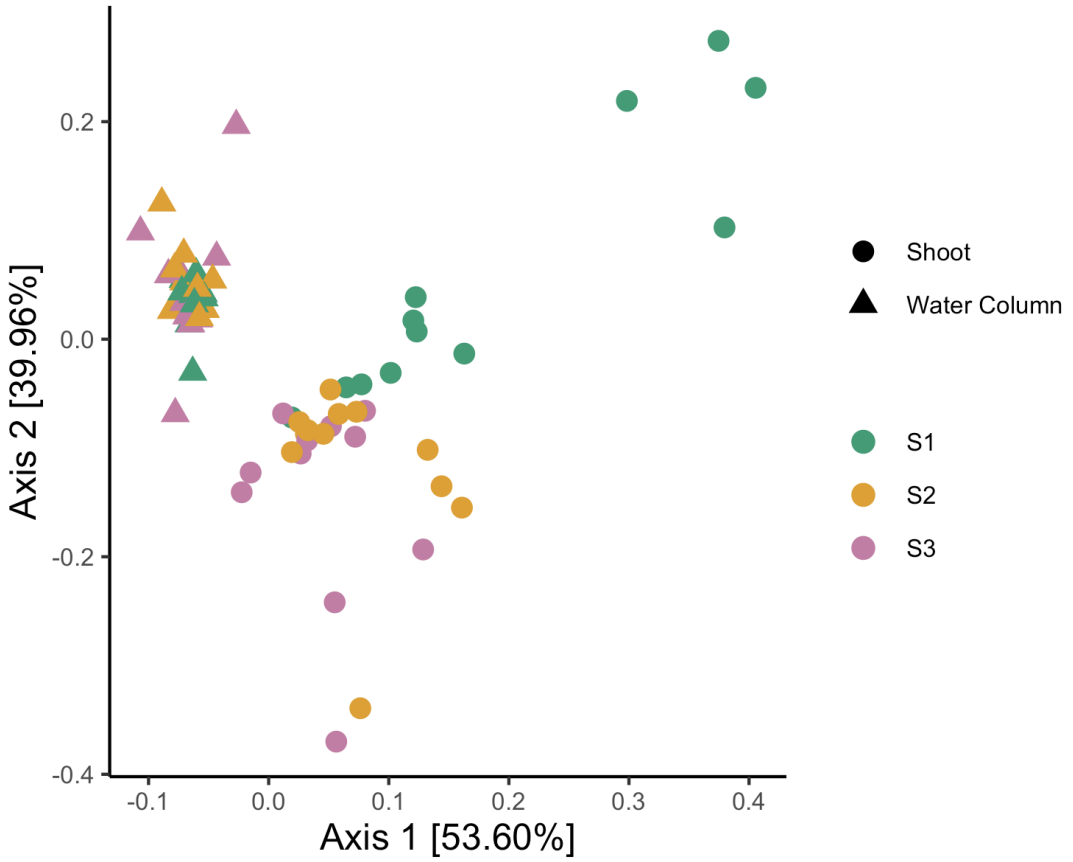

Figure 4.1 | Microbial communities associated with *P. oceanica* shoots and surrounding water column. Principle coordinate analysis plot of microbial community structure with first and second PCoA axes derived from Aitchson beta-diversity distance metrics of 16S amplicon data. Water column and shoot microbiomes cluster distinctly from each other (PERMANOVA, p = 0.001, pseudo-F = 27.98). Leaf microbiomes cluster different by site (PERMANOVA, p = 0.001, pseudo-F = 7.58), while there was no site effect on water column microbiomes (PERMANOVA, p = 0.430, pseudo-F = 0.72). S1 represents ambient samples, while S2 and S3 represent acidified samples.

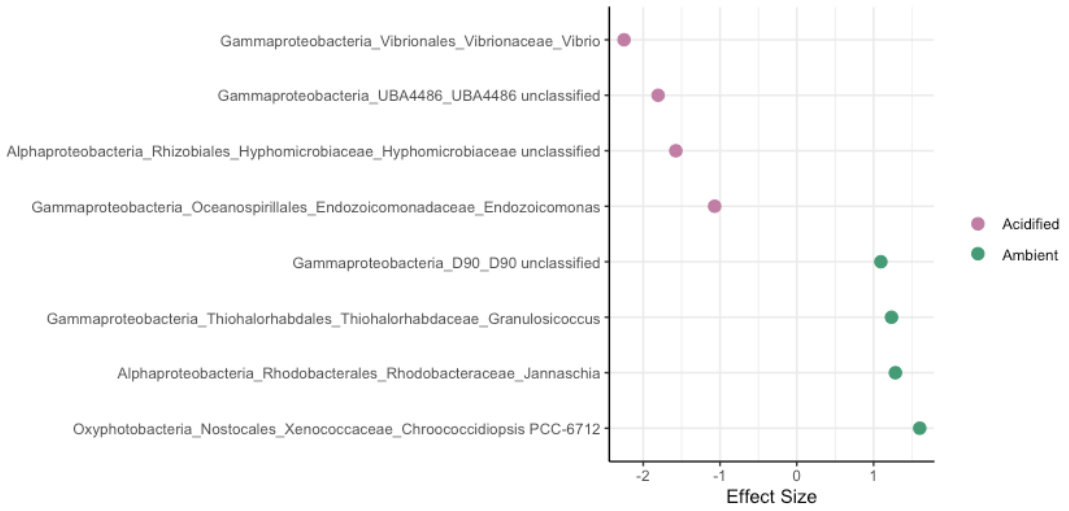

Figure 4.2 | Differentially abundant genera in acidified and ambient groups, derived from ALDEx2 analysis of 16S amplicon data. X-axis represents median effect size of each taxon, calculated as a ratio of the median difference in centered log ratio values and the median of the largest difference in centered log ratio values between ambient and acidified groups. Taxonomic features with correct p-values < 0.05 and effect size > | 1 | are represented here.

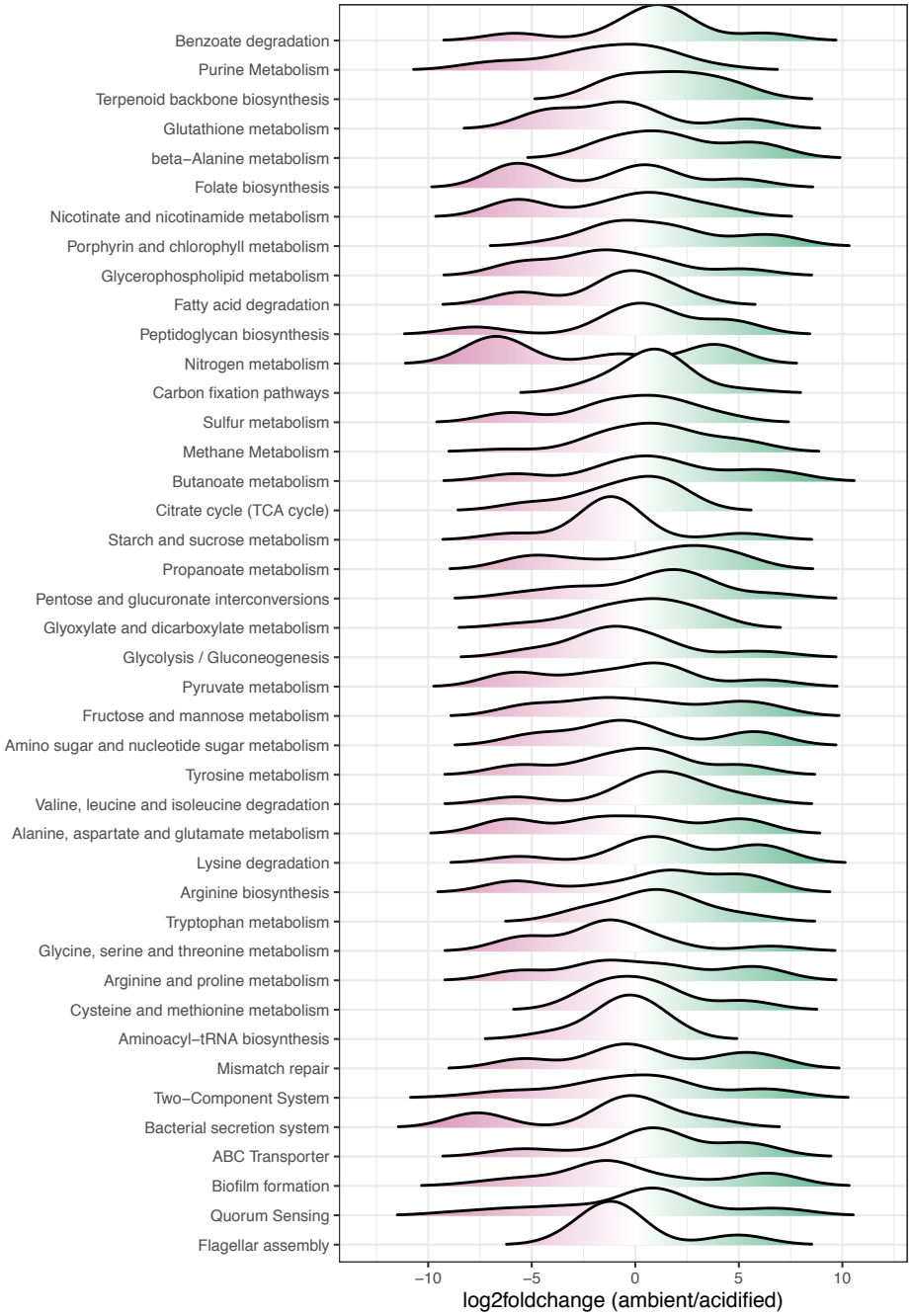

Figure 4.3 | Differential functional potential of metagenomes derived from acidified (pink) and ambient (green) *P. oceanica* leaf samples. Density plots represent the number of genes annotated to KEGG Orthology (KO) groups plotted as a function of the log 2 fold change within each pathway that were significantly enriched in either acidified or ambient conditions. Differential abundance was calculated using DESeq2.

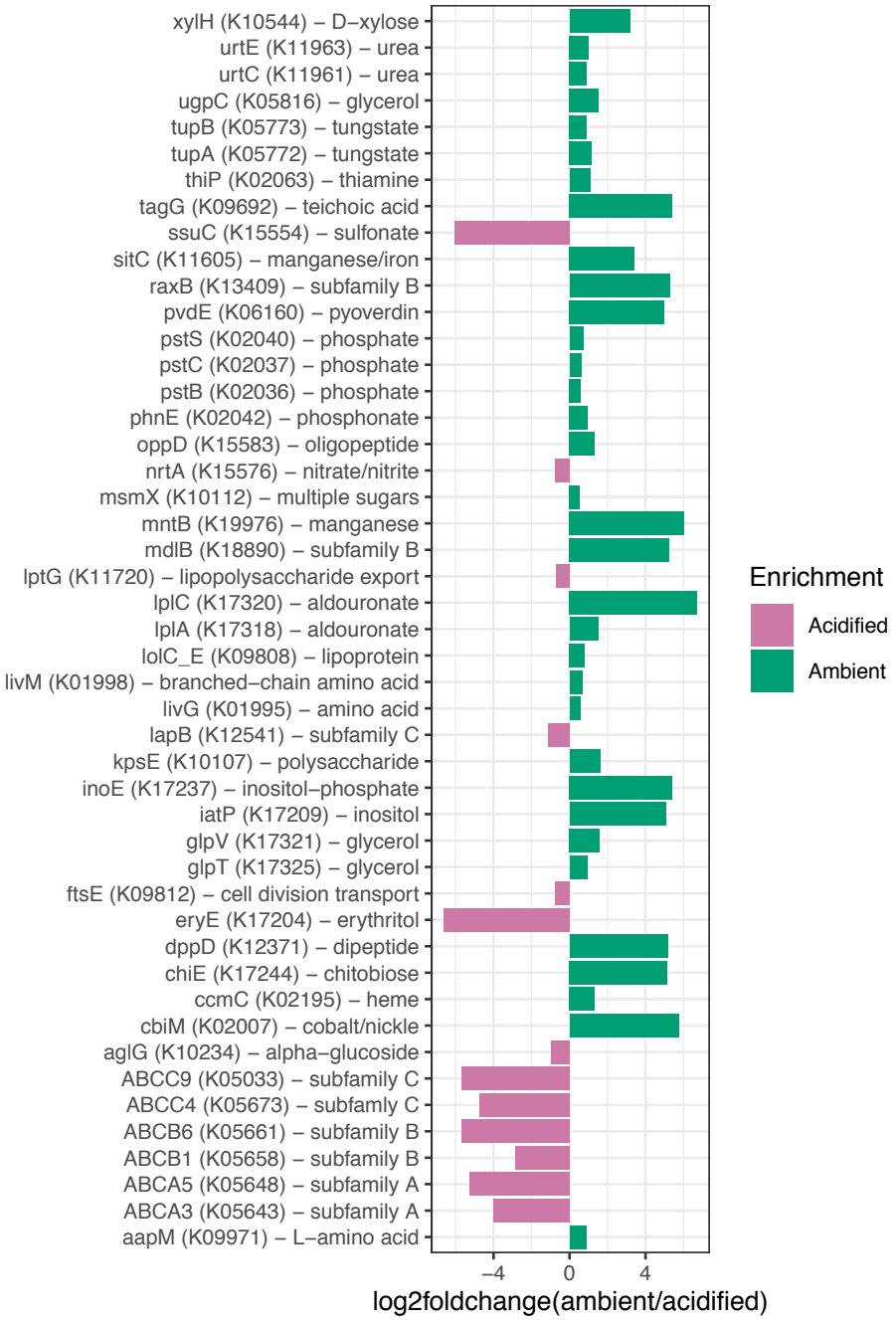

Figure 4.4 | Differential abundance of genes annotated to KEGG orthology (KO) groups within the ABC transporter pathway. X-axis represents the log 2 fold change of KOs between acidified and ambient metagenomes.

5 Recovery and Community Succession of the *Zostera marina* Rhizobiome After Transplantation

Lu Wang

MK English

Fiona Tomas

Ryan S. Mueller

Manuscript Under Review

Applied and Environmental Microbiology

1752 N St. NW, Washington DC, 20036, USA

5.1 Abstract

Seagrasses can form mutualisms with their microbiomes that facilitate the exchange of energy sources, nutrients, and hormones, and ultimately impact plant stress resistance. Little is known about community succession within the belowground seagrass microbiome after disturbance and its potential role in the plant's recovery after transplantation. We transplanted *Zostera marina* shoots with and without an intact rhizosphere, and cultivated plants for four weeks while characterizing microbiome recovery and effects on plant traits. Rhizosphere and root microbiomes were compositionally distinct, likely representing discrete microbial niches. Furthermore, microbiomes of washed transplants were initially different from those of sod transplants and recovered to resemble an undisturbed state within fourteen days. Conspicuously, changes in microbial communities of washed transplants corresponded with changes in rhizosphere sediment mass and root biomass, highlighting the strength and responsive nature of the relationship between plants, their microbiome, and the environment. Potential mutualistic microbes that were enriched over time include those that function in the cycling and turnover of sulfur, nitrogen, and plant-derived carbon in the rhizosphere environment. These findings highlight the importance and resiliency of the seagrass microbiome after disturbance. Consideration of the microbiome will have meaningful implications on habitat restoration practices.

5.2 Introduction

The rhizobiome has long been recognized to have important impacts on plant growth and health (Hiltner 1904). The microbes of the rhizobiome, which directly

interact with and are influenced by the roots (Bandyopadhyay *et al.* 2017), can benefit their plant hosts through recycling and producing bioavailable nutrients (Welsh *et al.* 1996a; Welsh 2000; Brodersen *et al.* 2017), increasing disease resistance through competition with or inhibition of pathogens (Bais, Fall and Vivanco 2004), and influencing plant growth and stress tolerance through production of phytohormones (Morgan, Bending and White 2005; Yang, Kloepper and Ryu 2009b). Community composition within the rhizobiome is shaped by plant metabolism and physiology, which controls rhizodeposition, exudation of organic carbon and nitrogen, and release of defense compounds (Morgan, Bending and White 2005; Bais *et al.* 2006; Lebeis *et al.* 2015). The quantity and composition of exudates can impact microbial activity in the rhizosphere and vary as a result of many factors (Carvalhais *et al.* 2013; Chaparro, Badri and Vivanco 2014; Tkacz *et al.* 2015; Lareen, Burton and Schäfer 2016). While plant-rhizobiome interactions are relatively well-defined for terrestrial plants, analogous interactions between aquatic plants and their microbiomes have only recently started to become known (Cúcio *et al.* 2016; Garcias-Bonet *et al.* 2016).

Seagrasses are marine vascular plants that form key ecosystems on coastal areas worldwide, where they provide numerous ecosystem services (Orth *et al.* 2006). Recent evidence suggests that members of the seagrass microbiome may modulate host growth and response to environmental stresses (Cúcio *et al.* 2016; Fahimipour *et al.* 2017; Crump *et al.* 2018). In addition to fixing nitrogen and producing phytohormones (Lehnen *et al.* 2016; Tarquinio *et al.* 2019), the seagrass microbiome is proposed to mitigate the toxic effects of hydrogen sulfide in sediments, which have been linked to declines in seagrass health and localized die-back events (Holmer and

Bondgaard 2001; Borum *et al.* 2005; Martin *et al.* 2019). The seagrass rhizobiome is thought to be primarily influenced by exudation of carbon compounds, which can provide up to 60% of the carbon assimilated by these microbes (Donnelly and Herbert 1998; Kaldy *et al.* 2006), and by radial oxygen loss from roots, which may promote colonization of the rhizosphere by distinct bacteria (Brodersen *et al.* 2015b; Martin *et al.* 2019).

The effect of rhizosphere disturbance on the composition of seagrass microbiomes and plant health has rarely been explored (Milbrandt, Greenawalt-Boswell and Sokoloff 2008). Yet, it may be important both for plant recovery after a disturbance and in the context of restoration outcomes, which are highly variable and dependent on methodology (van Katwijk *et al.* 2009, 2016; Cunha *et al.* 2012; Matheson *et al.* 2017). Sod transplants, which transfer shoots with intact rhizospheres, have historically been one of the more successful methods, potentially because the intact rhizosphere sediment acts as a natural anchor and retains functional relationships between the plant and its rhizobiome (van Katwijk *et al.* 2009). Conversely, bare root transplants are generally less successful and could experience a decrease or lag in plant performance as the rhizobiome redevelops after transplantation. Importantly, microbial community succession after disturbance can strongly affect host health in several microbiome-host systems (e.g., algae, corals, and humans), whereby dysbiosis disrupts host functioning and increases susceptibility to disease (Cochetière *et al.* 2005; Ritchie 2006; Longford *et al.* 2019a). Thus, it is important to understand the recovery of seagrass microbiomes after disturbance, as this may impact seagrass health and resistance to environmental stresses.

In this study, we characterized the recovery of seagrass rhizobiomes post-disturbance by transplanting *Zostera marina*, commonly referred to as eelgrass, with and without an intact rhizosphere and sampling for plant and microbiome characteristics over the course of 28 days. We expected to see the rhizobiome of seagrass transplanted without an intact rhizosphere recover over time to resemble that of the control plants, with a corresponding delay in the response of plant growth traits.

5.3 Materials and Methods

5.3.1 Experimental Setup

Sediment (top ~15 cm) and 90 healthy *Z. marina* primary shoots were manually collected at low tide from intertidal eelgrass beds in Yaquina Bay, OR, USA (44.624518, -124.044372) during July 2018. Seagrasses in this estuary typically grow under eutrophic conditions with $NO_2 + NO_3$ concentrations reaching ≥ 30 μM during summer months when upwelling is active along the Oregon coast (Brown and Ozretich 2009). Additionally, sediments in the estuary are strongly anoxic with high porewater concentrations of sulfide (10 - 80 μM) and total dissolved inorganic nitrogen (≥ 10 μM) (Morse *et al.* 2003; Wang, Tomas and Mueller 2020). After collection, sediment was sieved through wire mesh with 0.25 cm^2 openings and held in buckets filled with seawater for 24 h. Plants were manually extracted from the beds by excavating a ~3 cm radius sediment ball around the roots and collecting terminal shoots with attached rhizome fragments, a method that is similar to those previously used in studies on seagrass transplantation (Davis and Short 1997; Zhou *et al.* 2014; Novak *et al.* 2017). The loosely attached, non-rhizosphere sediment was dislodged

from the rhizome fragment by gentle agitation. This procedure adheres to the operational definition of the rhizosphere -- the sediment attached to the roots after manually shaking (Lundberg *et al.* 2012; Cúcio *et al.* 2016) -- while also capturing the biological definition of the rhizobiome, i.e., the microbial community that is closely associated with plant roots and is influenced by plant metabolism (Hiltner 1904). Plants were placed in plastic bags and processed for transplantation within three hours of collection.

Individual plants were randomly assigned to either the "wash" or "sod" transplant treatment group. The rhizospheres of plants in the washed group were removed by a gentle seawater rinse, retaining the rhizoplane bacteria and replicating the potential rhizosphere loss in transplantation efforts. The rhizospheres of plants assigned to the sod treatment group were left undisturbed. The rhizomes of plants in the wash treatment were trimmed to retain five internodes connected to the first five root bundles (Kaldy 2012), and rhizomes of sod transplants were standardized by trimming to lengths matching those of washed plants. Plant leaves were standardized across treatments by trimming to 50 cm (Tomas *et al.* 2011). PVC cylinders (18h x 7.6d cm) were filled with sediment and the meristem of each plant was positioned near the top of each. Sediment was added to cover the rhizome, roots, and rhizosphere (if attached). Planters were randomly and evenly placed inside a 2000-liter outdoor flow-through tank filled with water from Yaquina Bay.

5.3.2 Plant Sampling and Morphometric Analyses

Whole plant sampling was performed on the initial day of the experiment (t = 0) prior to transplantation and on days 1, 3, 7, 14, 21, and 28 post-transplantation. At least five plants from each treatment were collected and destructively sampled at each time point. Plants were removed from the mesocosm tank and initially agitated in air to remove loosely attached sediment, via 2-5 shakes with consistent force. The rhizosphere sediment was then washed from plant roots in 25 ml of sterile seawater and collected in sterile tubes. One ml of the resulting slurry was transferred to a sterile microcentrifuge tube and stored at -80 °C until DNA extraction. One pair of the youngest root cluster was then removed from the plant, transferred to a sterile microcentrifuge tube, and stored at -80 °C for DNA extraction.

Roots not used for extractions were removed from plants, counted, and measured to calculate average lengths. Rhizome lengths and longest leaf lengths were recorded for plants. Biomass measurements were recorded for the component parts of plants (i.e., leaves, rhizomes, and roots) after drying for seven days at 40 °C. The residual sediment slurries from plants (~24 ml/plant) were vacuum-filtered through pre-weighed GFF membranes, dried as above, and net weights were recorded as rhizosphere masses.

5.3.3 DNA Extraction, PCR, and Amplicon Sequencing

Microbial community DNA was extracted from frozen roots and sediment slurries using a CTAB and phenol:chloroform extraction method (Crump *et al.* 2003). within six weeks of sample collection. DNA was extracted from the root phytoplane

but may also include DNA from the root endosphere. Amplicon sequencing libraries were constructed from 25-100 ng of template DNA using a one-step PCR with bar-coded 515F and 806R universal 16S rRNA (v3-v4) primers (Kieft *et al.* 2018). PCRs were performed using AccuStart II ToughMix Polymerase following the manufacturer's instructions and performing a thermal cycle program of: 94 °C (3 min.); 25 cycles of 94 °C (45 sec.), 50 °C (60 sec.), 72 °C (90 sec.); 72 °C (10 min.); 4 °C (hold).

Successful amplification reactions (139 of 143 samples) were purified using Agencourt AMPure XP beads following the manufacturer's instructions, with the exception that a 1:1 ratio of bead solution and PCR product was used. A Qubit 2.0 fluorometer (Thermo Fisher Scientific, Waltham, MA, USA) was used to quantify concentrations of purified amplicons, and these values were used to evenly pool libraries prior to sequencing with the Illumina MiSeq (Illumina Inc., San Diego, CA, USA).

The 'DADA2' package (v 1.10.1) (Callahan *et al.* 2016) within the Bioconductor software environment (v 3.8) (Morgan 2018) of the R Project (v 3.5.2) (R Core Team 2018) was used to process raw sequencing reads. All reads were initially quality filtered using the 'filterAndTrim' command with default settings ("maxN=0, maxEE=c(2,2), truncQ=2"). To avoid computational limitations resulting from the fact that multiple libraries contained >>100000 reads, the resulting high-quality reads of libraries were randomly down-sampled to 15000 paired-end reads (BioProject ID: PRJNA591021). This resulted in 126 libraries with ≥ 8891 high-

quality paired-end reads used as inputs for the remaining DADA2 pipeline (i.e., error-rate training, sample inference, paired-read merging, chimera removal, amplicon sequence variant (ASV) counting, and taxonomic assignment against the SILVA Ref NR 132 database) (Quast *et al.* 2013). An average of 7819 ± 1430 sequences were retained across all libraries (Table S5.1), and sequence counts were rarefied to the library with the minimum count (n = 4881) using the 'rrarefy' function of 'vegan' (v 2.5-5) (Oksanen *et al.* 2018). A final count table with individual samples containing 119 ± 27 ASVs and 2296 ASVs detected across all samples was generated.

A filtered alignment of representative ASV sequences against the pre-computed SILVA Ref NR 132 alignment was created using the 'align.seqs' and 'filter.seqs' commands of the mothur software package (v 1.40.5) (Schloss *et al.* 2009). FastTreeMP (v 2.1.7) (Price, Dehal and Arkin 2010) calculated a phylogenetic tree from the filtered alignment applying a generalized time-reversible model of evolution (Tavaré and Miura 1986). The resulting tree was midpoint rooted using 'reroot.pl' (Junier *et al.* 2010).

5.3.4 Statistical Analyses

The 'phyloseq' package (v 1.26.1) (McMurdie and Holmes 2013) was used to import the phylogenetic tree, count table, taxonomy table, sequence FASTA of ASVs, and a matrix containing plant trait data, sampling date, plant compartment information, and treatment assignments for each sequence library into R. Single pseudocounts were added to plant trait variables containing zeros, allowing for $\log_2$-transformation. All statistical testing was performed in R and plots were created using

‘ggplot2’ (v 3.1.1) (Wickham 2016) and ‘ggpubr’ (v 0.2.1) (Kassambara 2019). Summary statistics are reported as means (M) plus/minus standard deviation, unless otherwise stated.

The ‘vegdist’ function of ‘vegan’ was used to create a Euclidean distance matrix of samples based on $\log_2$-transformed, centered, and scaled plant morphometric data. The ‘UniFrac’ function of ‘phyloseq’ created weighted UNIFRAC distance matrices (Lozupone *et al.* 2012). from count tables and the phylogenetic tree. To test for the significance of sample clustering, the ‘adonis2’ function of ‘vegan’ was used with 1000 permutations (Anderson 2001). Two- and three-way tests were performed multiple times with the order of the independent variables in the formula changed to ensure consistency of test results, regardless of term precedence. To visualize sample distance relationships, Principal Coordinates Analyses (PCoAs) (Borg and Groenen 2005) were performed using the ‘pcoa’ command of ‘ape’ (v 5.3) (Paradis and Schliep 2018). In figures, percentages on axes labels of PCoA plots report the percent variation captured by each coordinate, and axes lengths are scaled to this number. Spearman’s rank correlations (ρ) between distance matrices of plant trait and ASV count data were determined using the ‘bioenv’ and ‘mantel’ functions of ‘vegan’.

Significant effects of treatment and/or time on response variables were assessed with Student’s T-tests and Analyses of Covariance (ANCOVAs) using the ‘t.test’ and ‘ancova’ functions of ‘stats’ (v 3.5.2) and ‘HH’ (v 3.1-37) (Heiberger 2019). If no significant interactions between the treatment effect and the time

covariate were detected, an Analysis of Variance (ANOVA) was performed on a reduced model without the interaction term using the 'Anova' function of the 'car' package and applying Type II sum of squares calculations (Fox and Weisberg 2019). Significant differences in ASV abundances between plant compartments ($\alpha \leq .01$) were tested using the 'DESeq' function of 'DESeq2' (v 1.22.2) (Love, Huber and Anders 2014).

Generalized linear mixed models (GLMMs) (Bolker *et al.* 2009) were used to determine significantly different temporal trends in abundance for microbial taxa. A Tweedie compound Poisson distribution was chosen for this model given that it best captures the nature of amplicon sequence datasets (e.g., overdispersion, zero-inflated datasets, and continuous values) (Sharpton *et al.* 2017). The 'cpglmm' function of the 'cplm' R package (Zhang 2013) was used for time-series analyses following the general procedure outlined in (Sharpton *et al.* 2017). Summarized sequence count tables of family-level taxonomic units were created and full GLMMs were fit relating counts to treatment, days post transplantation, the interaction of main effects, and random effects of each taxon. Taxa detected in > 25% of samples and with cumulative sequence counts > 100 reads were tested to focus on the most abundant, prevalent, statistically robust groups in our samples. *P*-values of modeled slopes and intercepts were obtained via likelihood ratio tests between the full model and two reduced models where the interaction or the treatment variable was removed. Slope and intercept *p*-values were adjusted using the Benjamini-Hochberg method (Benjamini and Hochberg 1995), and adjusted values ≤ .05 were considered significant. Resulting intercepts with positive values indicated that a taxon's initial

abundance was higher in washed versus sod transplant rhizospheres, with negative intercepts implying the opposite. Modeled slopes with positive coefficients indicated that rate of increase for a given taxon's abundance was greater over the course of the experiment in the wash treatment than in sod samples, and vice versa for negative slope coefficients.

5.4 Results

5.4.1 Changes in *Z. marina* Traits After Transplantation

We quantified several traits to assess plant growth (i.e., biomass and lengths of leaves, rhizomes, and roots) and to measure the mass of rhizosphere sediment (i.e., the sediment firmly attached to roots after plant collection; Figure S5.1). Plant traits varied significantly due to an interaction between days post transplantation (DPT) and treatment (PERMANOVA: DPT x Treatment $F_{1,61} = 2.85$, $p = .036$, $R^2 = .03$). While plant traits did not differ amongst treatments at the beginning of the experiment (PERMANOVA: Day 0 Treatment $F_{1,8} = 1.12$, $p = .304$, $R^2 = .12$; Figures 5.1B and S5.1), they exhibited overall differences within seven days after transplantation, and plant traits of the wash treatment began to more strongly resemble those of the sod treatment after one week (Figure 5.1A). For sod transplants, the most variation in traits occurred within the first seven days of the experiment, after which these measures stabilized and remained relatively constant (Figures 5.1B and S5.1). Conversely, changes in the traits of washed plants occurred more slowly, stabilizing only after fourteen days. By the end of the experiment no between-treatment variation in traits was evident (PERMANOVA: Day 28 Treatment $F_{1,13} = 1.00$, $p = .422$, $R^2 = .07$; Figures 5.1B and S5.1).

Principle coordinate analysis showed that 22.8% of the overall variation of plant traits was synchronized between treatments (Figure 5.1B). This variation likely relates to significant increases in the measurements of most traits over the course of the experiment in both treatment groups, indicating overall growth of *Z. marina* shoots after transplantation regardless of rhizosphere presence (Figure S5.1). For instance, upon experiment completion, total biomass of transplants had increased 1.5-fold on average, and lengths of leaves and rhizomes had increased 1.5 and 1.8-fold, respectively (Figure S5.1). Whereas differences in traits due to treatment were minimal at the beginning and end of the experiment, they were most pronounced from days one to fourteen of the experiment when sod transplants consistently demonstrated greater increases compared to those of the washed transplants (Figure 5.1C). For example, root biomass and root length were not significantly affected by rhizosphere removal at the beginning of the experiment (Student's t-test [root biomass]: Wash M = 0.016 ± 0.012 g, Sod M = 0.012 ± 0.006 g, $t(8) = -0.57$, $p = .58$; Student's t-test [root length]: Wash M = 6.04 ± 1.91 cm, Sod M = 4.46 ± 0.92 cm, $t(8) = -1.67$, $p = .13$). Importantly, though, sod transplants increased 1.7- fold in root biomass on average and wash transplants increased 1.1-fold by the end of the experiment (ANCOVA: Treatment $F_{1,72} = 16.16$, $p = .0001$; Figures 5.1C, S5.1C). As expected, rhizosphere sediment mass significantly varied with the interaction between the time covariate and the main treatment effect (ANCOVA: DPT x Treatment $F_{1,71} = 18.78$, $p < .00005$; Figure S5.1D). That is, the rhizosphere sediment mass attached to roots of sod transplants did not change significantly during the experiment, whereas sediment accumulation on washed roots rapidly increased after seven days

post transplantation and recovered to levels observed on sod transplants by the end of the experiment (Welch's t-test: Wash M= 16.34 ± 10.03 g, Sod M = 25.25 ± 13.26 g, $t(13) = 1.48$, $p = .16$, Figure S5.1D).

5.4.2 Microbial Community Differences Between *Z. marina* Rhizosphere and Roots

When considering all samples, microbial communities were most strongly clustered based on the belowground compartment (i.e., root vs. rhizosphere compartment; PERMANOVA: $F_{1,112} = 26.33$, $p = .001$, $R^2 = .16$; Figure 5.2A). Forty-two prokaryotic amplicon sequence variants (ASVs) exhibited significantly different relative abundances in the rhizosphere versus roots (Table S5.1). Twenty-five were enriched in the rhizosphere, while the remaining 17 were in greater relative abundance on roots (Figure 5.2B). Significant ASVs were most commonly assigned to the Proteobacteria and Bacteroidetes phyla (n = 18 and 12, respectively), with 66% of the former taxon and 75% of the latter detected in higher relative abundance in rhizosphere over root communities. Conversely, ASVs of the Epsilonbacteraeota phylum were typically in higher relative abundances in root samples (five of seven ASVs). Due to the strong effect of compartment on microbial community structure, the remaining microbial diversity results are presented separately for rhizosphere and root samples.

5.4.3 Changes in Rhizosphere Microbiomes After Transplantation

Temporal changes in the structure of rhizosphere microbial communities mirror the patterns observed for plant trait data. That is, initial differences were observed between rhizosphere communities from plants of different treatment groups,

but communities became more similar in structure by the end of the experiment (Figure 5.3A). The most variation was due to a shift of rhizosphere communities of washed transplants along the first principle coordinate to more strongly resemble sod samples after seven days. As observed for plant traits, a significant interactive effect of treatment and time on the rhizosphere community structure was detected (PERMANOVA: DPT x Treatment $F_{1,58} = 2.53$, $p = .005$, $R^2 = .03$).

To further investigate the effect of rhizosphere disruption on the recovery of the rhizosphere communities, we analyzed the different treatment samples separately. Structural changes in the rhizosphere communities of the sod and wash treatment groups both demonstrated significant time effects, but a stronger temporal correlation was detected for the washed than sod transplant rhizosphere communities (PERMANOVA: DPT [Wash transplants] $F_{1,25} = 6.47$, $p = .001$, $R^2 = .21$; DPT [Sod transplants] $F_{1,33} = 3.57$, $p = .001$, $R^2 = .10$). A shift in community structure of washed transplants occurred at seven days and corresponded to the point of accelerating sediment accumulation on washed roots. Additionally, overall community changes were significantly correlated to rhizosphere sediment masses of all washed plants (Mantel test $p = .004$, Spearman's $\rho = .25$; Figure 5.3B). For sod transplants, however, sediment mass was not correlated with rhizosphere community structure (Mantel test $p = .43$, Spearman's $\rho = .0001$; Figure 5.3C), and was instead most strongly correlated with plant growth traits (Mantel test: Leaf Length + Rhizome Length + Leaf Biomass $p = .001$, Spearman's $\rho = .27$).

Using regression analyses with summarized sequence counts of family-level taxonomic units, we identified microbial taxonomic families that were specifically associated with *Z. marina* rhizosphere development during the experiment (GLMM: *adjusted* $p \leq .05$; Table S5.2). Thirty-two families had significantly different modeled intercepts between treatments, and 14 families exhibited significant differences in modeled slopes. Six families were found with significant differences in both slopes and intercepts (Figure 5.3D). Of these six, the Ruminococcaceae and Sulfurovaceae had negative intercepts and positive slope coefficients. For example, higher relative abundances of the Ruminococcaceae were detected in the sod samples on average, but the rate of increase of this taxon's abundance was greater in washed samples over time. The Sulfurovaceae showed a similar temporal pattern of abundance in washed samples, but in sod transplants this taxon generally demonstrated a decrease over time. The remaining four families (Clostridiales Family XII, Sandaracinaceae, Chromatiaceae, and Rhizobiales [Incertae sedis]) all showed similar patterns (Figure 5.3D); in washed transplants they rapidly decreased to low levels within the first seven days of the experiment, whereas in sod transplants there was little to no detection of them throughout the experiment.

5.4.4 Changes in Root Microbiomes After Transplantation

Recovery dynamics of root microbiomes were largely similar to those observed for rhizosphere communities (Figure 5.4A). A significant effect of the interaction between time and treatment on the structure of all root communities was detected (PERMANOVA: DPT x Treatment $F_{1,58} = 2.01$, $p = .043$, $R^2 = .03$). A relatively strong effect of time was evident for communities from wash transplants

(PERMANOVA: $F_{1,26} = 5.91$, $p = .001$, $R^2 = .19$; Figure 5.4B), but not for sod transplants (PERMANOVA: $F_{1,28} = 1.78$, $p = .096$, $R^2 = .06$; Figure 5.4C). Changes in washed root microbiome community structure were not correlated with sediment mass accumulation (Mantel test: $p = .085$, Spearman's $\rho = .13$), and were instead most strongly correlated with leaf length and rhizome mass (Mantel test: $p = .001$, Spearman's $\rho = .32$). In contrast, the root microbiomes of sod transplants were relatively stable over time (PERMANOVA: $F_{1,28} = 1.78$, $p = .096$, $R^2 = .06$; Figure 5.4C), and not correlated with any single plant trait or combination thereof.

Regression analyses identified 25 taxonomic families with significant differences in modeled intercepts between treatments, but no differences in modeled slopes (Table S5.3). Another four families were found to have no detectable differences in intercepts, but significant differences in slopes. Five families were found to have significant differences in both modeled intercepts and slopes (Figure 5.4D). The Lentimicrobiaceae, Ruminococcaceae, and the Desulfobacteraceae were all modeled to have largely similar dynamics, with negative intercepts and positive slope coefficients. Abundances of these taxa on roots of sod transplants rapidly declined within seven days of transplantation, followed by a more gradual increase in abundance over the last two weeks of the experiment (Figure 5.4D). Conversely, on roots of washed transplants these taxonomic families were nearly undetectable initially, but their abundances recovered by experiment completion. The Sulfurovaceae also exhibited gradual increases in relative abundance on washed roots, but in sod transplants this taxon's abundance increased after seven days and subsequently decreased (Figure 5.4D). Vibrionaceae showed an altogether different

pattern; high abundances were detected in initial wash samples, but by day seven these taxa were rarely detected. In sod transplants, abundances of sequences assigned to the Vibrionaceae were generally absent throughout the entire experiment.

5.5 Discussion

Our results indicate that *Zostera marina* rhizobiome communities are distinct, linked to seagrass performance, and resilient to disturbance. Indeed, eelgrass belowground root biomass suffered negatively from rhizosphere disruption, but recovered after approximately two weeks. Concomitantly, their microbial communities in the rhizospheres of washed transplants resembled those of sod transplants by experiment end, indicating that *Z. marina* and its belowground microbiome are resilient to stresses associated with transplantation.

The observation of consistently distinct microbial communities between compartments of *Z. marina* is in line with studies describing the structure of seagrass microbiomes from field-collected samples, where large differences are observed between plant microbial communities and those in the surrounding environment (Jensen *et al.* 1998; Cúcio *et al.* 2016; Mejia *et al.* 2016; Ettinger *et al.* 2017; Fahimipour *et al.* 2017; Crump *et al.* 2018; Ugarelli, Laas and Stingl 2019). In the study by Cúcio et al. (Cúcio *et al.* 2016) where the rhizosphere compartment was specifically analyzed, significant differences were found between communities of bulk and rhizosphere sediments. Our work further distinguishes the root-attached microbiome as different from the microbiota of the rhizosphere, and suggests that these two compartments are separate microbial niches shaped by prevailing redox and

nutrient gradients formed across sub-millimeter ranges by plant metabolic processes (Brodersen *et al.* 2018). These results are supported by previous observations (Fahimipour *et al.* 2017; Wang, Tomas and Mueller 2020) and a proposed model of microbiome assembly via selection of bulk sediment microbes (Fahimipour *et al.* 2017).

Although the mechanisms controlling assembly of seagrass microbiomes are largely unknown, evidence from terrestrial plant studies suggest that they are based on metabolic interactions and nutrient exchange between plants and microbes. For instance, changes in abiotic factors and/or the presence of pathogens can induce or restrict exudation of nutritional and allelopathic compounds, contributing to the selection of a root microbiome (Lakshmanan *et al.* 2013; Lebeis *et al.* 2015). Root exudation is known to be metabolically costly for plants, though, and can result in significant losses of carbon and nitrogen (Morgan, Bending and White 2005). However, these costs are likely offset by the beneficial functions of the belowground microbiome (e.g., disease suppression, nutrient acquisition, stress tolerance, and growth enhancement) (Morgan, Bending and White 2005; Yang, Kloepper and Ryu 2009b; Wei *et al.* 2015).

Similar to these terrestrial plant examples, we propose that exudation is an important factor modulating belowground microbiomes of seagrasses. Seagrass exudation is known to change with environmental conditions (light restriction) (Martin *et al.* 2018b), and can act as an important resource for sediment microbes (Kaldy *et al.* 2006; Säwström *et al.* 2016). Our concomitant observations of

belowground root biomass loss in washed *Z. marina* plants and large-scale changes in the microbiome structure within the first week after transplantation may be related to changes in root exudation, which would imply a rapid and coordinated response by both the microbiome and plant to disturbance. An alternative explanation for our results is that root damage may have occurred during seawater rinses to remove the rhizosphere prior to transplantation. Although we cannot fully disprove this hypothesis, our data do suggest that no observable and significant root biomass loss occurred from initial washes. Further experimentation specifically characterizing exudation patterns of seagrasses after rhizosphere disturbance will be needed to definitively resolve these hypotheses.

When considering the timing of recovery between belowground compartments, it is notable that the change in microbial community structure of washed roots was detected three days after transplantation, whereas a similar change in the rhizosphere was detected on day seven (Figures 5.3B & 5.4B). Interestingly, almost all of the root- and rhizosphere-associated taxonomic families that significantly changed in abundance over time demonstrated an inflection point in their abundance trajectories between three and seven days post transplantation (Figures 5.3D & 5.4D). When considered with the changes observed for plant traits, these data suggest that the first week after transplantation is a critical transition period for the plant and its associated microbiome.

Rapid and resilient responses of microbiomes to disturbance, such as those seen here, have also been observed for microbiomes of terrestrial plants (Maignien *et*

al. 2014; Edwards *et al.* 2015) and marine algae (Longford *et al.* 2019b). Interestingly, the speed of recovery may be dependent on the physical route of microbial transmission, as microbiomes of the phyllosphere of *Arabidopsis thaliana* appear to be acquired from the air and converge to mature communities only after 60 days (Maignien *et al.* 2014). In contrast, recovery of microbiomes colonizing biotic surfaces found in water-saturated environments (e.g., algal surfaces and rice roots) occurs within days to weeks. For example, community assembly on the surface of *Delisia pulchra* was found to be deterministic, recovering to a pre-disturbed state within twelve days. In this system, the production of anti-fouling chemicals (i.e., halogenated furanones), either by early-colonizing bacteria or by the algae, is an important factor controlling community succession. Seagrasses can also produce a diverse set of anti-fouling chemicals on their surfaces (Papazian *et al.* 2019). Their precise role in modulating the epibiont community structure is currently unknown, but we suggest that the collective results of ours and the aforementioned studies support the hypothesis that these compounds and nutritional exudates act to deterministically shape microbiome community structure.

Our results also show several ASVs assigned to taxonomic groups that have previously been proposed to benefit plants or enhance turnover of nutrients in sediments are enriched in seagrass-associated compartments after transplantation. For instance, ASVs enriched in rhizosphere over root samples were assigned to taxonomic groups (e.g., Marinilabiliaceae, Bacteroidetes BD2-2 and SB-5, Flavobacteriaceae, Sandaracinaceae) widely recognized to be important degraders of complex organic material, such as rhizodeposits and algal cell wall polysaccharides

(Mohr *et al.* 2012; McBride 2014; McIlroy and Nielsen 2014; Coskun *et al.* 2018; Garcia, La Clair and Müller 2018; Wang *et al.* 2020). Notable taxa that were enriched on roots include ASVs with potential important roles in turnover of plant exudates. For example, all detected ASVs assigned to the methylotrophic lineages (i.e., Methylomonaceae, Methylophagaceae, and Methylophilaceae) were found in higher relative abundance on the root vs. rhizosphere, supporting a potential symbiotic role for these populations based on their described abilities to consume plant-derived methanol and produce plant phytohormones (Trotsenko, Ivanova and Doronina 2001; Zhang *et al.* 2019). Additionally, ASVs of the Lachnospiraceae and Colwelliaceae families, which were enriched on roots, may have potential roles in consumption of plant-derived polysaccharides and lignin (Boutard *et al.* 2014; Woo and Hazen 2018). In fact, the former group may have an additional symbiotic role with plants, as a novel species of Lachnospiraceae is proposed to be diazotrophic (Igai *et al.* 2016).

Other taxa found enriched in either the root or rhizosphere compartment appear to rely on respiratory metabolisms linked to sulfur and nitrogen cycles, a common feature of populations of the seagrass microbiome (Cúcio *et al.* 2018; Tarquinio *et al.* 2018). Previous reports suggest that organic matter inputs from seagrass roots can stimulate microbial activities that control these cycles, ultimately leading to higher sulfate reduction, denitrification, and nitrogen fixation rates in seagrass bed sediments, as well as stimulating the release of bioavailable phosphorus and iron (Hansen *et al.* 2000; Chisholm and Moulin 2003; Deborde *et al.* 2008; Cole and McGlathery 2012; Brodersen *et al.* 2017; Wang, Tomas and Mueller 2020). ASVs assigned to the Desulfobulbaceae, which can act either as anaerobic sulfate

reducers (e.g., *Desulforhopalus sp.*) (Isaksen and Teske 1996) or as sulfide oxidizers who transfer electrons from reduced sulfur compounds to either oxygen or nitrate (e.g., *Ca. Electrothrix sp.*) (Pfeffer *et al.* 2012; Kessler *et al.* 2019), were commonly enriched in the rhizosphere compartment and have been frequently detected within rhizospheres of aquatic plants (Martin *et al.* 2019; Scholz *et al.* 2019). In addition, several ASVs found enriched on roots were designated as known or putative sulfur-oxidizing bacteria , including Sedimenticolaceae (Bourque, Vega-Thurber and Fourqurean 2015), Thiovulaceae, and Arcobacteraceae (Waite *et al.* 2017), supporting the hypothesis that seagrasses facilitate the activities of sulfur-oxidizing bacteria as a way to combat sulfide toxicity (Jensen, Kühl and Priemé 2007).

Summarized sequence counts representing relative abundance changes of the Ruminococcaceae and the Sulfurovaceae stand out in our time-course analyses, as both exhibited similar abundance differences initially and over time in both root and rhizosphere samples. ASVs of these taxa, along with those of the Lentimicrobiaceae and Desulfobacteraceae, were noticeably absent on washed roots at the start of the experiment, but all recovered to the relatively high levels found on roots of sod transplants by the end of the experiment. Many of these taxa are known to drive sulfur cycling in marine sediments (Rodriguez-Mora *et al.* 2016; Probandt *et al.* 2017; Waite *et al.* 2017) and their functional roles may be important in long-term associations with plants. In contrast, the Vibrionaceae were the only taxa that rapidly decreased from high relative abundances on washed roots to undetectable levels after seven days. Given that many *Vibrio* species are fast-growing copiotrophs that rapidly form biofilms on marine surfaces (Mueller *et al.* 2007; Lilburn *et al.* 2010) it is

possible that these ASVs rapidly colonize the rhizosphere and root environment, and that plants respond by changing their physiology as a way to discourage growth of these bacteria while encouraging growth of beneficial microbes shortly after disturbance.

Seagrass health after transplantation is often unpredictable (van Katwijk *et al.* 2016) and restoration success is thought to be dependent on many factors, with root growth and sediment anchoring identified as keys to long-term success (van Katwijk *et al.* 2009; Suykerbuyk *et al.* 2016; Thom *et al.* 2018). Despite the importance of these belowground processes, few studies have explicitly examined the impact of microbiome community structure on transplantation success. A study by Milbrandt and colleagues is, perhaps, an instructive exception (Milbrandt, Greenawalt-Boswell and Sokoloff 2008). Similar to our findings, washed and sod transplants of *Thalassia testudinum* showed few differences in plant traits several weeks after transplantation. Critically, though, transplants that were planted into autoclaved sediment demonstrated a strong and significant die-off starting at seven weeks post transplantation, leading the authors to conclude that an intact microbial community is essential to the plant's ability to combat transplantation shock.

An important distinction of our work is that growth traits of washed transplants consistently lagged behind those of sod transplants during the first week of the experiment when microbiome recovery was most pronounced. Notably, root biomass showed rapid and significant decreases for plants assigned the wash treatment versus those assigned to the sod treatment. The potential implications of

root biomass loss after bare-root restoration attempts should be further considered and investigated due to the established roles of roots in physical anchoring (Zenone *et al.* 2020), microbial recruitment (Garcia-Martinez *et al.* 2005), and resource acquisition (Hemminga 1998). When considering our results in light of the highly variable nature of restoration outcomes, it is apparent that understanding the roles of the seagrass microbiome in optimizing plant physiology, combating transplantation shock, and contributing to anchoring effects at the bed-scale will be essential to the development of best practices for future seagrass restoration programs.

5.6 Acknowledgments

We acknowledge Oregon State University's Summer Undergraduate Research Experience program, HMSC's Mamie Markham Research Award, and the Joan Countryman Suit Scholarship for financial support, the CGRB core facility for sequencing support, C. Moffett and I. Cheung at HMSC for facility and administrative support, and E. Slick for help with sample collection.

5.7 Figures

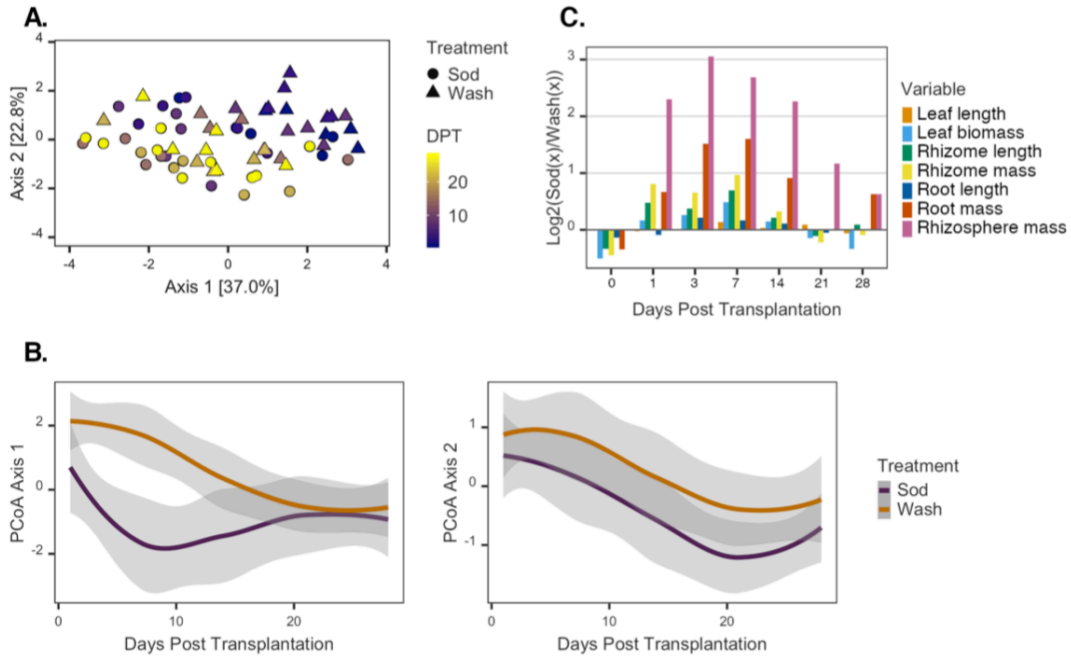

Figure 5.1 | Variance in *Z. marina* Traits Over Time. (A) PCoA of *Z. marina* plants based on a Euclidean distance matrix relating plant traits. Color gradient represents the day of plant collection (DPT), and symbols represent the treatment assignment of each plant. (B) Locally estimated scatterplot smoothing (LOESS) of the first two principal coordinate summary variables over time (cumulative variance = 59.8%) illustrates how variation in traits of plants from each treatment (purple lines = sod transplants, gold lines = washed transplants) significantly diverges over time (left) and co-varies over the course of the experiment (right). Shaded areas represent 95% confidence intervals of estimates. (C) Relative differences in log transformed values of *Z. marina* morphometric data at sampling points over time. Positive values indicate higher values in sod transplants than washed, and negative values indicate the opposite.

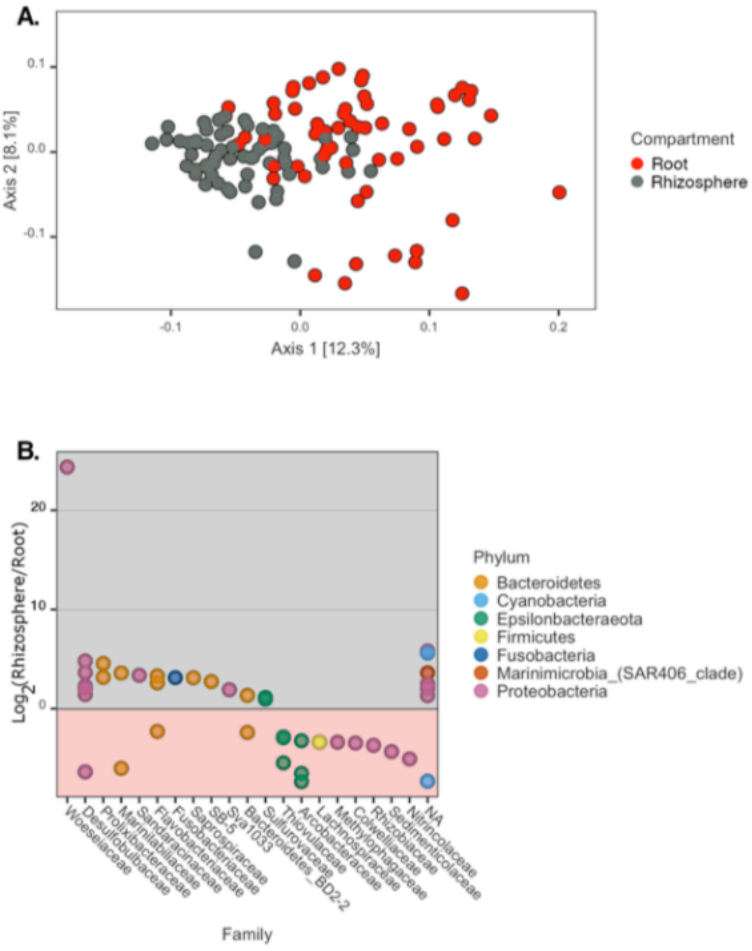

Figure 5.2 | Microbial Community Differences Between *Z. marina* Compartments. (A) PCoA of *Z. marina* all sampled microbial communities based on a weighted UNIFRAC distance matrix. Colors indicate the compartment of each sample (Red = Root, Gray = Rhizosphere). (B) Taxa with significant relative abundance differences between compartments. Positive values indicate higher relative abundances of ASVs in rhizospheres than roots, and negative values indicate the opposite. ASVs assigned to the same phylum have the same color. ASVs are grouped by column by taxonomic family.

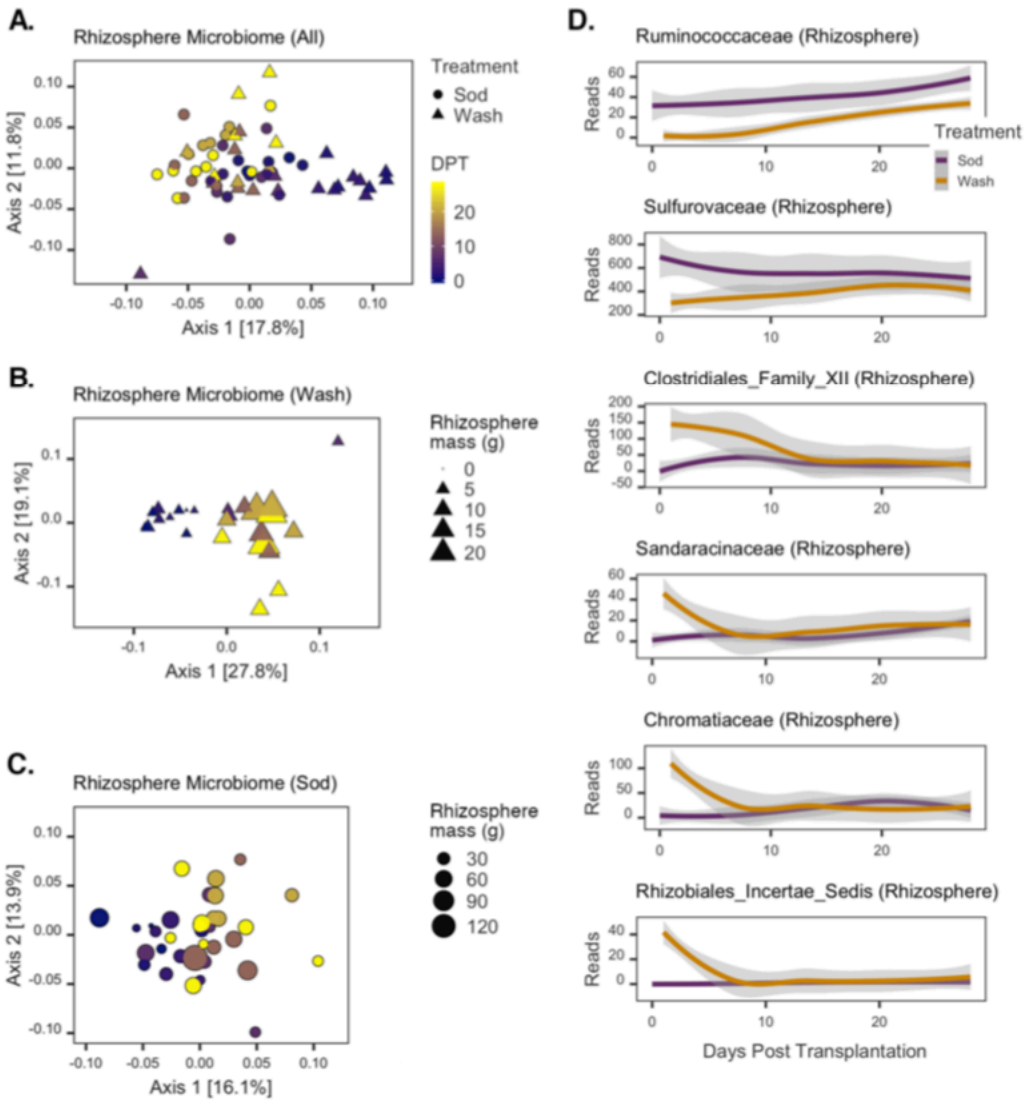

Figure 5.3 | Changes in Rhizosphere Microbial Communities Post-transplantation. PCoAs of (A) all rhizosphere, (B) washed rhizosphere, and (C) sod transplant rhizosphere communities. Color gradient represents the day of sample collection (DPT), and symbols represent the treatment assignment of each sample. Symbol size in (B) and (C) is scaled to the grams of rhizosphere sediment collected from each corresponding sampled plant. (D) Rhizosphere ASVs with significant Time x Treatment interaction intersects. LOESS was applied to the sequence counts for each taxon; shaded areas represent 95% confidence intervals of estimates. Colors designate each respective treatment group (purple = sod transplants, gold = washed transplants).

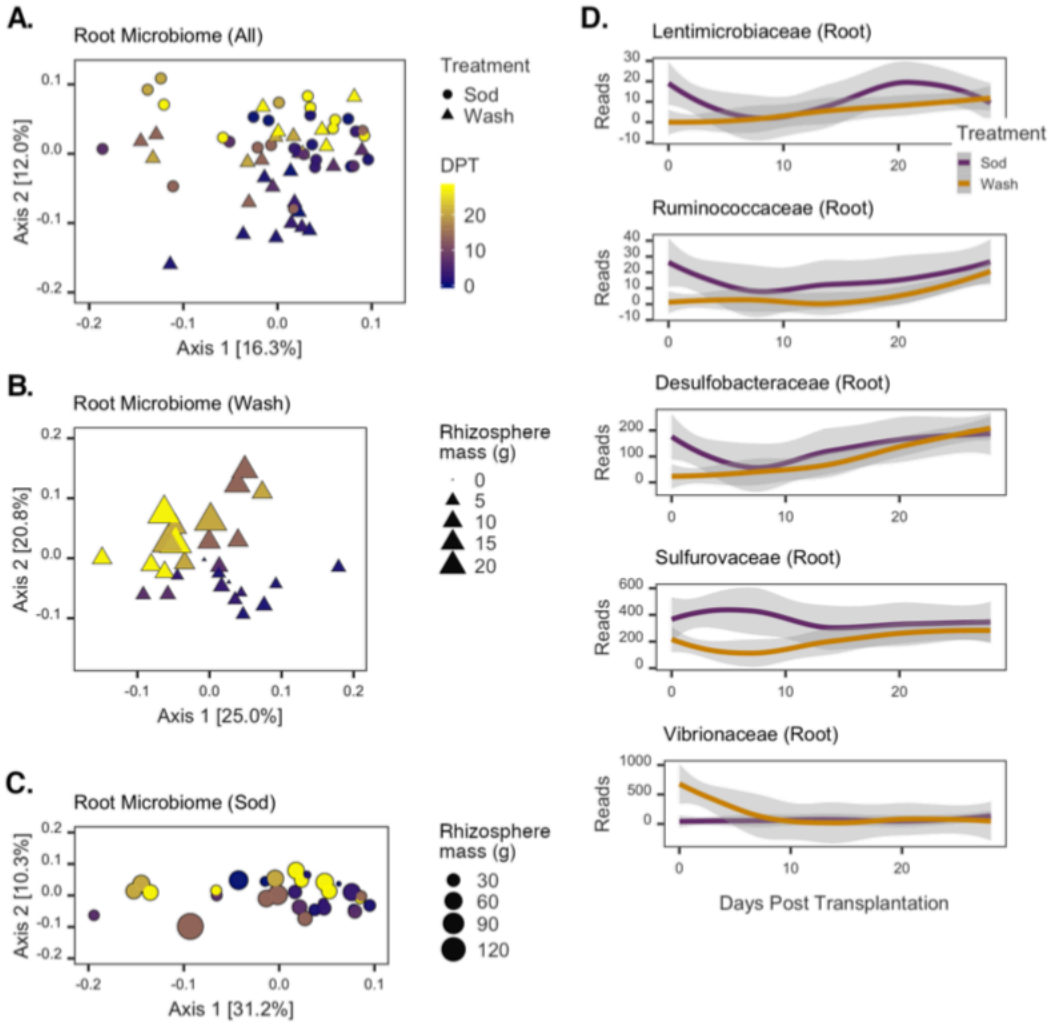

Figure 5.4 | Changes in Root Microbial Communities Post-transplantation. PCoAs of (A) all root, (B) washed root, and (C) sod transplant root communities. Color gradient represents the day of sample collection (DPT), and symbols represent the treatment assignment of each sample. Symbol size in (B) and (C) is scaled to the grams of rhizosphere sediment collected from each corresponding sampled plant. (D) Root ASVs with significant Time x Treatment interaction intersects. LOESS was applied to the sequence counts for each taxon; shaded areas represent 95% confidence intervals of estimates. Colors designate each respective treatment group (purple = sod transplants, gold = washed transplants).

6 Conclusion

The body of work in this dissertation aimed to understand how environmental stressors associated with global change impact the microbial communities associated with seagrasses and corals. The importance of these host systems is illustrated by the many important ecological and economic services and resources that they provide, such as sustaining biodiversity and providing coastal protection (Hughes *et al.* 2017; Holmer 2019). Additionally, seagrass meadows are capable of storing carbon within coastal sediments and contribute to "blue carbon" processes, whereby atmospheric CO_2 can be sequestered for long periods in marine sediments (Oreska *et al.* 2018). The microbiomes of seagrasses and corals have important roles in ecosystem functioning and structure, primarily through nutrient cycling activities and mutualisms (Wilkins *et al.* 2019). Considering how holobionts, i.e., the microbiome and their host organisms, will be impacted by global change, such as ocean warming, eutrophication, and ocean acidification is an important challenge for research. The results of these studies will help understanding ecological responses to disturbance and informing future management and restoration practices aimed at mitigating or reversing environmental deterioration.

Oceans absorb the consequences of global change resulting from anthropogenic actions, including atmospheric CO_2, heat, and nutrient runoff. Under current climate change models, the heat absorbed by oceans is leading to a rise of 1-4 °C in mean sea surface temperature globally (Bindoff *et al.* 2019; Pörtner *et al.* 2019). Alarmingly, any increase above 1.5 °C is predicted to be disastrous for coral and seagrass populations (Bindoff *et al.* 2019). Concurrent with overall rises in average

sea surface temperatures, intermittent marine heat waves are becoming more severe and frequent, in part due to climate change and human activities, which can be an important factor in coral bleaching and seagrass loss worldwide (Smale *et al.* 2019). Rising temperatures are associated with coral bleaching – loss of the photosynthetic symbiont Symbiodiniaceae, and holobiont dysbiosis, shifting to a community enriched with potentially pathogenic microbes such as *Vibrio sp.* (Bourne *et al.* 2008; Tout *et al.* 2015). Nitrogen and phosphorus pollution from sewage treatment plants and agricultural sources can create ecological imbalance through stimulation of both autotrophic and heterotrophic organisms (Howarth, Sharpley and Walker 2002). Eutrophication may lead to proliferation of algae, which may outcompete seagrasses, and dysbiosis within coral holobionts. Lastly, if anthropogenic emissions are left unchecked, the ocean pH is predicted to decrease by 0.3 by 2100 (Bindoff *et al.* 2019), leading to ocean acidification (OA) and negatively impacting calcifying organisms such as molluscs and corals (Gazeau *et al.* 2013; Mollica *et al.* 2018). However, as seagrasses have been shown to be carbon limited in most environment, they may thrive under future OA conditions (Koch *et al.* 2013), where enhanced primary production may mitigate changes to seawater carbonate chemistry and pH (Unsworth *et al.* 2012b; Su *et al.* 2020a). OA effects on marine host-associated organisms have a pattern of enrichment for pathogenic microbes (Vega Thurber *et al.* 2009; Hassenrück *et al.* 2015; Aires *et al.* 2018), decrease in the symbiotic genus *Endozoicomonas* within coral holobionts, and disruptions in the transport of exogenous compounds (Botté *et al.* 2019).

Chapter 2 of this dissertation originally aimed to tease apart the effects of individual nutrient pollutants (nitrogen and phosphorus) on coral health and the coral microbiome. This was the first study to date to study the effects of phosphorus on *Agaricia sp.* and *Siderastrea siderea* corals and their microbiomes. Serendipitously, this *in situ* nutrient pollution experiment coincided with a thermal anomaly that resulted as the warmest summer and winter on record in the Florida Keys (Manzello 2015) and presented an opportunity to study the synergistic effects of heat and nutrient stress on coral microbiomes. The results illustrated how differential interactions of nitrogen and phosphorus with heat stress manifest in divergent bleaching and disease states of corals. In this experiment, the effects of heat stress and disease, which increased community alpha diversity and resulted in dysbiosis, outweighed the effects of nutrient supplementation on the *S. siderea* microbiome. These results also show that the combination of environmental stressors have the potential to act upon marine organisms in an additive, synergistic, or independent manner depending on the site and characteristics of the host organism. Responses of foundational species, such as corals, to future global conditions will be complex and will have ecosystem-level implications.

Compared to corals, seagrass microbiome research is fairly nascent and has been focused primarily on observational studies that characterize and catalog the microbes associated with different hosts and parts of the plant. I set out to add to this understanding by identifying the core microbiome of *Zostera marina* leaf, root, and rhizosphere compartments, and to provide a working definition of the different compartments of this seagrass, highlighting the strength and nature of the relationship

between the plant and its microbes. Beyond these initial questions, I also aimed to characterize how the seagrass and its microbiome responds to environmental stressors, providing some of the first studies to consider the seagrass holobiont in the context of environmental disturbance.

Previous work examining eutrophication of seagrass systems has measured environmental and seagrass responses, including quantifying algal blooms, epiphyte load, and biogeochemical measures. Chapter 3 aimed to characterize the effects of nutrient pollution on the *Zostera marina* microbiome and morphology. *Z. marina* plants in this mesocosm experiment appeared to be nutrient limited, as increases in the number of leaves were observed after 28 days in nutrient addition treatments. There was no indication of algal blooms or increases in epiphyte loading in fertilized samples. Many previous studies on the effects of eutrophication on seagrasses have resulted in algal proliferation and/or seagrass die offs (van Katwijk *et al.* 1997; Govers *et al.* 2014b). Contradictory results from this experiment may be due to the characteristics of the experimental setup, such as rapid water turnover or light saturation. Interestingly, microbial community changes were highly dependent on seagrass compartment they were sampled from, with samples collected from sediments responding differently than those from the water column. Notably, the root-associated microbiota of fertilized treatments were enriched in taxa associated with nitrogen and sulfur metabolism. Based on this evidence and the nutrient limitation of *Z. marina* plants in our study, it is likely that these root-associated taxa were stimulated by both nutrient inputs and enhanced growth of fertilized eelgrasses,

which potentially produced increased root exudation of labile carbon, supporting heterotrophic root-associated microbes.

Chapter 4 further explores the effects of environmental stressors on the seagrass holobiont by characterizing the effects of long-term high pCO_2 and low pH exposure on the leaf microbiome of *Posidonia oceanica*. The novelty of this system lies within the field site that samples were taken from, a naturally occurring volcanic CO_2 vents in Ischia, Italy (Hall-Spencer *et al.* 2008). This naturally occurring site represents a reasonable analog for what seagrass may experience under future OA conditions, and allows the sampling of *P. oceanica* microbiomes are presumably acclimated to high CO_2/low pH conditions. Previous results from this location have shown that seagrass productivity is highest in acidified areas near CO_2 vents (Hall-Spencer *et al.* 2008). When considering these results in conjunction with those that support a mechanism whereby seagrass photosynthate supports symbiotic associations with members of its phyllosphere (Kaldy 2012), I hypothesized that corresponding changes to microbial metabolism would be observed between samples collected from seagrass leaves across the sampled pH gradient. My findings support this hypothesis, by indicating that primary producers were enriched in ambient samples, whereas samples from vent sites were enriched for heterotrophic bacteria encoding more genes involved in the metabolism of photosynthetic material. Taken together, these results suggest that OA conditions decrease carbon restrictions on seagrass productivity, as has been seen previously, which appears to stimulate the abundances of specialized microbial heterotrophic populations on the seagrass leaf surface. To date, work examining the response of algal epiphytes and the

microbiomes of seagrasses to OA have focused on structural and compositional shifts in the communities, without fully considering functional implications (Hassenrück *et al.* 2015; Guilini *et al.* 2017). Results of chapter 4 corroborate previous findings and expands upon those works by revealing changes in the functional potential of the *P. oceanica* leaf microbiome under OA, including enrichment for genes encoding for biofilm formation from a diverse array of taxa, use of alternate electron acceptors in respiration, and carbon metabolism. Through the nutrient and oxygen gradients within biofilms, and the increased concentration of seagrass photosynthates, the environment on seagrass leaves is able to support a wide array of metabolic processes under OA conditions.

Chapter 5 aimed to characterize the succession of the *Z. marina* root and rhizosphere community after transplantation. This project originated from chapter 3 experiments, where bare-root *Z. marina* transplants were planted without a rhizosphere, but developed robust rhizospheres after three weeks. This observation led me to want to explore the dynamics of rhizosphere development further by tracking microbial community changes through time on seagrass roots and within the rhizosphere and to correspond these changes to measured changes in plants. The work presented in Chapter 5 attempts to answer these questions, as *Z. marina* shoots were transplanted with and without rhizospheres (henceforth “sod” and “wash” treatments) and followed plant morphology and microbiome succession for four weeks. Initial root and rhizosphere microbial communities of wash treatments were distinct from those of sod treatments, with apparent proliferation of fast growing and opportunistic microbes, such as *Vibrio sp.*, in the first two weeks. These results lead me to conclude

that washed plants were recruiting their microbiome from surrounding porewater and sediment. Moreover, microbial communities on washed plants recovered after 14 days to resemble communities on plants assigned to sod treatments. Strikingly, these changes were concomitant with an observed loss and subsequent recovery of root biomass exclusively in washed plants. These results show that seagrass microbiomes are resilient to transplantation in mesocosm conditions, and that community development and recruitment may be influenced directly by temporally related changes in plant physiology. Further experimentation investigating the chemical drivers of plant-microbiome interactions during rhizosphere development and recovery will help to elucidate the mechanisms behind these observations and may provide further insights into the symbioses and dependencies between seagrasses and their microbiomes. For example, to test the role of seagrass exudates in recruiting the root microbiome, exudates could be collected and characterized, and then used to enrich for both water column and sediment associated microbes. From a practical perspective, these findings have important implications on management decisions related to seagrass bed restoration attempts, as these results insinuate that the inclusion of the rhizosphere during transplantation may impact plant health, which may, in turn, impact chances of restoration success (Milbrandt, Greenawalt-Boswell and Sokoloff 2008; Boyer and Wyllie-Echeverria 2010).

Since many chapters of this dissertation have already published or are under peer review, the majority of the research is presented in “neat” packages, which don’t necessarily convey the numerous limitations and challenges associated with each experiment. For instance, although mesocosm experiments are useful for controlling

and testing for specific conditions and outcomes, a major limitation is that subjects within these systems can and will respond differently from those in the field. On the other hand, *in situ* experiments have their own limitations and considerations related to uncontrolled factors. For example, unforeseen circumstances, such as interference from local fauna, or interactions and changes in local conditions, such as the incidence of a thermal anomaly during the chapter 2 experiment, can lead to complex relationships between factors that complicates interpretations of results. By working with mesocosms in Chapter 3 & 5, the intent was to minimize the influence of uncontrolled factors in experimental outcomes, allowing for greater clarity in the relationships between measured variables to be defined. Though these results may not replicate the processes of the field, they provide relatively simple and foundational knowledge that can act as a lens through which future *in situ* experiments can be conducted and interpreted. Lastly, the through line of my dissertation involved utilizing 16S amplicon and metagenomic sequencing. Though the advent of high-throughput sequencing and its application to microbial ecology has opened up and unprecedented opportunity to study the vast majority of unculturable organisms found in natural systems, the biases and limitations associated with these methods are well known and must be acknowledged when the significance of findings based on this approach. A major caveat is that taxonomic results from 16S amplicon studies do not provide evidence of function, further the detection functional genes in metagenome studies do not provide direct evidence of activity. Additional biases arise from DNA extraction, PCR, 16S rRNA copy number variation, library preparation, and downstream analyses, including use of genomic databases that are biased in their

taxonomic composition (Acinas *et al.* 2005; Janda and Abbott 2007; McLaren, Willis and Callahan 2019). Nonetheless, results and conclusions from past and present next-generation sequencing experiments do have value in providing a high-level understanding of microbial community dynamics that can inform the design of appropriate and testable explanatory hypotheses, fueling the iterative process of scientific experimentation and incremental advancement of knowledge.

Throughout my graduate training I've grappled with identifying the "right" way to analyze microbiome data. The microbiome field is developing and rapidly evolving. Even during my short time as a graduate researcher, there was a mainstream adaptation of utilizing Amplicon Sequence Variants (ASVs) over Operational Taxonomic Units (OTUs) to define unique entities in microbial communities (Callahan, McMurdie and Holmes 2017). Additionally, a multitude of tools and pipelines for analysis of amplicon and metagenome data has been developed (Schloss *et al.* 2009; Anders and Huber 2010; Li *et al.* 2015; Mandal *et al.* 2015; Callahan *et al.* 2016; Nurk *et al.* 2017; Bolyen *et al.* 2019), each promoting their advantages over the rest, leading to ambiguity in best practices and prohibiting wide-spread adoption of any singular tool. Moreover, an increasing number of computational pipelines each offering their own advantages (and disadvantages) are published with each passing year. As I've learned, an important factor to account for in choosing an analytical approach is the nature of microbiome data, which are often over dispersed and do not fit the assumptions associated with standard statistical tests of differential abundance, such as ANOVAs or T-tests. Further, microbiome data is commonly analyzed as proportions, which may not be truly representative of absolute abundance in the

sample source. As a result of the count data generated from high-throughput sequencing experiments being compositional (Mandal *et al.* 2015; Gloor *et al.* 2017; Knight *et al.* 2018), spurious negative correlations between counts are common making it difficult to distinguish true biological signals from random noise. Throughout this dissertation, I endeavored to use the best available and most appropriate tools to answer each specific research question. This has necessitated an interactive approach to data analysis for several of my chapters presented here, analyzing microbiome data using ANOVA, generalized linear mixed models, DESeq2, ALDEx2, indicator species analysis, and corncob to name a few (Bolker *et al.* 2009; Schloss *et al.* 2009; Anders and Huber 2010; Gloor *et al.* 2017; Martin, Witten and Willis 2020). An interesting conclusion from these iterations is that I generally saw very similar results across the board regardless of the statistical model applied or the treatment of the data (e.g., consistent patterns were observed when I analyzed 16S amplicon sequencing data from Chapter 4 for differential abundance using corncob, ALDEx2, and indicator species analysis; data not shown). These results lead me to conclude that each of these microbiome analysis methods possess their own merits, and that studies applying different analytical approaches can and should be compared when evaluating the validity and consistency of observations across a field of research.

One of the biggest lessons I learned is the importance of asking the right questions. The mesocosm experiment for Chapter 3 was my first large-scale mesocosm experiment. Most of the literature on seagrass eutrophication at the time focused on analyzing one type of measurement. While designing the experiment, I

aimed to characterize a holistic view of eutrophication effects on the microbiome, including any indirect effects arising from plant responses. Thus, I set out to collect measurements of plant growth rates, photosynthesis, above and belowground biomass, and samples for analysis of microbiomes, nutrient concentrations, dissolved pCO_2, volatile organic compounds (VOC), and leaf C:N ratio. Measuring photosynthesis rates alone took 3-4 hours given my available methodology. The time needed to collect all these parameters was 16 person-hours per sampling day, and I was working alone for most sampling days. I quickly needed to adapt and reduce the parameters sampled, such as reducing the frequency of photosynthesis measurements. I learned that I need to identify and limit the scope of experiments and understand what parameters need to be measured to answer the research questions prior to conducting the experiment. Not all measurements are included in the final manuscript, such as VOC profiles or pCO_2 measurements. Other measurements had no significant differences between ambient and fertilized samples. Photosynthesis rates in macrophytes may not change over the short time span of the experiment, though we had originally hypothesized that nutrient enrichment may impact photosynthesis. I took these lessons with me when designing the experiment for Chapter 5. Sample collection for this experiment more streamlined and manageable, and we were able to answer our research question.

Despite and because of challenges and lessons arising from these various chapters, I was able to build upon the literature, confirm previous findings, and contribute novel findings to marine host-microbiome research. I found that disease phenotypes may not always be microbe-mediated in corals and identified individual

and synergistic effects of warming and nutrient pollution on two coral species. As part of my work in seagrass systems, I established new and reliable protocols for seagrass microbiome research, including sampling procedures for belowground seagrass root, rhizosphere, and bulk sediment compartments. By focusing on these compartments, important compartment-specific differences were observed leading to a more nuanced understanding of the niches relevant for seagrass microbiome research, that are historically overlooked. For instance, my work has established both biogeochemical and microbial gradients stretching from the seagrass root to the bulk sediment, indicating a need to differentiate these distinct compartments. I was also able to identify core seagrass microbiome members across geographic and species, including the *Granulosicoccus sp.*, abundant on both *Z. marina* and *P. oceanica*. A large part of my observational work in the seagrass system is hypothesis generation, through identifying taxa of interest. It would be interesting for future work to pursue the metabolic relationship between seagrasses and *Granulosicoccus sp.*

There is a solid foundation of marine host-microbiome research on which this field can grow. Future work should examine microbiomes under multiple stressors, *in situ*, and/or under long term experiments. To expand upon chapter 5, long term and *in situ* seagrass transplantation experiments should be conducted to allow for the tracking of outcomes for realistic restoration conditions. Given our results showing the importance of sulfur-cycling bacteria to seagrasses and of their previously documented importance to lucinid clams, future studies should also focus on multi-species interactions between plants, sulfur-oxidizing bacteria, and clams that co-occur in seagrass beds (Heide *et al.* 2012). By taking a holistic approach to understanding

relationships between the environment, host organisms, and their microbiomes, the predictive power for the fitness of marine ecosystems under future global change scenarios should expand and better account for how microscale interactions between host and microbiome can impact system-level outcomes. It will also be interesting to characterize host-microbial interactions at the molecular and metabolic level. For example, the results of Chapter 5 point to potential chemical interactions between seagrasses and rhizosphere microbes; follow-up experiments characterizing seagrass root exudates and specific microbial responses to changing exudate patterns will help to validate mechanistic hypotheses underlying the observed phenomena. The results of my dissertation research also putatively identify several mutualistic taxa within the core seagrass microbiome and the mechanism of mutualism. One important group is methylotrophic bacteria, which can enhance growth of terrestrial plants through the production of phytohormones (Madhaiyan *et al.* 2005). Importantly, because the research conducted ultimately looked to explore ecosystem processes through the explicit inclusion of microbial communities, it should be viewed in the context of its implications on future management decisions and policy development. Work has already been done to use healthy and perturbed seagrass root microbiomes as indicators of seagrass stress (Martin *et al.* 2020). Marine microbial ecology researchers should look to expand upon these ideas through applying the knowledge gained to the enhancement of conservation efforts. For example, knowledge gained about the mechanistic relationships between host and microbiomes may lead to practices involving the inoculation or manipulation of the microbiome of marine organisms with the goals of mitigating disease and enhancing host fitness. Many

amazing researchers may already be conducting or contemplating these experiments, and I look forward to the papers to come.

7 References

Abramoff MD, Magalhaes PJ, Ram SJ. *Image Processing with Image J.* Biophotonics Int.z, 2004.

Acinas SG, Sarma-Rupavtarm R, Klepac-Ceraj V *et al.* PCR-Induced Sequence Artifacts and Bias: Insights from Comparison of Two 16S rRNA Clone Libraries Constructed from the Same Sample. *Appl Environ Microbiol* 2005;**71**:8966–9.

Agawin NSR, Ferriol P, Cryer C *et al.* Significant nitrogen fixation activity associated with the phyllosphere of Mediterranean seagrass Posidonia oceanica: first report. *Mar Ecol Prog Ser* 2016;**551**:53–62.

Ainsworth TD, Fordyce AJ, Camp EF. The Other Microeukaryotes of the Coral Reef Microbiome. *Trends in Microbiology* 2017;**25**:980–91.

Aires T, Serebryakova A, Viard F *et al.* Acidification increases abundances of Vibrionales and Planctomycetia associated to a seaweed-grazer system: potential consequences for disease and prey digestion efficiency. *PeerJ* 2018;**6**:e4377.

Anders S, Huber W. Differential expression analysis for sequence count data. *Genome Biology* 2010;**11**:R106.

Anders S, Pyl PT, Huber W. HTSeq—a Python framework to work with high-throughput sequencing data. *Bioinformatics* 2015;**31**:166–9.

Anderson MJ. A new method for non-parametric multivariate analysis of variance. *Austral Ecology* 2001;**26**:32–46.

Anderson MJ. Permutational Multivariate Analysis of Variance (PERMANOVA). *Wiley StatsRef: Statistics Reference Online*. American Cancer Society, 2017, 1–15.

Andrews S. *FastQC: A Quality Control Tool for High Throughput Sequence Data*., 2010.

Aoki LR, McGlathery KJ. Restoration enhances denitrification and DNRA in subsurface sediments of Zostera marina seagrass meadows. *Marine Ecology Progress Series* 2018;**602**:87–102.

Apostolaki ET, Vizzini S, Hendriks IE *et al.* Seagrass ecosystem response to long-term high CO2 in a Mediterranean volcanic vent. *Marine Environmental Research* 2014;**99**:9–15.

Apprill A. Marine Animal Microbiomes: Toward Understanding Host–Microbiome Interactions in a Changing Ocean. *Front Mar Sci* 2017;**4**, DOI: 10.3389/fmars.2017.00222.

Arias-Ortiz A, Serrano O, Masqué P *et al.* A marine heatwave drives massive losses from the world's largest seagrass carbon stocks. *Nature Climate Change* 2018;**8**:338.

Armitage AR, Frankovich TA, Heck KL *et al.* Experimental nutrient enrichment causes complex changes in seagrass, microalgae, and macroalgae community structure in Florida Bay. *Estuaries* 2005;**28**:422–34.

Asplund ME, Baden SP, Russ S *et al.* Ocean acidification and host-pathogen interactions: blue mussels, Mytilus edulis, encountering Vibrio tubiashii: Ocean acidification and host-pathogen interactions. *Environ Microbiol* 2014;**16**:1029–39.

Bais HP, Fall R, Vivanco JM. Biocontrol of *Bacillus subtilis* against Infection of *Arabidopsis* Roots by *Pseudomonas syringae* Is Facilitated by Biofilm Formation and Surfactin Production. *Plant Physiology* 2004;**134**:307–19.

Bais HP, Weir TL, Perry LG *et al.* The Role of Root Exudates in Rhizosphere Interactions with Plants and Other Organisms. *Annual Review of Plant Biology* 2006;**57**:233–66.

Bandyopadhyay P, Bhuyan SK, Yadava PK *et al.* Emergence of plant and rhizospheric microbiota as stable interactomes. *Protoplasma* 2017;**254**:617–26.

Barbier EB, Hacker SD, Kennedy C *et al.* The value of estuarine and coastal ecosystem services. *Ecological Monographs* 2011;**81**:169–93.

Barnes BB, Hallock P, Hu C *et al.* Prediction of coral bleaching in the Florida Keys using remotely sensed data. *Coral Reefs* 2015;**34**:491–503.

Barr JJ, Auro R, Furlan M *et al.* Bacteriophage adhering to mucus provide a non-host-derived immunity. *Proceedings of the National Academy of Sciences* 2013;**110**:10771–6.

Barrón C, Duarte C. Dissolved organic matter release in a Posidonia oceanica meadow. *Mar Ecol Prog Ser* 2009;**374**:75–84.

Bates D, Mächler M, Bolker B *et al.* Fitting Linear Mixed-Effects Models Using lme4. *Journal of Statistical Software* 2015;**67**, DOI: 10.18637/jss.v067.i01.

Bengtsson MM, Bühler A, Brauer A *et al.* Eelgrass Leaf Surface Microbiomes Are Locally Variable and Highly Correlated with Epibiotic Eukaryotes. *Front Microbiol* 2017;**8**, DOI: 10.3389/fmicb.2017.01312.

Benjamini Y, Hochberg Y. Controlling the False Discovery Rate: A Practical and Powerful Approach to Multiple Testing. *J R Stat Soc Ser B Methodol* 1995;**57**:289–300.

Bentis CJ, Kaufman L, Golubic S. Endolithic fungi in reef-building corals (Order: Scleractinia) are common, cosmopolitan, and potentially pathogenic. *The Biological Bulletin* 2000;**198**:254–260.

Béraud E, Gevaert F, Rottier C *et al.* The response of the scleractinian coral Turbinaria reniformis to thermal stress depends on the nitrogen status of the coral holobiont. *Journal of Experimental Biology* 2013;**216**:2665–74.

Biagi E, Caroselli E, Barone M *et al.* Patterns in microbiome composition differ with ocean acidification in anatomic compartments of the Mediterranean coral Astroides calycularis living at CO2 vents. *Science of The Total Environment* 2020;**724**:138048.

Bindoff NL, Cheung WWL, Kairo JG *et al. IPCC Special Report on the Ocean and Cryosphere in a Changing Climate*., 2019.

Bolger AM, Lohse M, Usadel B. Trimmomatic: a flexible trimmer for Illumina sequence data. *Bioinformatics* 2014;**30**:2114–20.

Bolker BM, Brooks ME, Clark CJ *et al.* Generalized linear mixed models: a practical guide for ecology and evolution. *Trends in Ecology & Evolution* 2009;**24**:127–35.

Bolyen E, Rideout JR, Dillon MR *et al.* Reproducible, interactive, scalable and extensible microbiome data science using QIIME 2. *Nature Biotechnology* 2019;**37**:852–7.

Borg I, Groenen P. *Modern Multidimensional Scaling: Theory and Applications*. 2nd ed. New York: Springer-Verlag, 2005.

Borger JL. Dark spot syndrome: a scleractinian coral disease or a general stress response? *Coral Reefs* 2005;**24**:139–44.

Borum J, Pedersen O, Greve TM *et al.* The potential role of plant oxygen and sulphide dynamics in die-off events of the tropical seagrass, Thalassia testudinum. *Journal of Ecology* 2005;**93**:148–58.

Botté ES, Nielsen S, Abdul Wahab MA *et al.* Changes in the metabolic potential of the sponge microbiome under ocean acidification. *Nature Communications* 2019;**10**:1–10.

Bourne D, Iida Y, Uthicke S *et al.* Changes in coral-associated microbial communities during a bleaching event. *The ISME Journal* 2008;**2**:350–63.

Bourne DG, Morrow KM, Webster NS. Insights into the Coral Microbiome: Underpinning the Health and Resilience of Reef Ecosystems. *Annual Review of Microbiology* 2016;**70**:317–40.

Bourque A, Vega-Thurber R, Fourqurean J. Microbial community structure and dynamics in restored subtropical seagrass sediments. *Aquat Microb Ecol* 2015;**74**:43–57.

Boutard M, Cerisy T, Nogue P-Y *et al.* Functional Diversity of Carbohydrate-Active Enzymes Enabling a Bacterium to Ferment Plant Biomass. *PLOS Genetics* 2014;**10**:e1004773.

Boyer KE, Wyllie-Echeverria S. Eelgrass Conservation and Restoration in San Francisco Bay: Opportunities and Constraints. 2010:84.

Bracht AJ, Brudek RL, Ewing RY *et al.* Genetic identification of novel poxviruses of cetaceans and pinnipeds. *Arch Virol* 2006;**151**:423–38.

Brandt ME, McManus JW. Disease incidence is related to bleaching extent in reef-building corals. *Ecology* 2009;**90**:2859–67.

Brodersen KE, Koren K, Moßhammer M *et al.* Seagrass-Mediated Phosphorus and Iron Solubilization in Tropical Sediments. *Environ Sci Technol* 2017;**51**:14155–63.

Brodersen KE, Lichtenberg M, Paz L-C *et al.* Epiphyte-cover on seagrass (Zostera marina L.) leaves impedes plant performance and radial O2 loss from the below-ground tissue. *Frontiers in Marine Science* 2015a;**2**, DOI: 10.3389/fmars.2015.00058.

Brodersen KE, Nielsen DA, Ralph PJ *et al.* Oxic microshield and local pH enhancement protects *Zostera muelleri* from sediment derived hydrogen sulphide. *New Phytologist* 2015b;**205**:1264–76.

Brodersen KE, Siboni N, Nielsen DA *et al.* Seagrass rhizosphere microenvironment alters plant-associated microbial community composition: Seagrass rhizosphere microbes. *Environmental Microbiology* 2018;**20**:2854–64.

Brown CA, Ozretich RJ. Coupling Between the Coastal Ocean and Yaquina Bay, Oregon: Importance of Oceanic Inputs Relative to Other Nitrogen Sources. *Estuaries and Coasts* 2009;**32**:219–37.

Bruno JF, Petes LE, Drew Harvell C *et al.* Nutrient enrichment can increase the severity of coral diseases. *Ecology Letters* 2003;**6**:1056–61.

Burke M, Dennison W, Moore K. Non-structural carbohydrate reserves of eelgrass Zostera marina. *Mar Ecol Prog Ser* 1996;**137**:195–201.

Burkholder JM, Mason KM, Glasgow HB. Water-column nitrate enrichment promotes decline of eelgrass Zostera marina: evidence from seasonal mesocosm experiments. *Mar Ecol Prog Ser* 1992:16.

Burkholder JM, Tomasko DA, Touchette BW. Seagrasses and eutrophication. *Journal of Experimental Marine Biology and Ecology* 2007;**350**:46–72.

Callahan BJ, McMurdie PJ, Holmes SP. Exact sequence variants should replace operational taxonomic units in marker-gene data analysis. *The ISME Journal* 2017;**11**:2639–43.

Callahan BJ, McMurdie PJ, Rosen MJ *et al.* DADA2: High-resolution sample inference from Illumina amplicon data. *Nature Methods* 2016;**13**:581–3.

Campbell JE, Fourqurean JW. Ocean acidification outweighs nutrient effects in structuring seagrass epiphyte communities. *J Ecol* 2014;**102**:730–7.

Carpenter KE, Abrar M, Aeby G *et al.* One-Third of Reef-Building Corals Face Elevated Extinction Risk from Climate Change and Local Impacts. *Science* 2008;**321**:560–3.

Carvalhais LC, Dennis PG, Fan B *et al.* Linking Plant Nutritional Status to Plant-Microbe Interactions. *PLoS ONE* 2013;**8**:e68555.

Carvalho D, R CCC. Marine Biofilms: A Successful Microbial Strategy With Economic Implications. *Front Mar Sci* 2018;**5**, DOI: 10.3389/fmars.2018.00126.

Castejón-Silvo I, Terrados J. Experimental assessment of Posidonia oceanica-associated gastropods grazing on an early-successional biofilm community: nutrient availability and species-specific effects. *Marine Ecology* 2017;**38**:e12381.

Celdrán D, Espinosa E, Sánchez-Amat A *et al.* Effects of epibiotic bacteria on leaf growth and epiphytes of the seagrass Posidonia oceanica. *Mar Ecol Prog Ser* 2012;**456**:21–7.

Cervino J, Goreau TJ, Nagelkerken I *et al.* Yellow band and dark spot syndromes in Caribbean corals: distribution, rate of spread, cytology, and effects on abundance and division rate of zooxanthellae. *Hydrobiologia* 2001;**460**:53–63.

Chaparro JM, Badri DV, Vivanco JM. Rhizosphere microbiome assemblage is affected by plant development. *ISME J* 2014;**8**:790–803.

Chapin III FS, Schulze E-D, Mooney HA. The Ecology and Economics of Storage in Plants. *Annual Review of Ecology and Systematics* 1990;**2**:423–47.

Chisholm J, Moulin P. Stimulation of nitrogen fixation in refractory organic sediments by *Caulerpa taxifolia* (Chlorophyta). *Limnology and Oceanography* 2003;**48**:787–94.

Cochetière MFDL, Durand T, Lepage P *et al.* Resilience of the Dominant Human Fecal Microbiota upon Short-Course Antibiotic Challenge. *Journal of Clinical Microbiology* 2005;**43**:5588–92.

Cole LW, McGlathery KJ. Nitrogen fixation in restored eelgrass meadows. *Marine Ecology Progress Series* 2012;**448**:235–46.

Coskun ÖK, Pichler M, Vargas S *et al.* Linking Uncultivated Microbial Populations and Benthic Carbon Turnover by Using Quantitative Stable Isotope Probing. *Appl Environ Microbiol* 2018;**84**, DOI: 10.1128/AEM.01083-18.

Crump BC, Fine LM, Fortunato CS *et al.* Quantity and quality of particulate organic matter controls bacterial production in the Columbia River estuary. *Limnology and Oceanography* 2017;**62**:2713–31.

Crump BC, Kling GW, Bahr M *et al.* Bacterioplankton Community Shifts in an Arctic Lake Correlate with Seasonal Changes in Organic Matter Source. *Appl Environ Microbiol* 2003;**69**:2253–68.

Crump BC, Wojahn JM, Tomas F *et al.* Metatranscriptomics and Amplicon Sequencing Reveal Mutualisms in Seagrass Microbiomes. *Front Microbiol* 2018;**9**, DOI: 10.3389/fmicb.2018.00388.

Cúcio C, Engelen AH, Costa R *et al.* Rhizosphere Microbiomes of European Seagrasses Are Selected by the Plant, But Are Not Species Specific. *Front Microbiol* 2016;**7**, DOI: 10.3389/fmicb.2016.00440.

Cúcio C, Overmars L, Engelen AH *et al.* Metagenomic Analysis Shows the Presence of Bacteria Related to Free-Living Forms of Sulfur-Oxidizing Chemolithoautotrophic Symbionts in the Rhizosphere of the Seagrass Zostera marina. *Front Mar Sci* 2018;**5**, DOI: 10.3389/fmars.2018.00171.

Cunha AH, Marbá NN, van Katwijk MM *et al.* Changing Paradigms in Seagrass Restoration. *Restoration Ecology* 2012;**20**:427–30.

Cunning R, Baker AC. Excess algal symbionts increase the susceptibility of reef corals to bleaching. *Nature Climate Change* 2013;**3**:259.

Dang H, Lovell CR. Microbial Surface Colonization and Biofilm Development in Marine Environments. *Microbiol Mol Biol Rev* 2016;**80**:91–138.

Das S, Mangwani N. Ocean acidification and marine microorganisms: responses and consequences. *Oceanologia* 2015;**57**:349–61.

Davis RC, Short FT. Restoring eelgrass, *Zostera marina* L., habitat using a new transplanting technique: The horizontal rhizome method. *Aquatic Botany* 1997;**59**:1–15.

Deborde J, Abrill G, Mouret A *et al.* Effects of seasonal dynamics in a Zostera noltii meadow on phosphorus and iron cycles in a tidal mudflat (Arcachon Bay, France). *Marine Ecology Progress Series* 2008;**355**:59–71.

D'Esposito D, Orrù L, Dattolo E *et al.* Transcriptome characterisation and simple sequence repeat marker discovery in the seagrass Posidonia oceanica. *Scientific Data* 2016;**3**:1–9.

Dogs M, Wemheuer B, Wolter L *et al.* Rhodobacteraceae on the marine brown alga Fucus spiralis are abundant and show physiological adaptation to an epiphytic lifestyle. *Systematic and Applied Microbiology* 2017;**40**:370–82.

Doney SC, Busch DS, Cooley SR *et al.* The Impacts of Ocean Acidification on Marine Ecosystems and Reliant Human Communities. *Annual Review of Environment and Resources* 2020;**45**:null.

Doney SC, Ruckelshaus M, Duffy JE *et al.* Climate Change Impacts on Marine Ecosystems. *Annual Review of Marine Science* 2012;**4**:11–37.

Donnarumma L, Lombardi C, Cocito S *et al.* Settlement pattern of Posidonia oceanica epibionts along a gradient of ocean acidification: an approach with mimics. *Mediterranean Marine Science* 2014;**15**, DOI: 10.12681/mms.677.

Donnelly AP, Herbert RA. Bacterial interactions in the rhizosphere of seagrass communities in shallow coastal lagoons. *J Appl Microbiol* 1998;**85 Suppl 1**:151S-160S.

Dorokhov YL, Sheshukova EV, Komarova TV. Methanol in Plant Life. *Front Plant Sci* 2018;**9**, DOI: 10.3389/fpls.2018.01623.

Doronina N, Kaparullina E, Trotsenko Y. The Family Methylophilaceae. In: Rosenberg E, DeLong EF, Lory S, et al. (eds.). *The Prokaryotes: Alphaproteobacteria and Betaproteobacteria*. Berlin, Heidelberg: Springer Berlin Heidelberg, 2014, 869–80.

Duarte CM, Holmer M, Marbà N. Plant–Microbe Interactions in Seagrass Meadows. In: Kristensen E, Haese RR, Kostka JE (eds.). *Interactions Between Macro- and Microorganisms in Marine Sediments*. American Geophysical Union, 2005, 31–60.

Dufrêne M, Legendre P. Species Assemblages and Indicator Species:the Need for a Flexible Asymmetrical Approach. *Ecological Monographs* 1997;**67**:345–66.

Edwards J, Johnson C, Santos-Medellín C *et al.* Structure, variation, and assembly of the root-associated microbiomes of rice. *Proceedings of the National Academy of Sciences* 2015;**112**:E911–20.

Eichner M, Rost B, Kranz SA. Diversity of ocean acidification effects on marine N2 fixers. *Journal of Experimental Marine Biology and Ecology* 2014;**457**:199–207.

Elliff CI, Kikuchi RKP. Ecosystem services provided by coral reefs in a Southwestern Atlantic Archipelago. *Ocean & Coastal Management* 2017;**136**:49–55.

Ettinger CL, Voerman SE, Lang JM *et al.* Microbial communities in sediment from Zostera marina patches, but not the Z. marina leaf or root microbiomes, vary in relation to distance from patch edge. *PeerJ* 2017;**5**:e3246.

Ezzat L, Towle E, Irisson J-O *et al.* The relationship between heterotrophic feeding and inorganic nutrient availability in the scleractinian coral T. reniformis under a short-term temperature increase. *Limnol Oceanogr* 2016;**61**:89–102.

Fahimipour AK, Kardish MR, Eisen JA *et al.* Global-scale structure of the eelgrass microbiome. *bioRxiv* 2016:089797.

Fahimipour AK, Kardish MR, Lang JM *et al.* Global-Scale Structure of the Eelgrass Microbiome. *Appl Environ Microbiol* 2017;**83**:e03391-16.

Ferdie M, Fourqurean JW. Responses of seagrass communities to fertilization along a gradient of relative availability of nitrogen and phosphorus in a carbonate environment. *Limnology and Oceanography* 2004;**49**:2082–94.

Fernandes AD, Reid JN, Macklaim JM *et al.* Unifying the analysis of high-throughput sequencing datasets: characterizing RNA-seq, 16S rRNA gene sequencing and selective growth experiments by compositional data analysis. *Microbiome* 2014;**2**:15.

Ferrier-Pagès C, Godinot C, D'Angelo C *et al.* Phosphorus metabolism of reef organisms with algal symbionts. *Ecol Monogr* 2016;**86**:262–77.

Finster K, Liesack W, Tindall BJ. Sulfurospirillum arcachonense sp. nov., a New Microaerophilic Sulfur-Reducing Bacterium. *International Journal of Systematic and Evolutionary Microbiology* 1997;**47**:1212–7.

Flemming H-C, Wingender J. The biofilm matrix. *Nat Rev Microbiol* 2010;**8**:623–33.

Fourqurean JW, Duarte CM, Kennedy H *et al.* Seagrass ecosystems as a globally significant carbon stock. *Nature Geosci* 2012;**5**:505–9.

Fox J, Weisberg S. *An R Companion to Applied Regression*. Third. Thousand Oaks CA: Sage, 2019.

Frederiksen MS, Glud RN. Oxygen dynamics in the rhizosphere of Zostera marina: A two-dimensional planar optode study. *Limnology and Oceanography* 2006;**51**:1072–83.

Fuentes-Lema A, Sanleón-Bartolomé H, Lubián LM *et al.* Effects of elevated CO2 and phytoplankton-derived organic matter on the metabolism of bacterial communities from coastal waters. *Biogeosciences; Katlenburg-Lindau* 2018;**15**:6927–40.

Galbally IE, Kirstine W. The Production of Methanol by Flowering Plants and the Global Cycle of Methanol. *Journal of Atmospheric Chemistry* 2002;**43**:195–229.

Garcia R, La Clair JJ, Müller R. Future Directions of Marine Myxobacterial Natural Product Discovery Inferred from Metagenomics. *Marine Drugs* 2018;**16**:303.

Garcia-Martinez M, Kuo J, Kilminster K *et al.* Microbial colonization in the seagrass Posidonia spp. roots. *Marine Biology Research* 2005;**1**:388–95.

Garcias-Bonet N, Arrieta JM, Duarte CM *et al.* Nitrogen-fixing bacteria in Mediterranean seagrass (Posidonia oceanica) roots. *Aquatic Botany* 2016;**131**:57–60.

Garcias-Bonet N, Arrieta JM, de Santana CN *et al.* Endophytic bacterial community of a Mediterranean marine angiosperm (Posidonia oceanica). *Front Microbiol* 2012;**3**, DOI: 10.3389/fmicb.2012.00342.

Garcias-Bonet N, Fusi M, Ali M *et al.* High denitrification and anaerobic ammonium oxidation contributes to net nitrogen loss in a seagrass ecosystem in the central Red Sea. *Biogeosciences* 2018;**15**:7333–46.

Garrard SL, Beaumont NJ. The effect of ocean acidification on carbon storage and sequestration in seagrass beds; a global and UK context. *Marine Pollution Bulletin* 2014;**86**:138–46.

Garrard SL, Gambi MC, Scipione MB *et al.* Indirect effects may buffer negative responses of seagrass invertebrate communities to ocean acidification. *Journal of Experimental Marine Biology and Ecology* 2014;**461**:31–8.

Gazeau F, Parker LM, Comeau S *et al.* Impacts of ocean acidification on marine shelled molluscs. *Mar Biol* 2013;**160**:2207–45.

George R, Gullström M, Mtolera MSP *et al.* Methane emission and sulfide levels increase in tropical seagrass sediments during temperature stress: A mesocosm experiment. *Ecology and Evolution* 2020;**10**:1917–28.

Gil-Agudelo DL, Garzón-Ferreira J. Spatial and seasonal variation of dark spots disease in coral communities of the Santa Marta area (Colombian Caribbean). *Bulletin of Marine Science* 2001;**69**:619–629.

Glasl B, Herndl GJ, Frade PR. The microbiome of coral surface mucus has a key role in mediating holobiont health and survival upon disturbance. *The ISME Journal* 2016;**10**:2280.

Gloor GB, Macklaim JM, Pawlowsky-Glahn V *et al.* Microbiome Datasets Are Compositional: And This Is Not Optional. *Front Microbiol* 2017;**8**, DOI: 10.3389/fmicb.2017.02224.

Gochfeld D, Olson J, Slattery M. Colony versus population variation in susceptibility and resistance to dark spot syndrome in the Caribbean coral Siderastrea siderea. *Diseases of Aquatic Organisms* 2006;**69**:53–65.

Govers LL, de Brouwer JHF, Suykerbuyk W *et al.* Toxic effects of increased sediment nutrient and organic matter loading on the seagrass Zostera noltii. *Aquatic Toxicology* 2014a;**155**:253–60.

Govers LL, Lamers LPM, Bouma TJ *et al.* Eutrophication threatens Caribbean seagrasses – An example from Curaçao and Bonaire. *Marine Pollution Bulletin* 2014b;**89**:481–6.

Grech A, Coles R, Marsh H. A broad-scale assessment of the risk to coastal seagrasses from cumulative threats. *Marine Policy* 2011;**35**:560–7.

Gruber N. Warming up, turning sour, losing breath: ocean biogeochemistry under global change. *Philosophical Transactions of the Royal Society A: Mathematical, Physical and Engineering Sciences* 2011;**369**:1980–96.

Guevara R, Ikenaga M, Dean AL *et al.* Changes in Sediment Bacterial Community in Response to Long-Term Nutrient Enrichment in a Subtropical Seagrass-Dominated Estuary. *Microb Ecol* 2014;**68**:427–40.

Guilini K, Weber M, Beer D de *et al.* Response of Posidonia oceanica seagrass and its epibiont communities to ocean acidification. *PLOS ONE* 2017;**12**:e0181531.

Haapkylä J, Unsworth RKF, Flavell M *et al.* Seasonal Rainfall and Runoff Promote Coral Disease on an Inshore Reef. *PLOS ONE* 2011;**6**:e16893.

Hall-Spencer JM, Rodolfo-Metalpa R, Martin S *et al.* Volcanic carbon dioxide vents show ecosystem effects of ocean acidification. *Nature* 2008;**454**:96–9.

Halpern BS, Walbridge S, Selkoe KA *et al.* A Global Map of Human Impact on Marine Ecosystems. *Science* 2008;**319**:948–52.

Hansen J, Udy J, Perry C *et al.* Effect of the seagrass Zostera capricorni on sediment microbial processes. *Marine Ecology Progress Series* 2000;**199**:83–96.

Hargreaves SK, Williams RJ, Hofmockel KS. Environmental Filtering of Microbial Communities in Agricultural Soil Shifts with Crop Growth. *PLOS ONE* 2015;**10**:e0134345.

Hasler-Sheetal H, Holmer M. Sulfide Intrusion and Detoxification in the Seagrass Zostera marina. *PLoS One* 2015;**10**, DOI: 10.1371/journal.pone.0129136.

Hassenrück C, Fink A, Lichtschlag A *et al.* Quantification of the effects of ocean acidification on sediment microbial communities in the environment: the importance of ecosystem approaches. King G (ed.). *FEMS Microbiology Ecology* 2016;**92**:fiw027.

Hassenrück C, Hofmann LC, Bischof K *et al.* Seagrass biofilm communities at a naturally CO2-rich vent. *Environmental Microbiology Reports* 2015;**7**:516–25.

Hauxwell J, Cebrián J, Valiela I. Eelgrass Zostera marina loss in temperate estuaries:: relationship to land-derived nitrogen loads and effect of light limitation imposed by algae. *Marine Ecology Progress Series* 2003;**247**:59–73.

Heiberger RM. *HH: Statistical Analysis and Data Display: Heiberger and Holland.*, 2019.

Heide T van der, Govers LL, Fouw J de *et al.* A Three-Stage Symbiosis Forms the Foundation of Seagrass Ecosystems. *Science* 2012;**336**:1432–4.

Hemminga MA. The root/rhizome system of seagrasses: an asset and a burden. *Journal of Sea Research* 1998;**39**:183–96.

Hemminga MA, Harrison PG, Lent F van. The balance of nutrient losses and gains in seagrass meadows. *Marine Ecology Progress Series* 1991;**71**:85–96.

Hentschel U, Piel J, Degnan SM *et al.* Genomic insights into the marine sponge microbiome. *Nature Reviews Microbiology* 2012;**10**:641–54.

Hernán G, Ramajo L, Basso L *et al.* Seagrass (Posidonia oceanica) seedlings in a high-CO 2 world: from physiology to herbivory. *Scientific Reports* 2016;**6**:38017.

Hervé M. *RVAideMemoire: Testing and Plotting Procedures for Biostatistics*., 2018.

Hessing-Lewis ML, Hacker SD, Menge BA *et al.* Are large macroalgal blooms necessarily bad? nutrient impacts on seagrass in upwelling-influenced estuaries. *Ecological Applications* 2015;**25**:1330–1347.

Hiltner L. Über nevere Erfahrungen und Probleme auf dem Gebiet der Boden Bakteriologie und unter besonderer Beurchsichtigung der Gründüngung und Broche. *Arbeit Deut Landw Ges Berlin* 1904;**98**:59–78.

Hoegh-Guldberg O, Smith GJ. Influence of the population density of zooxanthellae and supply of ammonium on the biomass and metabolic characteristics of the reef corals Seriatopora hystrix and Stylophora pistillata. *Marine Ecology Progress Series* 1989;**57**:173–86.

Holmer M. Productivity and Biogeochemical Cycling in Seagrass Ecosystems. *Coastal Wetlands*. Elsevier, 2019, 443–77.

Holmer M, Andersen FØ, Nielsen SL *et al.* The importance of mineralization based on sulfate reduction for nutrient regeneration in tropical seagrass sediments. *Aquatic Botany* 2001;**71**:1–17.

Holmer M, Bondgaard EJ. Photosynthetic and growth response of eelgrass to low oxygen and high sulfide concentrations during hypoxic events. *Aquatic Botany* 2001;**70**:29–38.

Holmer M, Duarte C, Boschker H *et al.* Carbon cycling and bacterial carbon sources in pristine and impacted Mediterranean seagrass sediments. *Aquatic Microbial Ecology* 2004;**36**:227–37.

Holmer M, Frederiksen MS, Møllegaard H. Sulfur accumulation in eelgrass (Zostera marina) and effect of sulfur on eelgrass growth. *Aquatic Botany* 2005;**81**:367–79.

Hong H, Shen R, Zhang F *et al.* The complex effects of ocean acidification on the prominent N2-fixing cyanobacterium Trichodesmium. *Science* 2017;**356**:527–31.

Hood-Nowotny R, Umana NH-N, Inselbacher E *et al.* Alternative Methods for Measuring Inorganic, Organic, and Total Dissolved Nitrogen in Soil. *Soil Science Society of America Journal* 2010;**74**:1018–27.

Hooidonk R van, Maynard J, Tamelander J *et al.* Local-scale projections of coral reef futures and implications of the Paris Agreement. *Scientific Reports* 2016;**6**:39666.

Hothorn T, Bretz F, Westfall P. Simultaneous inference in general parametric models. *Biom J* 2008;**50**:346–63.

Howarth RW. Coastal nitrogen pollution: A review of sources and trends globally and regionally. *Harmful Algae* 2008;**8**:14–20.

Howarth RW, Sharpley A, Walker D. Sources of nutrient pollution to coastal waters in the United States: Implications for achieving coastal water quality goals. *Estuaries* 2002;**25**:656–76.

Hughes TP, Barnes ML, Bellwood DR *et al.* Coral reefs in the Anthropocene. *Nature* 2017;**546**:82–90.

Hurtado-McCormick V, Kahlke T, Petrou K *et al.* Regional and Microenvironmental Scale Characterization of the Zostera muelleri Seagrass Microbiome. *Front Microbiol* 2019;**10**, DOI: 10.3389/fmicb.2019.01011.

Hyatt D, Chen G-L, LoCascio PF *et al.* Prodigal: prokaryotic gene recognition and translation initiation site identification. *BMC Bioinformatics* 2010;**11**:119.

Igai K, Itakura M, Nishijima S *et al.* Nitrogen fixation and *nifH* diversity in human gut microbiota. *Sci Rep* 2016;**6**:1–11.

Invers O, Zimmerman RC, Alberte RS *et al.* Inorganic carbon sources for seagrass photosynthesis: an experimental evaluation of bicarbonate use in species inhabiting temperate waters. *Journal of Experimental Marine Biology and Ecology* 2001;**265**:203–17.

Isaksen MF, Finster K. Sulphate reduction in the root zone of the seagrass Zostera noltii on the intertidal flats of a coastal lagoon (Arcachon, France). *Marine Ecology Progress Series* 1996;**137**:187–94.

Isaksen MF, Teske A. *Desulforhopalus vacuolatus* gen. nov., sp. nov., a new moderately psychrophilic sulfate-reducing bacterium with gas vacuoles isolated from a temperate estuary. *Arch Microbiol* 1996;**166**:160–8.

Janda JM, Abbott SL. 16S rRNA Gene Sequencing for Bacterial Identification in the Diagnostic Laboratory: Pluses, Perils, and Pitfalls. *Journal of Clinical Microbiology* 2007;**45**:2761–4.

Jensen PR, Jenkins KM, Porter D *et al.* Evidence that a New Antibiotic Flavone Glycoside Chemically Defends the Sea Grass Thalassia testudinum against Zoosporic Fungi. *Appl Environ Microbiol* 1998;**64**:1490–6.

Jensen SI, Kühl M, Priemé A. Different bacterial communities associated with the roots and bulk sediment of the seagrass Zostera marina. *FEMS Microbiol Ecol* 2007;**62**:108–17.

Jiang Z, Liu S, Zhang J *et al.* Eutrophication indirectly reduced carbon sequestration in a tropical seagrass bed. *Plant Soil* 2018;**426**:135–52.

Jiang ZJ, Huang X-P, Zhang J-P. Effects of CO2 Enrichment on Photosynthesis, Growth, and Biochemical Composition of Seagrass Thalassia hemprichii (Ehrenb.) Aschers. *Journal of Integrative Plant Biology* 2010;**52**:904–13.

Jones P, Garcia BJ, Furches A *et al.* Plant Host-Associated Mechanisms for Microbial Selection. *Front Plant Sci* 2019;**10**, DOI: 10.3389/fpls.2019.00862.

Junier P, Molina V, Dorador C *et al.* Phylogenetic and functional marker genes to study ammonia-oxidizing microorganisms (AOM) in the environment. *Appl Microbiol Biotechnol* 2010;**85**:425–40.

Jurburg SD, Nunes I, Stegen JC *et al.* Autogenic succession and deterministic recovery following disturbance in soil bacterial communities. *Sci Rep* 2017;**7**:45691.

Kaczmarsky L, Richardson LL. Do elevated nutrients and organic carbon on Philippine reefs increase the prevalence of coral disease? *Coral Reefs* 2011;**30**:253–7.

Kaldy J. Influence of light, temperature and salinity on dissolved organic carbon exudation rates in Zostera marinaL. *Aquatic Biosystems* 2012;**8**:19.

Kaldy JE, Eldridge PM, Cifuentes LA *et al.* Utilization of DOC from seagrass rhizomes by sediment bacteria: 13C-tracer experiments and modeling. *Mar Ecol Prog Ser* 2006;**317**:41–55.

Kanehisa M, Sato Y, Kawashima M *et al.* KEGG as a reference resource for gene and protein annotation. *Nucl Acids Res* 2016;**44**:D457–62.

Kang I, Lim Y, Cho J-C. Complete genome sequence of Granulosicoccus antarcticus type strain IMCC3135T, a marine gammaproteobacterium with a putative dimethylsulfoniopropionate demethylase gene. *Marine Genomics* 2018;**37**:176–81.

Kassambara A. *Ggpubr: "Ggplot2" Based Publcation Ready Plots.*, 2019.

van Katwijk M, Vergeer L, Schmitz G *et al.* Ammonium toxicity in eelgrass Zostera marina. *Marine Ecology Progress Series* 1997;**157**:159–73.

van Katwijk MM, Bos AR, de Jonge VN *et al.* Guidelines for seagrass restoration: Importance of habitat selection and donor population, spreading of risks, and ecosystem engineering effects. *Marine Pollution Bulletin* 2009;**58**:179–88.

van Katwijk MM, Thorhaug Anitra, Marbà Núria *et al.* Global analysis of seagrass restoration: the importance of large-scale planting. *Journal of Applied Ecology* 2016;**53**:567–78.

Kellogg CA, Piceno YM, Tom LM *et al.* Comparing Bacterial Community Composition of Healthy and Dark Spot-Affected Siderastrea siderea in Florida and the Caribbean. *PLOS ONE* 2014;**9**:e108767.

Kessler AJ, Wawryk M, Marzocchi U *et al.* Cable bacteria promote DNRA through iron sulfide dissolution. *Limnology and Oceanography* 2019;**64**:1228–38.

Kieft B, Li Z, Bryson S *et al.* Microbial Community Structure–Function Relationships in Yaquina Bay Estuary Reveal Spatially Distinct Carbon and Nitrogen Cycling Capacities. *Front Microbiol* 2018;**9**, DOI: 10.3389/fmicb.2018.01282.

Kilminster K, Garland J. Aerobic heterotrophic microbial activity associated with seagrass roots: effects of plant type and nutrient amendment. *Aquat Microb Ecol* 2009;**57**:57–68.

Knight R, Vrbanac A, Taylor BC *et al.* Best practices for analysing microbiomes. *Nature Reviews Microbiology* 2018;**16**:410–22.

Koch M, Bowes G, Ross C *et al.* Climate change and ocean acidification effects on seagrasses and marine macroalgae. *Global Change Biology* 2013;**19**:103–32.

Kolowith LC, Ingall ED, Benner R. Composition and cycling of marine organic phosphorus. *Limnology and Oceanography* 2001;**46**:309–20.

Koweek DA, Zimmerman RC, Hewett KM *et al.* Expected limits on the ocean acidification buffering potential of a temperate seagrass meadow. *Ecol Appl* 2018;**28**:1694–714.

Kroeker KJ, Kordas RL, Crim RN *et al.* Meta-analysis reveals negative yet variable effects of ocean acidification on marine organisms. *Ecology Letters* 2010;**13**:1419–34.

Krueger F. *"Trim Galore." A Wrapper Tool around Cutadapt and FastQC to Consistently Apply Quality and Adapter Trimming to FastQ Files*., 2015.

Kuever J. The Family Desulfobacteraceae. In: Rosenberg E, DeLong EF, Lory S, et al. (eds.). *The Prokaryotes: Deltaproteobacteria and Epsilonproteobacteria*. Berlin, Heidelberg: Springer Berlin Heidelberg, 2014a, 45–73.

Kuever J. The Family Desulfobulbaceae. In: Rosenberg E, DeLong EF, Lory S, et al. (eds.). *The Prokaryotes: Deltaproteobacteria and Epsilonproteobacteria*. Berlin, Heidelberg: Springer Berlin Heidelberg, 2014b, 75–86.

Kurilenko VV, Christen R, Zhukova NV *et al.* Granulosicoccus coccoides sp. nov., isolated from leaves of seagrass (Zostera marina). *INTERNATIONAL JOURNAL OF SYSTEMATIC AND EVOLUTIONARY MICROBIOLOGY* 2010;**60**:972–6.

Kurm V, Geisen S, Hol WHG. A low proportion of rare bacterial taxa responds to abiotic changes compared to dominant taxa. *Environmental Microbiology* 2018;**0**, DOI: 10.1111/1462-2920.14492.

Kurm V, van der Putten WH, de Boer W *et al.* Low abundant soil bacteria can be metabolically versatile and fast growing. *Ecology* 2017;**98**:555–64.

Lakshmanan V, Castaneda R, Rudrappa T *et al.* Root transcriptome analysis of *Arabidopsis thaliana* exposed to beneficial *Bacillus subtilis* FB17 rhizobacteria revealed genes for bacterial recruitment and plant defense independent of malate efflux. *Planta* 2013;**238**:657–68.

Lamb JB, van de Water JA, Bourne DG *et al.* Seagrass ecosystems reduce exposure to bacterial pathogens of humans, fishes, and invertebrates. *Science* 2017;**355**:731–733.

Langmead B, Salzberg SL. Fast gapped-read alignment with Bowtie 2. *Nat Methods* 2012;**9**:357–9.

Lapointe BE, Barile PJ, Matzie WR. Anthropogenic nutrient enrichment of seagrass and coral reef communities in the Lower Florida Keys: discrimination of local versus regional nitrogen sources. *Journal of Experimental Marine Biology and Ecology* 2004;**308**:23–58.

Lareen A, Burton F, Schäfer P. Plant root-microbe communication in shaping root microbiomes. *Plant Mol Biol* 2016;**90**:575–87.

Larkum AWD, Davey PA, Kuo J *et al.* Carbon-concentrating mechanisms in seagrasses. *J Exp Bot* 2017;**68**:3773–84.

Lebeis SL, Paredes SH, Lundberg DS *et al.* Salicylic acid modulates colonization of the root microbiome by specific bacterial taxa. *Science* 2015;**349**:860–4.

Lehnen N, Marchant HK, Schwedt A *et al.* High rates of microbial dinitrogen fixation and sulfate reduction associated with the Mediterranean seagrass Posidonia oceanica. *Systematic and Applied Microbiology* 2016;**39**:476–83.

Lei J, Nepf H. Wave damping by flexible vegetation: Connecting individual blade dynamics to the meadow scale. *Coastal Engineering* 2019;**147**:138–48.

Li D, Liu C-M, Luo R *et al.* MEGAHIT: an ultra-fast single-node solution for large and complex metagenomics assembly via succinct de Bruijn graph. *Bioinformatics* 2015;**31**:1674–6.

Li H, Handsaker B, Wysoker A *et al.* The Sequence Alignment/Map format and SAMtools. *Bioinformatics* 2009;**25**:2078–9.

Lidbury I, Johnson V, Hall-Spencer JM *et al.* Community-level response of coastal microbial biofilms to ocean acidification in a natural carbon dioxide vent ecosystem. *Marine Pollution Bulletin* 2012;**64**:1063–6.

Lilburn TG, Gu J, Cai H *et al.* Comparative genomics of the family Vibrionaceae reveals the wide distribution of genes encoding virulence-associated proteins. *BMC Genomics* 2010;**11**:369.

Lindow SE, Brandl MT. Microbiology of the Phyllosphere. *Appl Environ Microbiol* 2003;**69**:1875–83.

Liu J, Weinbauer M, Maier C *et al.* Effect of ocean acidification on microbial diversity and on microbe-driven biogeochemistry and ecosystem functioning. *Aquatic Microbial Ecology* 2010;**61**:291–305.

Liu S, Jiang Z, Deng Y *et al.* Effects of nutrient loading on sediment bacterial and pathogen communities within seagrass meadows. *MicrobiologyOpen* 2018;**0**:e00600.

Liu S, Jiang Z, Wu Y *et al.* Effects of nutrient load on microbial activities within a seagrass-dominated ecosystem: Implications of changes in seagrass blue carbon. *Marine Pollution Bulletin* 2017a;**117**:214–21.

Liu S, Jiang Z, Zhang J *et al.* Sediment microbes mediate the impact of nutrient loading on blue carbon sequestration by mixed seagrass meadows. *Science of The Total Environment* 2017b;**599–600**:1479–84.

Longford SR, Campbell AH, Nielsen S *et al.* Interactions within the microbiome alter microbial interactions with host chemical defences and affect disease in a marine holobiont. *Sci Rep* 2019a;**9**:1–13.

Longford SR, Campbell AH, Nielsen S *et al.* Interactions within the microbiome alter microbial interactions with host chemical defences and affect disease in a marine holobiont. *Sci Rep* 2019b;**9**:1–13.

López NI, Duarte CM, Vallespinós F *et al.* Bacterial activity in NW Mediterranean seagrass (Posidonia oceanica) sediments. *Journal of Experimental Marine Biology and Ecology* 1995;**187**:39–49.

López NI, Duarte CM, Vallespinós F *et al.* The effect of nutrient additions on bacterial activity in seagrass (Posidonia oceanica) sediments. *Journal of Experimental Marine Biology and Ecology* 1998;**224**:155–66.

Love MI, Huber W, Anders S. Moderated estimation of fold change and dispersion for RNA-seq data with DESeq2. *Genome Biol* 2014;**15**, DOI: 10.1186/s13059-014-0550-8.

Lozupone C, Knight R. UniFrac: a New Phylogenetic Method for Comparing Microbial Communities. *Appl Environ Microbiol* 2005;**71**:8228–35.

Lozupone CA, Stombaugh JI, Gordon JI *et al.* Diversity, stability and resilience of the human gut microbiota. *Nature* 2012;**489**:220–30.

Lu Y, Edmonds JW, Yamashita Y *et al.* Spatial variation in the origin and reactivity of dissolved organic matter in Oregon-Washington coastal waters. *Ocean Dynamics* 2015;**65**:17–32.

Lundberg DS, Lebeis SL, Paredes SH *et al.* Defining the core *Arabidopsis thaliana* root microbiome. *Nature* 2012;**488**:86–90.

Lundberg DS, Yourstone S, Mieczkowski P *et al.* Practical innovations for high-throughput amplicon sequencing. *Nature Methods* 2013;**10**:999–1002.

Madhaiyan M, Poonguzhali S, Lee HS *et al.* Pink-pigmented facultative methylotrophic bacteria accelerate germination, growth and yield of sugarcane clone Co86032 (Saccharum officinarum L.). *Biol Fertil Soils* 2005;**41**:350–8.

Magris RA, Heron SF, Pressey RL. Conservation Planning for Coral Reefs Accounting for Climate Warming Disturbances. *PLOS ONE* 2015;**10**:e0140828.

Maignien L, DeForce EA, Chafee ME *et al.* Ecological Succession and Stochastic Variation in the Assembly of Arabidopsis thaliana Phyllosphere Communities. *mBio* 2014;**5**:e00682-13.

Mandal S, Van Treuren W, White RA *et al.* Analysis of composition of microbiomes: a novel method for studying microbial composition. *Microb Ecol Health Dis* 2015;**26**, DOI: 10.3402/mehd.v26.27663.

Manzello DP. Rapid Recent Warming of Coral Reefs in the Florida Keys. *Scientific Reports* 2015;**5**:16762.

Marietou A. Nitrate reduction in sulfate-reducing bacteria. *FEMS Microbiol Lett* 2016;**363**, DOI: 10.1093/femsle/fnw155.

Martin BC, Alarcon MS, Gleeson D *et al.* Root microbiomes as indicators of seagrass health. *FEMS Microbiol Ecol* 2020;**96**, DOI: 10.1093/femsec/fiz201.

Martin BC, Bougoure J, Ryan MH *et al.* Oxygen loss from seagrass roots coincides with colonisation of sulphide-oxidising cable bacteria and reduces sulphide stress. *The ISME Journal* 2019;**13**:707.

Martin BC, Gleeson D, Statton J *et al.* Low Light Availability Alters Root Exudation and Reduces Putative Beneficial Microorganisms in Seagrass Roots. *Frontiers in Microbiology* 2018a;**8**, DOI: 10.3389/fmicb.2017.02667.

Martin BC, Statton J, Siebers AR *et al.* Colonizing tropical seagrasses increase root exudation under fluctuating and continuous low light. *Limnology and Oceanography* 2018;**63**:S381–91.

Martin BD, Witten D, Willis AD. Modeling microbial abundances and dysbiosis with beta-binomial regression. *Ann Appl Stat* 2020;**14**:94–115.

Martin M. Cutadapt removes adapter sequences from high-throughput sequencing reads. *EMBnet.journal* 2011:3.

Martin S, Rodolfo-Metalpa R, Ransome E *et al.* Effects of naturally acidified seawater on seagrass calcareous epibionts. *Biology Letters* 2008;**4**:689–92.

Martino C, Morton JT, Marotz CA *et al.* A Novel Sparse Compositional Technique Reveals Microbial Perturbations. *mSystems* 2019;**4**, DOI: 10.1128/mSystems.00016-19.

Martiny AC, Coleman ML, Chisholm SW. Phosphate acquisition genes in Prochlorococcus ecotypes: Evidence for genome-wide adaptation. *PNAS* 2006;**103**:12552–7.

Marubini F, Davies PS. Nitrate increases zooxanthellae population density and reduces skeletogenesis in corals. *Mar Biol* 1996;**127**:319–28.

Matheson FE, Reed J, Santos VMD *et al.* Seagrass rehabilitation: successful transplants and evaluation of methods at different spatial scales. *New Zealand Journal of Marine and Freshwater Research* 2017;**51**:96–109.

Maynard J, Hooidonk R van, Eakin CM *et al.* Projections of climate conditions that increase coral disease susceptibility and pathogen abundance and virulence. *Nature Climate Change* 2015;**5**:688.

Mazel F, Davis KM, Loudon A *et al.* Is Host Filtering the Main Driver of Phylosymbiosis across the Tree of Life? *mSystems* 2018;**3**:e00097-18.

McBride MJ. The Family Flavobacteriaceae. In: Rosenberg E, DeLong EF, Lory S, et al. (eds.). *The Prokaryotes: Other Major Lineages of Bacteria and The Archaea*. Berlin, Heidelberg: Springer, 2014, 643–76.

McDevitt-Irwin JM, Baum JK, Garren M *et al.* Responses of Coral-Associated Bacterial Communities to Local and Global Stressors. *Front Mar Sci* 2017;**4**, DOI: 10.3389/fmars.2017.00262.

McGlathery KJ. Macroalgal Blooms Contribute to the Decline of Seagrass in Nutrient-Enriched Coastal Waters. *Journal of Phycology* 2001;**37**:453–6.

McIlroy S, Nielsen P. The Family Saprospiraceae. *The Prokaryotes: Other Major Lineages of Bacteria and The Archaea*. 2014, 863–89.

McLaren MR, Willis AD, Callahan BJ. Consistent and correctable bias in metagenomic sequencing experiments. Turnbaugh P, Garrett WS, Turnbaugh P, et al. (eds.). *eLife* 2019;**8**:e46923.

McMurdie PJ, Holmes S. phyloseq: An R Package for Reproducible Interactive Analysis and Graphics of Microbiome Census Data. *PLOS ONE* 2013;**8**:e61217.

Mejia AY, Rotini A, Lacasella F *et al.* Assessing the ecological status of seagrasses using morphology, biochemical descriptors and microbial community analyses. A study in *Halophila stipulacea* (Forsk.) Aschers meadows in the northern Red Sea. *Ecological Indicators* 2016;**60**:1150–63.

Menzel P, Ng KL, Krogh A. Fast and sensitive taxonomic classification for metagenomics with Kaiju. *Nature Communications* 2016;**7**:1–9.

Meron D, Atias E, Kruh LI *et al.* The impact of reduced pH on the microbial community of the coral Acropora eurystoma. *ISME J* 2011;**5**:51–60.

Meyer JL, Rodgers JM, Dillard BA *et al.* Epimicrobiota Associated with the Decay and Recovery of Orbicella Corals Exhibiting Dark Spot Syndrome. *Front Microbiol* 2016;**7**, DOI: 10.3389/fmicb.2016.00893.

Milbrandt EC, Greenawalt-Boswell J, Sokoloff PD. Short-term indicators of seagrass transplant stress in response to sediment bacterial community disruption. *Botanica Marina* 2008;**51**, DOI: 10.1515/BOT.2008.020.

Mincer TJ, Aicher AC. Methanol Production by a Broad Phylogenetic Array of Marine Phytoplankton. *PLOS ONE* 2016;**11**:e0150820.

Mitchell HM, Rocha GA, Kaakoush NO *et al.* The Family Helicobacteraceae. In: Rosenberg E, DeLong EF, Lory S, et al. (eds.). *The Prokaryotes: Deltaproteobacteria and Epsilonproteobacteria*. Berlin, Heidelberg: Springer Berlin Heidelberg, 2014, 337–92.

Mohr KI, Garcia RO, Gerth K *et al. Sandaracinus amylolyticus* gen. nov., sp. nov., a starch-degrading soil myxobacterium, and description of Sandaracinaceae fam. nov. *International Journal of Systematic and Evolutionary Microbiology,* 2012;**62**:1191–8.

Mollica NR, Guo W, Cohen AL *et al.* Ocean acidification affects coral growth by reducing skeletal density. *PNAS* 2018;**115**:1754–9.

Morgan JAW, Bending GD, White PJ. Biological costs and benefits to plant–microbe interactions in the rhizosphere. *Journal of Experimental Botany* 2005;**56**:1729–39.

Morgan M. *BiocManager: Access the Bioconductor Project Package Repository*., 2018.

Moriarty DJW, Pollard PC. Diel variation of bacterial productivity in seagrass (Zostera capricorni) beds measured by rate of thymidine incorporation into DNA. *Marine Biology* 1982;**72**:165–73.

Morrow KM, Bourne DG, Humphrey C *et al.* Natural volcanic CO 2 seeps reveal future trajectories for host–microbial associations in corals and sponges. *The ISME Journal* 2015;**9**:894–908.

Morrow KM, Moss AG, Chadwick NE *et al.* Bacterial Associates of Two Caribbean Coral Species Reveal Species-Specific Distribution and Geographic Variability. *Appl Environ Microbiol* 2012;**78**:6438–49.

Morse JW, Dimarco SF, Sell KS *et al.* Determination of the Optimum Sampling Intervals in Sediment Pore Waters Using the Autocovariance Function. *Aquatic Geochemistry* 2003;**9**:41–57.

Mueller RS, McDougald D, Cusumano D *et al. Vibrio cholerae* Strains Possess Multiple Strategies for Abiotic and Biotic Surface Colonization. *Journal of Bacteriology* 2007;**189**:5348–60.

Munn CB. The Role of Vibrios in Diseases of Corals. *Microbiology Spectrum* 2015;**3**, DOI: 10.1128/microbiolspec.VE-0006-2014.

Muscatine L, Falkowski PG, Dubinsky Z *et al.* The effect of external nutrient resources on the population dynamics of zooxanthellae in a reef coral. *Proc R Soc Lond B* 1989;**236**:311–24.

Nayfach S, Bradley PH, Wyman SK *et al.* Automated and accurate estimation of gene family abundance from shotgun metagenomes. *PLoS Comput Biol* 2015;**11**:e1004573.

Neave MJ, Apprill A, Ferrier-Pagès C *et al.* Diversity and function of prevalent symbiotic marine bacteria in the genus Endozoicomonas. *Appl Microbiol Biotechnol* 2016;**100**:8315–24.

Neave MJ, Michell CT, Apprill A *et al.* Endozoicomonas genomes reveal functional adaptation and plasticity in bacterial strains symbiotically associated with diverse marine hosts. *Scientific Reports* 2017;**7**:40579.

Nielsen LB, Finster K, Welsh DT *et al.* Sulphate reduction and nitrogen fixation rates associated with roots, rhizomes and sediments from Zostera noltii and Spartina maritima meadows. *Environmental Microbiology* 2001;**3**:63–71.

NOAA and Coral Reef Watch, US Department of Commerce. *2014 Annual Summaries of Thermal Conditions Related to Coral Bleaching for U.S. National Coral Reef Monitoring Program (NCRMP) Jurisdictions.*, 2014.

Norström AV, Nyström M, Jouffray J-B *et al.* Guiding coral reef futures in the Anthropocene. *Frontiers in Ecology and the Environment* 2016;**14**:490–8.

Novak AB, Plaisted HK, Hays CG *et al.* Limited effects of source population identity and number on seagrass transplant performance. *PeerJ* 2017;**5**, DOI: 10.7717/peerj.2972.

Nowicki R, Heithaus M, Thomson J *et al.* Indirect legacy effects of an extreme climatic event on a marine megafaunal community. *Ecological Monographs* 2019;**0**:e01365.

Nowicki R, Thomson J, Burkholder D *et al.* Predicting seagrass recovery times and their implications following an extreme climate event. *Marine Ecology Progress Series* 2017;**567**:79–93.

Nurk S, Meleshko D, Korobeynikov A *et al.* metaSPAdes: a new versatile metagenomic assembler. *Genome Res* 2017;**27**:824–34.

O'Brien PA, Morrow KM, Willis BL *et al.* Implications of Ocean Acidification for Marine Microorganisms from the Free-Living to the Host-Associated. *Front Mar Sci* 2016;**3**, DOI: 10.3389/fmars.2016.00047.

Oksanen JF, Blanchet G, Friendly M *et al. Vegan: Community Ecology Package*., 2018.

van Oppen MJH, Blackall LL. Coral microbiome dynamics, functions and design in a changing world. *Nature Reviews Microbiology* 2019;**17**:557–67.

Oreska MPJ, Wilkinson GM, McGlathery KJ *et al.* Non-seagrass carbon contributions to seagrass sediment blue carbon. *Limnology and Oceanography* 2018;**63**:S3–18.

Orth RJ, Carruthers TJB, Dennison WC *et al.* A Global Crisis for Seagrass Ecosystems. *BioScience* 2006;**56**:987–96.

Ow YX, Collier CJ, Uthicke S. Responses of three tropical seagrass species to CO2 enrichment. *Mar Biol* 2015;**162**:1005–17.

Pacella SR, Brown CA, Waldbusser GG *et al.* Seagrass habitat metabolism increases short-term extremes and long-term offset of CO2 under future ocean acidification. *Proceedings of the National Academy of Sciences* 2018;**115**:3870–5.

Papazian S, Parrot D, Burýšková B *et al.* Surface chemical defence of the eelgrass Zostera marina against microbial foulers. *Scientific Reports* 2019;**9**:3323.

Paradis E, Schliep K. ape 5.0: an environment for modern phylogenetics and evolutionary analyses in R. *Bioinformatics* 2018;**35**:526–8.

Park S, Jung Y-T, Won S-M *et al.* Granulosicoccus undariae sp. nov., a member of the family Granulosicoccaceae isolated from a brown algae reservoir and emended description of the genus Granulosicoccus. *Antonie van Leeuwenhoek* 2014;**106**:845–52.

Paterson E, Sim A. Soil-specific response functions of organic matter mineralization to the availability of labile carbon. *Global Change Biology* 2013;**19**:1562–71.

Pedersen O, Binzer T, Borum J. Sulphide intrusion in eelgrass (Zostera marina L.). *Plant, Cell & Environment* 2004;**27**:595–602.

Pérez M, Invers O, Ruiz JM *et al.* Physiological responses of the seagrass Posidonia oceanica to elevated organic matter content in sediments: An experimental assessment. *Journal of Experimental Marine Biology and Ecology* 2007;**344**:149–60.

Pfeffer C, Larsen S, Song J *et al.* Filamentous bacteria transport electrons over centimetre distances. *Nature* 2012;**491**:218–21.

Piontek J, Lunau M, Händel N *et al.* Acidification increases microbial polysaccharide degradation in the ocean. *Biogeosciences* 2010;**7**:1615–24.

Pollard P, Moriarty D. Organic carbon decomposition, primary and bacterial productivity, and sulphate reduction, in tropical seagrass beds of the Gulf of Carpentaria, Australia. *Marine Ecology Progress Series* 1991;**69**:149–59.

Porter JW, Torres C, Sutherland KP *et al.* Prevalence, severity, lethality, and recovery of dark spots syndrome among three Floridian reef-building corals. *Journal of Experimental Marine Biology and Ecology* 2011;**408**:79–87.

Pörtner H-O, Roberts DC, Masson-Delmotte V *et al. IPCC, 2019. Summary for Policymakers. In: IPCC Special Report on the Ocean and Cryosphere in a Changing Climate*., 2019.

Pratchett MS, Hoey AS, Wilson SK. Reef degradation and the loss of critical ecosystem goods and services provided by coral reef fishes. *Current Opinion in Environmental Sustainability* 2014;**7**:37–43.

Prentice C, Hessing-Lewis M, Sanders-Smith R *et al.* Reduced water motion enhances organic carbon stocks in temperate eelgrass meadows. *Limnology and Oceanography* 2019;**0**, DOI: 10.1002/lno.11191.

Price MN, Dehal PS, Arkin AP. FastTree 2 – Approximately Maximum-Likelihood Trees for Large Alignments. *PLoS ONE* 2010;**5**:e9490.

Probandt D, Knittel K, Tegetmeyer HE *et al.* Permeability shapes bacterial communities in sublittoral surface sediments. *Environmental Microbiology* 2017;**19**:1584–99.

Qiu X, Liu G-P, Zhu Y-Q. Determination of water-soluble ammonium ion in soil by spectrophotometry. *Analyst* 1987;**112**:909–11.

Quast C, Pruesse E, Yilmaz P *et al.* The SILVA ribosomal RNA gene database project: improved data processing and web-based tools. *Nucleic Acids Res* 2013;**41**:D590–6.

R Core Team. *R: A Language and Environment for Statistical Computing.* Vienna, Austria, 2018.

Ralph PJ, Durako MJ, Enríquez S *et al.* Impact of light limitation on seagrasses. *Journal of Experimental Marine Biology and Ecology* 2007;**350**:176–93.

Randall CJ, Jordán-Garza AG, Muller EM *et al.* Does Dark-Spot Syndrome Experimentally Transmit among Caribbean Corals? *PLOS ONE* 2016;**11**:e0147493.

Richardson LL. Coral diseases: what is really known? *Trends in Ecology & Evolution* 1998;**13**:438–43.

Ritchie K. Regulation of microbial populations by coral surface mucus and mucus-associated bacteria. *Mar Ecol Prog Ser* 2006;**322**:1–14.

Rodriguez-Mora MJ, Edgcomb VP, Taylor C *et al.* The Diversity of Sulfide Oxidation and Sulfate Reduction Genes Expressed by the Bacterial Communities of the Cariaco Basin, Venezuela. *The Open Microbiology Journal* 2016;**10**, DOI: 10.2174/1874285801610010140.

Rohwer F, Breitbart M, Jara J *et al.* Diversity of bacteria associated with the Caribbean coral Montastraea franksi. *Coral Reefs* 2001;**20**:85–91.

Rolny N, Costa L, Carrión C *et al.* Is the electrolyte leakage assay an unequivocal test of membrane deterioration during leaf senescence? *Plant Physiology and Biochemistry* 2011;**49**:1220–7.

Román M, Fernández E, Méndez G. Anthropogenic nutrient inputs in the NW Iberian Peninsula estuaries determined by nitrogen and carbon isotopic signatures of Zostera noltei seagrass meadows. *Marine Environmental Research* 2019;**143**:30–8.

Rosenberg E, Koren O, Reshef L *et al.* The role of microorganisms in coral health, disease and evolution. *Nature Reviews Microbiology* 2007;**5**:355–362.

Ruiz J, Romero J. Effects of in situ experimental shading on the Mediterranean seagrass Posidonia oceanica. *Marine Ecology Progress Series* 2001;**215**:107–20.

Russell BD, Connell SD, Findlay HS *et al.* Ocean acidification and rising temperatures may increase biofilm primary productivity but decrease grazer consumption. *Philos Trans R Soc Lond B Biol Sci* 2013;**368**, DOI: 10.1098/rstb.2012.0438.

Säwström C, Serrano O, Rozaimi M *et al.* Utilization of carbon substrates by heterotrophic bacteria through vertical sediment profiles in coastal and estuarine seagrass meadows. *Environmental Microbiology Reports* 2016:n/a-n/a.

Schloss PD, Westcott SL, Ryabin T *et al.* Introducing mothur: Open-Source, Platform-Independent, Community-Supported Software for Describing and Comparing Microbial Communities. *Appl Environ Microbiol* 2009;**75**:7537–41.

Schmidt AL, Wysmyk JKC, Craig SE *et al.* Regional-scale effects of eutrophication on ecosystem structure and services of seagrass beds. *Limnology and Oceanography* 2012;**57**:1389–402.

Schoepf V, Grottoli AG, Levas SJ *et al.* Annual coral bleaching and the long-term recovery capacity of coral. *Proc R Soc B* 2015;**282**:20151887.

Scholz VV, Mueller H, Koren K *et al.* The rhizosphere of aquatic plants is a habitat for cable bacteria. *FEMS Microbiol Ecol* 2019;**95**:fiz062.

Schreiber L, Kjeldsen KU, Funch P *et al.* Endozoicomonas Are Specific, Facultative Symbionts of Sea Squirts. *Front Microbiol* 2016;**7**, DOI: 10.3389/fmicb.2016.01042.

Shantz AA, Burkepile DE. Context-dependent effects of nutrient loading on the coral–algal mutualism. *Ecology* 2014;**95**:1995–2005.

Shantz AA, Lemoine NP, Burkepile DE. Nutrient loading alters the performance of key nutrient exchange mutualisms. *Ecol Lett* 2016;**19**:20–8.

Sharpton T, Lyalina S, Luong J *et al.* Development of Inflammatory Bowel Disease Is Linked to a Longitudinal Restructuring of the Gut Metagenome in Mice. *mSystems* 2017;**2**:e00036-17.

Shaver EC, Shantz AA, McMinds R *et al.* Effects of predation and nutrient enrichment on the success and microbiome of a foundational coral. *Ecology* 2017;**98**:830–9.

Sherman K, DeBruyckere LA. Eelgrass habitats on the U.S. West Coast: state of the knowledge of eelgrass ecosystem services and eelgrass extent. 2018:97.

Short F, Carruthers T, Dennison W *et al.* Global seagrass distribution and diversity: A bioregional model. *Journal of Experimental Marine Biology and Ecology* 2007;**350**:3–20.

Short FT, Burdick DM. Quantifying Eelgrass Habitat Loss in Relation to Housing Development and Nitrogen Loading in Waquoit Bay, Massachusetts. *Estuaries* 1996;**19**:730.

Short FT, Burdick DM, Kaldy JE. Mesocosm experiments quantify the effects of eutrophication on eelgrass, Zostera marina. *Limnology and Oceanography* 1995;**40**:740–9.

Short FT, Coles RG. *Global Seagrass Research Methods*. Elsevier, 2001.

Short FT, Green EP. *World Atlas of Seagrasses*. University of California Press, 2003.

Short FT, Wyllie-Echeverria S. Natural and human-induced disturbance of seagrasses. *Environmental Conservation* 1996;**23**:17.

Siboni N, Ben-Dov E, Sivan A *et al.* Global distribution and diversity of coral-associated Archaea and their possible role in the coral holobiont nitrogen cycle. *Environmental microbiology* 2008;**10**:2979–2990.

Sinha E, Michalak AM, Balaji V. Eutrophication will increase during the 21st century as a result of precipitation changes. *Science* 2017;**357**:405–8.

Sipler RE, Kellogg CTE, Connelly TL *et al.* Microbial Community Response to Terrestrially Derived Dissolved Organic Matter in the Coastal Arctic. *Front Microbiol* 2017;**8**, DOI: 10.3389/fmicb.2017.01018.

Smale DA, Wernberg T, Oliver ECJ *et al.* Marine heatwaves threaten global biodiversity and the provision of ecosystem services. *Nature Climate Change* 2019;**9**:306–12.

Smith CR, Austen MC, Boucher G *et al.* Global Change and Biodiversity Linkages across the Sediment–Water Interface. *BioScience* 2000;**50**:1108–20.

Smith GW, Ives LD, Nagelkerken IA *et al.* Caribbean sea-fan mortalities. *Nature* 1996;**383**:487–487.

Sowell SM, Wilhelm LJ, Norbeck AD *et al.* Transport functions dominate the SAR11 metaproteome at low-nutrient extremes in the Sargasso Sea. *ISME J* 2009;**3**:93–105.

Stapel J, Hemminga MA. Nutrient resorption from seagrass leaves. *Marine Biology* 1997;**128**:197–206.

Stein O, Granot D. An Overview of Sucrose Synthases in Plants. *Front Plant Sci* 2019;**10**, DOI: 10.3389/fpls.2019.00095.

Su J, Cai W-J, Brodeur J *et al.* Chesapeake Bay acidification buffered by spatially decoupled carbonate mineral cycling. *Nature Geoscience* 2020a;**13**:441–7.

Suykerbuyk W, Govers LL, Bouma TJ *et al.* Unpredictability in seagrass restoration: analysing the role of positive feedback and environmental stress on Zostera noltii transplants. *Journal of Applied Ecology* 2016;**53**:774–84.

Sweet M, Burn D, Croquer A *et al.* Characterisation of the Bacterial and Fungal Communities Associated with Different Lesion Sizes of Dark Spot Syndrome Occurring in the Coral Stephanocoenia intersepta. *PLOS ONE* 2013;**8**:e62580.

Sweet M, Bythell J. The role of viruses in coral health and disease. *Journal of Invertebrate Pathology* 2017;**147**:136–44.

Tarquinio F, Bourgoure J, Koenders A *et al.* Microorganisms facilitate uptake of dissolved organic nitrogen by seagrass leaves. *The ISME Journal* 2018;**12**:2796.

Tarquinio F, Hyndes GA, Laverock B *et al.* The seagrass holobiont: understanding seagrass-bacteria interactions and their role in seagrass ecosystem functioning. *FEMS Microbiol Lett* 2019, DOI: 10.1093/femsle/fnz057.

Tavaré S, Miura R. Some probabilistic and statistical problems in the analysis of DNA sequences. *Lectures on mathematics in the life sciences* 1986;**17**:57–86.

Taylor DI, Nixon SW, Granger SL *et al.* Responses of coastal lagoon plant communities to different forms of nutrient enrichment—a mesocosm experiment. *Aquatic Botany* 1995;**52**:19–34.

Teira E, Fernández A, Álvarez-Salgado X *et al.* Response of two marine bacterial isolates to high CO<sub>2 concentration. *Mar Ecol Prog Ser* 2012;**453**:27–36.

Thom R, Gaeckle J, Borde A *et al.* Eelgrass (Zostera marina L.) Restoration in the Pacific Northwest: Recommendations to Improve Project Success. 2008:33.

Thom R, Gaeckle J, Buenau K *et al.* Eelgrass (Zostera marina L.) restoration in Puget Sound: development of a site suitability assessment process: Puget Sound eelgrass restoration site selection. *Restoration Ecology* 2018;**26**:1066–74.

Thompson JR, Rivera HE, Closek CJ *et al.* Microbes in the coral holobiont: partners through evolution, development, and ecological interactions. *Front Cell Infect* 2015;**4**:176.

Thompson LR, Sanders JG, McDonald D *et al.* A communal catalogue reveals Earth's multiscale microbial diversity. *Nature* 2017;**551**:457–63.

Tkacz A, Cheema J, Chandra G *et al.* Stability and succession of the rhizosphere microbiota depends upon plant type and soil composition. *ISME J* 2015;**9**:2349–59.

Touchette BW, Burkholder JM, Glasgow HB. Variations in eelgrass (Zostera marina L.) morphology and internal nutrient composition as influenced by increased temperature and water column nitrate. *Estuaries* 2003;**26**:142–55.

Tomas F, Abbott JM, Steinberg C *et al.* Plant genotype and nitrogen loading influence seagrass productivity, biochemistry, and plant–herbivore interactions. *Ecology* 2011;**92**:1807–17.

Tout J, Siboni N, Messer LF *et al.* Increased seawater temperature increases the abundance and alters the structure of natural Vibrio populations associated with the coral Pocillopora damicornis. *Front Microbiol* 2015;**6**, DOI: 10.3389/fmicb.2015.00432.

Trotsenko YuA, Ivanova EG, Doronina NV. Aerobic Methylotrophic Bacteria as Phytosymbionts. *Microbiology* 2001;**70**:623–32.

Turner TR, James EK, Poole PS. The plant microbiome. *Genome Biology* 2013;**14**:209.

Udy JW, Dennison WC. Growth and physiological responses of three seagrass species to elevated sediment nutrients in Moreton Bay, Australia. *Journal of Experimental Marine Biology and Ecology* 1997;**217**:253–77.

Ugarelli K, Chakrabarti S, Laas P *et al.* The Seagrass Holobiont and Its Microbiome. *Microorganisms* 2017;**5**:81.

Ugarelli K, Laas P, Stingl U. The Microbial Communities of Leaves and Roots Associated with Turtle Grass (*Thalassia testudinum*) and Manatee Grass (*Syringodium filliforme*) are Distinct from Seawater and Sediment Communities, but Are Similar between Species and Sampling Sites. *Microorganisms* 2019;**7**, DOI: 10.3390/microorganisms7010004.

Unsworth RKF, Collier CJ, Henderson GM *et al.* Tropical seagrass meadows modify seawater carbon chemistry: implications for coral reefs impacted by ocean acidification. *Environ Res Lett* 2012a;**7**:024026.

Vega Thurber R, Payet JP, Thurber AR *et al.* Virus–host interactions and their roles in coral reef health and disease. *Nature Reviews Microbiology* 2017;**15**:205–16.

Vega Thurber R, Willner-Hall D, Rodriguez-Mueller B *et al.* Metagenomic analysis of stressed coral holobionts. *Environmental Microbiology* 2009;**11**:2148–2163.

Vega Thurber RL, Burkepile DE, Fuchs C *et al.* Chronic nutrient enrichment increases prevalence and severity of coral disease and bleaching. *Global Change Biology* 2014;**20**:544–54.

Venables WN, Ripley BD. *Modern Applied Statistics with S.* 4th ed. New York: Springer, 2002.

Vizzini S, Di Leonardo R, Costa V *et al.* Trace element bias in the use of CO2 vents as analogues for low pH environments: Implications for contamination levels in acidified oceans. *Estuarine, Coastal and Shelf Science* 2013;**134**:19–30.

Voss JD, Richardson LL. Nutrient enrichment enhances black band disease progression in corals. *Coral Reefs* 2006;**25**:569–76.

Wagner DE, Kramer P, van Woesik R. Species composition, habitat, and water quality influence coral bleaching in southern Florida. *Marine Ecology Progress Series* 2010;**408**:65–78.

Waite DW, Vanwonterghem I, Rinke C *et al.* Comparative Genomic Analysis of the Class Epsilonproteobacteria and Proposed Reclassification to Epsilonbacteraeota (phyl. nov.). *Front Microbiol* 2017;**8**, DOI: 10.3389/fmicb.2017.00682.

Walter RK, O'Leary JK, Vitousek S *et al.* Large-scale erosion driven by intertidal eelgrass loss in an estuarine environment. *Estuarine, Coastal and Shelf Science* 2020;**243**:106910.

Wang F-Q, Chen Z-J, Yang J-M *et al.* Labilibacter sediminis sp. nov., isolated from marine sediment. *International Journal of Systematic and Evolutionary Microbiology,* 2020;**70**:321–6.

Wang L, Tomas F, Mueller RS. Nutrient enrichment increases size of Zostera marina shoots and enriches for sulfur and nitrogen cycling bacteria in root-associated microbiomes. *FEMS Microbiology Ecology* 2020;**96**:fiaa129.

Wang Y, Tian RM, Gao ZM *et al.* Optimal Eukaryotic 18S and Universal 16S/18S Ribosomal RNA Primers and Their Application in a Study of Symbiosis. *PLOS ONE* 2014;**9**:e90053.

Warnes GR, Bolker B, Bonebakker L *et al. Gplots: Various R Programming Tools for Plotting Data*., 2016.

Waycott M, Duarte CM, Carruthers TJB *et al.* Accelerating loss of seagrasses across the globe threatens coastal ecosystems. *PNAS* 2009;**106**:12377–81.

Webster NS, Negri AP, Botté ES *et al.* Host-associated coral reef microbes respond to the cumulative pressures of ocean warming and ocean acidification. *Sci Rep* 2016a;**6**:1–9.

Webster NS, Negri AP, Botté ES *et al.* Host-associated coral reef microbes respond to the cumulative pressures of ocean warming and ocean acidification. *Scientific Reports* 2016b;**6**:19324.

Wegley L, Edwards R, Rodriguez-Brito B *et al.* Metagenomic analysis of the microbial community associated with the coral Porites astreoides. *Environmental Microbiology* 2007;**9**:2707–19.

Wegley L, Yu Y, Breitbart M *et al.* Coral-associated archaea. *Marine Ecology Progress Series* 2004;**273**:89–96.

Wei Z, Yang T, Friman V-P *et al.* Trophic network architecture of root-associated bacterial communities determines pathogen invasion and plant health. *Nat Commun* 2015;**6**:1–9.

Weigel BL, Pfister CA. Successional Dynamics and Seascape-Level Patterns of Microbial Communities on the Canopy-Forming Kelps Nereocystis luetkeana and Macrocystis pyrifera. *Front Microbiol* 2019;**10**, DOI: 10.3389/fmicb.2019.00346.

Weil E. Coral Reef Diseases in the Wider Caribbean. *Coral Health and Disease*. Springer, Berlin, Heidelberg, 2004, 35–68.

Weiss S, Xu ZZ, Peddada S *et al.* Normalization and microbial differential abundance strategies depend upon data characteristics. *Microbiome* 2017;**5**, DOI: 10.1186/s40168-017-0237-y.

Welsh D, Wellsbury P, Bourgues S *et al.* Relationship between porewater organic carbon content, sulphate reduction and nitrogen fixation (acetylene reduction) in the rhizosphere of *Zostera noltii*. *Hydrobiologia* 1996a;**329**:175–83.

Welsh DT. Nitrogen fixation in seagrass meadows: Regulation, plant–bacteria interactions and significance to primary productivity. *Ecology Letters* 2000;**3**:58–71.

Welsh DT, Bourgués S, de Wit R *et al.* Seasonal variations in nitrogen-fixation (acetylene reduction) and sulphate-reduction rates in the rhizosphere of Zostera noltii: nitrogen fixation by sulphate-reducing bacteria. *Marine Biology* 1996b;**125**:619–28.

Welsh RM, Rosales SM, Zaneveld JR *et al.* Alien vs. predator: bacterial challenge alters coral microbiomes unless controlled by Halobacteriovorax predators. *PeerJ* 2017;**5**, DOI: 10.7717/peerj.3315.

Wetzel RG, Penhal P a. Transport of carbon and excretion of dissolved organic carbon by leaves and roots/rhizomes in seagrasses and their epiphytes. *Aquatic Botany* 1979;**6**:149–58.

Weynberg KD, Laffy PW, Wood-Charlson EM *et al.* Coral-associated viral communities show high levels of diversity and host auxiliary functions. *PeerJ* 2017;**5**, DOI: 10.7717/peerj.4054.

Whitfield AK. The role of seagrass meadows, mangrove forests, salt marshes and reed beds as nursery areas and food sources for fishes in estuaries. *Rev Fish Biol Fisheries* 2017;**27**:75–110.

Wickham H. *Ggplot2: Elegant Graphics for Data Analysis*. Springer-Verlag New York, 2016.

Wiedenmann J, D'Angelo C, Smith EG *et al.* Nutrient enrichment can increase the susceptibility of reef corals to bleaching. *Nature Climate Change* 2013;**3**:160.

Wilkins LGE, Leray M, O'Dea A *et al.* Host-associated microbiomes drive structure and function of marine ecosystems. *PLOS Biology* 2019;**17**:e3000533.

Wirsen CO, Sievert SM, Cavanaugh CM *et al.* Characterization of an Autotrophic Sulfide-Oxidizing Marine Arcobacter sp. That Produces Filamentous Sulfur. *Appl Environ Microbiol* 2002;**68**:316–25.

Woo HL, Hazen TC. Enrichment of Bacteria From Eastern Mediterranean Sea Involved in Lignin Degradation via the Phenylacetyl-CoA Pathway. *Front Microbiol* 2018;**9**, DOI: 10.3389/fmicb.2018.00922.

Wood DE, Salzberg SL. Kraken: ultrafast metagenomic sequence classification using exact alignments. *Genome Biol* 2014;**15**:R46.

Wood-Charlson EM, Weynberg KD, Suttle CA *et al.* Metagenomic characterization of viral communities in corals: mining biological signal from methodological noise: Methodological biases in coral viromics. *Environmental Microbiology* 2015;**17**:3440–9.

Woodhead AJ, Hicks CC, Norström AV *et al.* Coral reef ecosystem services in the Anthropocene. *Functional Ecology* 2019;**33**:1023–34.

Wooldridge SA. Excess seawater nutrients, enlarged algal symbiont densities and bleaching sensitive reef locations: 1. Identifying thresholds of concern for the Great Barrier Reef, Australia. *Marine Pollution Bulletin* 2020;**152**:107667.

Wooldridge SA, Done TJ. Improved water quality can ameliorate effects of climate change on corals. *Ecological Applications* 2009;**19**:1492–9.

Yang J, Kloepper JW, Ryu C-M. Rhizosphere bacteria help plants tolerate abiotic stress. *Trends in Plant Science* 2009a;**14**:1–4.

Yarden O. Fungal association with sessile marine invertebrates. *Front Microbiol* 2014;**5**, DOI: 10.3389/fmicb.2014.00228.

York PH, Smith TM, Coles RG *et al.* Identifying knowledge gaps in seagrass research and management: An Australian perspective. *Marine Environmental Research* 2017;**127**:163–72.

Zaneveld JR, Burkepile DE, Shantz AA *et al.* Overfishing and nutrient pollution interact with temperature to disrupt coral reefs down to microbial scales. *Nat Commun* 2016;**7**, DOI: 10.1038/ncomms11833.

Zaneveld JR, McMinds R, Thurber RV. Stress and stability: applying the Anna Karenina principle to animal microbiomes. *Nature Microbiology* 2017;**2**:17121.

Zayas-Santiago CC, Rivas-Ubach A, Kuo L-J *et al.* Metabolic Profiling Reveals Biochemical Pathways Responsible for Eelgrass Response to Elevated CO2 and Temperature. *Sci Rep* 2020;**10**, DOI: 10.1038/s41598-020-61684-x.

Zenone A, Alagna A, D'Anna G *et al.* Biological adhesion in seagrasses: The role of substrate roughness in Posidonia oceanica (L.) Delile seedling anchorage via adhesive root hairs. *Marine Environmental Research* 2020;**160**:105012.

Zhang P, Jin T, Kumar Sahu S *et al.* The Distribution of Tryptophan-Dependent Indole-3-Acetic Acid Synthesis Pathways in Bacteria Unraveled by Large-Scale Genomic Analysis. *Molecules* 2019;**24**, DOI: 10.3390/molecules24071411.

Zhang Y. *Likelihood-Based and Bayesian Methods for Tweedie Compound Poisson Linear Mixed Models*., 2013.

Zheng P, Wang C, Zhang X *et al.* Community Structure and Abundance of Archaea in a Zostera marina Meadow: A Comparison between Seagrass-Colonized and Bare Sediment Sites. *Archaea* 2019;**2019**:1–11.

Zhou Y, Liu P, Liu B *et al.* Restoring Eelgrass (*Zostera marina* L.) Habitats Using a Simple and Effective Transplanting Technique. *PLoS One* 2014;**9**, DOI: 10.1371/journal.pone.0092982.

Ziegler M, Roik A, Porter A *et al.* Coral microbial community dynamics in response to anthropogenic impacts near a major city in the central Red Sea. *Marine Pollution Bulletin* 2016;**105**:629–40.

Zieman J. Methods for the study of the growth and production of turtle grass, Thalassia testudinum konig. *Aquaculture* 1974;**4**:139–43.

Zimmer DP, Soupene E, Lee HL *et al.* Nitrogen regulatory protein C-controlled genes of Escherichia coli: Scavenging as a defense against nitrogen limitation. *Proc Natl Acad Sci U S A* 2000;**97**:14674–9.

8 Appendices

8.1 Appendix A: Ch. 2 Supplemental Tables

Coral	Date	Species	Treat	Nit	Pho	Transect	BiteScars	DSSPrese	PercDSS	BleachPres	PercBleacl	Mortality
A1	7/11/14	Agaricia	C	0	0	1	0	0	0	0	0	0
A4	7/11/14	Agaricia	C	0	0	1	0	0	0	0	0	0
A7	7/11/14	Agaricia	C	0	0	2	0	0	0	0	0	0
A20	7/11/14	Agaricia	C	0	0	2	0	0	0	0	0	0
A14	7/11/14	Agaricia	C	0	0	2	0	0	0	0	0	0
A19	7/11/14	Agaricia	N	1	0	1	0	0	0	0	0	0
A11	7/11/14	Agaricia	N	1	0	1	0	0	0	0	0	0
A5	7/11/14	Agaricia	N	1	0	1	0	0	0	0	0	0
A12	7/11/14	Agaricia	N	1	0	2	0	0	0	0	0	0
A16	7/11/14	Agaricia	N	1	0	2	0	0	0	0	0	0
A2	7/11/14	Agaricia	NP	1	1	1	0	0	0	0	0	0
A6	7/11/14	Agaricia	NP	1	1	1	0	0	0	0	0	0
A8	7/11/14	Agaricia	NP	1	1	2	0	0	0	0	0	0
A10	7/11/14	Agaricia	NP	1	1	2	0	0	0	0	0	0
A15	7/11/14	Agaricia	NP	1	1	2	0	0	0	0	0	0
A3	7/11/14	Agaricia	P	0	1	1	0	0	0	0	0	0
A18	7/11/14	Agaricia	P	0	1	2	0	0	0	0	0	0
A9	7/11/14	Agaricia	P	0	1	2	0	0	0	0	0	0
A17	7/11/14	Agaricia	P	0	1	2	0	0	0	0	0	0
A13	7/11/14	Agaricia	P	0	1	2	0	0	0	0	0	0
S3	7/11/14	Siderastrea	C	0	0	1	1	0	0	0	0	0
S5	7/11/14	Siderastrea	C	0	0	1	0	0	0	0	0	0
S9	7/11/14	Siderastrea	C	0	0	1	0	0	0	0	0	0
S12	7/11/14	Siderastrea	C	0	0	2	0	0	0	0	0	0
S20	7/11/14	Siderastrea	C	0	0	2	0	0	0	0	0	0
S2	7/11/14	Siderastrea	N	1	0	1	0	0	0	0	0	0
S10	7/11/14	Siderastrea	N	1	0	2	0	0	0	0	0	0
S11	7/11/14	Siderastrea	N	1	0	2	0	0	0	0	0	0
S15	7/11/14	Siderastrea	N	1	0	2	0	0	0	0	0	0
S18	7/11/14	Siderastrea	N	1	0	2	0	0	0	0	0	0
S1	7/11/14	Siderastrea	NP	1	1	1	0	0	0	0	0	0
S6	7/11/14	Siderastrea	NP	1	1	1	0	0	0	0	0	0

S8	7/11/14	Siderastrea	NP	1	1	1	0	0	0	0	0	0
S14	7/11/14	Siderastrea	NP	1	1	2	0	0	0	0	0	0
S16	7/11/14	Siderastrea	NP	1	1	2	0	0	0	0	0	0
S4	7/11/14	Siderastrea	P	0	1	1	0	0	0	0	0	0
S7	7/11/14	Siderastrea	P	0	1	1	0	0	0	0	0	0
S17	7/11/14	Siderastrea	P	0	1	1	0	0	0	0	0	0
S13	7/11/14	Siderastrea	P	0	1	2	0	0	0	0	0	0
S19	7/11/14	Siderastrea	P	0	1	2	0	0	0	0	0	0
A1	8/13/14	Agaricia	C	0	0	1	0	0	0	1	90	0
A4	8/13/14	Agaricia	C	0	0	1	0	0	0	0	0	0
A7	8/13/14	Agaricia	C	0	0	2	0	0	0	1	10	0
A20	8/13/14	Agaricia	C	0	0	2	0	0	0	0	0	0
A14	8/13/14	Agaricia	C	0	0	2	0	0	0	0	0	10
A19	8/13/14	Agaricia	N	1	0	1	0	0	0	0	0	0
A11	8/13/14	Agaricia	N	1	0	1	0	0	0	0	0	0
A5	8/13/14	Agaricia	N	1	0	1	0	0	0	0	0	0
A12	8/13/14	Agaricia	N	1	0	2	0	0	0	0	0	0
A16	8/13/14	Agaricia	N	1	0	2	0	0	0	0	0	0
A2	8/13/14	Agaricia	NP	1	1	1	0	0	0	1	40	0
A6	8/13/14	Agaricia	NP	1	1	1	0	0	0	0	0	2
A8	8/13/14	Agaricia	NP	1	1	2	0	0	0	1	15	0
A10	8/13/14	Agaricia	NP	1	1	2	0	0	0	0	0	0
A15	8/13/14	Agaricia	NP	1	1	2	0	0	0	0	0	0
A3	8/13/14	Agaricia	P	0	1	1	0	0	0	0	0	5
A18	8/13/14	Agaricia	P	0	1	2	0	0	0	0	0	0
A9	8/13/14	Agaricia	P	0	1	2	0	0	0	1	15	0
A17	8/13/14	Agaricia	P	0	1	2	0	0	0	0	0	0
A13	8/13/14	Agaricia	P	0	1	2	0	0	0	1	12	0
S3	8/13/14	Siderastrea	C	0	0	1	0	0	0	0	0	0
S5	8/13/14	Siderastrea	C	0	0	1	0	1	5	0	0	0
S9	8/13/14	Siderastrea	C	0	0	1	0	0	0	0	0	0
S12	8/13/14	Siderastrea	C	0	0	2	0	1	5	0	0	0
S20	8/13/14	Siderastrea	C	0	0	2	0	1	5	0	0	0

S2	8/13/14	Siderastrea	N	1	0	1	0	1	3	0	0	0
S10	8/13/14	Siderastrea	N	1	0	2	0	0	0	0	0	0
S11	8/13/14	Siderastrea	N	1	0	2	0	0	0	0	0	0
S15	8/13/14	Siderastrea	N	1	0	2	0	1	3	0	0	0
S18	8/13/14	Siderastrea	N	1	0	2	0	0	0	0	0	0
S1	8/13/14	Siderastrea	NP	1	1	1	0	0	0	0	0	0
S6	8/13/14	Siderastrea	NP	1	1	1	0	1	2	0	0	0
S8	8/13/14	Siderastrea	NP	1	1	1	0	0	0	0	0	0
S14	8/13/14	Siderastrea	NP	1	1	2	0	1	10	0	0	0
S16	8/13/14	Siderastrea	NP	1	1	2	0	1	15	0	0	0
S4	8/13/14	Siderastrea	P	0	1	1	0	1	20	0	0	0
S7	8/13/14	Siderastrea	P	0	1	1	0	0	0	0	0	0
S17	8/13/14	Siderastrea	P	0	1	1	0	1	10	0	0	0
S13	8/13/14	Siderastrea	P	0	1	2	0	0	0	0	0	0
S19	8/13/14	Siderastrea	P	0	1	2	0	0	0	0	0	0
A1	9/11/14	Agaricia	C	0	0	1	0	0	0	1	98	0
A4	9/11/14	Agaricia	C	0	0	1	0	0	0	1	99	0
A7	9/11/14	Agaricia	C	0	0	2	0	0	0	1	100	0
A20	9/11/14	Agaricia	C	0	0	2	0	0	0	1	100	0
A14	9/11/14	Agaricia	C	0	0	2	0	0	0	1	100	0
A19	9/11/14	Agaricia	N	1	0	1	0	0	0	1	100	3
A11	9/11/14	Agaricia	N	1	0	1	0	0	0	1	100	5
A5	9/11/14	Agaricia	N	1	0	1	0	0	0	1	99	0
A12	9/11/14	Agaricia	N	1	0	2	0	0	0	1	100	30
A16	9/11/14	Agaricia	N	1	0	2	0	0	0	1	90	0
A2	9/11/14	Agaricia	NP	1	1	1	0	0	0	1	96	0
A6	9/11/14	Agaricia	NP	1	1	1	0	0	0	1	100	3
A8	9/11/14	Agaricia	NP	1	1	2	0	0	0	1	75	0
A10	9/11/14	Agaricia	NP	1	1	2	0	0	0	1	80	0
A15	9/11/14	Agaricia	NP	1	1	2	0	0	0	1	100	0
A3	9/11/14	Agaricia	P	0	1	1	0	0	0	1	100	95
A18	9/11/14	Agaricia	P	0	1	2	0	0	0	1	100	0
A9	9/11/14	Agaricia	P	0	1	2	0	0	0	1	99	0

A17	9/11/14	Agaricia	P	0	1	2	0	0	0	1	100	0
A13	9/11/14	Agaricia	P	0	1	2	0	0	0	1	100	0
S3	9/11/14	Siderastrea	C	0	0	1	0	1	4	0	0	0
S5	9/11/14	Siderastrea	C	0	0	1	0	1	15	0	0	0
S9	9/11/14	Siderastrea	C	0	0	1	0	1	15	0	0	0
S12	9/11/14	Siderastrea	C	0	0	2	0	0	0	0	0	0
S20	9/11/14	Siderastrea	C	0	0	2	0	1	8	0	0	0
S2	9/11/14	Siderastrea	N	1	0	1	0	1	20	0	0	0
S10	9/11/14	Siderastrea	N	1	0	2	0	1	2	0	0	0
S11	9/11/14	Siderastrea	N	1	0	2	0	1	10	0	0	0
S15	9/11/14	Siderastrea	N	1	0	2	0	1	9	0	0	0
S18	9/11/14	Siderastrea	N	1	0	2	0	1	3	0	0	0
S1	9/11/14	Siderastrea	NP	1	1	1	0	1	3	0	0	0
S6	9/11/14	Siderastrea	NP	1	1	1	0	1	4	0	0	0
S8	9/11/14	Siderastrea	NP	1	1	1	0	1	20	0	0	0
S14	9/11/14	Siderastrea	NP	1	1	2	0	1	15	0	0	0
S16	9/11/14	Siderastrea	NP	1	1	2	0	1	40	0	0	0
S4	9/11/14	Siderastrea	P	0	1	1	0	1	30	0	0	0
S7	9/11/14	Siderastrea	P	0	1	1	0	0	0	0	0	0
S17	9/11/14	Siderastrea	P	0	1	1	0	1	12	0	0	0
S13	9/11/14	Siderastrea	P	0	1	2	0	0	0	0	0	0
S19	9/11/14	Siderastrea	P	0	1	2	0	1	6	0	0	0
A1	10/17/14	Agaricia	C	0	0	1	0	0	0	1	90	0
A4	10/17/14	Agaricia	C	0	0	1	0	1	2	1	85	0
A7	10/17/14	Agaricia	C	0	0	2	0	0	0	1	100	10
A20	10/17/14	Agaricia	C	0	0	2	0	0	0	1	90	4
A14	10/17/14	Agaricia	C	0	0	2	0	0	0	1	100	0
A19	10/17/14	Agaricia	N	1	0	1	0	0	0	1	100	65
A11	10/17/14	Agaricia	N	1	0	1	NA	NA	NA	NA	NA	100
A5	10/17/14	Agaricia	N	1	0	1	0	0	0	1	95	0
A12	10/17/14	Agaricia	N	1	0	2	0	0	0	1	98	1
A16	10/17/14	Agaricia	N	1	0	2	0	0	0	1	99	10
A2	10/17/14	Agaricia	NP	1	1	1	0	0	0	1	100	2

A6	10/17/14	Agaricia	NP	1	1	1	0	0	0	1	95	4
A8	10/17/14	Agaricia	NP	1	1	2	0	0	0	1	100	1
A10	10/17/14	Agaricia	NP	1	1	2	0	0	0	1	90	20
A15	10/17/14	Agaricia	NP	1	1	2	0	0	0	1	98	8
A3	10/17/14	Agaricia	P	0	1	1	NA	NA	NA	NA	NA	100
A18	10/17/14	Agaricia	P	0	1	2	0	0	0	1	99	4
A9	10/17/14	Agaricia	P	0	1	2	0	0	0	1	95	0
A17	10/17/14	Agaricia	P	0	1	2	0	0	0	1	95	1
A13	10/17/14	Agaricia	P	0	1	2	0	0	0	1	100	0
S3	10/17/14	Siderastrea	C	0	0	1	0	1	5	0	0	0
S5	10/17/14	Siderastrea	C	0	0	1	2	1	6	0	0	3
S9	10/17/14	Siderastrea	C	0	0	1	0	0	0	0	0	0
S12	10/17/14	Siderastrea	C	0	0	2	0	0	0	0	0	0
S20	10/17/14	Siderastrea	C	0	0	2	0	0	0	0	0	0
S2	10/17/14	Siderastrea	N	1	0	1	0	1	3	0	0	1
S10	10/17/14	Siderastrea	N	1	0	2	0	0	0	0	0	0
S11	10/17/14	Siderastrea	N	1	0	2	0	0	0	0	0	0
S15	10/17/14	Siderastrea	N	1	0	2	0	1	1	0	0	0
S18	10/17/14	Siderastrea	N	1	0	2	0	1	30	0	0	0
S1	10/17/14	Siderastrea	NP	1	1	1	0	1	3	0	0	0
S6	10/17/14	Siderastrea	NP	1	1	1	0	0	0	0	0	0
S8	10/17/14	Siderastrea	NP	1	1	1	0	1	10	0	0	0
S14	10/17/14	Siderastrea	NP	1	1	2	0	1	11	0	0	0
S16	10/17/14	Siderastrea	NP	1	1	2	0	1	40	0	0	0
S4	10/17/14	Siderastrea	P	0	1	1	0	1	20	0	0	0
S7	10/17/14	Siderastrea	P	0	1	1	0	0	0	0	0	0
S17	10/17/14	Siderastrea	P	0	1	1	0	1	9	0	0	0
S13	10/17/14	Siderastrea	P	0	1	2	0	0	0	0	0	0
S19	10/17/14	Siderastrea	P	0	1	2	0	1	2	0	0	0
A1	11/7/14	Agaricia	C	0	0	1	NA	0	0	1	10	10
A4	11/7/14	Agaricia	C	0	0	1	NA	0	0	1	50	15
A7	11/7/14	Agaricia	C	0	0	2	NA	0	0	1	NA	NA
A20	11/7/14	Agaricia	C	0	0	2	NA	0	0	1	50	95

A14	11/7/14	Agaricia	C	0	0	2	NA	NA	NA	NA	NA	NA
A19	11/7/14	Agaricia	N	1	0	1	NA	NA	NA	NA	NA	100
A11	11/7/14	Agaricia	N	1	0	1	NA	NA	NA	NA	NA	100
A5	11/7/14	Agaricia	N	1	0	1	NA	0	0	1	90	90
A12	11/7/14	Agaricia	N	1	0	2	NA	0	0	1	NA	10
A16	11/7/14	Agaricia	N	1	0	2	NA	0	0	1	95	NA
A2	11/7/14	Agaricia	NP	1	1	1	NA	0	0	1	100	0
A6	11/7/14	Agaricia	NP	1	1	1	NA	0	0	1	25	75
A8	11/7/14	Agaricia	NP	1	1	2	NA	0	0	1	100	0
A10	11/7/14	Agaricia	NP	1	1	2	NA	NA	NA	NA	NA	100
A15	11/7/14	Agaricia	NP	1	1	2	NA	0	0	1	10	50
A3	11/7/14	Agaricia	P	0	1	1	NA	NA	NA	NA	NA	100
A18	11/7/14	Agaricia	P	0	1	2	NA	0	0	1	100	NA
A9	11/7/14	Agaricia	P	0	1	2	NA	0	0	1	50	NA
A17	11/7/14	Agaricia	P	0	1	2	NA	0	0	1	10	NA
A13	11/7/14	Agaricia	P	0	1	2	NA	0	0	1	100	NA
S3	11/7/14	Siderastrea	C	0	0	1	NA	NA	NA	NA	NA	NA
S5	11/7/14	Siderastrea	C	0	0	1	NA	1	3	0	0	0
S9	11/7/14	Siderastrea	C	0	0	1	NA	0	0	0	0	0
S12	11/7/14	Siderastrea	C	0	0	2	2	0	0	0	0	0
S20	11/7/14	Siderastrea	C	0	0	2	NA	0	0	0	0	0
S2	11/7/14	Siderastrea	N	1	0	1	NA	1	33	0	0	0
S10	11/7/14	Siderastrea	N	1	0	2	NA	1	10	0	0	0
S11	11/7/14	Siderastrea	N	1	0	2	NA	0	0	0	0	0
S15	11/7/14	Siderastrea	N	1	0	2	NA	1	4	0	0	0
S18	11/7/14	Siderastrea	N	1	0	2	NA	1	5	0	0	0
S1	11/7/14	Siderastrea	NP	1	1	1	NA	1	15	0	0	0
S6	11/7/14	Siderastrea	NP	1	1	1	NA	1	20	0	0	0
S8	11/7/14	Siderastrea	NP	1	1	1	NA	1	5	0	0	0
S14	11/7/14	Siderastrea	NP	1	1	2	NA	1	40	0	0	0
S16	11/7/14	Siderastrea	NP	1	1	2	NA	1	50	0	0	0
S4	11/7/14	Siderastrea	P	0	1	1	NA	1	33	0	0	0
S7	11/7/14	Siderastrea	P	0	1	1	NA	0	0	0	0	0

S17	11/7/14	Siderastrea	P	0	1	1	NA	1	50	0	0	0
S13	11/7/14	Siderastrea	P	0	1	2	NA	1	NA	NA	NA	NA
S19	11/7/14	Siderastrea	P	0	1	2	NA	0	0	0	0	0
A1	12/18/14	Agaricia	C	0	0	1	0	0	0	1	100	40
A4	12/18/14	Agaricia	C	0	0	1	0	0	0	1	10	35
A7	12/18/14	Agaricia	C	0	0	2	0	0	0	1	50	0
A20	12/18/14	Agaricia	C	0	0	2	0	0	0	0	0	95
A14	12/18/14	Agaricia	C	0	0	2	0	0	0	0	0	75
A19	12/18/14	Agaricia	N	1	0	1	0	0	0	1	50	90
A11	12/18/14	Agaricia	N	1	0	1	NA	NA	NA	NA	NA	100
A5	12/18/14	Agaricia	N	1	0	1	0	0	0	0	0	90
A12	12/18/14	Agaricia	N	1	0	2	0	0	0	1	12	10
A16	12/18/14	Agaricia	N	1	0	2	0	0	0	1	85	15
A2	12/18/14	Agaricia	NP	1	1	1	0	0	0	1	85	40
A6	12/18/14	Agaricia	NP	1	1	1	0	0	0	0	0	70
A8	12/18/14	Agaricia	NP	1	1	2	0	0	0	1	55	0
A10	12/18/14	Agaricia	NP	1	1	2	NA	NA	NA	NA	NA	100
A15	12/18/14	Agaricia	NP	1	1	2	0	0	0	1	5	80
A3	12/18/14	Agaricia	P	0	1	1	NA	NA	NA	NA	NA	100
A18	12/18/14	Agaricia	P	0	1	2	0	0	0	1	100	95
A9	12/18/14	Agaricia	P	0	1	2	0	0	0	1	10	30
A17	12/18/14	Agaricia	P	0	1	2	0	0	0	1	2	85
A13	12/18/14	Agaricia	P	0	1	2	0	0	0	1	70	10
S3	12/18/14	Siderastrea	C	0	0	1	1	1	35	0	0	0
S5	12/18/14	Siderastrea	C	0	0	1	0	0	0	0	0	0
S9	12/18/14	Siderastrea	C	0	0	1	0	0	0	0	0	0
S12	12/18/14	Siderastrea	C	0	0	2	0	1	10	0	0	0
S20	12/18/14	Siderastrea	C	0	0	2	0	0	0	0	0	0
S2	12/18/14	Siderastrea	N	1	0	1	2	1	3	0	0	0
S10	12/18/14	Siderastrea	N	1	0	2	0	1	5	0	0	0
S11	12/18/14	Siderastrea	N	1	0	2	1	0	0	0	0	0
S15	12/18/14	Siderastrea	N	1	0	2	7	1	4	0	0	0
S18	12/18/14	Siderastrea	N	1	0	2	0	1	40	0	0	0

S1	12/18/14	Siderastrea	NP	1	1	1	0	1	12	0	0	0
S6	12/18/14	Siderastrea	NP	1	1	1	0	1	8	0	0	0
S8	12/18/14	Siderastrea	NP	1	1	1	0	1	21	0	0	2
S14	12/18/14	Siderastrea	NP	1	1	2	0	1	8	0	0	0
S16	12/18/14	Siderastrea	NP	1	1	2	0	1	55	0	0	0
S4	12/18/14	Siderastrea	P	0	1	1	0	1	45	0	0	3
S7	12/18/14	Siderastrea	P	0	1	1	0	1	20	0	0	0
S17	12/18/14	Siderastrea	P	0	1	1	0	1	30	0	0	0
S13	12/18/14	Siderastrea	P	0	1	2	0	0	0	0	0	0
S19	12/18/14	Siderastrea	P	0	1	2	0	0	0	1	10	0
A1	1/14/15	Agaricia	C	0	0	1	0	0	0	1	15	85
A4	1/14/15	Agaricia	C	0	0	1	0	0	0	0	0	35
A7	1/14/15	Agaricia	C	0	0	2	0	0	0	0	0	40
A20	1/14/15	Agaricia	C	0	0	2	0	0	0	0	0	95
A14	1/14/15	Agaricia	C	0	0	2	0	0	0	0	0	80
A19	1/14/15	Agaricia	N	1	0	1	0	0	0	1	0	90
A11	1/14/15	Agaricia	N	1	0	1	NA	NA	NA	NA	NA	100
A5	1/14/15	Agaricia	N	1	0	1	0	0	0	0	0	95
A12	1/14/15	Agaricia	N	1	0	2	0	0	0	0	0	10
A16	1/14/15	Agaricia	N	1	0	2	0	0	0	1	100	85
A2	1/14/15	Agaricia	NP	1	1	1	0	0	0	1	10	50
A6	1/14/15	Agaricia	NP	1	1	1	0	0	0	0	0	50
A8	1/14/15	Agaricia	NP	1	1	2	0	0	0	1	50	0
A10	1/14/15	Agaricia	NP	1	1	2	NA	NA	NA	NA	NA	100
A15	1/14/15	Agaricia	NP	1	1	2	0	0	0	0	0	90
A3	1/14/15	Agaricia	P	0	1	1	NA	NA	NA	NA	NA	100
A18	1/14/15	Agaricia	P	0	1	2	0	0	0	0	0	100
A9	1/14/15	Agaricia	P	0	1	2	0	0	0	0	0	50
A17	1/14/15	Agaricia	P	0	1	2	0	0	0	1	2	85
A13	1/14/15	Agaricia	P	0	1	2	0	0	0	1	10	50
S3	1/14/15	Siderastrea	C	0	0	1	2	1	30	0	0	0
S5	1/14/15	Siderastrea	C	0	0	1	1	0	0	0	0	0
S9	1/14/15	Siderastrea	C	0	0	1	0	0	0	0	0	0

S12	1/14/15	Siderastrea	C	0	0	2	0	1	10	0	0	0
S20	1/14/15	Siderastrea	C	0	0	2	0	0	0	0	0	0
S2	1/14/15	Siderastrea	N	1	0	1	0	1	1	0	0	0
S10	1/14/15	Siderastrea	N	1	0	2	2	1	5	0	0	0
S11	1/14/15	Siderastrea	N	1	0	2	1	0	0	0	0	0
S15	1/14/15	Siderastrea	N	1	0	2	7	1	5	0	0	0
S18	1/14/15	Siderastrea	N	1	0	2	0	1	20	0	0	0
S1	1/14/15	Siderastrea	NP	1	1	1	0	1	20	0	0	0
S6	1/14/15	Siderastrea	NP	1	1	1	0	1	8	0	0	0
S8	1/14/15	Siderastrea	NP	1	1	1	0	1	15	0	0	2
S14	1/14/15	Siderastrea	NP	1	1	2	0	1	5	0	0	0
S16	1/14/15	Siderastrea	NP	1	1	2	0	1	60	0	0	0
S4	1/14/15	Siderastrea	P	0	1	1	0	1	35	0	0	3
S7	1/14/15	Siderastrea	P	0	1	1	0	1	15	0	0	0
S17	1/14/15	Siderastrea	P	0	1	1	1	1	15	0	0	0
S13	1/14/15	Siderastrea	P	0	1	2	0	0	0	0	0	0
S19	1/14/15	Siderastrea	P	0	1	2	0	0	0	0	0	0

Table S2.1 | Disease and bleaching data for *Agaricia sp.* and *Siderastrea siderea* corals.

Date	Treatment	#Reads	#Reads Post QC	%Reads PostQC	% of > Q30
7/14/14	C	3,520,020	3,080,760	87.52%	89.64
7/14/14	C	3,960,020	3,420,536	86.38%	89.62
7/14/14	C	2,553,668	1,872,348	73.32%	88.35
7/14/14	C	9,678,784	7,295,266	75.37%	89
7/14/14	C	674,660	485,740	72.00%	88
9/14/14	C	4,473,072	3,458,532	77.32%	88.32
9/14/14	C	4,489,466	3,219,786	71.72%	89.02
9/14/14	C	6,473,708	5,188,274	80.14%	89.45
9/14/14	C	9,945,962	7,394,600	74.35%	89
9/14/14	C	2,351,646	1,887,344	80.26%	88.68
8/13/14	C	1,685,280	1,268,430	75.27%	89.84
8/13/14	C	949,170	669,550	70.54%	89.47
8/13/14	C	7,349,140	5,872,162	79.90%	90.03
8/13/14	C	3,678,414	3,116,742	84.73%	89.04
8/13/14	C	4,312,652	3,475,696	80.59%	89.73
10/17/14	C	3,441,300	2,476,100	71.95%	90.17
10/17/14	C	6,677,300	4,941,820	74.01%	89.76
10/17/14	C	2,861,290	2,201,218	76.93%	90.02
10/17/14	C	11,682,346	9,564,388	81.87%	89.16
10/17/14	C	836,360	578,446	69.16%	89.38
7/14/14	N	5,324,156	4,597,272	86.35%	88.56
7/14/14	N	450,178	276,864	61.50%	87.75
7/14/14	N	5,669,970	4,490,714	79.20%	89.27
7/14/14	N	5,525,900	4,225,236	76.46%	88.79
7/14/14	N	4,011,386	2,986,664	74.45%	88.33
9/14/14	N	9,238,678	6,730,332	72.85%	88.97
9/14/14	N	7,948,666	5,890,266	74.10%	88.7
9/14/14	N	6,271,772	4,616,666	73.61%	89.33
9/14/14	N	5,725,144	4,896,922	85.53%	89.66
9/14/14	N	3,257,542	2,407,606	73.91%	88.65
8/13/14	N	8,258,470	6,608,466	80.02%	89.58
8/13/14	N	11,340,584	8,223,064	72.51%	89.98
8/13/14	N	1,450,996	1,229,122	84.71%	87.49
8/13/14	N	472,920	396,742	83.89%	87.98
10/17/14	N	1,626,006	1,206,728	74.21%	89.61
10/17/14	N	1,353,122	916,966	67.77%	89.64
10/17/14	N	1,603,352	1,199,528	74.81%	90.33
10/17/14	N	4,643,792	4,007,866	86.31%	89.12
10/17/14	N	3,618,280	3,071,760	84.90%	89.88
7/14/14	NP	9,889,976	6,850,626	69.27%	88.58
7/14/14	NP	8,642,392	6,502,044	75.23%	88.98
7/14/14	NP	7,815,494	5,263,620	67.35%	87.34
7/14/14	NP	3,493,490	2,625,756	75.16%	88.44
7/14/14	NP	474,154	342,506	72.24%	89.25
9/14/14	NP	4,374,668	3,326,024	76.03%	89.07
9/14/14	NP	5,791,162	4,377,722	75.59%	88.77
9/14/14	NP	4,719,180	3,433,916	72.77%	88.36
9/14/14	NP	2,615,442	2,201,218	84.16%	88.31
9/14/14	NP	3,895,442	3,247,090	83.36%	88.7

(continued from previous page)

8/13/14	NP	1,507,922	1,121,248	74.36%	89.74
8/13/14	NP	504,532	340,472	67.48%	84.36
8/13/14	NP	2,317,904	1,695,874	73.16%	89.54
8/13/14	NP	1,556,338	1,333,306	85.67%	87.83
8/13/14	NP	1,511,494	1,309,382	86.63%	88.29
10/17/14	NP	810,722	582,674	71.87%	89.45
10/17/14	NP	551,818	370,722	67.18%	88.89
10/17/14	NP	798,592	616,484	77.20%	88.91
10/17/14	NP	2,526,566	1,877,630	74.32%	89.15
10/17/14	NP	3,209,994	2,631,188	81.97%	85.45
7/14/14	P	13,352,194	10,976,030	82.20%	89.13
7/14/14	P	6,281,130	5,338,718	85.00%	88.08
7/14/14	P	6,577,756	5,410,922	82.26%	89.34
7/14/14	P	9,185,564	6,913,500	75.26%	89.22
7/14/14	P	3,069,110	2,451,258	79.87%	88.33
9/14/14	P	8,328,034	5,992,188	71.95%	85.08
9/14/14	P	7,370,474	6,292,880	85.38%	89.2
9/14/14	P	7,948,190	6,520,900	82.04%	89.24
9/14/14	P	8,351,698	6,927,072	82.94%	89.25
9/14/14	P	7,949,562	6,377,644	80.23%	88.13
8/13/14	P	4,027,634	3,251,386	80.73%	89.46
8/13/14	P	1,208,774	843,058	69.74%	89.53
8/13/14	P	3,778,108	3,016,354	79.84%	89.99
8/13/14	P	19,266,106	14,134,228	73.36%	88.57
10/17/14	P	818,950	590,424	72.10%	87.96
10/17/14	P	4,258,636	3,656,702	85.87%	89.47
10/17/14	P	5,015,000	4,228,322	84.31%	89.46
10/17/14	P	884,284	651,870	73.72%	89.4
10/17/14	P	292,876	206,162	70.39%	89.06
7/14/14	SW1	5,729,158	4,169,328	72.77%	87.43
8/13/14	SW1	9,125,480	7,214,774	79.06%	89.04
10/17/14	SW1	1,270,922	998,118	78.53%	88.7
7/14/14	SW2	1,441,102	1,113,558	77.27%	87.21
9/14/14	SW2	15,306,914	12,735,186	83.20%	88.71
10/17/14	SW2	2,079,508	1,747,504	84.03%	89.91

Table S2.2 | Metagenome sequencing and quality control data

	Mean Monthly Temp 2014	Mean Monthly Temp 2014 Stdev	Mean Monthly Temp 1987-2013	Mean Monthly Temp 1987-2013 Stdev
Jan	24.3512	0.8553	23.4833	1.1
Feb	24.9001	0.703	23.3201	1.1
March	24.3199	0.5419	23.732	1.1
April	25.5664	0.7425	25.1863	0.9
May	26.9868	0.3123	26.7661	1
June	28.1996	0.6855	28.4833	0.7
July	29.8267	0.4462	29.4004	0.5
Aug	30.8219	0.3388	30.0096	0.5
Sept	29.8574	0.4605	29.6307	0.6
Oct	28.5813	0.8583	28.0996	0.9
Nov	25.6189	0.8414	26.311	0.9
Dec	24.7671	0.6805	24.8235	0.9

Table S2.3 | Mean monthly temperature data from the NOAA Molasses Buoy in the Florida Keys

Month	Treatment	Chao1	SEM Chao1
July	C	3291.447	88.81019
July	C	4992.94	96.89722
July	C	4990.684	90.80251
July	C	4272.396	86.01224
July	C	5556.7	73.01245
July	NP	4955.172	101.28371
July	NP	5599.411	86.28117
July	NP	2970.874	79.70153
July	NP	5689.688	88.74211
July	NP	5608.551	98.33213
July	N	5257.535	91.68429
July	N	4823.475	82.42628
July	N	5182.587	77.94739
July	N	2684.344	67.43487
July	N	5180.862	84.56827
July	P	4624.37	86.23417
July	P	5385.142	77.09781
July	P	5586.094	80.433
July	P	5807.612	66.65327
July	P	5291.971	76.22146
August	C	5101.621	95.80392
August	C	4081.27	93.15395
August	C	5380.253	79.36922
August	C	3293.391	74.98181
August	C	5057.953	96.10586
August	NP	4070.125	86.90536
August	NP	4059.586	86.32176
August	NP	3866.296	90.41123
August	NP	4229.656	83.43742
August	NP	3056.517	95.55999
August	N	5407.845	67.59308
August	N	4117	88.61351
August	N	5261.781	67.52284
August	N	3151.027	81.04124
August	P	5988.669	61.99326
August	P	4885.008	90.28719
August	P	4959.101	91.46568
August	P	3579.751	86.64181
September	C	5333.279	80.46186
September	C	5157.75	105.24185
September	C	5677.37	79.93169
September	C	4962.938	91.29756
September	C	4881.504	104.68789
September	NP	5035.757	99.93592

(continued from previous page)

September	NP	5038.336	93.47351
September	NP	4970.089	93.73528
September	NP	5019.763	75.23734
September	NP	5308.88	107.3578
September	N	5287.772	87.28924
September	N	5509.799	85.11695
September	N	5443.029	76.81876
September	N	5263.254	79.19281
September	N	4571.047	90.49402
September	P	5609.566	78.35727
September	P	5832.225	83.45029
September	P	5522.409	78.70205
September	P	5522.458	86.78305
September	P	5596.358	84.29585
October	C	5115.143	76.02297
October	C	4426.107	81.08235
October	C	4436.056	84.92005
October	C	3318.661	86.44253
October	C	5736.519	66.00982
October	NP	2819.8	70.55177
October	NP	4331.828	86.6599
October	NP	3333.687	79.26529
October	NP	3244.777	75.10741
October	NP	4878.809	101.39746
October	N	3851.124	83.13216
October	N	4944.556	93.63655
October	N	5198.726	89.13546
October	N	3918.741	87.5771
October	N	3653.48	91.6116
October	P	3304.527	77.17427
October	P	5171.098	81.62922
October	P	3486.548	102.44256
October	P	4965.579	81.39615
October	P	2473.519	59.94393

Figure S2.4 | Alpha diversity (Chao1) indices for *Siderastrea siderea* metagenomes

8.2 Appendix B: Ch. 2 Supplemental Figures

Figure S2.1 | Photo of a nutrient diffuser adjacent to an experimental coral

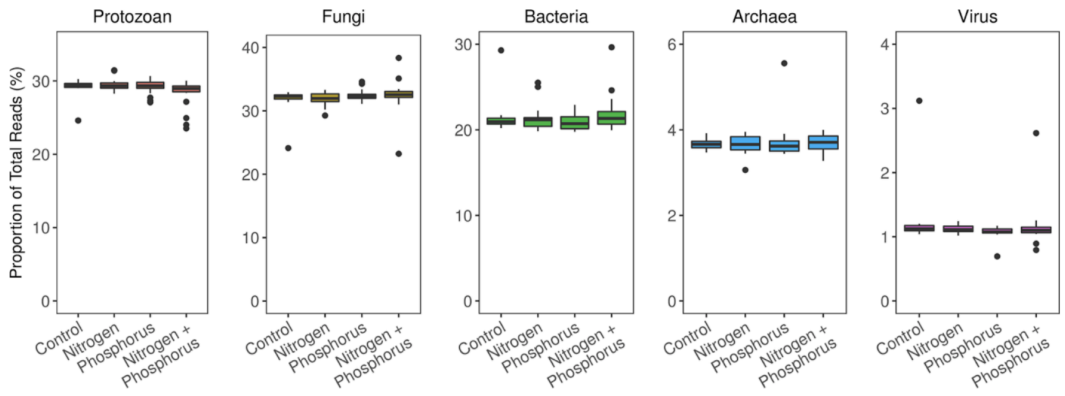

Figure S2.2 | Taxonomic distribution of *Siderastrea siderea* microbiomes from metagenomes of control and treated corals. Results are normalized as the relative abundance of taxonomic groups in each treatment. There were no significant differences in taxonomic relative abundance between the treatments.

8.3 Appendix C: Ch. 3 Supplemental Tables

		Weighted UniFrac		Unweighted UniFrac	
Sampling compartment	**Df**	**Pseudo-F**	**P-value**	**Pseudo-F**	**P-value**
Immediate (weeks 1/2) vs. sustained (weeks 3/4) effects					
Leaf	1, 43	2.16	**p = 0.018**	1.42	**p = 0.006**
Water column	1, 40	6.03	**p = 0.001**	1.69	**p = 0.001**
Root associated	1, 46	2.31	**p = 0.048**	1.41	**p = 0.023**
Rhizosphere	1, 57	1.49	p = 0.142	1.10	p = 0.094
Bulk sediment	1, 49	1.09	p = 0.269	1.01	p = 0.263

Table S3.1 | Results of PERMANOVA tests conducted on weighted and unweighted UniFrac metrics of microbial communities associated with *Zostera marina* sampling compartments; leaf, water column, root associated sediment, rhizosphere sediment, and bulk sediment, to elucidate differences between the first half of the experiment (weeks 1, 2) and the second half of the experiment (weeks 3, 4). Statistically significant results ($p < 0.05$) are denoted in bold.

Figure S3.2 (following page) | Results of generalized linear mixed models examining changes in ammonium and nitrate concentrations between treatment, time, and the interaction of treatment and time. Significant results ($p < 0.05$) are denoted in bold.

Response variable	Effects	Df	χ^2	P-value	SD
Water column					
Ammonium	Treatment	1	0.56	0.455	
	Time	7	6.21	0.515	
	Treatment x Time	7	0.99	0.995	
	Tank				<0.001
Nitrate	Treatment	1	2.11	0.147	
	Time	7	26.82	**<0.001**	
	Treatment x Time	7	15.42	**0.031**	
	Tank				0.039
Rhizosphere sediment porewater					
Ammonium	Treatment	1	9.17	**0.002**	
	Time	7	23.85	**0.001**	
	Treatment x Time	7	3.37	0.849	
	Tank				0.001
Nitrate	Treatment	1	3.90	**0.048**	
	Time	7	60.90	**<0.001**	
	Treatment x Time	7	13.06	0.071	
	Tank				0.348
Plant associated sediment porewater					
Ammonium	Treatment	1	18.26	**<0.001**	
	Time	7	21.76	**0.003**	
	Treatment x Time	7	26.49	**<0.001**	
	Tank				<0.001
Nitrate	Treatment	1	1.31	0.252	
	Time	7	14.30	**0.046**	
	Treatment x Time	7	6.56	0.476	
	Tank				0.179
Bulk sediment porewater					
Ammonium	Treatment	1	13.47	**<0.001**	
	Time	7	11.81	0.107	
	Treatment x Time	7	1.73	0.973	
	Tank				<0.001
Nitrate	Treatment	1	2.28	0.131	
	Time	7	73.16	**<0.001**	
	Treatment x Time	7	21.47	**0.003**	
	Tank				0.564
Sediment porewater compartments					
Ammonium	Treatment	1	25.03	**<0.001**	Tukey's post-hoc comparison by source: PA – BS: p = 0.004 R – BS: p = 4.12 e-5 R – PA: p = 0.082
	Source	2	23.03	**<0.001**	
	Time	7	17.73	**0.013**	
	Tank				<0.001
Nitrate	Treatment	1	6.32	**0.012**	Tukey's post-hoc comparison by source: PA – BS: p = 0.345 R – BS: p = 3.17 e-7 R– PA: p = 3.74 e-10
	Source	2	66.79	**<0.001**	
	Time	7	128.32	**<0.001**	
	Tank				0.352

Figure S3.2

		Weighted UniFrac		Unweighted UniFrac	
Sampling compartment	**Df**	**Pseudo-F**	**P-value**	**Pseudo-F**	**P-value**
Sampling day effects, weeks 1 and 2					
Leaf	4, 18	1.79	**p = 0.007**	1.16	**p = 0.001**
Water column	4, 13	4.20	**p = 0.001**	1.39	**p = 0.001**
Root associated	3, 29	1.02	p = 0.378	1.10	p = 0.110
Rhizosphere	4, 24	1.73	**p = 0.013**	1.06	p = 0.055
Bulk sediment	4, 20	1.27	p = 0.072	1.05	**p = 0.021**
Sampling day effects, weeks 3 and 4					
Leaf	3, 18	1.54	**p = 0.032**	1.23	**p = 0.001**
Water column	3, 19	1.87	**p = 0.016**	1.23	**p = 0.011**
Root associated	3, 11	0.66	p = 0.800	0.94	p = 0.734
Rhizosphere	3, 26	2.21	**p = 0.022**	1.22	**p = 0.016**
Bulk sediment	3, 22	1.92	**p = 0.003**	1.10	**p = 0.002**

Table S3.3 | Results of PERMANOVA tests conducted on weighted and unweighted UniFrac metrics of microbial communities associated with *Zostera marina* sampling compartments; leaf, water column, root associated sediment, rhizosphere sediment, and bulk sediment, to elucidate the temporal effects. Tests were conducted within each sampling compartment, comparing between sampling days 0, 1, 3, 7, and 14 for weeks 1 and 2, and comparing between sampling days 15, 17, 21, and 28 for weeks 3 and 4. Statistically significant results ($p < 0.05$) are denoted in bold.

Table S3.4 (following page) | Indicator OTUs of root associated and rhizosphere samples from weeks 3 and 4 of the experiment. OTUs are identified to the genus level or to the highest taxonomic resolution possible.

OTU	Compartment	Treatment	Genus	16S rRNA V4-V5 Amplicon Sequence
Otu00011	Root Associated	Ambient	Alphaproteobacteria unclassified	TACGAAGGGGGCTAGCGTTGTTCGGAATTACTGGGCGTAAAGAGTACGTAGGCTGATTAGAAAGTTAGGGGTGAAATCCCAGGGCTCAACCCTGGAACTGCCTCTAAAACTCCTAATCTTGAGTTCGAGAGAGGTGAGTGGAATTCCGAGTGTAGAGGTGAAATTCGTAGATATTCGGAGGAACACCAGTGGCGAAGGCGGCTCACTGGCTCGATACTGACGCTGAGGTACGAAAGCGTGGGGAGCAAACAGG
Otu00017	Root Associated	Ambient	Glaciecola	TACGGAGGGTGCGAGCGTTAATCGGAATTACTGGGCGTAAAGCGCACGCAGGCGGTTTGTTAAGCTAGATGTGAAAGCCCCGGGCTCAACCTGGGAATAGCATTTAGAACTGGCAGGCTAGAGTCTTGGAGAGGGGAGTGGAATTTCTGGTGTAGCGGTGAAATGCGTAGATATCAGAAGGAACATCAGTGGCGAAGGCGACTCCCTGGCCAAAGACTGACGCTCATGTGCGAAAGTGTGGGTAGCGAACACAGG
Otu00018	Root Associated	Ambient	Verrucomicrobiaceae unclassified	TACGAAGGTCCCAAGCGTTGTTCGGAATAACTGGGCGTAAAGCGTGTGTAGGCTGCGCGGAAAGTCAAATGTGAAAGCCAGGGGCTCAACCTCTGAACTGCATTCGATACTCCCGTGCTAGAGTAATGGAGAGGTAAGTGGAATTCCCGGTGTAGCAGTGAAATGCGTAGATATCGGGAGGAACATCAATGGCGAAGGCAACTTACTGGACATTTACTGACGCTCAGACACGAAGGCTAGGGGAGCGAAAGGG
Otu00032	Root Associated	Ambient	Sulfitobacter	TACGGAGGGGGTTAGCGTTGTTCGGAATTACTGGGCGTAAAGCGTACGTAGGCGGATCAGAAAGTATGGGGTGAAATCCCGAGGCTCAACCTCGGAACTGCCTCATAAACTCCTGGTCTTGAGTTCGAGAGAGGTGAGTGGAATTCCAAGTGTAGAGGTGAAATTCGTAGATATTTGGAGGAACACCAGTGGCGAAGGCGGCTCACTGGCTCGATACTGACGCTGAGGTACGAAAGTGTGGGGAGCAAACAGG
Otu00033	Root Associated	Ambient	Winogradskyella	TACGGAGGATCCAAGCGTTATCCGGAATCATTGGGTTTAAAGGGTCCGTAGGGTGGATAATTAAGTCAGAGGTGAAATCCTGCAGCTCAACTGTAGAATTGCCTTTGAAACTGGTTATCTTGAATTATTGTGAAGTGGTTAGAATATGTAGTGTAGCGGTGAAATGCATAGATATTACATAGAATACCAATTGCGAAGGCAGATCACTAACAATATATTGACACTGATGGACGAAAGCGTGGGGAGCGAACAGG
Otu00048	Root Associated	Ambient	Granulosicoccus	TACGGAGGGTGCAAGCGTTAATCGGAATTACTGGGCGTAAAGCGCGCGTAGGCGGCTTGGTCAGTCAGATGTGAAATCCCCGAGCTCAACTTGGGAACTGCATTTGATACTGCCAAGCTAGAGTATGTTAGAGGAAAGCGGAATTCCGGGTGTAGCGGTGAAATGCGTAGATATCCGGAGGAACATCAGTGGCGAAGGCGGCTTTCTGGAACAATACTGACGCTGAGGTGCGAAAGCGTGGGGAGCAAACAGG
Otu00068	Root Associated	Ambient	Litorimonas	TACGGAGGGGGCTAGCGTTGTTCGGAATTACTGGGCGTAAAGCGTGCGTAGGCGGATTAGAAAGTATGGGGTGAAATCCCAGGGCTCAACCCTGGAACTGCCTCATAAACTCCTAGTCTTGAGTTCTGGAGAGGTAAGTGGAATTCCTAGTGTAGAGGTGAAATTCGTAGATATTAGGAGGAACACCAGAGGCGAAGGCGGCTTACTGGACAGATACTGACGCTGAGGCACGAAAGTGTGGGGAGCAAACAGG
Otu00075	Root Associated	Ambient	Gammaproteobacteria unclassified	TACGGAGGGTGCAAGCGTTAATCGGAATTACTGGGCGTAAAGCGCGCGTAGGCGGTTGTTTAAGTCGGATGTGAAAGCCCTGGGCTCAACCTGGGAACTGCATTCGATACTGGGCAACTAGAGTATGAAAGAGGGAGGTAGAATTCCATGTGTAGCGGTGAAATGCGTAGATATGTGGAGGAATACCAGTGGCGAAGGCGGCCTCCTGGTTCAATACTGACGCTGAGGTGCGAAAGCGTGGGGAGCAAACAGG
Otu00078	Root Associated	Ambient	Lewinella	TACGGAGGGTGCAAGCGTTATCCGGAATCACTGGGTTTAAAGGGTGCGTAGGTGGACTAGTAAGTCAGAGGTGAAATCCCGTCGCTTAACGACGGAACTGCCTTTGATACTGCTTGTCTTGAATCAGGTTGAGGTATGCGGAATGTGGCATGTAGCGGTGAAATGCGTAGATATGCCATAGAACACCGATTGCGAAGGCAGCATACTGGCCCTGTATTGACACTGAGGCACGAAAGCGTGGGGAGCGAACAGG
Otu00079	Root Associated	Ambient	Marinicella unclassified	TACGGAGGGTGCGAGCGTTAATCGGAATTACTGGGCGTAAAGGGTACGTAGGCGGCTTAATAAGTCAGATGTGAAATCCCCGGGCTTAACCTGGGAACTGCATTTGAAACTGTTTGGCTAGAGTGAGTGAGAGGTTAGTGGAATTCAAGGCGTAGCGGTGAAATGCGTAGAGGTCTTGAGGAACATCAGTGGCGAAGGCGACTAACTGGCACTACACTGACGCTGAGGTACGAAAGCGTGGGGAGCGAACAGG
Otu00090	Root Associated	Ambient	Rhodobacteraceae unclassified	TACGGAGGGGACTAGCGTTGTTCGGAATTACTGGGCGTAAAGCGCACGTAGGCGGACCAGAAAGTATGGGGTGAAATCCCAGGGCTCAACCCTGGAACTGCCTCATAAACTCCTGGTCTAGAGTTCGAGAGAGGTGAGTGGAATTCCGAGTGTAGAGGTGAAATTCGTAGATATTCGGAGGAACACCAGTGGCGAAGGCGGCTCACTGGCTCGATACTGACGCTGAGGTGCGAAAGCGTGGGGAGCAAACAGG
Otu00098	Root Associated	Ambient	Bacteria unclassified	AACGGGAGGGGCAAGCGTTATTCGGCATAACTGGGCGTAAAGAGTCCGTAGACGGTAAAATAAGTTTTTTGTTAAATTTTAAATTCTAATTTTAAAACAAGCATTAAATACTGTTTTACTTTGAGTTTAGTACAGAAAAATGGAATTTTATATGAAAGGGTGAAATCTGCTAATATATAAAGGAATGCCATTAGCGAAGGCGATTTTTTGGTATAAACTGACGTTGAGGGACGAAAGTGTGGGTATCAAACAGG
Otu00099	Root Associated	Ambient	Gammaproteobacteria unclassified	TACGGAGGGTGCAAGCGTTAATCGGAATTACTGGGCGTAAAGCGCGCGTAGGCGGCTATATAAGTCGGATGTGAAAGCCCTGGGCTCAACCTGGGAACTGCATTCGATACTGTATAGCTAGAGTTTGGTAGAGGGAAGTGGAATTCCACATGTAGCGGTGAAATGCGTAGATATGTGGAGGAACACCAGTGGCGAAGG

				CGACTTCCTGGACCAGAACTGACGCTGAGGTGCGAAAGCGTGGGTAGCA AACAGG
Otu0 0104	Root Associated	Ambient	Bacteria unclassified	TACGGGAGGGGCAAGCGTTATTCGAAATAACTGGGCGTAAAGAGTTCGT AGACGGTAATACAAGTTATTTGTTAATTTTTAAAGCCTAACTTTAAGCCA GCAAATAAGACTATTTTACTTGAGTTTTTTTCAGAAGAGCAGAATTTTATA TTAAGGGGTGAGACCTGTAGATATATAAAGGAATACCATTAAAAGCGAA GGCGGCTCTTTGGTAAAAACTGACGTTGAGGAACGAAAGTATAGGGAGC AAACAGG
Otu0 0116	Root Associated	Ambient	Bacteroidetes unclassified	TACGGAGGATGCGAGCGTTATCCGGAATCACTGGGTTTAAAGGGTGCGTA GGCGGGAAAATAAGTCAGAGGTGAAATCTGGTCGCTTAACGATCAAATT GCCTTTGAAACTGTTTTTCTTGAAATATGATGAGGTTGGCAGAATGTGAC ATGTAGCGGTGAAATGCATAGATATGTCATAGAATACCAATTGCGAAGGC AGCTGACTGGTCATTATTTGACGCTGAGGCACGAAAGCGTGGGGAGCGA ACAGG
Otu0 0144	Root Associated	Ambient	Lutibacter	TACGGAGGGTGCAAGCGTTATCCGGAATCATTGGGTTTAAAGGGTCCGTA GGCGGACTATTAAGTCAGAGGTGAAATCCCACAGCTCAACTGTGGAACTG CCTTTGATACTGGTAGTCTTGAGTTATATGGAAGTAGATAGAATGTGTAG TGTAGCGGTGAAATGCATAGATATTACACAGAATACCGATTGCGAAGGC AGTCTACTACGTATATACTGACGCTAATGGACGAAAGCGTGGGGAGCGA ACAGG
Otu0 0152	Root Associated	Ambient	Bacteria unclassified	TACGGGAGGGGCTAGCGTTATTCGAAGTAACTAGGCGTAAAGGGTTCGTA GACGGTATTTTAAGTCAAATATTAAACATTAAAAAACATTTAATACAATA TTTAACACTATTATACTAGAGTTTATTGCAGAAAAGAAGAATTTTATGAG TAAAAATAAAATTTACAGATACATAAAGGAATACCGAAAGCGAAGGCGT CTTTTTGGCAATAAACTGACGTTGAGGAACGAAAGTTTAGGTAGCAAATA GG
Otu0 0163	Root Associated	Ambient	Proteobacteria unclassified	TACAGAGGGTGCAAACGTTGCTCGGAATTACTGGGCGTAAAGCGCGTGTA GGCGGATTCGAAAGTCAGATGTGAAATCCCTGGGCTCAACCTAGGAACTG CATTTGAAACTTCGTGTCTAGAGTGATGGAGAGGAAAGCGGAATTATTGG TGTAGAGGTGAAATTCGTAGATATCAATAGGAACACCAGTGGCGAAGGC GGCTTTCTGGACATTTACTGACGCTGAGACGCGAAAGCATGGGGAGCAA ACAGG
Otu0 0181	Root Associated	Ambient	Gammaproteobacteria unclassified	TACGGAGGGATCGAACGTTAATCGGAATTACTGGGCGTAAAGCGCGCGT AGGCGGTTTGATAAGTGGGATGTGAAAGCCCCGGGCTTAACCTGGGAACT GCATTCCAAACTGTCAGACTAGAGTATGGTAGAGGGTGGTAGAATTTCCT GTGTAGCGGTGAAATGCGTAGATATAGGAAGGAATACCGATGGCGAAGG CAGCCACCTGGACCAATACTGACGCTGAGGTGCGAAAGCGTGGGGAGCA AACAGG
Otu0 0198	Root Associated	Ambient	Saprospiraceae unclassified	TACGGAGGGTGCAAGCGTTATCCGGAATCACTGGGTTTAAAGGGTGCGTA GGCGGGTAAATAAGTCAGAGGTGAAAGCTCACAGCTTAACTGTGGAATT GCCTTTGATACTGTTTATCTTGAATTGTGTTGAGGTTAGCGGAATGTGACA TGTAGCGGTGAAATGCATAGATATGTCATAGAACACCAATTGCGAAGGC AGCTAGCTAGGCATTGATTGACGCTGAGGCACGAAAGCGTGGGGAGCGA ACAGG
Otu0 0217	Root Associated	Ambient	Ekhidna	TACGGAGGGTGCAAGCGTTGTCCGGATTTATTGGGTTTAAAGGGTACGTA GGCGGATTTTTAAGTCCGTGGTGAAAGCCTACAGCTTAACTGTAGAACTG CCATGGATACTGGAAATCTTGAATTCAGTTGAGGTAAGCGGAATTTATGA TGTAGCGGTGAAATGCATAGATATCATAAAGAACACCAATTGCGAAGGC AGCTTGCTGGACTTGAATTGACGCTGAGGTACGAAAGCGTGGGGAGCGA ACAGG
Otu0 0256	Root Associated	Ambient	Hyphomonadaceae unclassified	TACGGAGGGGGCTAGCGTTGTTCGGAATTACTGGGCGTAAAGCGTACGTA GGCGGACTATTAAGTAAGATGTGAAATCCCAGGGCTCAACCCTGGAACTG CATTTTAAACTGGTAGTCTAGAGTTATGGAGAGGTAAGTGGAATTCCTAG TGTAGAGGTGAAATTCGTAGATATTAGGAGGAACACCAGAGGCGAAGGC GGCTTACTGGACATATACTGACGCTGAGGTACGAAAGTGTGGGGAGCAA ACAGG
Otu0 0267	Root Associated	Ambient	Flavobacteriaceae unclassified	TACGGAGGGTCCGAGCGTTATCCGGAATCATTGGGTTTAAAGGGTCCGTA GGCGGGCAGCTCAGTCAGTGGTGAAAGTCTGTGGCTCAACCATAGAATTG CCATTGATACTGGTTGTCTTGAATCAATGTGAAGTGGTTAGAATAAGTAG TGTAGCGGTGAAATGCATAGATATTACTTAGAATACCGATTGCGAAGGCA GATCACTAACATTGTATTGACGCTGAGGGACGAAAGCGTGGGGAGCGAA CAGG
Otu0 0281	Root Associated	Ambient	Luteolibacter	TACGAAGGTCCCAAGCGTTGTTCGGAATCACTGGGCGTAAAGGGAGCGT AGGCGGCGTGGTAAGTCAGATGTGAAATTCCGGGGCTCAACCTCGGAACT GCATCCGATACTGCCATGCTAGAGTGGTGGAGGGGCATCTGGAATTCACG GTGTAGCAGTGAAATGCGTAGATATCGTGAGGAACACTAGTGGCGAAGG CGAGATGCTGGACACCTACTGACGCTGAGGCTCGAAGGCCAGGGTAGCG AAAGGG
Otu0 0283	Root Associated	Ambient	Flammeovirgaceae unclassified	TACGGAGGGTGCAAGCGTTGTCCGGATTTATTGGGTTTAAAGGGTGCGTA GGCGGTCAATTAAGTCAGTGGTGAAATCCTATAGCTTAACTATAGAACTG CCATTGATACTGGTTGACTTGAGTACAGACGAGGTAGGCGGAATTTATGG TGTAGCGGTGAAATGCATAGATACCATAAAGAACACCGATAGCGAAGGC AGCTTACTGGACTGTAACTGACGCTGAGGCACGAAAGCATGGGTAGCGA ACAGG
Otu0 0008	Root Associated	Fertilized	Arcobacter	TACGGAGGGTGCAAGCGTTACTCGGAATCACTGGGCGTAAAGAGCGTGT AGGCGGATAGATAAGTTTGAAGTGAAATCCAATGGCTCAACCATTGAACT GCTTTGAAAACTGTTTATCTAGAATATGGGAGAGGTAGATGGAATTTCTG GTGTAGGGGTAAAATCCGTAGAGATCAGAAGGAATACCGATTGCGAAGG

				CGATCTACTGGAACATTATTGACGCTGAGACGCGAAAGCGTGGGGAGCA AACAGG
Otu0 0013	Root Associat ed	Fertilized	Sulfurovum	TACGGAGGGTGCAAGCGTTACTCGGAATCACTGGGCGTAAAGCGCGCGC AGGCGGCCTTTTAAGTTGGATGTGAAAGCCTATGGCTCAACCATAGAACT GCATCCAAAACTATCAGGCTAGAGTGTGGGAGAGGAAGATGGAATTAGT TGTGTAGGGGTAAAATCCGTAGAGATAACTAGGAATACCAAAAGCGAAG GCAATCTTCTGGAACATTACTGACGCTGAGGCGCGAAAGCGTGGGGAGC AAACAGG
Otu0 0015	Root Associat ed	Fertilized	Sulfurovum	TACGGAGGGTGCAAGCGTTACTCGGAATCACTGGGCGTAAAGCGCGCGC AGGCGGCCATTTAAGTTGGATGTGAAAGCCTACGGCTCAACCGTAGAACT GCATCCAAAACTATTTGGCTAGAGTGTGGGAGAGGAAGATGGAATTAGTT GTGTAGGGGTAAAATCCGTAGAGATAACTAGGAATACCAAAAGCGAAGG CAATCTTCTGGAACACTACTGACGCTGAGGCGCGAAAGCGTGGGGAGCA AACAGG
Otu0 0019	Root Associat ed	Fertilized	Colwellia	TACGAGGGGTGCAAGCGTTAATCGGAATTACTGGGCGTAAAGCGTTCGTA GGCGGTTATTTAAGCAAGATGTGAAAGCCCAGGGCTCAACCTTGGAACTG CATTTTGAACTGGGTAACTAGAGTACTGTAGAGGGTGGTGGAATTTCCAG TGTAGCGGTGAAATGCGTAGAGATTGGAAGGAACATCAGTGGCGAAGGC GGCCACCTGGACAGATACTGACGCTGAGGAACGAAAGCGTGGGGAGCGA ACAGG
Otu0 0024	Root Associat ed	Fertilized	Arcobacter	TACGGAGGGTGCAAGCGTTACTCGGAATTACTGGGCGTAAAGAGCGTGT AGGCGGGTAAATAAGTTGGAAGTGAAATCCTATGGCTCAACCATAGAAC TGCTTCCAAAACTGTTAACCTAGAATGTGGGAGAGGTAGATGGAATTTCT GGTGTAGGGGTAAAATCCGTAGATATCAGAAGGAATACCGATTGCGAAG GCGATCTACTGGAACATTATTGACGCTGAGACGCGAAAGCGTGGGGAGC AAACAGG
Otu0 0064	Root Associat ed	Fertilized	Sulfurospirillu m	TACGGAGGGTGCAAGCGTTACTCGGAATCACTGGGCGTAAAGGATGCGT AGGCGGATAATCAAGTCAAAAGTGAAATCCCACGGCTTAACCGTGGAAC TGCTTTCGAAACTGATTATCTAGAATATGGAAGAGGCAGATGGAATTAGT GGTGTAGGGGTAAAATCCGTAGAGATCACTAGGAATACCGATTGCGAAG GCGATCTGCTGGGACATTATTGACGCTGAGGCATGAAAGCGTGGGGAGC AAACAGG
Otu0 0073	Root Associat ed	Fertilized	Bacteroidetes unclassified	TACGGAGGGTGCAAGCGTTATCCGGATTTATTGGGTTTAAAGGGTGCGTA GGCGGAAGAATAAGTCAGTGGTGAAATCTTGCAGCTTAACTGTAAAACTG CCATTGATACTGTTTTTCTTGAGTATAGTTGAGGTAGGCGGAATGTGTAAT GTAGCGGTGAAATGCTTAGATATTACACAGAACACCGATTGCGTAGGCAG CTTACTAAGCTATAACTGACGCTGAGGCACGAAAGCGTGGGGAGCGAAC AGG
Otu0 0074	Root Associat ed	Fertilized	Gammaproteo bacteria unclassified	TACGGAGGGTGCAAGCGTTAATCGGAATTACTGGGCGTAAAGCGCACGT AGGCGGTTAGGTAAGTCAGATGTGAAAGCCCCGGGCTCAACCTGGGAAC TGCATTTGATACTGCTTAACTAGAGTATAGTAGAGGCAAGTGGAATTCCA GGTGTAGCGGTGAAATGCGTAGATATCTGGAGGAACATCAGTGGCGAAG GCGACTTGCTGGACTAATACTGACGCTGAGGTGCGAAAGCGTGGGGAGC AAACAGG
Otu0 0119	Root Associat ed	Fertilized	Desulfobactera ceae unclassified	TACGGGGGGTGCAAGCGTTATTCGGAATTATTGGGCGTAAAGGGCGCGTA GGCGGTCTTGTCGGTCAGATGTGAAAGCCCGGGGCTCAACCCTGGAAGTG CATTTGAAACAGCAAGACTTGAATACTGGAGAGGAGAGCGGAATTCCTG GTGTAGAGGTGAAATTCGTAGATATCAGGAGGAACACCGATGGCGAAGG CAGCTCTCTGGACAGATATTGACGCTGAGGCGCGAAGGCGTGGGTAGCG AACAGG
Otu0 0164	Root Associat ed	Fertilized	Vibrio	TACGGAGGGTGCGAGCGTTAATCGGAATTACTGGGCGTAAAGCGCATGC AGGTGGTCTGTTAAGTCAGATGTGAAAGCCCGGGGCTTAACCTCGGAATA GCATTTGAAACTGTCAGACTAGAGTACTGTAGAGGGGGGTAGAATTTCAG GTGTAGCGGTGAAATGCGTAGAGATCTGAAGGAATACCGGTGGCGAAGG CGGCCCCCTGGACAGATACTGACACTCAGATGCGAAAGCGTGGGGAGCA AACAGG
Otu0 0193	Root Associat ed	Fertilized	Flavobacteriac eae unclassified	TACGGAGGGTCTAAGCGTTATCCGGAATCATTGGGTTTAAAGGGTCCGTA GGCGGGCTAATAAGTCAGAGGTGAAATCCCACAGCTTAACTGTGGCACTG CCTTTGATACTGTTAGTCTTGAGTCATAATGAGGTAGATGGAATGTGTAG TGTAGCGGTGAAATGCATAGATATTACACAGAACACCGATTGCGAAGGC AGTCTACTAATTATGTACTGACGCTGAGGGACGAAAGCGTGGGTAGCGA ACAGG
Otu0 0228	Root Associat ed	Fertilized	Gp23 unclassified	TACGGAGGGGGCAAGCGTTATTCGGATTTACTGGGCGTAAAGCGCACGTA GGTGGCATGGTAAGTCAAAGGTGAAAGCCCTCGGCTCAACCGAGGAATT GCCTTTGAAACTGCTTTGCTTGAGTCCGGGAGGGGGGAGCGGAATTCCCA GTGTAGCGGTGAAATGCGTAGATACTGGGAGGAACACCGGTGGCGAAGG CGGCTCCCTGGACCGGTACTGACACTGAGGTGCGAAAGCGTGGGTAGCA AACAGG
Otu0 0330	Root Associat ed	Fertilized	Marinifilum unclassified	TACGGAGGATTCGAGCGTTATCCGGATTTATTGGGTTTAAAGGGTCCGTA GGCGGTTCTTTAAGTCAGTGGTGAAATCCCAGAGCTCAACTCTGGAACTG CCATTGAAACTGAAGAACTTGAATATGGTTGAGGTAGGCGGAATACGTTA TGTAGCGGTGAAATGCATAGATATAACGTAGAACACCAATTGCGAAGGC AGCTTACTAAACCATTATTGACGCTGATGGACGAAAGCGTGGGGAGCGA ACAGG
Otu0 0334	Root Associat ed	Fertilized	Bacteriovoraca ceae unclassified	TACGGAGGGTGCAAGCGTTGTTCGGATTTACTGGGCGTAAAGCGCGCGCA GGCGGACTAGCAAGTCAGATGTGAAATCTCGGGGCTTAACCCCGAAACT GCGTCTGAAACTGTTAGTCTAGAGTCTCACAGGGGGTAGGGGAATTTCAC GTGTAGGGGTAAAATCCGTAGAGATGTGAAGGAACACCGGTGGCGAAGG

				CGCCTACCTGGATGAGCACTGACGCTGAGGCGCGAAAGCGTGGGGAGCA AACAGG
Otu0 0365	Root Associat ed	Fertilized	Proteobacteria unclassified	TACGGAGGGGGCAAACGTTGTTCGGAATCACTGGGCGTAAAGCGCATGT AGGCGGCTTGTCATGTCAGATGTGAAAGCCCACGGCTCAACCGTGGAAGT GCATTTGAAACTGGCAGGATAGAATATGGGAGAGGGTTGTAGAATACCA GGTGTAGAGGTGAAATTCGTAGATATCTGGTAGAATACCGGTGGCGAAG GCGGCAACCTGGACCAATATTGACGCTGAGATGCGAAAGCGTGGGGAGC GAACAGG
Otu0 0402	Root Associat ed	Fertilized	Bacteria unclassified	TACGTAGGGTGCAAGCGTTGTTCGGAATCACTGGGCGTAAAGGGAGCGT AGGCGGGATTGTAAGTTAGGAGTTTAATGCATGGGCTTAACCCATGACCT GCTCTTAATACTGCGGTTCTTGAGTATGGGAGAGGGCGATGGAATTCCAG GTGTAGCGGTGGAATGCGTAGATATCTGGAAGAACACCAGTAGCGAAGG CGGTCGCCTGGCCCAATACTGACGCTGAGGCTCGAAAGCTAGGGGAGCA AACAGG
Otu0 0710	Root Associat ed	Fertilized	Cytophaga	TACGGAGGATGCGAGCGTTATCCGGATTCATTGGGTTTAAAGGGTGCGTA GGCGGTAGAATAAGTCAGTGGTGAAAGCCTGCAGCTCAACTGTAGAATT GCCATTGATACTGTTTTACTTGAGTATAATTGAGGTAGGCGGAATGTGTT GTGTAGCGGTGAAATGCATAGATATAACACAGAACACCAATTGCGAAGG CAGCTTACTAAGTTATAACTGACGCTGAGGCACGAAAGCGTGGGTAGCG AACAGG
Otu0 0185	Rhizosp here	Ambient	Lutibacter	TACGGAGGGTGCAAGCGTTATCCGGAATCATTGGGTTTAAAGGGTCCGTA GGCGGACTATTAAGTCAGAGGTGAAATCCCACAGCTCAACTGTGGAACTG CCTTTGATACTGGTAGTCTTGAGTTATATGGAAGTAGATAGAATGTGTAG TGTAGCGGTGAAATGCATAGATATTACACAGAATACCGATTGCGAAGGC AGTCTACTACGTATATACTGACGCTAATGGACGAAAGCGTGGGGAGCGA ACAGG
Otu0 0411	Rhizosp here	Ambient	Saprospiraceae unclassified	TACGGAGGGTGCAAGCGTTATCCGGAATCACTGGGTTTAAAGGGTGCGTA GGCGGCGTTATAAGTCAGAGGTGAAAGGCCACCGCTTAACGGTGGGACT GCCTTTGATACTGTAGTGCTTGAATAAGGTTGAGGTTAGCGGAATGTGAC ATGTAGCGGTGAAATGCATAGATATGTCATAGAACACCAATTGCGAAGG CAGCTGGCTAGACCTTTATTGACGCTGAGGCACGAAAGCGTGGGGAGCG AACAGG
Otu0 0205	Rhizosp here	Ambient	Sulfitobacter	TACGGAGGGGGTTAGCGTTGTTCGGAATTACTGGGCGTAAAGCGTACGTA GGCGGATCAGAAAGTAGGGGGTGAAATCCCAGGGCTCAACCCTGGAACT GCCTCCTAAACTCCTGGTCTTGAGTTCGAGAGAGGTGAGTGGAATTCCAA GTGTAGAGGTGAAATTCGTAGATATTTGGAGGAACACCAGTGGCGAAGG CGGCTCACTGGCTCGATACTGACGCTGAGGTACGAAAGTGTGGGGAGCA AACAGG
Otu0 0133	Rhizosp here	Ambient	Alphaproteoba cteria unclassified	TACGGAGGGGACTAGCGTTGTTCGGAATTACTGGGCGTAAAGAGTTCGTA GGCGGATAAGCAAGTAAGAGGTGAAAGCCCAGGGCTCAACCCTGGAACT GCCTTTTAAACTGCTTATCTAGAGACTGATAGAGGTTAGGGGAATACCTA GTGTAGAGGTGAAATTCGTAGATATTAGGTGGAACACCAGTGGCGAAGG CGCCTAACTGGATCAGTACTGACGCTGAGGAACGAAAGCGTGGGGAGCA AACAGG
Otu0 0445	Rhizosp here	Ambient	Actinobacteria unclassified	GACGTAGGGGGCGAGCGTTGTCCGGATTTATTGGGCGTAAAGGGCTCGTA GGCGGTTACGTAAGTCGGATGTGAAAACTCGAGGCTCAACTTCGAGACGC CATCCGATACTGCGTTGACTTGAGTCCGGTAGAGGAGTGTGGAATTCCTA GTGTAGCGGTGAAATGCGCAGATATTAGGAGGAACACCTATTGCGAAGG CAGCACTCTGGGCCGGTACTGACGCTGAGGAGCGAAAGCATGGGTAGCA AACAGG
Otu0 0218	Rhizosp here	Ambient	Flavobacteriac eae unclassified	TACGGAGGATCCAAGCGTTATCCGGAATCATTGGGTTTAAAGGGTCCGTA GGTGGATAATTAAGTCAGAGGTGAAAGTTTGCAGCTCAACTGTAAAATTG CCTTTGATACTGGTTATCTTGAGTTATTATGAAGTAGTTAGAATATGTAGT GTAGCGGTGAAATGCATAGATATTACATAGAATACCAATTGCGAAGGCA GATTACTAATAATATACTGACACTGATGGACGAAAGCGTGGGTAGCGAA CAGG
Otu0 0193	Rhizosp here	Ambient	Rhodobacterac eae unclassified	TACGGAGGGGGTTAGCGTTGTTCGGAATTACTGGGCGTAAAGCGCACGTA GGCGGATTGGAAAGTTGGGGGTGAAATCCCAGGGCTCAACCCTGGAACT GCCTCCAAAACTATCAGTCTAGAGTTCGAGAGAGGTGAGTGGAATTCCGA GTGTAGAGGTGAAATTCGTAGATATTCGGAGGAACACCAGTGGCGAAGG CGGCTCACTGGCTCGATACTGACGCTGAGGTGCGAAAGCGTGGGGAGCA AACAGG
Otu0 0217	Rhizosp here	Ambient	Haliscomenob acter	TACGGAGGGTGCAAGCGTTATCCGGAATCACTGGGTTTAAAGGGTGCGTA GGCGGCGTTATTAGTCAGAGGTGAAATCTTGCAGCTTAACTGTAAAATTG CCTTTGAAACTGTAATGCTTGAATCACGTTGAGGTCGGCGGAATGTGACA TGTAGCGGTGAAATGCATAGATATGTCATAGAACACCAATTGCGTAGGCA GCTGACTAGGCGTGTATTGACGCTGAGGCACGAAAGCGTGGGTAGCGAA CAGG
Otu0 0359	Rhizosp here	Ambient	Verrucomicrob iaceae unclassified	TACGAAGGTCCCGAGCGTTGTTCGGATTTACTGGGCGTAAAGAGTCTGTA GGCGGTAAAGTAAGTCAGGTGTGAAATCCCGAAGCTCAACTTCGGAACT GCACCCGATACTGCTTTACTAGAGTATTGGAGGGGAATCTGGAATTCTCG GTGTAGCAGTGAAATGCGTAGATATCGAGAGGAACACTAGTGGCGAAGG CGAGATTCTGGACAATTACTGACGCTGAGAGACGAAGGCCAGGGTAGCG AAAAGG
Otu0 0126	Rhizosp here	Ambient	Gammaproteo bacteria unclassified	TACGGAGGGTGCAAGCGTTAATCGGAATTACTGGGCGTAAAGCGCGCGT AGGCGGCTATTCAAGCCAGATGTGAAATCCCCGGGCTTAACCTGGGAACT GCATTTGGAACTGGGTAGCTAGAATACAGCAGAGGAGTGTGGAATTTCA GGTGTAGCGGTGAAATGCGTAGAGATCTGAAGGAACATCAGTGGCGAAG

				GCGACACTCTGGGCTGATATTGACGCTGAGGTGCGAAAGCGTGGGTAGC AAACAGG
Otu0 0257	Rhizosp here	Ambient	Rhodobacterac eae unclassified	TACGGAGGGGGTTAGCGTTGTTCGGAATTACTGGGCGTAAAGCGCACGTA GGCGGACTATTAAGTTAGAGGTGAAATCCCAGGGCTCAACCCTGGAACTG CCTTTAATACTGGTAGTCTTGAGTTCGAGAGAGGTGAGTGGAATTCCAAG TGTAGAGGTGAAATTCGTAGATATTTGGAGGAACACCAGTGGCGAAGGC GGCTCACTGGCTCGATACTGACGCTGAGGTGCGAAAGCGTGGGGAGCAA ACAGG
Otu0 0312	Rhizosp here	Ambient	Candidatus Brocadiaceae unclassified	TACGGAGAGGGCAAGCGTTGTTCGGAATCACTGGGCATAAAGCGCACGT AGGCGGATCTGTAAGTCGGTTGTGAAAGCCCGGGGCTCAACCCCGGAAT GGCTTCCGAAACTGCAGGTCTGGAGGACGAGAGGGGAGAGCGGAACTTC TGGTGGAGCGGTGAAATGCGTAGATATCAGAAGGAACACCGGTGGCGAA AGCGGCTCTCTGGCTCGTTTCTGACGCTGAGGTGCGAAAGCTAGGGGAGC AAACGGG
Otu0 0031	Rhizosp here	Fertilized	Methylophaga	TACGGAGGGTGCAAGCGTTAATCGGAATTACTGGGCGTAAAGCGCGCGT AGGCGGTTATTTAAGTCAGATGTGAAATCCCTGGGCTCAACCTAGGAACT GCATTTGATACTGGATAACTAGAGTATGGTAGAGGTGAGTGGAATTTCAG GTGTAGCGGTGAAATGCGTAGAGATCTGAAGGAACATCAGTGGCGAAGG CGACTCACTGGGCCATTACTGACGCTGAGGTGCGAAAGCGTGGGTAGCA AACAGG
Otu0 0097	Rhizosp here	Fertilized	Bacteria unclassified	TACGGGAAGGGCAAGCGTTATTCGGCATGACTGGGCGTAAAGAGTCCGT AGATGGTAAAGTAAGTTTTTGTTAAATTTTAAGACTTAATCTTAACACAG CAATAAATACTGCTTATTTACTAAGAGTTAAAGGAGAAAAGTAGAATTTT ATACGATTAGGGGTGAAATCCGTAGATATATAAAGGAATGCCAACAGCG AAGGCAGCTTTTTACTGTAAACTGACATTGAGGGACGAAAGTGTGGGTAG CAAACAGG
Otu0 0088	Rhizosp here	Fertilized	Flavobacteriac eae unclassified	TACGGAGGGTGCAAGCGTTATCCGGAATCATTGGGTTTAAAGGGTCCGTA GGCGGGTAATTAAGTCAGAGGTGAAATCCCACAGCTTAACTGTGGAACTG CCTTAGATACTGGTTATCTTGAGTTTTAGTGAAGTAGATAGAATGTGTAGT GTAGCGGTGAAATGCATAGATATTACACAGAATACCGATTGCGAAGGCA GTCTACTAACTAACAACTGACGCTAATGGACGAAAGCGTGGGGAGCGAA CAGG
Otu0 0297	Rhizosp here	Fertilized	Rubritalea	TACGAAGGTCCCGAGCGTTATTCGGAATCACTGGGCGTAAAGGGAGCGT AGGCTGTACGGTAAGTCAGATGTGAAATCTCAGAGCTCAACTCTGAAACT GCATCCGATACTGCCGTACTAGAGTAATGGAGGGGTAACTGGAATTCTCG GTGTAGCAGTGAAATGCGTAGATATCGAGAGGAAGACCAACGGCGAAGG CAGGTTACTGGACATTTACTGACGCTGAGGCTCGAAGGCTAGGGTAGCGA AAGGG
Otu0 0302	Rhizosp here	Fertilized	Sulfurospirillu m	TACGGAGGGTGCAAGCGTTACTCGGAATCACTGGGCGTAAAGGATGCGT AGGCGGATAATCAAGTCAAAAGTGAAATCCTACAGCTCAACTGTAGAAC TGCTTTCGAAACTGGTTATCTAGAATATGGAAGAGGCAGATGGAATTAGT GGTGTAGGGGTAAAATCCGTAGAGATCACTAGGAATACCGATTGCGAAG GCGATCTGCTGGGACATTATTGACGCTGAGGCATGAAAGCGTGGGGAGC AAACAGG
Otu0 0335	Rhizosp here	Fertilized	Gp22 unclassified	TACGGAGGGGGCCAGCGTTGTTCGGAATTATTGGGCGTAAAGGGCGCGT AGGCTGCTTTGCAAGTCGAAGGTGAAATCCCTCAGCTCAACTGAGGAACT GCCTCCGATACTGCAGGGCTTGAGTCCCGGAGAGGGTAGCGGAATTCCCA GTGTAGCGGTGAAATGCGTAGATACTGGGAGGAACACCGGTGGCGAAGG CGGCTACCTGGACGGGTACTGACGCTGAGGCGCGAAAGCGTGGGGAGCA AACAGG
Otu0 0588	Rhizosp here	Fertilized	Bacteroidetes unclassified	TACGGAGGATGCAAGCGTTATCCGGATTCATTGGGTTTAAAGGGTTCGCA GGCGGCGTATTAAGTCAGTGGTGAAATCTCTCGGCTCAACCGAGAAACTG CCATTGATACTGGTATGCTAGAGTATAGTTGGCGTAGGCGGAATGTATCA TGTAGCGGTGAAATGCTTAGATATGATACAGAACACCGATCGCGAAGGC AGCTTACGAAACTATAACTGACGCTCAGGAACGAAAGCGTGGGGAGCGA ACAGG
Otu0 0443	Rhizosp here	Fertilized	Flavobacteriac eae unclassified	TACGGAGGATCCAAGCGTTATCCGGAATCATTGGGTTTAAAGGGTCCGTA GGTGGACAATTAAGTCAGAGGTGAAAGTTTGCAGCTTAACTGTAAAATTG CCTTTGATACTGGTTGTCTTGAATCATTATGAAGTGGTTAGAATATGTAGT GTAGCGGTGAAATGCATAGATATTACATAGAATACCAATTGCGAAGGCA GATCACTAATAATGTATTGACACTGATGGACGAAAGCGTGGGGAGCGAA CAGG
Otu0 0357	Rhizosp here	Fertilized	Glaciecola	TACGGAGGGTGCAAGCGTTAATCGGAATTACTGGGCGTAAAGCGCACGC AGGCGGTTTGTTAAGCTAGATGTGAAAGCCCCGCGCTCAACGTGGGATGG TCATTTAGAACTGGCAGACTAGAGTCTTGGAGAGGGGAGTGGAATTTCTA GTGTAGCGGTGAAATGCGTAGATATTAGAAGGAACATCAGTGGCGAAGG CGACTCCCTGGCCAAAGACTGACGCTCATGTGCGAAAGTGTGGGTAGCGA ACAGG
Otu0 0849	Rhizosp here	Fertilized	Bacteria unclassified	GACGTAGGACGCAAGCGTTATCCGGATTTACTGGGCGTAAAGCGTCTGTA GGCGGAGGTATAAGTTGGGCGTGAAAGCTCCGGGCTCAACCCGGAGAGA GCGTTCAATACTGTATCACTAGAGGAGGTCAGAGGAGAGCGGAATTTCCG GTGTAGCGGTAAAATGCGCAGATATCGGAAGGAACACCAGTGGCGAAAG CGGCTCTCTGGGGCCCACCTGACGCTGAGAGACGAAAGCTAGGGGAGCA AACAGG

Table S3.4

8.4 Appendix D: Ch. 3 Supplemental Figures

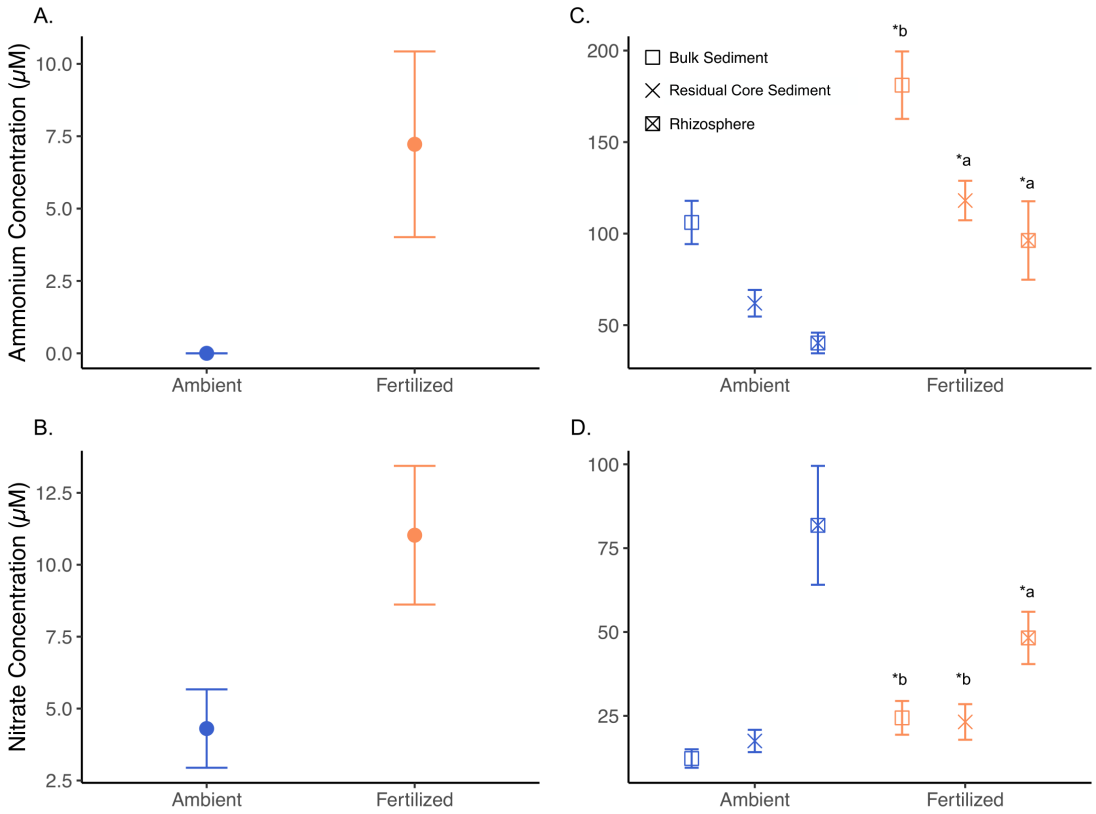

Figure S3.1 | Water column ammonium (A) and nitrate (B) concentration and porewater ammonium (C) and nitrate (D) concentration in bulk sediment, residual core sediment, and rhizosphere sediment. Significant effects ($p < 0.05$) of fertilization within compartments are denoted by asterisks, and significant differences between porewater compartments (regardless of treatment) are denoted by letters. Error bars represent SEM.

8.5 Appendix F: Ch. 4 Supplemental Figures

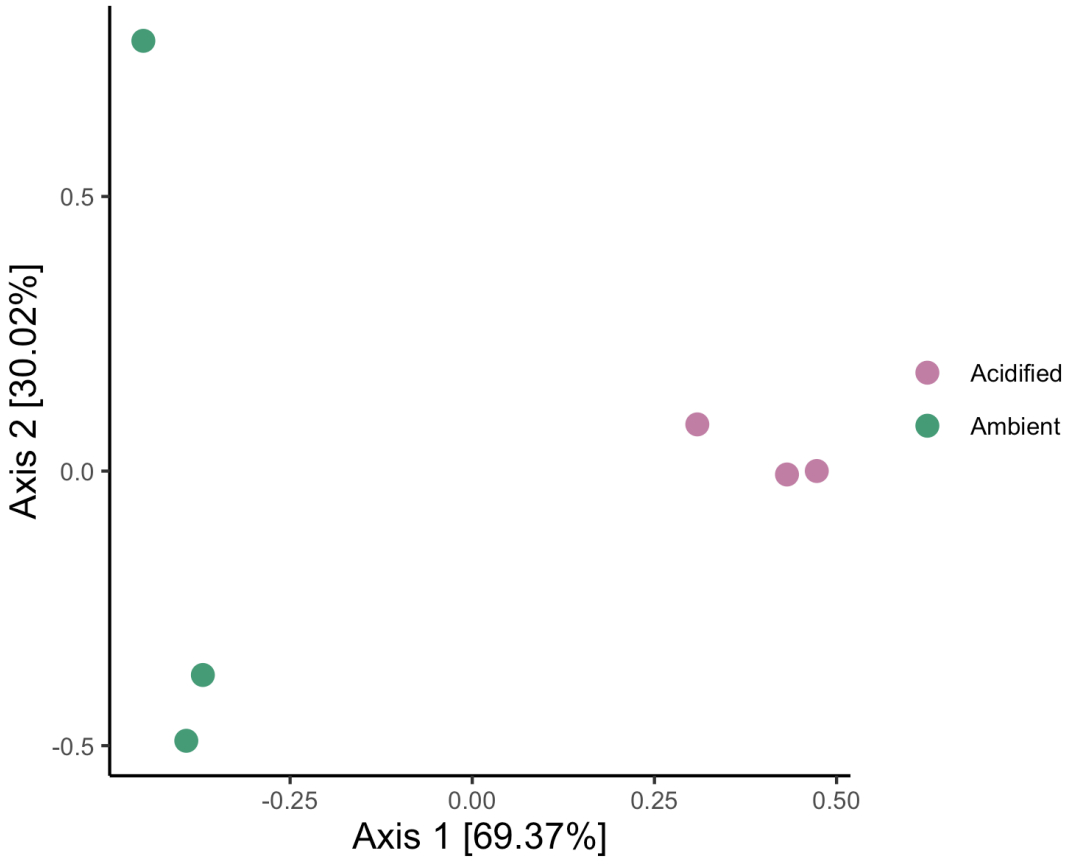

Figure S4.1 | Principle coordinate analysis plot of KEGG orthology (KO) groups within metagenomes derived from ambient (green) and acidified (pink) samples. PCoA axes are derived from Aitchison beta-diversity distance metrics of KO read counts.

8.6 Appendix G: Ch. 5 Supplemental Tables

ASV	Phylum	Class	Order	Family	Genus	lfc[a]	lfcSE[b]	stat[c]	padj[d]
asv0122	Proteobacteria	Gammaproteobacteria	Steroidobacterales	Woeseiaceae	Woeseia	24.370	2.310	10.548	0.000
asv0135	Proteobacteria	Gammaproteobacteria	BD7-8	NA	NA	5.817	1.622	3.587	0.004
asv0165	Cyanobacteria	Oxyphotobacteria	Chloroplast	NA	NA	5.610	1.572	3.568	0.004
asv0121	Proteobacteria	Deltaproteobacteria	Desulfobacterales	Desulfobulbaceae	Desulfopila	4.808	1.401	3.433	0.006
asv0089	Bacteroidetes	Bacteroidia	Bacteroidales	Prolixibacteraceae	Draconibacterium	4.554	0.969	4.700	0.000
asv0041	Proteobacteria	Deltaproteobacteria	Desulfobacterales	Desulfobulbaceae	Desulforhopalus	3.641	0.758	4.803	0.000
asv0173	Marinimicrobia	NA	NA	NA	NA	3.616	0.774	4.673	0.000
asv0105	Bacteroidetes	Bacteroidia	Bacteroidales	Marinilabiliaceae	NA	3.597	0.908	3.959	0.001
asv0138	Proteobacteria	Deltaproteobacteria	Myxococcales	Sandaracinaceae	NA	3.365	0.854	3.941	0.001
asv0147	Bacteroidetes	Bacteroidia	Flavobacteriales	Flavobacteriaceae	Aquibacter	3.305	0.926	3.570	0.004
asv0098	Bacteroidetes	Bacteroidia	Bacteroidales	Prolixibacteraceae	Draconibacterium	3.161	0.846	3.736	0.003
asv0118	Fusobacteria	Fusobacteriia	Fusobacteriales	Fusobacteriaceae	Propionigenium	3.124	0.852	3.668	0.003
asv0218	Bacteroidetes	Bacteroidia	Chitinophagales	Saprospiraceae	NA	3.112	0.882	3.528	0.005
asv0094	Bacteroidetes	Bacteroidia	Bacteroidales	SB-5	NA	2.735	0.521	5.253	0.000
asv0055	Bacteroidetes	Bacteroidia	Flavobacteriales	Flavobacteriaceae	Maritimimonas	2.598	0.504	5.152	0.000
asv0087	Proteobacteria	Deltaproteobacteria	Sva0485	NA	NA	2.490	0.484	5.139	0.000
asv0035	Proteobacteria	Deltaproteobacteria	Desulfobacterales	Desulfobulbaceae	NA	2.278	0.554	4.113	0.001
asv0022	Proteobacteria	Gammaproteobacteria	B2M28	NA	NA	2.039	0.561	3.637	0.004
asv0034	Proteobacteria	Deltaproteobacteria	Desulfobacterales	Desulfobulbaceae	NA	2.020	0.533	3.791	0.002
asv0018	Proteobacteria	Deltaproteobacteria	Desulfuromonadales	Sva1033	NA	1.910	0.297	6.430	0.000
asv0005	Proteobacteria	Deltaproteobacteria	Desulfobacterales	Desulfobulbaceae	NA	1.424	0.221	6.441	0.000
asv0009	Bacteroidetes	Bacteroidia	Bacteroidales	Bacteroidetes BD2-2	NA	1.343	0.247	5.430	0.000
asv0036	Proteobacteria	Gammaproteobacteria	NA	NA	NA	1.315	0.381	3.450	0.006
asv0002	Epsilonbacteraeota	Campylobacteria	Campylobacterales	Sulfurovaceae	Sulfurovum	1.134	0.174	6.501	0.000
asv0004	Epsilonbacteraeota	Campylobacteria	Campylobacterales	Sulfurovaceae	Sulfurovum	0.962	0.187	5.153	0.000
asv0020	Bacteroidetes	Bacteroidia	Flavobacteriales	Flavobacteriaceae	NA	-2.296	0.682	-3.364	0.007
asv0017	Bacteroidetes	Bacteroidia	Bacteroidales	Bacteroidetes BD2-2	NA	-2.402	0.715	-3.358	0.007
asv0068	Epsilonbacteraeota	Campylobacteria	Campylobacterales	Thiovulaceae	Sulfurimonas	-2.855	0.842	-3.392	0.007
asv0003	Epsilonbacteraeota	Campylobacteria	Campylobacterales	Thiovulaceae	Sulfurimonas	-2.940	0.590	-4.982	0.000
asv0011	Epsilonbacteraeota	Campylobacteria	Campylobacterales	Arcobacteraceae	Arcobacter	-3.233	0.707	-4.576	0.000
asv0026	Firmicutes	Clostridia	Clostridiales	Lachnospiraceae	NA	-3.376	1.008	-3.350	0.007
asv0001	Proteobacteria	Gammaproteobacteria	Nitrosococcales	Methylophagaceae	NA	-3.389	0.484	-7.000	0.000
asv0012	Proteobacteria	Gammaproteobacteria	Alteromonadales	Colwelliaceae	Colwellia	-3.473	0.879	-3.952	0.001
asv0093	Proteobacteria	Alphaproteobacteria	Rhizobiales	Rhizobiaceae	Cohaesibacter	-3.701	1.029	-3.598	0.004
asv0025	Proteobacteria	Gammaproteobacteria	Chromatiales	Sedimenticolaceae	NA	-4.338	0.926	-4.683	0.000
asv0060	Proteobacteria	Gammaproteobacteria	Oceanospirillales	Nitrincolaceae	Amphritea	-5.073	0.863	-5.881	0.000
asv0153	Epsilonbacteraeota	Campylobacteria	Campylobacterales	Thiovulaceae	Sulfurimonas	-5.471	1.618	-3.381	0.007
asv0129	Bacteroidetes	Bacteroidia	Bacteroidales	Marinilabiliaceae	Labilibacter	-6.020	1.032	-5.836	0.000
asv0131	Proteobacteria	Deltaproteobacteria	Desulfobacterales	Desulfobulbaceae	Desulforhopalus	-6.375	1.314	-4.851	0.000
asv0081	Epsilonbacteraeota	Campylobacteria	Campylobacterales	Arcobacteraceae	Arcobacter	-6.530	1.451	-4.501	0.000
asv0023	Cyanobacteria	Oxyphotobacteria	Chloroplast	NA	NA	-7.323	0.994	-7.365	0.000
asv0015	Epsilonbacteraeota	Campylobacteria	Campylobacterales	Arcobacteraceae	Arcobacter	-7.365	0.945	-7.794	0.000

[a] lfc: Log2-Fold Change (Rhizosophere/Root)
[b] lfcSE: Log2-Fold Change Standard Error
[c] stat: DESeq2 Test Statistic
[d] adjusted p-value: Benjamini-Hochberg FDR adjustment (Benjamini, Y., and Hochberg, Y. (1995). Journal of the Royal Statistical Society Series B, 57, 289–300.)

Table S5.1 | DESeq2 results: bacterial ASVs significantly different in relative abundance between compartments.

Family	padj intercept[a]	padj slope[a]	p intercept	p slope	coeff intercept	coeff slope
Ruminococcaceae	0.0362	0.0003	0.0140	0.0000	-2.5107	0.0772
Sandaracinaceae	0.0071	0.0095	0.0020	0.0006	2.6086	-0.1098
Rhizobiales Incertae Sedis	0.0000	0.0145	0.0000	0.0015	5.3061	-0.1891
Family XII	0.0002	0.0161	0.0000	0.0018	2.0881	-0.0907
Sulfurovaceae	0.0000	0.0169	0.0000	0.0021	-0.8038	0.0250
Chromatiaceae	0.0278	0.0221	0.0101	0.0030	2.5110	-0.1154
Mitochondria	NS	0.0056	0.2147	0.0001	-1.7061	0.1216
Rhodobacteraceae	NS	0.0069	0.1870	0.0003	-0.4555	0.0530
Thiotrichaceae	NS	0.0069	0.7446	0.0003	0.8323	-0.0579
Bacteroidales unknown	NS	0.0105	0.6650	0.0008	-0.8446	0.0564
Sulfurospirillaceae	NS	0.0122	0.0710	0.0011	-0.4319	0.0936
PHOS-HE36	NS	0.0337	0.3963	0.0051	1.6347	-0.1025
Puniceicoccaceae	NS	0.0410	0.0267	0.0067	-1.7858	0.0769
Prolixibacteraceae	NS	0.0429	0.0552	0.0075	-0.7010	0.0311
Woeseiaceae	0.0000	NS	0.0000	0.0135	3.8388	-0.1232
BD7-8 unknown	0.0000	NS	0.0000	0.0389	92.1933	-3.2501
MidBa8	0.0000	NS	0.0000	0.0556	-3.1286	0.0800
Arcobacteraceae	0.0000	NS	0.0000	0.3524	0.5868	0.0150
Bacteroidetes BD2-2	0.0000	NS	0.0000	0.4667	-0.7186	0.0091
Sva0485 unknown	0.0001	NS	0.0000	0.9385	-1.0274	0.0017
Aminicenantales unknown	0.0007	NS	0.0001	0.3686	-3.2495	0.0614
Flavobacteriaceae	0.0009	NS	0.0001	0.1348	0.1707	0.0122
Bacteroidetes VC2.1 Bac22 unknown	0.0012	NS	0.0002	0.3482	-1.0322	0.0191
Kiritimatiellaceae	0.0012	NS	0.0002	0.3722	-1.9842	0.0361
Kangiellaceae	0.0012	NS	0.0002	0.9123	-3.2161	0.0137
Vibrionaceae	0.0013	NS	0.0003	0.0175	1.2846	-0.0558
Clostridiales unknown	0.0017	NS	0.0004	0.0404	-2.3497	0.0730
Desulfarculaceae	0.0017	NS	0.0003	0.5608	-1.4059	-0.0346
Lentimicrobiaceae	0.0022	NS	0.0005	0.4866	-1.2693	0.0197
Saprospiraceae	0.0037	NS	0.0009	0.0918	0.2273	0.0281
Izimaplasmataceae	0.0040	NS	0.0010	0.7628	0.8973	0.0092
Latescibacteraceae	0.0040	NS	0.0011	0.8977	-2.3159	-0.0112
Desulfobacteraceae	0.0105	NS	0.0030	0.7374	-0.2745	-0.0036
Marinilabiliaceae	0.0112	NS	0.0034	0.5177	-0.5261	-0.0165
Colwelliaceae	0.0113	NS	0.0035	0.1343	0.4155	0.0516
WCHB1-41 unknown	0.0220	NS	0.0071	0.5389	-2.3508	0.0424
Proteobacteria unknown	0.0245	NS	0.0083	0.8178	1.5059	-0.0115
Unknown Family	0.0264	NS	0.0092	0.1624	-0.8442	0.0266
Halieaceae	0.0318	NS	0.0119	0.3466	-0.9307	0.0244
Woesearchaeia unknown	0.0463	NS	0.0185	0.0715	-1.3702	0.0493

[a] padj: Benjamini-Hochberg FDR adjustment

Table S5.2 | CPGLMM results of *Z. marina* rhizosphere microbes with significant modeled coefficients for Intercepts (Treatment effect) and/or Slopes (Time x Treatment Interaction).

Family	padj intercept[a]	padj slope[a]	p intercept	p slope	coeff intercept	coeff slope
Vibrionaceae	0.0006	0.0003	0.0001	0.0000	2.5618	-0.1250
Desulfobacteraceae	0.0053	0.0006	0.0010	0.0000	-1.5928	0.0653
Sulfurovaceae	0.0000	0.0398	0.0000	0.0045	-0.9518	0.0292
Gammaproteobacteria unknown	0.0006	0.0398	0.0001	0.0048	-1.8652	0.0618
Ruminococcaceae	0.0075	0.0398	0.0015	0.0047	-2.7013	0.0963
Lentimicrobiaceae	0.0331	0.0398	0.0119	0.0036	-3.0029	0.1190
Desulfobulbaceae	NS	0.0398	0.1321	0.0018	-0.5698	0.0291
Prolixibacteraceae	NS	0.0398	0.1831	0.0024	-1.1274	0.0552
Desulfuromonadaceae	NS	0.0398	0.4447	0.0044	-1.7078	0.0982
Spirochaetaceae	NS	0.0442	0.6357	0.0059	-0.8580	0.0475
Family XII	0.0000	NS	0.0000	0.8192	2.0464	-0.0076
Arcobacteraceae	0.0000	NS	0.0000	0.1349	0.8259	-0.0175
Milano-WF1B-44 unknown	0.0000	NS	0.0000	0.0861	-1.1001	0.0254
Bacteroidetes BD2-2	0.0002	NS	0.0000	0.0268	-0.9710	0.0282
Sva0485 unknown	0.0002	NS	0.0000	0.2264	-2.9168	0.0614
Halieaceae	0.0006	NS	0.0001	0.9297	-1.5484	-0.0036
Rhodobacteraceae	0.0006	NS	0.0001	0.0733	-0.2798	-0.0264
B2M28 unknown	0.0006	NS	0.0001	0.3630	-1.7880	0.0330
Thiovulaceae	0.0025	NS	0.0004	0.2917	-0.6728	0.0139
Mariprofundaceae	0.0045	NS	0.0008	0.2261	0.3012	0.0707
Unknown Family	0.0116	NS	0.0025	0.3822	-1.0717	0.0226
Bacteroidetes VC2.1 Bac22 unknown	0.0119	NS	0.0027	0.1061	-1.6932	0.0514
Anaerolineaceae	0.0148	NS	0.0038	0.2063	-1.8215	0.0461
Pirellulaceae	0.0148	NS	0.0036	0.3126	-2.1341	0.0480
Colwelliaceae	0.0175	NS	0.0047	0.1594	1.3529	-0.0426
Cyclobacteriaceae	0.0233	NS	0.0068	0.0332	0.0881	-0.0745
Nitrincolaceae	0.0233	NS	0.0066	0.7537	0.6226	0.0079
Pseudoalteromonadaceae	0.0281	NS	0.0086	0.8006	0.9853	-0.0087
JGI 0000069-P22 unknown	0.0326	NS	0.0113	0.4628	0.6018	0.0249
Rhizobiaceae	0.0326	NS	0.0106	0.1638	-0.2354	-0.0400
SB-5	0.0326	NS	0.0110	0.0150	-2.6256	0.0982
Marinifilaceae	0.0337	NS	0.0126	0.7723	0.8651	-0.0094
Bacteroidia unknown	0.0380	NS	0.0147	0.6902	0.7044	0.0157
Psychromonadaceae	0.0392	NS	0.0157	0.4327	0.7206	-0.0199
Izimaplasmataceae	0.0462	NS	0.0191	0.0523	-0.1934	0.1090

[a] padj: Benjamini-Hochberg FDR adjustment

Table S5.3 | CPGLMM results of *Z. marina* root microbes with significant modeled coefficients for Intercepts (Treatment effect) and/or Slopes (Time x Treatment Interaction).

8.7 Appendix H: Ch. 5 Supplemental Figures

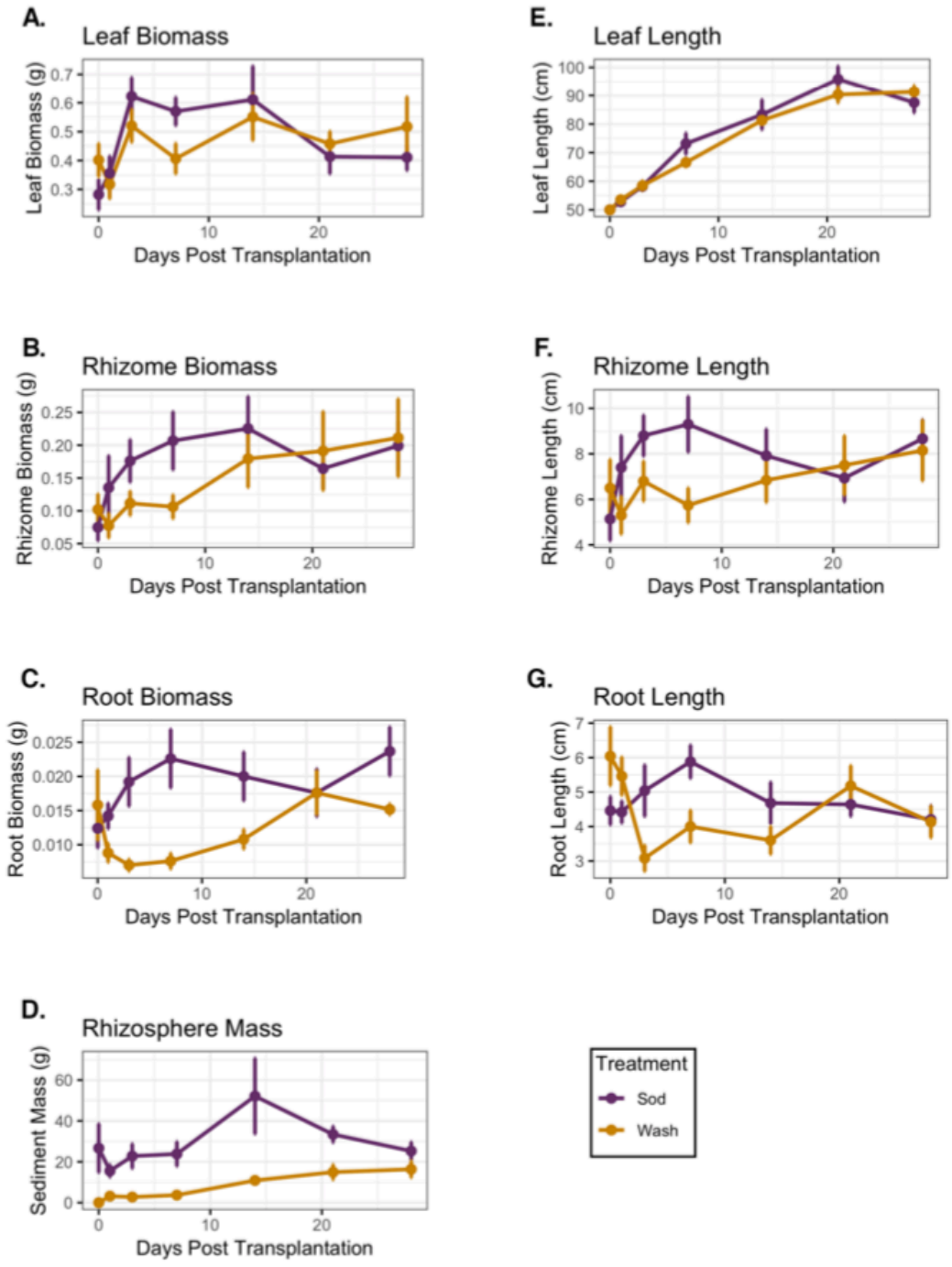

Figure S5.1 | *Z. marina* Morphometric Data. (A) Leaf Biomass, (B) Rhizome Biomass, (C) Root Biomass, (D) Rhizosphere Sediment Biomass, (E) Leaf Length, (F) Rhizome Length, (G) Root Length. Colors designate treatment group (purple = sod transplants, gold = washed transplants; mean values and standard errors are reported).